Development of chemogenetic methodology to investigate cortical mechanisms of cognition



Sanziana Maria Rotariu

Thesis submitted in partial fulfilment of the requirements

for the degree of Doctor of Philosophy

University of Oxford

Department of Pharmacology

Corpus Christi College

Trinity Term, 2019

Development of chemogenetic methodology to investigate cortical mechanisms of cognition

Sanziana Maria Rotariu, Corpus Christi College, D. Phil, Trinity Term 2019

Abstract

DREADDs (designer receptors exclusively activated by designer drugs) are virally mediated engineered muscarinic receptors that no longer bind their endogenous ligand acetylcholine but instead bind the clozapine metabolite, clozapine-N-oxide (CNO). These receptors are a very useful research tool for deconstructing behaviour due to their promoter-driven cell-specificity and potential spatial resolution, the low invasiveness associated with their use, reversibility and the temporal resolution of minutes to hours. This makes them ideal tools for linking cell-specific changes to behaviours that require longer testing duration such as learning and memory tasks.

Using an array of techniques, this thesis has provided an in-depth analysis of chemogenetic functionality in the hippocampus. Immunohistochemistry and *in situ* hybridisation studies assessed the spread and specificity of the CaMKIIa promoter driven excitatory (Gq-DREADD) and inhibitory (Gi-DREADD) constructs in the rat dorsal hippocampus. Slice electrophysiology, *in vivo* local field potential (LFP)-electrocorticography (ECoG) recordings and hippocampal-dependent behavioural tasks were used to assess the functionality of the constructs. Additionally, a liquid chromatography-mass spectrometry study directly tested the ability of CNO and clozapine to enter the brain as recent reports have found evidence that CNO is back-metabolised to clozapine, that then readily enters the brain and is in fact the activator of the DREADDs.

Expression of both the Gi- and Gq-DREADD was almost entirely restricted to the principal layers of the hippocampus, with the exception of transfection of a small population of interneurons in the hilar region of the dentate gyrus. In hippocampal slices expressing Gi-DREADD, both CNO and clozapine decreased excitatory transmission. Paradoxically, both ligands also decreased excitatory transmission in slices expressing an excitatory DREADD. Follow-up experiments ruled out the potential activation of inhibitory transmission or of the $mGlu_{2/3}$ receptors to be involved in this response.

In accordance with recent reports, the exposure study found evidence for back metabolism of CNO to clozapine, with the clozapine concentration in the brain after CNO injection being comparable to the clozapine concentration used to activate the DREADDs in the slice experiments (0.6 μM and 1 μM, respectively). The results also suggested a higher dose of CNO (10 mg/kg) might be needed for clozapine to enter the brain and activate the DREADDs.

In vivo LFP/ECoG recordings found decreased power in the beta, low gamma and high gamma frequencies in rats expressing a Gi-DREADD in the presence of CNO compared to saline. Somewhat surprising, there were no statistically significant changes in brain oscillations in Gq-DREADD expressing rats in the presence of CNO. This suggests that suppression of pyramidal cell activity disrupts the generation of gamma oscillations in the hippocampus by potentially modulating intraneuronal activity. Finally, object exploration, spatial short-term/working memory and locomotor activity were found to be unchanged regardless of viral construct or treatment. In addition, neither CNO (3 or 10 mg/kg) or clozapine (0.1 or 0.5 mg/kg) were found to affect behaviour in controls.

Collectively, these experiments provide evidence for DREADD functionality in the rat hippocampus. The results also suggest that despite evidence of *in vivo* functionality in the context of LFP signals, a behavioural phenotype might require a higher viral transfection rate. This emphasises the importance of correlating behavioural changes with neurophysiological measurements, as cell-specific manipulation might not be detected as changes in behaviour.

Acknowledgements

First and foremost I would like to thank my three supervisors: Trevor Sharp and David Bannerman at the University of Oxford and Kjartan Frisch Herrik at H. Lundbeck A/S who have given me the opportunity to work on this project. I am also very grateful for my funding bodies, the Medical Research Council UK and H. Lundbeck A/S for their generosity. Collectively, I'd like to thank my supervisors for their invaluable academic input during the past 4 years and during the writing of this thesis, the stimulating scientific conversations but also their kindness and continuous support.

I thank Trevor for his day to day supervision during my time in Oxford, for the opportunity to work in his group and for inspiring me beyond academia to run my first (and second) marathon.

I thank David for always making time for discussions, for imparting his knowledge on behaviour onto me and sparking my interest and for continuously cheering me on.

I thank Kjartan for making me feel very welcome at Lundbeck and making sure I'm integrating well into the Danish lifestyle, but also for his support and general positive attitude. I had a wonderful time at Lundbeck and I have you to thank for that.

I am grateful for the Sharp lab members, past and present. I thank Judith Schweimer for first welcoming me into the lab, teaching me all things lab related and looking after me until I found my feet but most importantly for her kindness and support. I thank Chris Barkus for teaching me how to perform behavioural studies and never hesitating to help. Lastly, I am very grateful that Raquel Pinacho joined our lab and shared DREADDfull experiences with me. I thank her for all her help throughout these years in all academic areas but also for all the chats during lunch and coffee breaks. Most importantly, I'd like to thank them all for their friendship and making Oxford more homely. I'd also like to thank Raquel and Chris for adopting me during my visits to Oxford and welcoming me into their home.

I'd like to thank all the skilled people I have met at Lundbeck and have helped me with my project. I thank Kasper Larsen for getting me settled in and answering all my questions. I thank Charlotte Hougaard and Lis Glasdam Jensen for guidance during my MEA experiments and the wonderful histology team – Camilla Stampe Jensen, Kirsten Jørgensen and Pia Møller Carstensen – for performing the *in situ* study. I thank Line Rørbæk Olsen and Hossein Armandi for help with the LC-MS/MS study. Lastly, I thank Ulrike Richter and Claus Agerskov for developing and providing me with the MatLab script and app for the LFP/ECoG study analysis. I'd like to extend my thanks to Ulrike for her endless patience and unwavering support through all my questions and requirements.

I am very grateful for the animal technicians I worked with during this project. In Oxford I'd like to thank Richard (OQF) and Nick and Debbie (BMS). In Lundbeck I'd like to thank the very skilled team from the dyrestalden – Nina, Heidi, Louise, Mette, Miki, Joy, Monica, Sofie, Allan, Louise, Susanne, Pernille and Sebrina. Thank you for taking care of my animals and allowing me to take weekends off.

A special thank you goes to my oldest and best friends from home, the three stars, Miru, Ioana and Alexandra. I thank them for all the laughs and limitless support. I also thank my dear friends, the neuro nerds: Ally, Mary and Megan for being my biggest cheerleaders and trusting in me.

I am most grateful for my family. I thank my dad, for his advice and for his continuous support throughout my life. I thank my mum, for her endless patience and love and always looking after me despite my grumpiness. I thank my brother Octav for calling me every other week to see how I'm doing, and I thank my brother Mihnea for bringing our niece Alma into our lives to brighten them up. Lastly, I'd like to thank Buni, who unfortunately had to leave us before this adventure was over but whose thoughts have been and will be with me always.

Finally, I thank Lars, who joined the party in Scotland and somehow decided to stay. Thank you for your kindness, patience, endless support and keeping me grounded but also for the numerous meals you've made for me.

The past 4 years would not have been possible without any of the people named above and many more that have helped along the way. Writing these words puts these past years into perspective and makes me realise just how lucky I am to have met and worked with such brilliant and kind people. And for that I'll be forever grateful.

Table of contents

Abstract ..... **II**

Acknowledgements ..... **III**

Table of contents ..... **IV**

Abbreviations ..... **IX**

Publications ..... **XII**

1. General introduction **1**

1.1 Scope of this thesis 1

1.2 G-protein coupled receptors 1

1.2.1 Engineering GPCR signalling 2

1.3 Designer receptors exclusively activated by designer drugs (DREADDs) 3

1.3.1 Viral construct configuration 3

1.3.2 Gq-coupled DREADDs 6

1.3.3 Gi-coupled DREADDs 8

1.3.4 DREADD agonists 10

1.3.5 Advantages of DREADDs in the hippocampus 14

1.4 The hippocampal formation 15

1.4.1 Hippocampal function 17

1.4.2 Behavioural tasks to study hippocampal function 19

1.5 Brain oscillations and local field potential 22

1.5.1 Hippocampal oscillations and behaviour 23

1.6 Aim of the thesis 24

2. Development of chemogenetic protocols to manipulate hippocampal function 27

2.1 Introduction 27

2.1.1 Tools to inhibit hippocampal function 27

2.1.2 Chemogenetic manipulation of neural activity 29

2.1.3 Use of chemogenetics to target the hippocampus 30

2.1.4 CNO as a DREADD activator 32

2.1.5 Chapter 2 experimental aims 33

2.2 Materials and methods 34

2.2.1 Animals 34

2.2.2 Viral constructs 35

2.2.3 Intracerebral viral injections 36

2.2.4 Immunohistochemistry 38

2.2.5 Fluorescence *in situ* hybridisation 39
2.2.6 Hippocampal *ex vivo* electrophysiology 41
2.2.7 Drugs 46
2.2.8 Statistical analysis 49
2.3 Results 50
2.3.1 DREADD delivery to the hippocampus 50
2.3.2 Cellular localisation of CaMKIIa promotor driven Gi-DREADD in hippocampus 57
2.3.3 Electrophysiological effect of CNO in Gi- and Gq-DREADD-expressing hippocampal slices 61
2.3.4 Electrophysiological effect of clozapine in Gi- and Gq-DREADD-expressing hippocampal slices 65
2.3.5 Effect of GABA receptor blockade on CNO-induced inhibition in Gq-DREADD-expressing hippocampal slices 68
2.3.6 Effect of metabotropic glutamate receptor blockade on CNO-induced inhibition in Gq-DREADD-expressing hippocampal slices 71
2.3.7 Effect of duration of application on CNO-induced inhibition in Gq-DREADD-expressing hippocampal slices 73
2.3.8 Electrophysiological effect of CNO in interneuron-targeted, Gq-DREADD-expressing hippocampal slices 74
2.4 Discussion 77
2.4.1 DREADD delivery to the dorsal hippocampus 78
2.4.2 Specificity of the CaMKIIa promoter 79
2.4.3 CNO as a DREADD agonist *ex vivo* 80
2.4.4 Investigation of inhibitory effect of CNO in the presence of Gq-DREADD 82
2.4.5 Clozapine as DREADD agonist *ex vivo* 84
2.4.6 Interneuron activation as an alternative approach to pyramidal neuron silencing 85
2.4.7 Conclusions 85
3. DREADDs as tools to modulate learning and memory behaviour 87
3.1 Introduction 87
3.1.1 Hippocampal dependent cognitive tasks 87
3.1.2 Short-term habituation, novelty and the hippocampus 90
3.1.3 Chapter 3 experimental aims 91
3.2. Materials and Methods 92
3.2.1. Animals 92
3.2.2 Viral constructs 92
3.2.3 Intracerebral viral injection 93
3.2.4 Drugs 94

3.2.5 Reward alternation T-maze 95
3.2.6 Spatial novelty preference Y-maze 97
3.2.7 Novelty-induced locomotor activity 98
3.2.8 Histology 98
3.2.9. Statistical analysis 99
3.3 Results 100
3.3.1 Spatial working memory in Gi-DREADD expressing rats in a familiar room 100
3.3.2 Spatial working memory in Gi-DREADD expressing rats in a novel room .. 103
3.3.3 Spatial novelty preference in Gi-DREADD expressing rats in the presence of clozapine 106
3.3.4 Novelty induced locomotor activity in the presence of clozapine 110
3.3.5. Post-hoc histological validation 112
3.4 Discussion 113
3.4.1 SWM on a rewarded alternation T-maze task in a familiar room in Gi-DREADD expressing rats 113
3.4.2 SWM on a rewarded alternation T-maze in a novel room in Gi-DREADD expressing rats 116
3.4.3 Short-term memory on a spatial novelty preference Y-maze task in Gi-DREADD expressing rats 118
3.4.4 Novelty induced locomotor activity in response to clozapine 119
3.4.5 Conclusions 120
4. Bioavailability of CNO and clozapine in relation to DREADD function 121
4.1 Introduction 121
4.1.1 c-Fos as marker of neuronal activity 121
4.1.2 c-Fos use in functional DREADD validation 122
4.1.3 CNO, designer drug or pro-drug? 123
4.1.4 Chapter 4 experimental aims 124
4.2 Materials and Methods 125
4.2.1 Animals 125
4.2.2 Viral constructs 126
4.2.3 Intracerebral viral injection 127
4.2.4 Drugs 127
4.2.5 Novel context-induced c-Fos activation 128
4.2.6 Immunohistochemistry (c-Fos fluorescence and DAB staining) 129
4.2.7 Fluorescence *in situ* hybridisation 131
4.2.8 Quantification of c-Fos positive cells 132
4.2.9 CNO/clozapine exposure study (LC-MS/MS) 134
4.2.10 Statistical analysis 136

4.3 Results 138
4.3.1 Effect of novel environment on c-Fos expression in hippocampus (Study 1) 138
4.3.2 Effect of CNO or clozapine on c-Fos in hippocampus with Gi-DREADD (Study 2) 139
4.3.3 Effect of higher dose CNO on c-Fos in hippocampus with Gi-DREADD or Gq-DREADD (Study 3) 142
4.3.4 Plasma levels of clozapine and CNO following systemic administration of clozapine and CNO 145
4.3.5 Brain levels of clozapine and CNO following systemic administration of clozapine and CNO 147
4.4 Discussion 150
4.4.1 Effects of CNO and clozapine on c-Fos after DREADD expression 151
4.4.2 CNO and clozapine pharmacokinetics 153
4.4.3 Conclusions 156
5. DREADDs as tool to study cortical mechanisms of cognition 157
5.1 Introduction 157
5.1.1 *In vivo* electrophysiological recordings 157
5.1.2 Hippocampal oscillations 158
5.1.3 DREADDs as tools to study hippocampal oscillations 160
5.1.4 Chapter 5 experimental aims 161
5.2 Materials and Methods 163
5.2.1 Animals 163
5.2.2 Viral constructs 164
5.2.3 Intracerebral viral injections 164
5.2.4 Stereotaxic electrode implantation 165
5.2.5 Drugs 166
5.2.6 Resting state ECoG/LFP recordings (study I and II) 167
5.2.7 Spatial novelty preference Y-maze 170
5.2.8 Locomotor activity 171
5.2.9 Spontaneous recognition task with 4 objects 172
5.2.10 Electrode placement confirmation and histology 174
5.2.11 rsECoG/LFP data analysis 174
5.2.12 Statistical analysis 176
5.3 Results 177
5.3.1 LFP profile of dorsal hippocampus Gi-DREADD expressing rats in the presence of CNO or clozapine – Study I 177
5.3.2 Novel environment hippocampal LFP recordings 192

5.3.3 Locomotor activity of Gi and Gq-DREADD and EGFP-control rats in the presence of CNO - Study II 195
5.3.4 Resting state LFP profile of rats expressing an inhibitory or excitatory DREADD in the dorsal hippocampus – study II 196
5.3.5. Histology 207
5.3.6 Novelty induced locomotor activity of Gi-DREADD and EGFP-control in the presence of CNO 211
5.3.7 Short-term memory of Gi-DREADD and EGFP-control in the presence of CNO 212
5.4 Discussion 214
5.4.1 LFP profile in response to CNO or clozapine Gi-DREADD activation – study I 215
5.4.2 LFP profile of Gi-DREADD expressing rats in a novel environment 216
5.4.3 LFP profile of Gq and Gi-DREADD rats in the presence of CNO – study II 217
5.4.4 Behavioural readout of decreased brain oscillations 220
5.4.5 Conclusion 221
6. General discussion 222
6.1 Chapter 2 summary: DREADDs as tool to manipulate hippocampal function *ex vivo* 223
6.2 Chapter 3 summary: DREADDs as a tool to manipulate hippocampal function *in vivo.* 226
6.3 Chapter 4 summary: CNO and clozapine bioavailability in relation to DREADD function 228
6.4 Chapter 5 summary: DREADDs as a tool to study cortical mechanisms of cognition 230
6.5 DREADD limitations 233
6.6 Unanswered questions 236
6.7 Conclusions 239
7. Appendix 241
7.1 Histology (LFP/ECoG Study I) 241
7.2 Resting state ECoG profile of rats expressing an inhibitory or excitatory DREADD in the dorsal hippocampus – study II 244
7.3 Resting state LFP profile recorded from the mPFC from rats expressing an inhibitory or excitatory DREADD in the dorsal hippocampus – study II 253
8. Bibliography 258

Abbreviations

2-AG	2-Arachidonoylglycerol
aCSF	Artificial cerebrospinal fluid
AAV	Adeno-associated virus
AMPA	α-amino-3-hydroxy-5-methyl-4-isoxazolepropionic acid
BBB	Blood-brain barrier
BNST	Bed nucleus of the stria terminalis
CA	Cornu ammonis
CaMKIIa	Ca2+/calmodulin-dependent protein kinase II
cAMP	Cyclic adenosine monophosphate
CB1	Cannabinoid receptor type 1
CLZ	Clozapine
CNO	Clozapine-N-oxide
CREB	cAMP response element binding
DG	Dentate gyrus
dHipp	Dorsal hippocampus
DMSO	Dimethyl sulfoxide
DREADDs	Designer receptor exclusively activated by designer drugs
ECoG	Electrocorticography
EGFP	Enhanced green fluorescent protein
Elk-1	ETS Like-1 protein
EPSC	Excitatory postsynaptic current
fEPSP	Field excitatory postsynaptic potential
FISH	Fluorescence in situ hybridisation
GABA	Gamma-aminobutyric acid
GAD1	Glutamic acid decarboxylase isoform 1
GIRK	G-protein-coupled inwardly-rectifying potassium channel
GLME	Generalised linear mixed-effects
GPCR	G-protein coupled receptor
HEK	Human embryonic kidney
i.p.	Intraperitoneal
IEG	Immediate early gene

ING	Interneuron gamma network
I-O	Input-output
ISH	In situ hybridisation
ITI	Intra-trial interval
KA	Kainate
KORD	κ-opioid receptor DREADD
LTD	Long term depression
MAPK	Mitogen-activated protein kinase
MEA	Multi electrode array
mPFC	Medial prefrontal cortex
mRNA	Messenger ribonucleic acid
MS	Medial septum
MSDB	Medial septal-diagonal band of Broca
NMDA	N-methyl-D-aspartate
NMDG	Meglumine / N-methyl-D-glucamine
NSAID	Nonsteroidal anti-inflammatory drug
MWM	Morris water maze
PBS	Phosphate buffered saline
PCR	Polymerase chain reaction
PD	Parkinson’s disease
PFA	Paraformaldehyde
PING	Pyramidal interneuron gamma network
PLC	Phospholipase C
PLCβ	Phospholipase C beta
PTX	Picrotoxin
PV	Parvalbumin
PVC	Polyvinyl chloride
REM	Rapid eye movement
ROI	Region of interest
RT	Room temperature
s.c.	Subcutaneous
SRM	Spatial reference memory
SWM	Spatial working memory

SWR	Sharp wave ripples
VTA	Ventral tegmental area

Publications

Parts of the work presented in the thesis has been presented as follows:

Investigation of the role of clozapine as a CNS DREADD activator (2018), Rotariu, S.M., Hougaard, C., Bannerman, D., Frisch Herrik, K., Sharp, T. Poster presented at BPS winter meeting, December 2018

Chapter 1

General introduction

1.1 Scope of this thesis

Correlating the basis of brain cellular function to behaviour is crucial for understanding mechanisms underlying normal brain function but also pathologies arising from abnormal cellular processes. Lesion studies have proved to be a useful tool in neuroscience research that brought further knowledge into the functions of different brain areas. Specifically, the hippocampus and its functions have been studied extensively with the help of lesions. However, this technique had its drawbacks in that it lacks cell specificity such that the arising behavioural changes that come as a consequence of lesions cannot be correlated with the underlying cellular mechanisms. Novel tools such as chemogenetics and optogenetics have tackled this limitation and provided a more refined approach to study brain function with a high level of cell-specificity. Experiments described in this thesis have used chemogenetics in the dorsal hippocampus of rats to investigate cortical mechanisms of cognition. The approaches used to achieve this are described in detail below.

1.2 G-protein coupled receptors

G-protein coupled receptors (GPCRs) are targeted by approximately a quarter of experimental and marketed drugs, making them the largest gene family targeted for drug discovery and development (Hopkins & Groom, 2002). G-protein mediated signalling is ubiquitous in practically all mammalian cells where GPCRs act as an on/off signalling switch. Due to their widespread distribution in the mammalian organism, GPCRs are involved in a multitude of physiological processes including hormonal function, cell growth and differentiation and synaptic transmission (Wettschureck & Offermanns, 2005). All these characteristics make GPCRs an ideal candidate for engineering synthetic signalling systems.

1.2.1 Engineering GPCR signalling

GPCR signalling is a transmembrane system that incorporates a receptor, a heterotrimeric protein and an effector (Wettschureck & Offermanns, 2005). This is unlike other transmembrane signalling systems that are only made up of a receptor and an effector. The typical pattern for GPCR – G-protein coupling is based on the activation of one of the canonical G-protein pathways: Gq, Gs and Gi. Briefly, Gq activation stimulates phospholipase C and increases intracellular calcium and Gs activation increases cyclic AMP. In contrast, Gi activation inhibits cAMP production (Conklin et al., 2008).

Engineering novel receptor/ligand pairs provides an opportunity to study physiological processes in different tissues and cell populations. The GPCR complex is an attractive target for receptor engineering through mutagenesis because it has modular architecture and is encoded by small genes (Conklin et al., 2008). The first attempt to develop a generation of engineered receptors called RASSLs (receptors activated solely by synthetic ligands) was by mutating the beta-adrenergic receptor (Strader et al., 1991). This report demonstrated the ability to develop a designer receptor by replacing a single amino acid residue which modified the ligand binding specificity. Thus, the mutated receptor would bind a newly synthesised molecule that would not activate the wild-type version of the receptor. However, the ligand was not suitable for experimental uses because of its very low affinity (Strader et al., 1991).

Next, a similar approach was employed to mutate the kappa opioid receptor (KOR). This time, the ligand was spiradoline. Site-directed mutagenesis rendered KOR no longer able to bind its endogenous peptide but instead preserved its ability to be activated by spiradoline (Coward et al., 1998). Despite successful attempts to engineer designer receptors, a number of drawbacks were associated with RASSLs. As was the case for the KOR, the ligands were binding to the mutated receptors but were also activating endogenous receptors. Secondly,

RASSLs also showed constitutive activity (Conklin et al., 2008). Thus, this prompted the search for designer receptors that would lack constitutive activity and ligands that show high affinity for the mutated receptor but are otherwise pharmacologically inert. As an alternative to DREADDs, ligand gated ion channel chemogenetic tools have also been developed, but will not be discussed further in this thesis (for review see Atasoy & Sternson, 2018).

1.3 Designer receptors exclusively activated by designer drugs (DREADDs)

DREADDs were first developed (for reviews see Rogan & Roth, 2011, Sternson & Roth, 2014, Zhu & Roth, 2014) by mutating the Gq-coupled human muscarinic M3 receptor which made them no longer responsive to their endogenous ligand, acetylcholine, but potently activated by binding of clozapine-N-oxide (CNO), a metabolite of clozapine. Gq-DREADD activation by CNO increased intracellular calcium. Subsequently, the Gi-coupled human muscarinic M4 receptor was designed, and when activated by CNO was shown to suppress hippocampal neuron activity by activating G protein-coupled inwardly-rectifying potassium channels (GIRKs) (Armbruster et al., 2007). A Gs-coupled DREADD was also developed but has not been widely used as its Gi and Gq counterparts (Guettier et al., 2009).

1.3.1 Viral construct configuration

DREADD constructs were originally created by Bryan Roth's lab and made commercially available. Typically, the constructs (**Figure 1.1**) are delivered by an adeno-associated virus (AAV) system that is flanked between two inverted terminal repeats. AAVs have been used successfully in gene delivery because of their safe profile and lack of immunogenicity (Daya & Berns, 2008; Naso et al., 2017). The AAV serotype controls the spread and efficacy of transfection. All viral constructs used in this thesis were of serotype AAV5/2 (widely referred to as AAV5) that was chosen based on its CNS transfection efficiency and tropism (Davidson

et al., 2000). This means that the genome of serotype 2 is packaged into the capsid of serotype 5 in order to improve efficiency of transfection.

The cell-specific delivery achieved by the viral construct is based on the promoter of choice that will dictate the tropism of the virus. All but one experiment described in this thesis used viral constructs under the control of a CaMKIIa promoter, to target excitatory neurons in the hippocampus by intracranial injection. This promoter has been shown previously to be specific in driving the transfection of viral constructs into excitatory neurons (Dittgen et al., 2004, Lopez et al., 2016, Mayford et al., 1996, White et al., 2011). Other promoters can be used to target different cell populations. For example, the hDlx promoter targets interneurons (Dimidschstein et al., 2016), the hSyn1 promoter targets neurons unspecifically (Lopez et al., 2016) and the GFAP promoter drives expression in glia (Scofield et al., 2015).

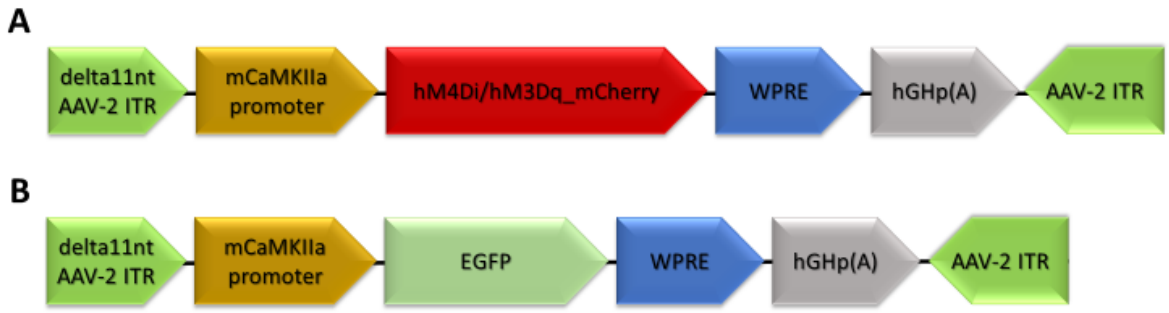


Figure 1.1 Typical structure of DREADD viral constructs

Schematic of DREADD vectors mediated by an adeno-associated virus (AAV) and driven by a CaMKIIa promoter. The mutated receptor, hM4Di or hM3Dq is tagged by a mCherry fluorophore (A). Control constructs lack the mutated receptor and express the EGFP fluorophore instead (B). WPRE: Woodchuck Hepatitis Virus Posttranscriptional Regulatory Element; hGHp(A): human growth hormone poly A; ITR: inverted terminal repeats.

The commonly used designer receptors, hM3Dq, hM4Di (Armbruster et al., 2007) act as a switch that is activated upon binding of a DREADD agonist. Thus, activation of the hM3Dq (Gq-DREADD) would be expected to lead to increased intracellular calcium and subsequent cell activation. In contrast, hM4Di (Gi-DREADD) activation should result in cell silencing

(Armbruster et al., 2007). A more recently described DREADD is a mutated kappa-opioid receptor DREADD (KORD) that is activated by SalB and was found to decrease neuronal firing by decreased cAMP (Vardy et al., 2015) (**Figure 1.2**). Finally, DREADD transfected cells are visualised by microscopy due to a fluorophore tagged to the mutated receptor or expressed by its own in control constructs. Commonly used fluorophores are mCherry, EGFP, mCitrine or dTomato.

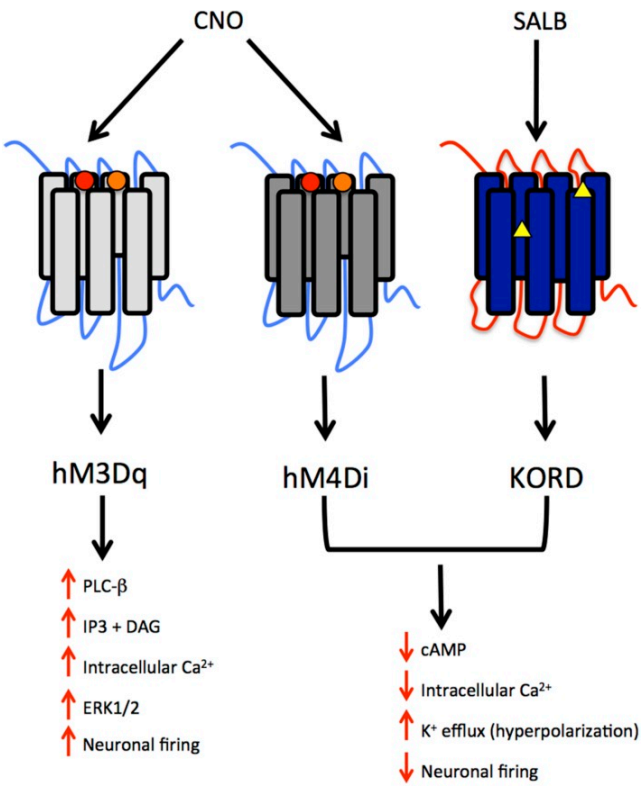


Figure 1.2 Summary of DREADD mechanisms

Schematic representation of DREADD mechanism of action. CNO binding to the hM3Dq receptor triggers a downstream cascade that is expected to lead to increased intracellular calcium and subsequent increased neuronal firing. In contrast, CNO and SalB binding to the hM4Di and KORD respectively, should cause decreased intracellular calcium and subsequent neuronal firing. Figure taken from Whisshell et al., 2016.

The combination of the virus with the mutated muscarinic receptor coupled to a promoter and tagged by a fluorophore allows for cell-specific transgene expression upon intracerebral delivery to the brain region of interest. CNO acts as an 'activator' for the DREADDs, thus

enabling transient cell-specific manipulation. The DREADD constructs used in this thesis were predominantly driven by the CaMKIIa promoter and targeted to pyramidal neurons in the dorsal hippocampus. Inhibitory, excitatory and control constructs were used throughout and they are introduced accordingly in the methods section of each chapter.

1.3.2 Gq-coupled DREADDs

The hM3Dq receptor was developed by using a modified M3 rat receptor containing a deletion on its third intracellular loop. A library of these mutants was created, and it was found that the mutants had lost their ability to bind their endogenous ligand (acetylcholine) in the process. They were then screened for affinity for clozapine. Finally, second generation mutants were created to be responsive to CNO. Their affinity to clozapine was however conserved and was 100-fold higher than CNO affinity (Armbruster et al., 2007).

Gq-DREADD function was later validated *in vivo* and *in vitro* using double transgenic mice expressing the Gq-DREADD in pyramidal neurons of the hippocampus and cortex (Alexander et al., 2009). The study reported that CNO induced cell depolarisation in Gq-DREADD expressing pyramidal cells *in vitro* as a result of a phospholipase C (PLC)-dependent mechanism, with evidence showing that a PLC inhibitor suppressed CNO induced depolarisation. The investigators suggested that the mechanisms underlying the depolarisation is a consequence of inhibition of the M-current that is carried by PIP_2 (phosphatidylinositol 4,5-biphosphate)-gated KCNQ (voltage-gated potassium) channels (Wang et al., 1998; Alexander et al., 2009). These findings indicate that Gq-DREADD signalling and function can vary on the basis of the local signalling machinery expressed by the cell population of interest.

Alexander et al., (2009) also found evidence of Gq-DREADD functionality *in vivo*. Specifically, using local field potential (LFP) recordings from the hippocampus of Gq-DREADD expressing mice, it was found that CNO evoked a dose-dependent increase in gamma power and interneuron firing rate. At a higher dose, (1 and 5 mg/kg) CNO even led to the onset of *status epilepticus* in this experiment. The study concluded that the CNO induced activation of pyramidal cells caused increased interneuron firing that subsequently gave rise to gamma oscillations, and that this mechanism underlies Gq-DREADD function in the hippocampus (Alexander et al., 2009). Hippocampal interneurons are predominantly GABAergic, meaning they mostly mediate inhibitory transmission and modulate the activity of excitatory pyramidal neurons (Danglot et al., 2006). By doing so, they control the excitatory/inhibitory balance in the hippocampus and thus regulate gamma rhythm (Bartos et al., 2007). Gamma oscillations are in the range of 30-90 Hz and are associated with cognitive functions, such as information processing or spatial navigation (Bartos et al., 2007). Gamma and other hippocampal oscillations are introduced more in Chapter 5.

Since the first reports validating the construct and its function, Gq-DREADD has been used successfully for investigating cell function and deconstructing certain behaviours. For example, studies reported that CNO increased neuronal firing of mouse hippocampal neurons expressing a Gq-DREADD (Zou et al., 2016), and depolarised neurons of the dorsal subiculum (Cordella et al., 2018). In other studies of Gq-DREADD, CNO was also reported to have an excitatory effect on hippocampal pyramidal cells (Sudarov et al., 2018; Lopez et al., 2016). At the behavioural level Gq-DREADD mediated activation of hippocampal pyramidal neurons was reported to enhance memory by transforming a sub-threshold event into long term memory (Lopez et al., 2016). Also in the hippocampus a c-Fos promoter driven Gq-DREADD construct was used to create an artificial memory trace based on neuronal activity induced DREADD expression (Garner et al., 2012). The immediate early gene (IEG) c-Fos is used as a marker of neuronal activity (Dragunow et al., 1989). Thus, in the study mentioned above

(Garner et al., 2012), the c-Fos promoter driven Gq-DREADD was expressed in cells where c-Fos expression was induced by exposure to a specific context. In a different study, Gq-DREADD was also expressed in the raphe serotonergic neurons and it was reported that acute activation resulted in antidepressant and increased anxiety related behaviours in an open field and light-dark box (Urban et al., 2016).

DREADDs have also been used successfully in other research areas. For example, Krashes et al., (2011) used Gq-DREADDs to investigate feeding behaviour and found that activating agouti-related protein (AgRP) neurons caused an increase in appetite. This effect was reversed upon deactivation of the neurons by means of absence of CNO induced Gq-DREADD stimulation (Krashes et al., 2011). Outside of the CNS, Gq-DREADD has been used to study hepatocytes function *in vivo* (Li et al., 2013) and to investigate G-protein function in pancreatic β-cells, with evidence showing increased insulin release (Guettier et al., 2009) and prevention of streptozotocin induced diabetes upon chronic activation of Gq-DREADD in β-cells (Jain et al., 2013).

1.3.3 Gi-coupled DREADDs

The hM4Di receptor was modelled alongside its Gq-coupled counterpart in that mutations at homologous residues rendered the wild-type muscarinic receptor no longer responsive to acetylcholine but responsive to CNO instead (Armbruster et al., 2007). The Gi-DREADD was then validated in HEK cells where it was found that CNO activated GIRKs, and in hippocampal cultured cells where CNO activation of Gi-DREADD hyperpolarised the cells and prevented action potential firing (Armbruster et al., 2007).

The underlying mechanism that leads to the inhibitory effect of the Gi-DREADD is not as clear as originally expected. Evidence from early studies indicated that hyperpolarisation and reduction in firing in HEK293 cells and cultured hippocampal neurons came about as a result of CNO binding to the Gi-DREADD to cause GIRK activation (Armbruster et al., 2007). Later research found another potential mechanism. Specifically, it was reported that by targeting a Gi-DREADD to axonal projections from hypothalamus to the midbrain, action potential propagation was not affected in the presence of CNO, as would be expected if hyperpolarisation had occurred and that the behavioural effects arising from the inhibition of this projection were correlated with inhibition of synaptic release rather than somatic hyperpolarisation (Stachniak et al., 2014).

In rat slices and *in vivo*, Gi-DREADD was validated by showing decreased excitability of striatal neurons in response to CNO application (Ferguson et al., 2011). In the same study investigators showed evidence that CNO activation of Gi-DREADD in the VTA decreased dopamine release in nucleus accumbens and reduced sensitivity to food reward. Lastly, the study also found that CNO activated Gi-DREADD decreased amphetamine induced c-fos activation (Ferguson et al., 2011).

Since its function has been validated, the Gi-DREADD had been used extensively to suppress activity in a number of cell types. To name a few examples, Gi-DREADDs have been shown to inactivate mediodorsal thalamic neurons and cause deficits in reversal and working memory (Parnandeau et al., 2013) and to impair fear learning upon suppression of somatostatin positive amygdala neurons (Li et al., 2013). In other instances, Gi-DREADDs have been targeted to serotonin neurons to investigate their role in respiratory and thermal control (Ray et al., 2011). Gi-DREADD activation was also reported to lead to decreased alcohol consumption upon inhibition of nucleus accumbens activity to a similar extent lesions of the

same region were shown to (Cassatero et al., 2014). Inhibitory DREADDs have also been used in rhesus monkeys to disrupt spatial working memory as a result of dorsolateral PFC inhibition (Upright et al., 2018).

In the hippocampus, Gi-DREADD was shown to suppress epileptiform activity upon CNO activation in organotypic slice hippocampal cultures and in newborn dentate gyrus cells (Avaliani et al., 2016, Zhou et al., 2019). Studies have also targeted Gi-DREADDs to the hippocampus to modulate memory. Specifically, a Gi-DREADD inhibited memory in an object location but not object recognition task (Lopez et al., 2016). Similarly, Tuscher et al. (2018) reported that CNO-induced CaMKIIa promoter driven Gi-DREADD activation in the hippocampus, impaired object-in-place performance but not object recognition (Tuscher et al., 2018). Lastly, Gi-DREADD mediated PV-interneuron inhibition was reported to impair social interaction, disrupt pre-pulse inhibition and induce a hyperactive state in the ventral hippocampus (Nguyen et al., 2014; Zou et al., 2016)

1.3.4 DREADD agonists

Until recently, the clozapine metabolite CNO has been the agonist of choice for the majority of studies using DREADD technology. CNO was originally considered suitable as a DREADD agonist based on it being bioavailable in humans and rodents, crosses the BBB, it being pharmacologically inert other than having affinity for DREADDs and it not being back metabolised to clozapine (Armbruster et al., 2007). The original study also provided evidence that shows clozapine has nM affinity for DREADDs and higher than that of CNO itself. Clozapine is an atypical antipsychotic as it blocks both D2 and 5-HT_{2A} receptors with high affinity (Seeman, 2014). Moreover, clozapine is known to have affinity for many other receptor types such as H1 histamine receptor, α2 adrenergic receptor and muscarinic M1 receptors

(Ereshefsky et al., 1989) to name a few. Thus, because of its mixed pharmacological profile, effects of clozapine as DREADD agonist would be difficult to interpret.

The reverse metabolism of CNO to clozapine had been previously reported in guinea pigs (Jann et al., 1994) and in humans (Chang et al., 1998), with little data on the CNO metabolism in rodents. To prevent off-target effects of CNO as a result of its conversion to clozapine and to avoid prolonged effects beyond the experimental window, it was recommended to keep the CNO dose low (0.1-3 mg/kg) (Roth, 2016). Many studies conducted in rat have been using a dose of 3 mg/kg CNO i.p. (Sengupta et al., 2016; Yau & McNally, 2015; Ferguson et al., 2011) but doses of up to 10 mg/kg CNO have been used without any non-specific effects being reported (Mahler et al., 2014).

In a pivotal study, Gomez and colleagues set out to describe the *in vivo* mechanism of CNO acting as a DREADD agonist and made a number of observations. A saturation binding experiment found no CNO but high clozapine binding in DREADD expressing human embryonic kidney (HEK) 293 cells or mouse brain tissue. Similar results were described following [^{3}H]clozapine and [^{3}H]CNO autoradiography using mouse and rat striatum expressing a Gq-DREADD. Furthermore, PET scans from striatal Gq-DREADD expressing rats revealed no CNO brain uptake in contrast to high clozapine uptake after CNO intravenous injection. The study also challenged the pharmacological inertness of CNO (10 µM) and showed evidence of competitive antagonism at a variety of receptors (H1, 5-HT_{2A} M1, M3, M4, D1, D2). Behaviourally, the investigators reported decreased locomotor activity as a result of nucleus accumbens Gi-DREADD activation by both clozapine (0.1 mg/kg) and CNO (10 mg/kg). Lastly, the study suggested the small dose of clozapine (0.1 mg/kg) to be sub-threshold in terms of lowering locomotor activity in naïve animals – in contrast to a higher dose

of clozapine (1 mg/kg) that decreased locomotor activity – and a more suitable DREADD activator that could have clinical therapeutic application (Gomez et al., 2017).

Other reports queried the 'pharmacological inertness' of CNO. A study performed in naïve rats showed that CNO (5 mg/kg but not 1 or 2 mg/kg i.p.) decreased amphetamine-induced dopamine increase and hyperlocomotion, in addition to showing conversion of CNO to clozapine in plasma (MacLaren et al., 2016). Similarly, Raper and colleagues assessed the pharmacokinetic properties of CNO (3 and 10 mg/kg s.c.) in rhesus monkeys and showed clozapine in the plasma and CSF at concentrations capable of activating endogenous serotonergic or dopaminergic receptors (Raper et al., 2017). Another study in monkeys reported a reduction in reaction time in stimulus-reward association tasks as a consequence of CNO administration in 2 of their subjects suggesting off-target effects of the drug (Eldridge et al., 2016). Taken together, the evidence put forward by these studies highlights the importance of employing appropriate controls in DREADD studies and question the mechanisms by which CNO generates its effects. Thus, the current study also addressed this limitation of CNO as a DREADD agonist.

As the potential for back-metabolism of CNO to clozapine has been a limitation in its use as a DREADD agonist and its translation into the clinic, there has been an interest in developing alternative agonists for DREADDs. Evidence from a structure-activity-relationship (SAR) analysis found Compound 21 (C21) to be a potent full agonist at the Gq-DREADD but not the endogenous muscarinic receptor. Perlapine, a commercially available hypnotic was also found to be more than 10 000 times more selective for the mutant hM3Dq compared to the wild type receptor (Chen et al., 2015).

A later study (Thompson et al., 2018), that was only published after the experiments presented in this thesis were initiated, carried out an extensive analysis on the pharmacokinetic and pharmacodynamic properties of Compound 21. Specifically, the study found Compound 21 to be brain permeable, have a good pharmacokinetic profile, and there was no evidence of back-metabolism to clozapine. In addition, Compound 21 was shown to be a potent agonist at modulating both Gi and Gq-DREADD in a rodent feeding model *in vivo* (Thompson et al., 2018).

A recent study carried out an extensive analysis in mice into the pharmacokinetics of clozapine, CNO and Compound 21 (Jendryka et al., 2019). The authors confirmed the back metabolism of CNO to clozapine in mice as reported previously in rats (Gomez et al., 2017, MacLaren et al., 2016). However, they provided evidence showing that while clozapine levels were high in the brain after CNO systemic administration, the majority of clozapine was bound to tissue and unable to activate the DREADDs. Instead, the CNO concentration, while present at lower levels than clozapine, was high enough to activate the DREADDs based on its pharmacokinetics. Additionally, the report found no significant behavioural effects of CNO (3.5 and 10 mg/kg), clozapine (0.1, 0.3, 1 mg/kg) or Compound 21 (0.3, 1 and 3 mg/kg) in a 5-choice serial-reaction-time task measuring a range of parameters including motivation, attention, impulsivity and locomotor activity, compared to animals that received vehicle treatment (Jendryka et al., 2019).

Collectively, these reports support the notion that CNO use has the risk of clozapine reverse-metabolism and non-DREADD mediated effects. However, its effectiveness as a DREADD agonist should not be overlooked with evidence from many studies that have used it successfully until now. As such, experiments in this thesis were predominantly carried out using CNO as an agonist. The reason for this choice was twofold. Firstly, as mentioned above

CNO has been used extensively in the DREADD literature and as long as appropriate controls are in place, CNO is likely to continue to be a suitable chemogenetic ligand. Secondly, pharmacokinetic and pharmacodynamic data of other potential DREADD agonists (i.e., Compound 21, perlapine) have only emerged once experiments in this thesis were already ongoing and validating yet another agonist would have required a well-described model of hippocampal deficit already, which was the overall aim of the thesis. It would be interesting for future experiments to establish the potential of other DREADD ligands in a similar model as presented in this thesis.

1.3.5 Advantages of DREADDs in the hippocampus

A number of features make DREADD technology appealing to neuroscientists. Firstly, and probably most importantly, their appeal lies in their ability to target selectively an array of different cell populations – based on the promotor of choice – in a variety of tissues. Secondly, their use is less invasive, compared to approaches such as optogenetics that require implantation of a fibre optic in the brain for activation. Moreover, light delivery through the optic fibre for prolonged periods of time can lead to over-heating of the brain and subsequent potential tissue damage (Deng et al., 2014). Additionally, in behavioural research or studies where neuronal modulation is required for extended periods of time, such as maze tasks, DREADDs have an advantage compared to optogenetics which typically operates on short time scales (Sternson & Roth, 2014), DREADD activation being dependent on the kinetics of the ligand. CNO is known to peak in the plasma in mice and rats after 30 min (Guettier et al., 2009; Manvich et al., 2018), but behavioural effects were still sustained after 9 hours (Alexander et al., 2009).

To deconstruct hippocampal dependent behaviours, DREADDs have a number of advantages over other approaches that manipulate hippocampal functions. Compared to lesions,

DREADDs allow for the preservation of the hippocampal inputs and outputs, and only transiently inhibit a neuronal population whilst lesions are irreversible and highly non-specific at cell level. Muscimol is a $GABA_A$ receptor agonist that is used in studies of hippocampal function because of its ability to inhibit neuronal activity without affecting fibres of passage (McEown & Treit, 2010). Thus, muscimol infusion would in theory be more similar to DREADD manipulations. However, brain micro-infusions are more invasive than systemic injections, pose the risk of infections and gliosis around the cannula tip/needle track which could cause back-flow of the drug. Moreover, DREADDs carry a fluorescent tag that enables the cell-specific localisation of the constructs *post mortem*, whilst muscimol diffusion is more difficult to assess. In addition, DREADDs are more versatile in that they can be used to both activate and inhibit a neuronal population, which allows for bi-directional control of the same neuronal population (Vardy et al., 2015), such manipulations not being possible by using muscimol infusions or lesions. Lastly, the less invasive nature of DREADD use is a critical aspect for translational application in the clinic (Rogan & Roth, 2011). Collectively, these attributes contribute to the appeal DREADDs have as a tool for deconstructing behaviours.

1.4 The hippocampal formation

The hippocampus has been historically regarded as a 'cognitive map' (O'Keefe & Nadel, 1978) but it is now known that its role expands beyond memory (see below). The hippocampal formation is formed by the granule cells of the dentate gyrus (DG), the pyramidal cells of the cornu Ammonis subfields CA1, CA2 and CA3 and the subiculum (Andersen et al., 2007). Synaptic transmission in the hippocampus happens mostly through the tri-synaptic circuit. **Figure 1.3** shows a schematic illustration and describes the hippocampal tri-synaptic circuit.

Briefly, the highly processed hippocampal multi-sensory input is delivered from neurons in layer II of the entorhinal cortex (EC) to the granule cells of the DG *via* perforant path axonal

projections. The granule cells axons will in turn project through mossy fibres onto dendrites of the CA3 that will innervate CA1 pyramidal neurons through Schaffer collateral-commissural pathway. Schaffer collaterals will then synapse in the subiculum, that is the main hippocampal output and entorhinal cortex (Neves et al., 2008). Besides this tri-synaptic circuit, transmission in the hippocampus happens by recurrent innervation of the CA3 pyramidal cells and by direct innervation of the CA3 and CA1 pyramidal cells by neurons in the entorhinal cortex *via* the perforant path and temporoammonic pathway, respectively (Neves et al., 2008). Stimulation of Schaffer collaterals is used routinely to study evoked field excitatory post-synaptic potentials in the CA1 subfield during slice electrophysiology recordings. This technique has also been used in experiments described in this thesis.

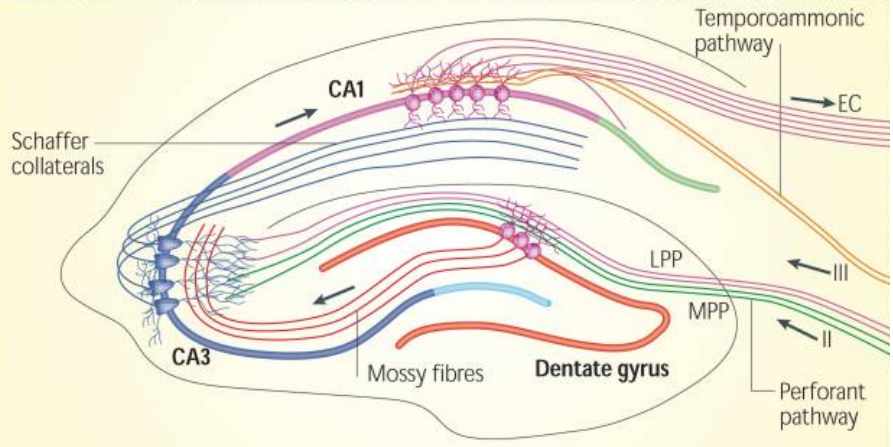


Figure 1.3 Tri-synaptic hippocampal circuit

Schematic representation of the tri-synaptic circuit. Sensory input enters the hippocampus from the entorhinal cortex *via* axons of the perforant path that synapse onto granule cells of the dentate gyrus. Information is then sent through the mossy fibres to the CA3 pyramidal neurons and to CA1 pyramidal neurons through the Schaffer collaterals. Input from the EC also innervates CA1 and CA3 pyramidal neurons through the temporoammonic and perforant path respectively. LPP: lateral perforant pathway, MPP: medial perforant pathway. Image taken from Deng et al., 2010.

However, this is not an exhaustive account of synaptic transmission in the hippocampus as it leaves out the CA2 subfield of the hippocampus, that is now emerging as more than just the anatomical area wedged between CA1 and CA3. The CA2 region receives inputs from the

Schaffer collaterals projecting from the CA3 subfield and targets the CA1 as its main output (Dudek et al., 2016). Anatomically, pyramidal cells in the CA2 have larger cell bodies compared to CA1 pyramidal neurons and lack the CA3 thorny excrescences that are thought to be the receivers of information from the mossy fibres (for review see Dudek et al., 2016). The role of the CA2 region in behaviour has been less studied compared to its neighbours CA1 and CA3 but it is now recognised that CA2 plays a role in different types of memory, such as social memory (Stevenson & Caldwell, 2014; Tzakis & Holahan, 2019).

1.4.1 Hippocampal function

The hippocampus plays a multifaceted role in behaviour, with the dorsal hippocampus being involved in cognitive processes, independent of emotional processing while the ventral hippocampus plays a role in emotionality and is involved in stress responses, anxiety, depression and fear (Gray, 1982; McNaughton & Gray, 2000; Fanselow & Dong, 2010). This knowledge comes mostly from lesion studies that have been an invaluable tool to study hippocampal function *in vivo*. For example, studies in rats with complete hippocampal lesions reported hippocampal dependence in novel object recognition (Clark et al., 2000). However, this is in contrast to reports showing similar performance in sham rats and rats with complete hippocampal lesions in novel object preference tasks (Piterkin et al., 2008). Similarly, it was reported that rats with hippocampal lesions had deficits in contextual fear learning that were not attributed to emotional deficits but were context dependent instead (Kim & Fanselow, 1992). In contrast, later evidence found that the animals can be trained on contextual fear learning task despite hippocampal lesions (Wiltgen et al., 2006) and attribute the ability to learn these tasks to adaptive changes in extra-hippocampal structures.

Further evidence about the function of the hippocampal structure came from the Moser lab, that studied its role in spatial learning along the rostrocaudal axis. Here they found that the

magnitude of spatial learning deficits positively correlated with the amount of dorsal hippocampal tissue that was lesioned (Moser et al., 1995). Specifically, rats that had 20-40% of the hippocampus intact at the dorsal pole showed sham level spatial learning in an open field water maze in contrast to rats that had 20-40% of the hippocampus spared at the ventral pole, that showed learning deficits comparable to rats that had complete hippocampal lesions. Rats that had up to 60% of the hippocampus at the ventral pole spared also displayed learning deficits (Moser et al., 1995). Thus, this report indicated that as little as 20% of the dorsal hippocampus is needed for normal performance on a spatial memory task, while the ventral hippocampus is not involved in this spatial memory domain. These findings are in line with later reports that ventral hippocampal lesions did not impact performance on spatial memory tasks but rather decreased anxiety levels (Bannerman et al., 2002, 2003).

Alternatively, hippocampal function can be studied by modulating afferents that innervate the hippocampal formation. Specifically, GABAergic, glutamatergic and cholinergic (Manseau et al., 2005) neurons of the medial septal-diagonal band of Broca (MSDB) project to the hippocampus and play a role in generating hippocampal theta rhythm (Buzsaki, 2002) (introduced below) and in learning and memory processes (Givens & Olton, 1990). For example, it was shown that by lesioning the medial septal input to the hippocampus rats were no longer able to learn to perform on the Morris water maze (MWM, see below) (McNaughton et al., 2006), a spatial task sensitive to hippocampal lesions (Morris, 1984; Morris et al., 1990). Similarly, a later study reported impaired performance on both a reference and working memory water maze after selective inactivation of GABAergic septal afferents to the hippocampus (Pang et al., 2011).

In terms of interactions with other brain areas the hippocampal-prefrontal connectivity has been of interest because of the role of the mPFC in cognitive processing. Like the

hippocampus, the mPFC is also involved in working memory and higher processes such as decision making, and it is believed that the interactions between the two regions serve as a way of solving complicated tasks (for review see Miller & Cohen, 2001). For example, it was found that the hippocampal-prefrontal synchrony is elevated in a spatial working memory tasks, indicating recruitment of both brain areas (Jones & Wilson, 2005). The ventral CA1 and subiculum regions of the hippocampus innervate the mPFC (Colgin, 2011), and disruption of this connectivity is thought to lead to neuropathologies such as schizophrenia (Godsil et al., 2013).

1.4.2 Behavioural tasks to study hippocampal function

As mentioned earlier, the hippocampus is known to play a role in spatial memory (O'Keefe & Nadel, 1978). Typically, hippocampal spatial memory is assessed in variations of either an open field water maze or in radial mazes (Bannerman et al., 2014). Both tasks provide a measure of spatial reference memory (SRM), also regarded as long-term memory and can be adapted to assess spatial working memory (SWM). SRM is traditionally tested in the Morris water maze (MWM), in which the animals are forced to swim to find a fixed location submerged platform (Morris et al., 1990). Thus, the animal must form spatial cue-platform associations to find the platform and guide itself to safety. The memory component is tested by introducing a probe trial, in which the platform is removed. Animals with no hippocampal deficits are then expected to spend more time in the quadrant where the platform was previously located whereas hippocampal lesioned animals search randomly (Clark et al., 2005).

In SRM memory tasks, the animal is thought to create a 'reference memory' by being trained to follow a set rule trial after trial. SRM can be assessed in radial mazes (Deacon & Rawlins, 2006) and can be adapted to assess SWM. Specifically, the animal is motivated by rewards

and trained to refrain from going into a previously visited arm (i.e. win-shift mazes), or is motivated by spontaneous alternation. For example, in the rewarded alternation T-maze, during the exposure phase, one arm of the maze is blocked and the animal is forced to run out of the start arm and into the open arm to collect the reward. After a delay – an intra trial interval (ITI) – the rat is returned to the start arm and allowed a free choice between the two goal arms. The 'correct' choice is the previously unvisited (novel) arm and it is the only rewarded arm on the choice trial (Deacon & Rawlins, 2006).

An alternative for testing hippocampal-dependent memory is the spatial novelty preference Y-maze task that assesses short-term spatial memory in which the animal is motivated by novelty and exploration and no food deprivation is required. Similarly, to the rewarded alternation T-maze, during the exposure phase the animal is allowed to explore two arms of the maze, but none of the arms are rewarded. The animal is returned to the maze after an ITI and allowed free exploration of all three arms. An animal with no spatial memory deficits is expected to spend significantly more time exploring the previously unvisited arm (novel) (Barkus et al., 2014). In contrast, evidence from rodent lesion studies on this task showed chance performance in mice with hippocampal lesions regardless of the ITI (1 min or 24 h) (Sanderson et al., 2009).

In the two tasks, the memory processes lie within the ITI. For example in the novelty preference Y-maze the ITI represents the short term memory component such that when the animal is returned to the maze it uses prominent spatial cues to solve the task (Barkus et al., 2014). In the rewarded alternation T-maze the ITI, but also the number of test trials given on the maze, form the 'working memory' component, when the animal keeps the information from the previous sample phase at the forefront of its memory and makes its next choice on the basis of previous decisions (Olton et al., 1979). As a result, increasing the ITI duration could

potentially increase the difficulty of the task but it also poses the risk to affect the performance of the control group. In rewarded alternation tasks, the animals are usually tested in blocks. Depending on the number of trials in one block, the memory acquired from a recent trial that is no longer informative can interfere and become counterproductive leading to errors (Deacon & Rawlins, 2006). Thus, increasing the number of trials in a block can subsequently increase the difficulty of the task and the working memory load. Rewarded alternation T-maze task could also be solved on the basis of familiarity (Sanderson & Bannerman, 2012) as opposed to working memory. The concept of short-term habituation and familiarity is discussed more in Chapter 3.

Counterbalancing is an important aspect of experimental design in behavioural studies when a subject is tested on the same task multiple times. For example, in the tasks described above it is important to counterbalance the novel arms in each trial between and within subjects. This is done to ensure that the rats do not have a preference for a specific arm. Usually, time of testing or order of injections are also accounted for as these as well can be factors contributing to behavioural outcomes (Zeelenberg & Pecher, 2014). Generally, in the behavioural studies described in this thesis, drug administration was done following a Latin square design in which each rat received vehicle and all drug doses once.

Ideally, behavioural outcomes are paired with neurophysiological measurements for a well-rounded understanding of the underlying mechanisms that give rise to changes at the behavioural level.

1.5 Brain oscillations and local field potential

As the underlying mechanism of DREADD function in various brain areas and neuronal populations is not fully known, behavioural changes arising from DREADD manipulations should be correlated with physiological measurements for a better understanding of the consequences of neuronal manipulation. As a result, pairing DREADD technology with recordings of electrical activity could offer insights into changes in brain activity resulting from DREADD induced neuronal modulation.

Local field potentials (LFP) are electrical signals recorded in rodents using a glass or metal electrode from the extracellular space of deep brain structures while electrocorticography (ECoG) uses stainless steel electrodes implanted in the skull above the brain region of interest (Buzsaki et al., 2012). Synaptic current is the main contributor to the recorded signal, however, the LFP represents the summation of all voltage fluctuations present in the surrounding tissue, such that any transmembrane ion exchange will contribute to the LFP (Buzsaki et al., 2012). Voltage fluctuations in the LFP and ECoG represent a summation of coordinated neuronal activity that gives rise to rhythmic oscillations at different frequencies. Here, brain oscillations were separated into the following frequency bands: theta (4-10 Hz), beta (10-30 Hz), low gamma (30-50 Hz) and high gamma (50-90 Hz) and high frequency oscillations (HFO; 90-150 Hz).

LFP recordings in rodents can be sustained over extended periods of time (hours to days). Thus, they provide an invaluable tool to assess changes in brain electrical activity with animals in the resting state. Hereinafter resting state will be defined as free movement of animals in a context they have been previously familiarised to such that natural home-cage behaviour in the absence of external stressors or stimuli is achieved. In humans ECoG are also performed

during their resting state, defined as awake stillness to avoid movement related artefacts, which differs from the rodent resting state (Hansen et al., 2019).

1.5.1 Hippocampal oscillations and behaviour

Synchronous neuronal ensemble activity (firing of cell assemblies) gives rise to oscillatory rhythms that are relevant to cognitive processes, such as memory. Neuronal assemblies are a group of neurons that will fire at the same time to contribute to a physiological outcome. For example, it was shown that pyramidal assemblies in the hippocampus fire in synchrony within 25 ms time windows, time that is thought to be essential for hippocampal synaptic plasticity (Harris et al., 2003). Using chemogenetics to manipulate hippocampal-dependent memory and associating changes in behaviour with changes in brain oscillation could provide insight into disorders where brain oscillatory activity is altered.

Each frequency band is generated by a different mechanism and is present during different behaviours (Colgin, 2016). For example, theta rhythms (4-10 Hz) are present during exploratory behaviour with theta power being increased during learning and memory retrieval, in short-term memory tasks (Vertes, 2005) and during rapid-eye movement (REM) sleep (Montgomery et al., 2008) but absent during periods of immobility (Buzsaki, 2002).

Enhanced cortical and basal ganglia oscillations in the beta range (10-30 Hz) are a neuropathological hallmark of Parkinson's disease (PD) and correlated with bradykinesia in patients (McCarthy et al., 2011; Little & Brown, 2014). The functional role of beta oscillations in PD is thought to be the conservation of the current movement pattern, maintenance of the '*status quo*' (Engel & Fries, 2010). Increased beta oscillations have been reported in the rat

hippocampus in a go/no-go odour discrimination task during odour sampling, suggesting the involvement of dorsal hippocampus in odour-discrimination learning (Martin et al., 2007).

Finally, gamma oscillations (30-90 Hz) are known to be involved in learning and memory processes with evidence from human studies showing increased gamma power during the ITI of a working memory task where gamma power was positively correlated with memory load (Howard et al., 2003). Failure in gamma regulation is a marker of neurological disorders and is thought to be at the root of cognitive deficits in schizophrenia (Gandal et al., 2012).

1.6 Aim of the thesis

Experiments described in this thesis aimed to capitalise on the potential of DREADD technology as tools to deconstruct cortical and subcortical mechanisms of cognition and at the same time evaluate their suitability for use in the rat hippocampus. Ultimately, by using DREADDs to manipulate hippocampal function, one could assess pro-cognitive effects of certain compounds. An interesting category of drugs to study in this model would have been the 5-HT_6 agonists and antagonists that were both, paradoxically, shown to cause pro-cognitive effects in models of hippocampal deficits (Woods et al., 20012). As the level of 5-HT_6 receptors in mouse is lower than in rats and has distinct pharmacology than the human and rat receptor (Hirst et al., 2003), the rat was a better animal model to study the mechanisms underlying the pro-cognitive effects of 5-HT_6 ligands. However, because of a lack of a detectable hippocampal impairment in the model presented in this thesis, experiments described below did not address this question but used the rat as an animal model nonetheless. Table 1.1 summarises the relevant DREADD studies that served as a framework for experiments in this thesis.

Reference	Main findings	Implications for the thesis
Armbruster et al., 2007	• First study to describe the development of DREADDs • First study to propose CNO as an otherwise pharmacologically inert DREADD agonist • Reported that clozapine has 100 times higher affinity than CNO to the DREADDs • Proposed Gi-DREADD mechanism *via* GIRKs and subsequent hyperpolarisation • Propsed Gq-DREADD mechanism as PLC-dependent and leading to increased intracellular calcium	• The study served as reference for the majority of DREADD literature • The reported clozapine affinity for DREADDs led to the design of electrophysiology experiments in Chapter 2 that assess direct functionality of clozapine at the DREADDs
Alexander et al., 2009	• Proof-of-concept study for Gq-DREADD in mouse glutamatergic hippocampal cells • The study reported depolarisation induced by CNO in hippocampal slices • *In vivo* CNO administration led to increased gamma power and epileptic seizures at a higher dose	• The study informed the hypothesis in Chapter 2, that CNO bath application will increase excitatory transmission in Gq-DREADD expressing slices • The study also informed the hypothesis in Chapter 5 that CNO administration will lead to decreased gamma power in Gi-DREADD rats and increased gamma power in Gq-DREADD rats
Lopez et al., 2016	• The study highlights the importance of the promoter of choice in DREADD studies • They report that using a pan-neuronal promoter (hSyn) in the hippocampus leads to opposite effects than expected in slice electrophysiology experiments (decreased excitatory transmission in Gq-DREADD expressing slices and increased excitatory transmission in Gi-DREADD expressing slices) • They suggest that this effect is attributed to the DREADDs being expressed in hippocampal interneurons • The study shows that using CaMKIIa promoter driven DREADDs leads to the expected outcomes (increased excitatory transmission in Gq-DREADD slices and decreased excitatory transmission in Gi-DREADD slices)	• Experiments in this study confirmed the decision of using a CaMKIIa promoter instead of a non-specific neuronal promoter for the DREADDs • The study served as the basis of the electrophysiology experiments described in Chapter 2 • The study informed the hypothesis that CNO bath application will lead to decreased fEPSP slope in Gi-DREADD expressing slices and the opposite effect was predicted in Gq-DREADD expressing slices

Gomez et al., 2017	• First study to propose clozapine as DREADD activator instead of CNO • Showed evidence for back-metabolism of CNO to clozapine in rats and mice • Showed evidence for lack of BBB penetration by CNO • Showed evidence of *in vivo* clozapine function as an agonist at the DREADDs at sub-threshold doses (0.1 mg/kg in rats)	• This report led to experiments in Chapter 3 to test clozapine instead of CNO as DREADD agonist in behavioural studies • The report prompted the re-evaluation of CNO as brain penetrant and led to the design of the exposure study in Chapter 4

Table 1.1: Relevant DREADD studies used to design experiments in this thesis

Representative citations that helped shape the hypotheses used in the experimental chapters of this thesis, their main findings and the implication for the thesis. GIRK: inward rectifying potassium channels, PLC: phospholipase C, fEPSP: field excitatory postsynaptic potential, BBB: blood-brain barrier.

Firstly, experiments in Chapter 2 aimed to interrogate the functionality of an excitatory and inhibitory DREADD in the rat hippocampus. As a result, a protocol for the delivery of the viral constructs to the dorsal hippocampus was developed to assess the DREADDs' spatial resolution and confirm their specificity in the pyramidal neurons by using a combination of stereotaxic intracerebral injection, immunohistochemistry and fluorescent *in situ* hybridisation. Next, the functionality of the constructs was examined in the presence of their agonists, CNO and clozapine, using multi-electrode array slice electrophysiology. Experiments in Chapter 3 aimed to assess the ability of DREADDs to modulate hippocampal-dependent behaviour in a working memory task and also a spatial memory task. Further, the aim of the experiments in Chapter 4 was to build on the *in vivo* results in the previous chapter and assess DREADD function in the context of neuronal activation using a c-Fos approach. Additionally, an exposure study was undertaken to investigate the bioavailability of CNO and clozapine in the rat brain and plasma. Lastly, the final chapter aimed to incorporate the knowledge of the previous chapters and re-assess DREADD functionality *in vivo* in hippocampal-dependent behavioural tasks and to investigate the impact of excitatory transmission manipulation on brain oscillations using LFP and ECoG recordings.

Chapter 2

Development of chemogenetic protocols to manipulate hippocampal function

2.1 Introduction

The hippocampus is known to be involved in cognitive processes such as learning and episodic memory (Bird & Burgess, 2008). The function of the hippocampus has been extensively studied in rodents, with early electrophysiological experiments from the lab of O'Keefe and Dostrovsky that discovered place cells that were firing when the animal was in a certain location, indicating the hippocampus as a spatial map (O'Keefe & Dostrovsky, 1971). However, besides the role the hippocampus plays in spatial and non-spatial memory it is now known that its role expands beyond memory altogether, for example in anxiety (Gray, 1982; McNaughton & Gray, 2000), as evidence from experiments involving lesions to ventral hippocampus show (Bannerman et al., 2003). As another example, a role for the hippocampus in a context independent memory task was evident in experiments showing that intra-hippocampal administration of the inhibitory agent muscimol disrupted object memory recognition (Cohen et al., 2013). Thus, the hippocampus plays a multifaceted role in emotional and cognitive processing as revealed by various techniques and tools aimed to disrupt hippocampal function.

2.1.1 Tools to inhibit hippocampal function

Lesion studies have been widely used to investigate hippocampal function. While these studies have provided valuable insights into the role of the hippocampus, they do not always reveal information on underlying mechanisms. For example, studies in rats with complete hippocampal lesions have been contradictory in terms of hippocampal dependence in novel object recognition with evidence from studies showing hippocampal importance in recognition

memory (albeit delay-dependent) (Clark et al., 2000) in contrast to reports showing similar performance to sham rats in novel object preference tasks (Piterkin et al., 2008). Contradictory studies from lesion studies about hippocampal dependence in contextual fear learning have also been reported (Wiltgen et al., 2006; Phillips & LeDoux, 1992). The ability to learn these tasks was most likely attributed to adaptive changes in extra-hippocampal structures compensating for the loss of hippocampal function. Other drawbacks of lesions include that they are invasive, do not discriminate between cell types, and cause non-reversible and permanent damage. Thus, researchers have explored ways to modulate hippocampal activity in a more refined manner, for example by using intra-hippocampal administration of the sodium channel blockers tetrodotoxin or lidocaine that cause a temporary deficit. Still, their use is limited by the fact that they do not target specific cell types and they disrupt axonal projections such that it can lead to a misattribution of cognitive processing and do not necessarily give a real measure of hippocampal activity (Fozzard et al., 2005).

Intra-hippocampal administration of the inhibitory agent muscimol, a $GABA_A$ agonist has been used extensively in hippocampal research because it causes a transient inhibition of the hippocampus (Mao & Robinson, 1998). However, with this approach it is unclear how large a deficit in hippocampal function is required to produce a behavioural effect. For example, some studies reported that only 1% of the volume of dorsal hippocampus is required to disrupt object recognition (Cohen et al., 2013), or ‘no more than 1 mm radius’ from the muscimol infusion site to inhibit context-dependent fear learning (Holt & Maren, 1999). In contrast, lesion studies report that object recognition is impaired only when more than 75% of the hippocampus is lesioned (Ainge et al., 2006; Broadbent et al., 2004).

Optogenetics, a more recently applied technique, has the ability to inhibit specific neuronal populations, including in the hippocampus (Hannapel et al., 2019; Kovács et al., 2016;

Sakaguchi et al., 2015). Optogenetics utilises genetically encoded light-sensitive ion channels or pumps called opsins such that neurons are activated by light stimulation (Boyden et al., 2005; Chow et al., 2010; Zemelman et al., 2002). For example, in the case of the chloride pump (e.g. NpHR, halorhodopsin being one of the most commonly used), cell silencing is achieved by the hyperpolarisation of the cell as a consequence of chloride entering the cell upon light activation of the ion pump (Guru et al., 2015).

This approach has high spatiotemporal resolution, enabling cell-specific manipulation of a restricted population of neurons. While optogenetics has been used extensively to understand the relationships between neuronal circuitry and behaviour (Bernstein & Boyden, 2011; Liu et al., 2012), light stimulation is generally applied for short periods of time which can be a hindrance in longer-lasting behavioural paradigms. Light is typically applied over short intervals since extended light delivery can lead to warming of the brain and potential damage. A recent study has shown that sustained light delivery to the brain tissue can increase brain temperature by 0.2-2ºC, and cause behavioural effects and changes in neural activity in the absence of opsins, which can lead to false positive findings (Owen et al., 2019). Finally, the optogenetic approach requires tethering of the animal and is invasive in that it requires the implantation of an optical fibre into the brain to ensure appropriate light delivery in deeper brain structures (Boyden, 2011).

2.1.2 Chemogenetic manipulation of neural activity

Chemogenetics is a technology that is based on the same principle as optogenetics, but it uses an exogenous ligand instead of light to activate specific neuron populations with receptor transfections. The technology involves targeting neurons with modified G-protein coupled receptors, also known as Designer Receptors Exclusively Activated by Designer Drugs, often abbreviated as DREADDs (for reviews see Rogan & Roth, 2011; Sternson & Roth, 2014; Zhu

& Roth, 2014). DREADDs are mutated human muscarinic receptors that are no longer responsive to their endogenous agonist, acetylcholine, but are activated upon binding of clozapine-N-oxide (CNO), a metabolite of clozapine. The most common DREADDs used in the experiments described in this thesis were Gi (hM4Di) and Gq (hM3Dq) coupled. Upon CNO binding to the hM4Di, cAMP levels decrease causing inhibition of transmission (Stachniak et al., 2014). Another proposed mechanism of inhibitory DREADDs is through the activation of the inward rectifying potassium channels (GIRKs) and hyperpolarisation resulting in cell silencing (Armbruster et al., 2007). To achieve neuronal excitation, CNO binds to the hM3Dq receptor causing activation of the phospholipase C (PLC) signalling cascade and leading to an increase in intracellular calcium that activates the cell (Armbruster et al., 2007).

Typically, DREADDs are virally delivered by adeno-associated viruses (AAVs), that cause a very minor immune response and are well tolerated *in vivo* (Miyake et al., 2011). The combination of the virus with the mutated muscarinic receptor coupled to a promoter and tagged by a fluorophore allows for cell-specific transgene expression when injected intracerebrally through stereotaxic surgery in the brain region of interest. CNO systemic administration (often intra-peritoneal injection) acts as a 'trigger' for the DREADDs, thus enabling transient cell-specific manipulation which have made DREADDs a very attractive tool in neuroscience research (Roth, 2016; Smith et al., 2016).

2.1.3 Use of chemogenetics to target the hippocampus

The aim of the current study was to study the effects of chemogenetic manipulation of hippocampal transmission on cognition. In a previous study, Alexander and colleagues showed CNO-induced depolarisation in mouse hippocampal cells expressing a CaMKIIa promoter driven excitatory DREADD. Furthermore, *in vivo*, they observed increased firing of hippocampal principal cells, hyperlocomotion and seizure-like behaviours (Alexander et al.,

2009). More recent studies have investigated the effect of Gi-DREADD transfection in organotypic slice hippocampal cultures and in newborn dentate gyrus cells on epileptic activity. These studies reported suppression of epileptiform activity in both models upon CNO induced Gi-DREADD activation (Avaliani et al., 2016; Zhou et al., 2019). Recently, Aitta-Aho et al. (2019) used CaMKIIa promoter driven Gi-DREADD expression in hippocampus and observed a CNO-induced decrease in hyperlocomotion in *Gria1-/-* mice (AMPA deficient GluA1 subunit mice) with no effect in wild type controls (Aitta-Aho et al., 2019). Studies have also reported the use of DREADDs to positively or negatively modulate long term memory. Specifically, an excitatory DREADD was used to transform a sub-threshold learning event to long-term memory in an object location, but not a recognition task. In contrast, an inhibitory DREADD blocked long-term memory for object location but not object recognition (López et al., 2016). Similarly, Tuscher et al. (2018) reported that CNO-induced CaMKIIa-Gi-DREADD activation of the hippocampus impaired object-in-place memory, but not object recognition (Tuscher et al., 2018). CNO-induced activation of an inhibitory DREADD was also shown to block recent, but not distant, contextual fear memory (Varela et al., 2016). Other groups have used DREADDs to manipulate hippocampal CA2 transmission. Boehringer et al. (2017) used a transgenic mouse line that specifically expressed Cre in the pyramidal neurons of the CA2 region. By bilaterally injecting a Cre-dependent Gi-DREADD, they reported increased spatial concentration of pyramidal cell spiking during locomotion upon CA2 pyramidal cell activity blockade by CNO (Boehringer et al., 2017). In a different transgenic mouse model, both CA2 activity increase and suppression during training was found to increase freezing in a context dependent fear task in female mice (Alexander et al., 2019). Finally, DREADDs have also served as a useful tool in targeting hippocampal interneurons in a Cre-dependent manner to investigate schizophrenia-like behaviours. CNO-induced PV-interneuron activation was reported to impair social interaction (Zou et al., 2016), while Gi-DREADD mediated PV-interneuron inhibition was reported to disrupt pre-pulse inhibition and induce a hyperactive state in the ventral hippocampus (Nguyen et al., 2014).

Although DREADD technology has been utilised for more than a decade, there are few studies in the literature that have used this approach to investigate the effects of manipulating hippocampal function in relation to cognitive processes. Moreover, there has been no study to date that validated the correct targeting of CaMKIIa-driven DREADD constructs in rat hippocampus, nor established that the constructs are functional in the way expected of their analogous endogenous GPCRs. Although Gi-DREADD-induced silencing is often considered as being mediated by activation of GIRKs, the levels of GIRK expression is cell-type specific, which could lead to different effects based on the type of cell and brain area in which the DREADDs are expressed (Rogan & Roth, 2011). This highlights the importance of assessing the functionality of DREADDs in the desired neuronal population in order to correctly interpret any behavioural phenotypes that are generated.

2.1.4 CNO as a DREADD activator

At the outset, it was thought that CNO targeted DREADDs, but was otherwise pharmacologically inert, readily crossed the blood brain barrier (BBB) and was not metabolised back to clozapine in rodents (Armbruster et al., 2007). However, while experiments described in this thesis were ongoing, the role of CNO as a selective DREADD activator came into question. Specifically, a study by Gomez et al., (2017) reported evidence that in rodents CNO poorly entered the brain and, that after systemic injection, it is back-metabolised to clozapine that subsequently enters the brain and binds with high affinity and potency to neuron-expressing DREADDs. Furthermore, it was reported that behavioural effects of CNO in mice and rats were caused by clozapine binding to DREADDs (Gomez et al., 2017). Other recent papers reported similar findings in non-human primates (Raper et al., 2017) and rats (MacLaren et al., 2016). Since then, more investigation has been done to understand the mechanism of clozapine-induced DREADD activation (Jendryka et al., 2019) and investigate

other potent DREADD agonists (Thompson et al., 2018). However, the functionality of clozapine as a DREADD agonist has not yet been confirmed.

2.1.5 Chapter 2 experimental aims

Experiments in this chapter were aimed to establish a protocol for successful delivery of two types of DREADDs to excitatory neurons in the rat dorsal hippocampus. Once this was achieved, the specificity of transfection of the viral constructs had to be confirmed. The second part of the chapter aimed to confirm the functionality of an excitatory, inhibitory and control construct in an *ex vivo* rat hippocampal slice electrophysiological model upon CNO and clozapine bath application. Follow-up experiments were undertaken for a better understanding of Gq-coupled signalling in the context of excitatory transmission in the hippocampus.

2.2 Materials and methods

Slice electrophysiology and *in situ* hybridisation experiments described in this chapter were carried out at H. Lundbeck A/S while immunohistochemical experiments were done at the University of Oxford.

2.2.1 Animals

All experimental procedures, housing and care were carried out in accordance with the Danish legislation regulating animal experiments; Law and Order on Animal experiments; Act No. 474 of 15/05/2014 and Order No. 12 of 07/01/2016, and with the specific license for these experiments issued by the National Authority. All experiments performed at the University of Oxford were in compliance with the UK Home Office Animals (Scientific Procedures) Act of 1986, and a Local Ethical Review Committee at the University of Oxford.

Male Lister Hooded rats were used in all experiments described in this thesis as this was the model used in our lab for behavioural tasks. Pigmented rats are known to have better vision compared to albino strains (Prusky et al., 2002), suggesting that Lister Hooded rats could be a preferred strain in behavioural tasks where visual spatial cues are present (Broersen & Uylings, 1999). Rats were generally group-housed at the University of Oxford and singly housed for experiments at H Lundbeck A/S, unless stated otherwise. Rats that took part in behavioural tasks were group-housed, because they were kept alive for longer periods of time (i.e. 2-4 months), with the exception of rats that had had electrode implants for rsECoG/LFP studies, as there was the risk of them pulling each other's implants out (Chapter 5). Rats were individually house for slice electrophysiology after viral injection as the duration between the time the rats had recovered from surgery and experimental day when they were culled was typically short (2-4 weeks).

Male Lister Hooded rats (Charles River, Germany or Harlan Laboratories, Bicester, UK), weighing between 250-300g on arrival were kept under environmentally controlled temperature (20 ± 2ºC) and humidity (50 ± 20%) with *ad libitum* access to food and water. Rats were group-housed until the viral injections, after which they were separated and either housed individually until the end of the experiment or paired with a littermate (experiments performed at the University of Oxford and follow up slice electrophysiology experiments at H. Lundbeck A/S). Rats were housed in open Makrolon polycarbonate cages with a wire lid (at both facilities) and kept in a ventilated scantainer (at H. Lundbeck A/S) in a 12h light/dark cycle (lights on at 06:00 and at 07:00 at the University of Oxford). Sawdust was used as bedding and cages were environmentally enriched with wooden chew blocks, a polycarbonate rectangular house (Rat Retreats™, Bio-Serv, Flemington, NJ, USA) or a cardboard house (University of Oxford).

2.2.2 Viral constructs

For all the experiments performed at H. Lundbeck A/S, the viral constructs were purchased from the Viral Vector Facility (VVF) of the Neuroscience Centre Zurich (ZNZ). Details about the viral constructs used to produce the experiments described in this thesis can be found in the table below (**Table 2.1**). For the immunohistochemical experiments performed at the University of Oxford, the viral construct AAV5-CaMKIIa-hM4D(Gi)-mCherry (titer approx. 3 x 10^{12} vg/mL) was obtained from UNC Vector Core (University of North Carolina), having been originally created by Bryan Roth.

Name	Abbreviation	Description	Identifier	Titre (vector genomes /ml)
ssAAV-5/2-CaMKIIa-hM3D(Gq)_mCherry-WPRE-hGHp(A)	Gq-DREADD	Pyramidal excitatory DREADD	V96-5	4.7 x 10^{12} vg/ml
ssAAV-5/2-CaMKIIa-hM4D(Gi)_mCherry-WPRE-hGHp(A)	Gi-DREADD	Pyramidal inhibitory DREADD	V102-5	7.3 x 10^{12} vg/ml
ssAAV-5/2-CaMKIIa-EGFP-WPRE-hGHp(A)	EGFP-control	Pyramidal control construct	V113-5	7.5 x 10^{12} vg/ml
ssAAV-5/2-hDlx-HBB-chl-HA_hM3d(Gq)_2A_NLS_ dTomato_WPRE_SV40p(A)	hDlx-Gq-DREADD	Interneuronal excitatory DREADD	V128-5	3.8 x 10^{12} vg/ml

Table 2.1: Viral constructs used at H.Lundbeck A/S. Purchased from Viral Vector Facility (VVF) of the Neuroscience Centre Zurich (ZNZ)

2.2.3 Intracerebral viral injections

For surgeries performed at H. Lundbeck A/S, rats were housed in the surgery suite at least 24h prior to the surgery. Anaesthesia was induced with 4% isoflurane (0.3 L/min oxygen and 0.7 L/min nitrous oxide) and maintained with 1-2% isoflurane for the duration of the surgery (0.3 L/min oxygen and 0.7 L/min nitrous oxide). Once anaesthesia was induced, the scalp was shaved, and the rat was placed in the stereotaxic frame (Kopf Instruments). Eye gel was applied (Neutral Ophtha Eye Gel, Teva Pharmaceuticals) to prevent dryness and the scalp was sterilised prior to injection of the local anaesthetic (2 mg/kg s.c., Marcain Polyamp Steripack 0.5% AstraZeneca, UK). The temperature of the rat was kept constant at 37 ºC using a homeothermic heating blanket. The skull was exposed through a small incision made in the scalp, and two small holes per hemisphere were drilled above the dorsal hippocampus using coordinates from the Rat Brain Atlas (Paxinos and Watson, 2007). A total of 6 injection sites

(**Figure 2.1**) was used for the delivery of the viral construct to the CA1 and CA3 regions of the dorsal hippocampus (from bregma):

i, ii) AP -3.6 mm, ML ±3 mm, DV -3 mm (from brain surface)

iii, iv) AP -3.6 mm, ML ±3 mm, DV -2.2 mm (from brain surface)

v, vi) AP -3.6 mm, ML ± 2 mm, DV -2.2 mm (from brain surface)

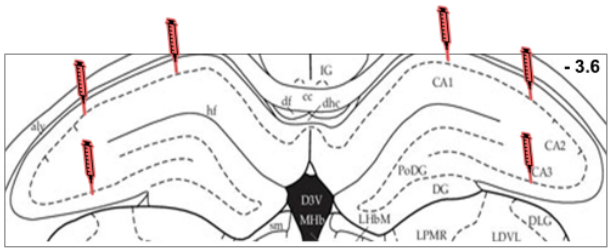


Figure 2.1: Schematic illustration (Paxinos and Watson, 2007) of the stereotaxic injection sites used for viral delivery of DREADDs to the dorsal hippocampus (AP:-3.6 mm from bregma)

Viral construct (330 nl) was injected at a rate of 200 nl/min using a 5 µl Hamilton syringe (75 RN, 700 series, VWR International) with a 26 gauge blunt needle (51 mm, tip style 3, VWR International) fixed to the arm of an injection pump (Stoelting Co., USA). The needle was kept in place for 3-5 min after the injection to prevent backflow of the viral construct. The scalp was then sutured and the rat was administered 1 ml of sterile saline solution (s.c.), an antibiotic (150 mg/kg, Noromox Prolongatum Vet., ScanVet, Fredensborg, Denmark) and a non-steroidal anti-inflammatory drug (NSAID) (5 mg/kg s.c., Norodyl (carprofen), Scan Vet, Fredensborg, Denmark). After the surgery rats were returned to a clean cage and placed under a heating lamp for a minimum of 2 h. Recovering rats were monitored, weighed and administered post-operative care daily for 5 consecutive days post-surgery.

Surgeries performed at the University of Oxford followed a similar protocol and the same coordinates were used. Here, the rats were brought to a temporary holding room at least 1 h prior to the surgery and returned to the main holding room once they have recovered for at

least 2 h in a heated cabinet. Peri-operative care included administration of a local anaesthetic (2 mg/kg s.c., Marcain Polyamp Steripack 0.5% AstraZeneca, UK), 1 ml of sterile glucose saline solution (s.c.), 1 mg/kg, s.c. metacam (Boehringer Ingelheim Vetmedica, Germany) and 0.03 mg/kg, s.c. vetergesic (Ceva Animal Health, France), but no antibiotics.

2.2.4 Immunohistochemistry

Confirmation of expression of the viral construct, either mCherry or EGFP tagged, was assessed post hoc for each experiment following transcardial perfusion and collection of the brain for immunohistochemical analysis. The extent of construct spread was visualised by either epifluorescence or confocal microscopy. The specificity of the CaMKIIa promoter driven viral constructs was assessed by double labelling with a CaMKIIa antibody. The specificity of this antibody has been characterised previously in a study that aimed to validate the specificity of a CaMKIIa-driven AAV construct to pyramidal neurons in the mPFC of rats (Wu et al., 2015), and a more recent one where the investigators targeted a CaMKIIa-driven Gq-DREADD to glutamatergic neurons in the motor cortex of rats (Hu et al., 2019). Both studies showed high specificity of the antibody in glutamatergic cells in rats.

Perfused brains from rats expressing a Gi-DREADD were collected 2-3 weeks after the viral injection to allow for expression of the construct and kept in PFA 4% overnight at 4ºC. Brains were then transferred into a 30% sucrose solution and stored at 4ºC until they were ready for sectioning. Coronal sections (30 µm) of dorsal hippocampus were cut on a cryostat at -20ºC and collected in PBS for storage at 4ºC. Free-floating sections were then washed 3 times (10 min) in PBS, followed by 10 min in 50 mM ammonium chloride to quench free aldehyde groups and reduce autofluorescence. The sections were then washed 3 more times in PBS containing 0.3% Triton-X (PBS-X) and blocked to avoid non-specific binding for 1 h in PBS-X with 10% donkey serum at room temperature. All steps in this protocol were done with gentle agitation,

except for the primary antibody incubation that took place at 4ºC. Sections were incubated overnight with a monoclonal anti-CaMKIIa antibody raised in mouse (Sigma-Aldrich) diluted 1:100 in PBS-X with 2% donkey serum. The following day, the sections were washed 3 times in PBS (10 min) and then incubated for 1 h in a donkey anti-mouse Alexa Fluor 647 (1:500, Invitrogen, UK) secondary antibody in PBS-X and 2% donkey serum. Finally, sections were washed once in PBS-X followed by PBS and then mounted and cover-slipped with Vectashield (Vector Labs, USA). Controls used for the immunolabeling included slices without primary antibody and slices without the secondary antibody. Colocalisation of CaMKIIa labelling with mCherry expressing cells was visualised using an epifluorescent microscope (DM-500B, Leica Microsystems, Wetzlar, Germany) to confirm the expression of the viral construct in the cell population of choice. Acquired images were exported into Image J (NIH) for further processing.

2.2.5 Fluorescence *in situ* hybridisation

Fluorescence *in situ* hybridisation (FISH) was performed by Kirsten Jørgensen and Pia Møller Carstensen under the guidance of Dr. Camilla Stampe Jensen. The oligonucleotide probes were designed specifically to hybridise the mRNA from the protein of interest (here, GAD1 and mCherry). FISH is based on genetic sequences recognising mRNA which makes it highly specific. The GAD1 marker has been previously validated in-house, so no controls were used in this case. FISH was used to verify whether there was off-target expression of the CaMKIIa promoter driven constructs in interneurons. This was achieved by labelling a pan-GABAergic interneuronal marker, GAD1. The GAD1 labelling was used to check whether the CaMKIIa promoter was indeed specific to pyramidal neurons and it did not transfect interneurons. For this purpose, rats were injected in one hemisphere of the dorsal hippocampus (as described above) with a Gi or Gq-DREADD, and a control construct (EGFP) was injected in the contralateral hemisphere to minimise the number of animals used. As a functioning EGFP probe was not available, only mCherry and GAD1 probes were used.

Rats were killed by guillotine 2-3 weeks after the viral injection. Brains were quickly dissected and snap frozen on blended dry ice. Coronal sections (12 µm) were cut on a cryostat at -20ºC and every other section was collected. Collection of the sections was done between approximately AP -3.1 and -4.1 mm from bregma around the site of injection.

FISH was performed using ViewRNA ISH Tissue, 2-Plex Assay Kit 96 assay (Affymetrix, Santa Clara, USA) to assess the qualitative expression of the CaMKIIa promoter driven mCherry tagged constructs (Type 1, Fast Red probe) in GAD1 expressing interneurons (Type 6, Fast Blue). Brain sections (two sections mounted per microscope slide) were fixed in PFA 4% overnight at 4ºC. The following day sections were washed twice in PBS (1 min) and dehydrated in increasing concentrations of alcohol: 50%, 70%, 96%, 99% (10 min each). The slides were left to dry and heated to 40ºC by the ThermoBrite system (Abbott). Incubations were made in the ThermoBrite system at 40ºC, unless stated otherwise. Next, the sections were incubated with Protease QF 1:100 for 30 min. Prior to hybridisation, sections were washed consecutively in PBS (1 min), PFA 4% (5 min) and PBS again twice (3 min). For the hybridisation, the sections were incubated with 400 µl of the Probe Set Diluent containing 10 µl of each of the two probe sets (Type 1 and Type 6) overnight. Sections were washed in the corresponding washing buffer after each incubation. The sections were then incubated in PreAmplifier Mix QT for 30 min followed by 15 min incubations with Amplifier Mix QT. Label Probe 6 – alkaline phosphatase (AP) solution in dilution of 1:1000 with Label Probe Diluent QF was added to the sections for 1 h, followed by Fast Blue substrate for 45 min at room temperature (RT) in the dark. AP Stop QF was then added for 30 min before incubating the sections with Label Probe 1-AP solution in dilution of 1:1000 with Label Probe Diluent QF for 1 hour at 40ºC. AP Enhancer was added for 5 min at RT followed by Fast Red substrate for 30 min. Finally, after a series of washes with PBS (1 min), PFA 4% (5 min), PBS (1 min) and dH_2O, Hematoxylin (15 s at RT) and Hoechst (0.6 µl/ml, 3 min) were added as a counterstain.

Finally, sections were washed once more in PBS and dH_2O and cover-slipped using CC/Mount (Sigma-Aldrich).

To visualise the signals of hybridised mRNA and check for GAD1/mCherry co-labelling, confocal images were acquired (Nikon Eclipse Ti confocal microscope) using the Volocity software (PerkinElmer, USA). Three z-slices (0.2 µm step size) images were taken and 4 x 4 fields with 20% overlap were stitched in Volocity where contrast was enhanced using the same settings for all the images captured.

For quantification, colour images were acquired from the CA1 pyramidal region and DG hilar region under a brightfield microscope using 40X magnification. Images were exported into Image J (NIH) and the number of GAD1 positive cells was counted. Next, the number of GAD1 cells also expressing mCherry were counted and an average percentage of co-expression was calculated. In the CA1 region counting was restricted to the pyramidal layer. For the DG hilar quantification, cells were only counted outside the DG granule cell layer.

2.2.6 Hippocampal *ex vivo* electrophysiology

Once successful hippocampal transfection of the DREADDs was confirmed, DREADD functionality was characterised by means of multi-electrode array (MEA) recordings *ex vivo*. The aim of these experiments was to assess whether excitatory synaptic transmission was altered in Gi and Gq-DREADD expressing rat hippocampal slices upon CNO or clozapine bath application. Briefly, field excitatory post-synaptic potentials (fEPSPs) were evoked in the CA1 area of the dorsal hippocampus upon stimulation of Shaffer collaterals.

Rats were decapitated by guillotine 2-3 weeks post bilateral viral injection. The brain was extracted and immediately collected in ice cold 'slicing' solution made up of the following concentrations: NMDG (100 mM), 37% w/v HCl (100 mM), NaCl (26 mM), KCl (2.5 mM), NaH_2PO_4 (1.24 mM), $CaCl_2$ (1 mM), $MgCl_2$ (3 mM), $NaHCO_3$ (26.2 mM), glucose (10mM), kynurenic acid (2 mM), L-ascorbic acid/Na pyruvate (0.3/1 mM). Cutting solution was kept at a physiological pH by carbogen, a mixture of 95% O_2/5% CO_2 prior to brain collection. Upon collection, the brain was quickly dissected on a cell culture dish placed on ice and covered by filter paper (Munktell, 90mm diameter). The cerebellum and frontal cortex were cut out by single edge blades (Fischer Scientific) and the rest of the brain was carefully transferred and glued onto the steel platform inside the slicing chamber. The chamber was filled with cutting solution that was kept cold by ice and a carbogenator was introduced to the bath to keep the pH constant. Whole brain coronal slices (350 µm) from rats expressing one of Gi-DREADD, Gq-DREADD or EGFP-control constructs were cut by a vibratome (Leica VT 1200S) at a speed of 0.08 mm/s. The two dorsal hippocampi were separated and trimmed from the rest of the tissue using a carbon steel blade scalpel (Swann-Morton, handle 3) and gently transferred with the help of a pipette to the well of a 200 mL BSK1 submerged slice chamber with a carbogenator rock (Scientific Systems Design Inc, Mississauga, Canada). The slice chamber was filled up with artificial cerebrospinal fluid (aCSF) containing the following: NaCl (124 mM), $NaHCO_3$ (25 mM), NaH_2PO_4 (1 mM), KCl (4.4 mM), $MgCl_2$ (1.3 mM), $CaCl_2$ (2.5 mM), glucose (10 mM), L-ascorbic acid/Na pyruvate (0.3/1 mM). Cutting and aCSF solutions were prepared with Sigma-Aldrich reagents. Slices were kept under these conditions at room temperature or at least 1 h before the beginning of the recordings.

Three parallel set-ups of the MEA60 electrophysiological suite (Multi Channel Systems, Reutlingen, Germany) connected to two PCs were used to record fEPSPs. In order to do so, a hippocampal slice was transferred into the well of a MEA biochip (Ayanda Biosystems, Lausanne, Switzerland) comprising of 60 tip shaped 3D platinum electrodes (40 µm diameter)

arranged in a 5x13 matrix (200 µm spacing, 450-650 kΩ impedance) that was connected to a MEA1060-BC pre-amplifier case. The electrodes were used for stimulation and recording as described below. The slice was guided into place using a fine brush. ACSF was continuously perfused at rate of 3.5 ml/min using a peristaltic pump (VWR International Ismatec MS-4/8 Reglo Digital) connected to PVC tubing. Prior to being delivered into the well the aCSF was heated to 32ºC by a PHO1 temperature-controlled perfusion cannula (Multi Channel Systems, Reutlingen, Germany). A vacuum was used to keep the volume of aCSF in the well constant. Slices were visualised by brightfield microscopes (Axio Vert.A1 and Axiovert 40C, Carl Zeiss). Once the slice was in the desired position, and the stimulating and recording electrode have been chosen, the slice was covered and set into place by a metal ring with nylon mesh attached. A U-1C micromanipulator (You Ltd, Tokyo, Japan) was used to lower the mesh onto the surface of the slice.

Despite having to choose from 60 electrodes, only one stimulating and one recording electrode were chosen in each experiment (**Figure 2.2**). This was done to keep the distance between the two electrodes constant (between 140-400µm) throughout experiments and ensure the stimulation of the Schaffer collateral commissural pathway and recording from the CA1b region of dorsal hippocampus (Lopez et al., 2016). Monopolar stimulation was delivered to stratus radiatum of the CA1c region using a STG2004 stimulus generator and MC_stimulus II software (Multi Channel Systems, Reutlingen, Germany) that controls the amplitude, duration and frequency of the stimulus.

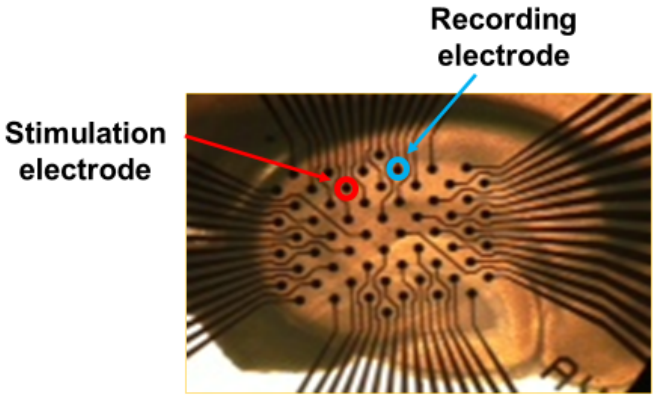


Figure 2.2: Example brightfield image showing a transverse dorsal hippocampal slice positioned on top of the electrodes in the MEA well. The stimulating (red) and recording (blue) electrodes for Schaffer collateral stimulation are circled. Imaged acquired by and used with permission of Lis Glasdam Jensen.

After approximately a 30 min equilibrium period, an input-output (I-O) curve was recorded. This was achieved by a series of 13 consecutive sweeps of biphasic voltage pulses each of 100 µs duration and applied every 15 s as follows (in mV): 0, 0, 100, 500, 750, 1000, 1250, 1500, 2000, 2500, 3000, 3500 and 4000. Subsequent baseline stimulus intensity was set to evoke 40-50% of the maximal fEPSP achieved by the I-O stimulus. Typically, a 20 min baseline with 100 µs stimulation every 30 s was recorded followed by 30 min bath application of either CNO or clozapine with continuous stimulation throughout drug application. The drug effects on fEPSPs from each group were baseline-normalised and quantified by comparing the values from all the slices recorded from one viral construct group at minute 49 (T49). This represented the end of drug application and recording period. The values for each group at T49 were also analysed statistically against one value of 100% representing the baseline. **Table 2.2** provides a summary of the drugs, concentrations and durations of application used in the electrophysiology experiments. The experiment was usually finalised with another I-O curve post drug application.

Confirmation of viral expression from the recorded slices was done post hoc. Because of the thickness of the slices, the location of the virus could not be determined precisely but it was

possible to make the assessment of whether or not the virus was expressed. Slices not expressing mCherry were excluded from the analysis. As a total of three slices were recorded at the same time and drug application was done simultaneously, all exclusions had to be done post-hoc and were made blindly to viral construct expressed, to avoid bias. Exclusions were made based on lack of a stable baseline, approximately ± 20% deviation from the 100% normalised baseline but also at least 10 min of stable recording prior to bath application of compound. If the baseline is unstable, the effect of the drug may be either masked or exaggerated by the unstable response. Slices were also excluded if the fEPSP was lost during the recording or if there was a constant decrease in the fEPSPs from the beginning of the baseline recording that continued throughout the recording, even if the baseline was still within the ±20% range. The I-O curve post drug application was a good indicator of whether the signal was completely lost, or it had decreased as a consequence of drug application. For the first four experimental days of experiment 1 (see **Table 2.2**), transverse hippocampal sections were used. From day 5, coronal sections were used instead as this enabled the visualisation of the injection site. Results from the transverse and coronal slices were pooled as no differences in responses were observed.

The negative-going slope of the fEPSP was used as a measure for quantification of the synaptic strength. The fEPSP slope was measured at 20-80% fall of the slope (**Figure 2.3**) (MC_Rack software). fEPSP raw data (but not I-O data) were normalised to baseline and analysed using GraphPad Prism 7 (GraphPad Software, Inc., San Diego, CA).

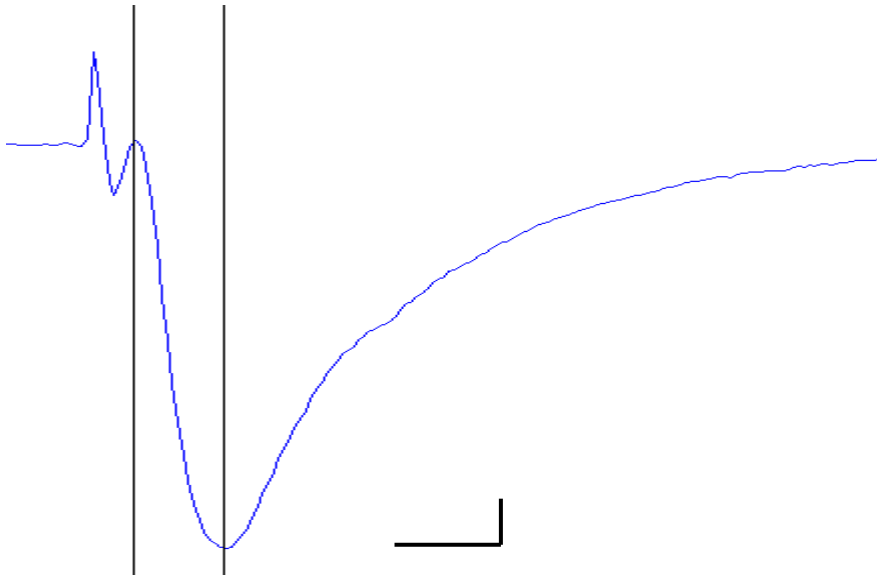


Figure 2.3. Negative-going fEPSP slope

Example fEPSP showing two cursors used for the analysis of the slope. The first cursor is placed at the second peak and the second cursor is placed at the main trough, delimitating the negative-going fEPSP slope. Calibration: 0.2 mV, 20 ms.

2.2.7 Drugs

CNO (stock of 100 mM) (Tocris Biosciences for experiments 1 and 6 and made in house for experiments 3, 4 and 5; **Table 2.2**) and CGP52432 (stock of 10 mM) (Tocris Bioscience) were dissolved in deionised water and subsequently diluted in aCSF to the required concentration. Picrotoxin (PTX) (stock of 100mM) (Sigma-Aldrich and Tocris Biosciences), clozapine (CLZ) (stock of 1 mM) (Enamine) and LY341495 (stock of 1 mM) (Tocris Biosciences) were all dissolved in 100% DMSO (Sigma-Aldrich) and subsequently diluted in aCSF to the required working concentration. This led to a total DMSO concentration in aCSF of 0.01% for clozapine experiments, and 0.1% for experiments using picrotoxin. CB1 antagonist SR141716A (Tocris Biosicences) was dissolved in 100% DMSO, but precipitated in aCSF due to its lipophilicity. As a result, the electrophysiology experiment using the CB1 antagonist had to be abandoned.

The drug concentrations have been chosen based on either previous experiments carried out in the lab or based on literature. Specifically, CNO (10 μM) has been previously used to assess DREADD functionality in slice electrophysiology experiments (Ferguson et al., 2011; Robinson et al., 2014; Zou, 2016; Corella et al., 2018), with one study reporting a small hyperpolarisation caused by 1 μM CNO compared to 10 μM CNO in mouse hippocampal slices expressing a Gi-DREADD, indicating a dose-dependent response (Zhu et al., 2014). Clozapine concentration was chosen based on the first report describing the DREADDs that indicates that clozapine is approximately 100 times more potent that CNO at the DREADDs (Armbruster et al., 2007). However, in the current study in a small subset of slices, no marked effect was seen using 100 nM clozapine (data not shown), such that the concentration was increased to 1 μM. Later, a report has successfully used clozapine (5 μM) to validate the DREADDs in their model (Zhou et al., 2018). $GABA_A$ (picrotoxin) and $GABA_B$ (CGP52432) blockers and the concentrations were chosed based on previous experiments that were done in our lab, where inhibitory transmission was blocked in hippocampal slices. Nonetheless, Lopez et al., (2016) also used 100 μM picrotoxin to block $GABA_A$ mediated transmission in DREADD expressing slices. Moreover, the study has also used a 20 min period as baseline as described in the present study (Lopez et al., 2016). LY341495 is a $mGluR_{2/3}$ blocker and was chosen based on a report showing successful blockade of the effect of a $mGluR_{2/3}$ agonist in slices at a concentration of 10 nM (Trepanier et al., 2013). Finally, the CB1 antagonist and concentration that was intended to be used was chosen based on a study that showed reversal of Gq-DREADD effect in slices by bath application of the SR 141716A (5 μM) CB1 antagonist (Mazzone et al., 2018).

Experiment number	**Viral construct**	**Drugs (concentration)**	**Timeline**	**Number of slices (rats)**
1) CNO-induced DREADD activation	Gi-DREADD	CNO (10 µM)	**Baseline** (0-20 min): aCSF **Drug application**: (20-50 min): CNO	19 (6)
	Gq-DREADD			18 (6)
	EGFP-Control			19 (6)
2) Clozapine-induced DREADD activation	Gi-DREADD	Clozapine (1 µM)	**Baseline** (0-20 min): aCSF **Drug application**: (20-50 min): Clozapine	5 (2)
	Gq-DREADD			5 (2)
	EGFP-Control			5 (2)
3) GABAergic blockade	Gq-DREADD	Picrotoxin (100 µM) CGP52432 (2 µM) CNO (10 µM)	**Baseline** (0-20 min): Picrotoxin & CGP52432 **Drug application**: (20-50 min): Picrotoxin & CGP52432, CNO	8 (3)
	EGFP-Control			4 (2)
4) GABAergic & $mGlu_{2/3}$ transmission inhibition	Gq-DREADD	Picrotoxin (100 µM) CGP52432 (2 µM) LY341495 (10 nM) CNO (10 µM)	**Baseline** (0-20 min): Picrotoxin & CGP52432 & LY341495 **Drug application**: (20-50 min): Picrotoxin & CGP52432 & LY341495, CNO	11 (4)
	EGFP-Control			6 (2)
5) CNO washout	Gq-DREADD	CNO (10 µM)	**Baseline** (0-20 min): aCSF **Drug application**: (20-25 min): CNO **Washout:** (25-90 min): aCSF	8 (3)
6) Activation of inhibitory transmission	hDlx-Gq-DREADD	CNO (10 µM)	**Baseline** (0-20 min): aCSF **Drug application**: (20-50 min): CNO	13 (4)

Table 2.2: Summary of MEA experiments in Chapter 2. The table describes the sample numbers in each experiment and the protocol and drugs used.

2.2.8 Statistical analysis

All data in this chapter were analysed using GraphPad Prism 7 (GraphPad Software, Inc., San Diego, CA). For the MEA experiments, data was tested for normality using the D'Agostino & Pearson or Shapiro-Wilk (for small samples) normality test where appropriate. One sample t-test against a value of 100 was used to compare drug effect to baseline. Ordinary one-way ANOVA followed by Tukey's multiple comparison post hoc test (or non-parametric equivalent Kruskal-Wallis followed by Dunn's post-hoc) and repeated measures 2-way ANOVA were used to compare treatment effects between groups and I-O data respectively. When only two groups were compared, an unpaired t-test or its non-parametric equivalent the Mann-Whitney U test was used. Significance was set at a P value of $p<0.05$.

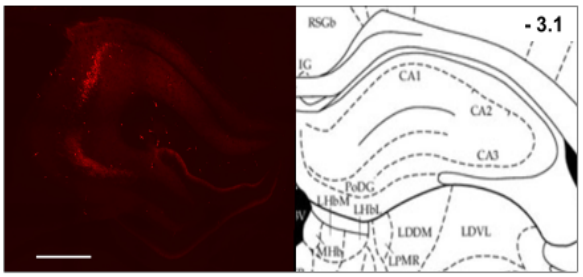
2.3 Results

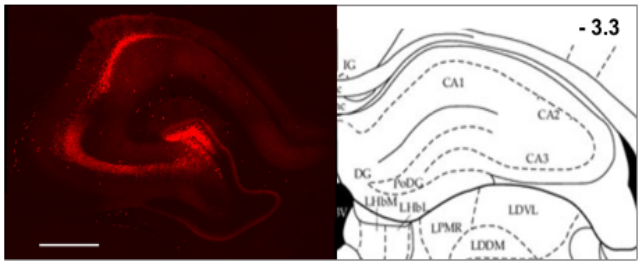
2.3.1 DREADD delivery to the hippocampus

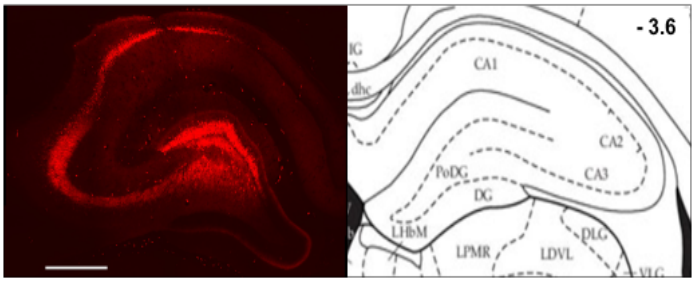
The hippocampus is critical for cognitive functions that include formation of new memories and information processing, with the dorsal region being particularly important in this regard (Fanselow & Dong, 2010). The organisation of newly formed memories and their retrieval is attributed to the principal cells of the hippocampus, the excitatory pyramidal neurons. These neurons are also responsible for transmitting the hippocampal output to neighbouring brain areas (Graves et al., 2012).

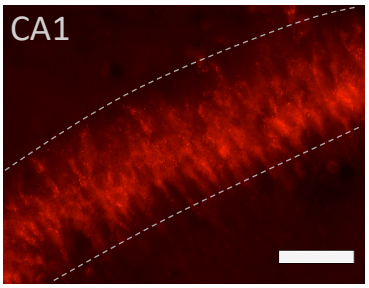
CaMKIIa promoter driven AAV constructs tagged to either mCherry (Gi-DREADD, **Figure 2.4** and Gq-DREADD, **Figure 2.5**) or EGFP (EGFP-control, **Figure 2.6**) fluorescent markers were delivered to the CA1 and CA3 regions of the dorsal hippocampus by stereotaxic injection. Perfused brains were collected from rats expressing one of the three aforementioned constructs and coronal brain sections were used to assess the qualitative spread of the DREADDs along in the dorsal hippocampus.

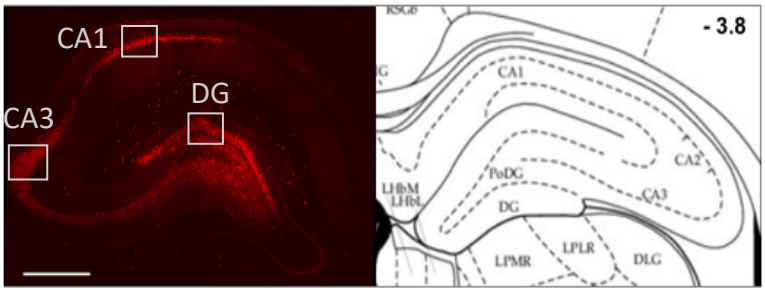
Figures 2.4-2.6 show fluorescent confocal images of the dorsal hippocampus from DREADD expressing rats accompanied by an illustration of the dorsal hippocampus at the specific AP location taken from the Rat Brain Atlas (Paxinos & Watson, 2007). Each figure represents one the viral spread in one single animal and high magnification insets of the pyramidal layer for the CA1, CA3 and DG regions are shown on the right.

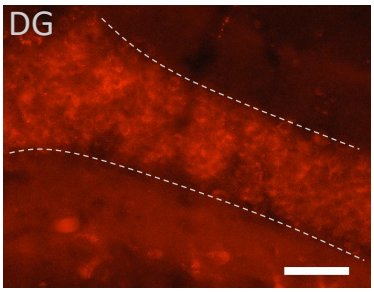

- 3.1
RSGb
IG
CA1
CA2
CA3
PoDG
LHbM
LHbL
IV
MHb
LDDM
LDVL
LPMR

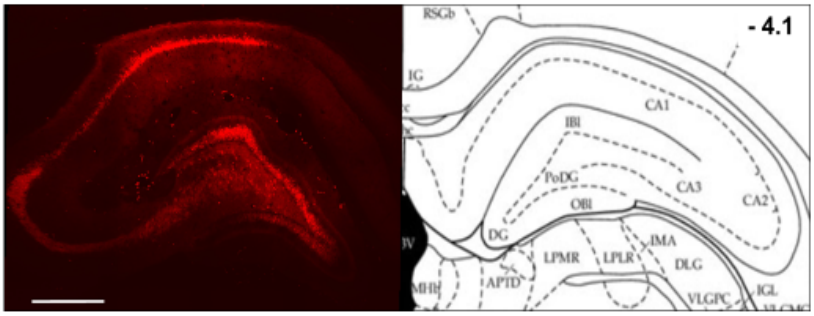

- 3.3
IG
CA1
CA2
CA3
DG
PoDG
LHbM
LHbL
IV
LPMR
LDVL
LDDM

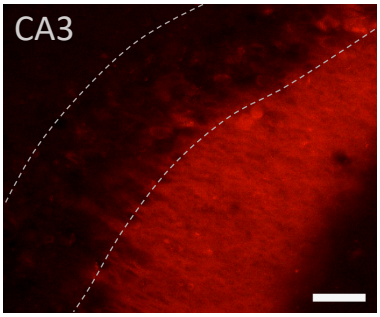

- 3.6
IG
dhc
CA1
CA2
PoDG
CA3
DG
LHbM
LPMR
LDVL
DLG
VLG


CA1


CA1
DG
CA3
- 3.8
RSGb
IG
CA1
CA2
PoDG
CA3
LHbM
LHbL
DG
LPMR
LPLR
DLG


DG


- 4.1
RSGb
IG
CA1
IBI
PoDG
CA3
CA2
OBI
DG
IV
LPMR
LPLR
IMA
DLG
MHb
APTD
VLGPC
IGL


CA3

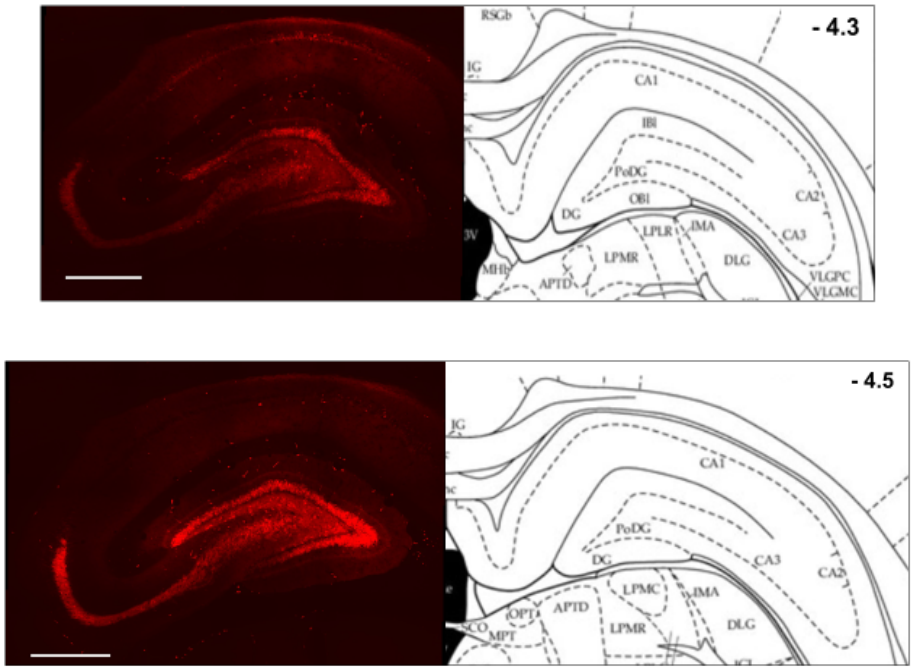
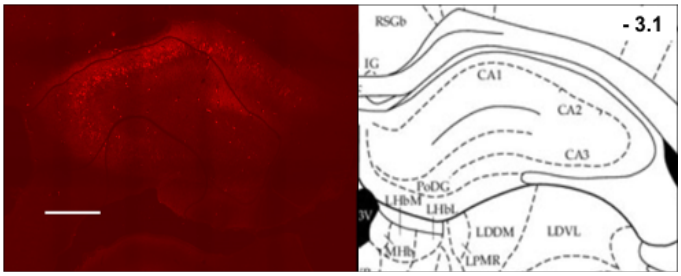
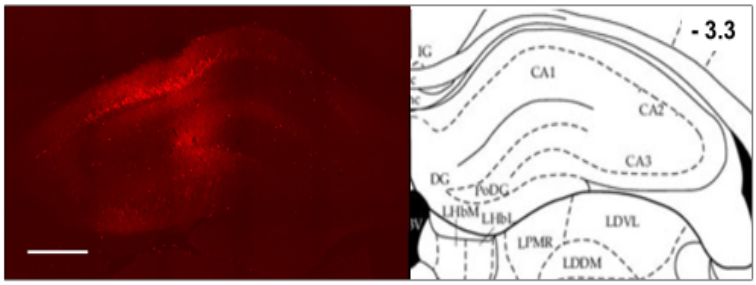
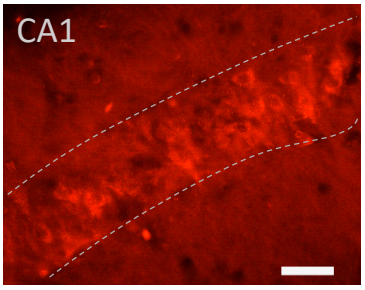


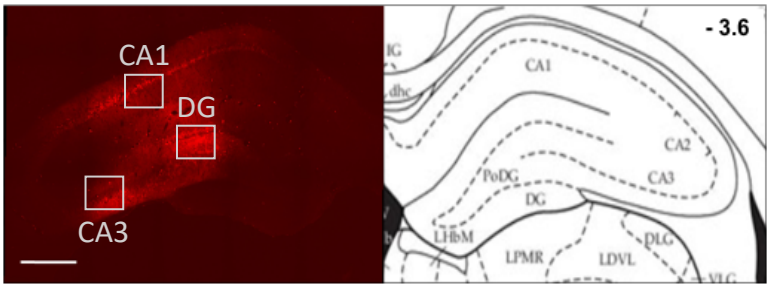
Figure 2.4: Gi-DREADD expression along the AP axis of the dorsal hippocampus.

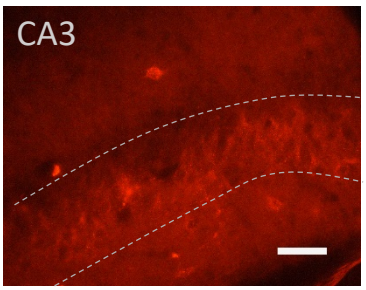
Fluorescent confocal stacks showing the spread of mCherry (red) tagged Gi-DREADD throughout the dorsal hippocampus of one single animal and corresponding illustration of the sections at the specific AP positioning. Numbers in the top right corner are AP coordinates measured from bregma (Paxinos & Watson, 2007). Scale bar = 500 µm. Confocal images were taken using a 10x objective and 4x4 fields with 20% overlap were stitched together. High magnification insets from the CA1, CA3 and DG areas are shown on the right. Fluorescent images were taken from one slice as indicated by the white boxes. Pyramidal (CA regions)/granule (DG) cell layer is delineated by the white dotted line in the insets. Scale bar = 50 µm.

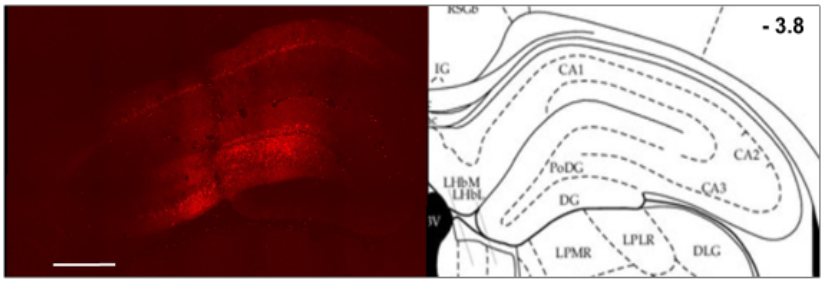

RSGb
IG
CA1
CA2
CA3
PoDG
LHbM
LHbl
LDDM
LDVL
MHb
LPMR
- 3.1

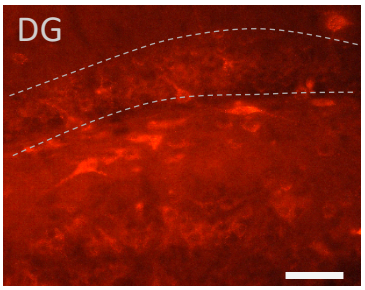

IG
CA1
CA2
CA3
DG
PoDG
LHbM
LHbl
LDVL
LPMR
LDDM
- 3.3

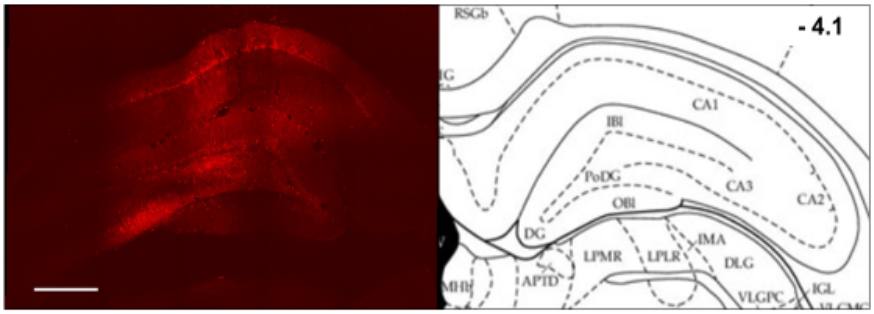

CA1


CA1
DG
CA3
IG
dhc
CA1
CA2
CA3
PoDG
DG
LHbM
LPMR
LDVL
DLG
VLG
- 3.6


CA3


RSGb
IG
CA1
CA2
CA3
PoDG
LHbM
LHbl
DG
LPMR
LPLR
DLG
- 3.8


DG


RSGb
CA1
IBl
PoDG
CA3
CA2
OBl
DG
IMA
LPMR
LPLR
DLG
APTD
VLGPC
IGL
- 4.1

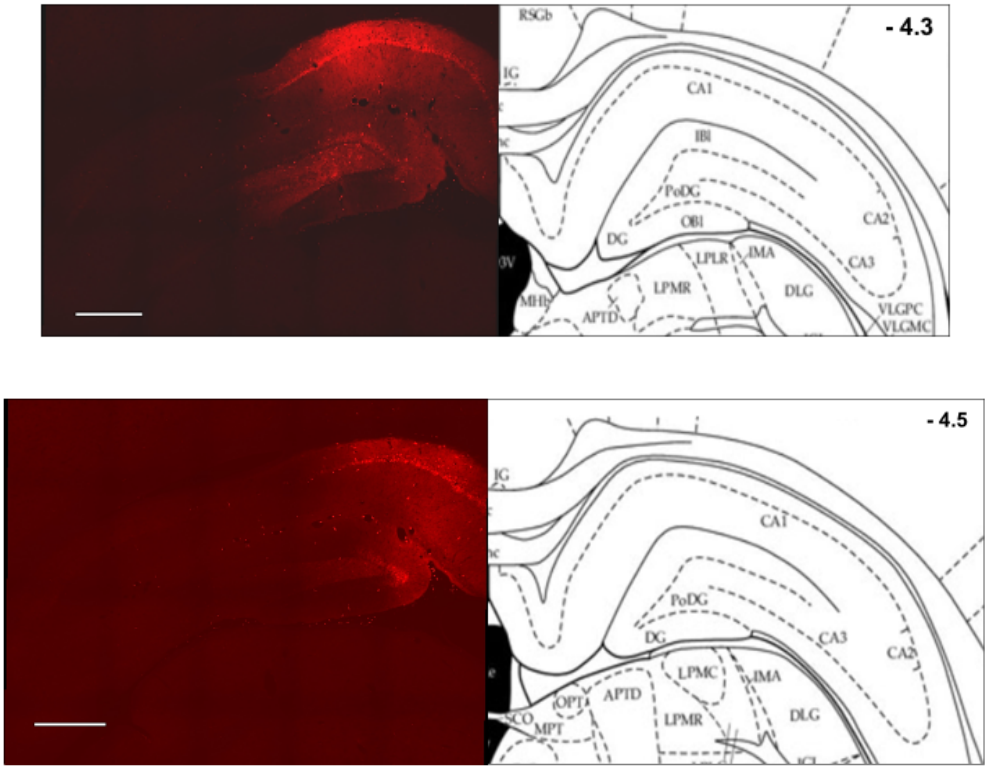
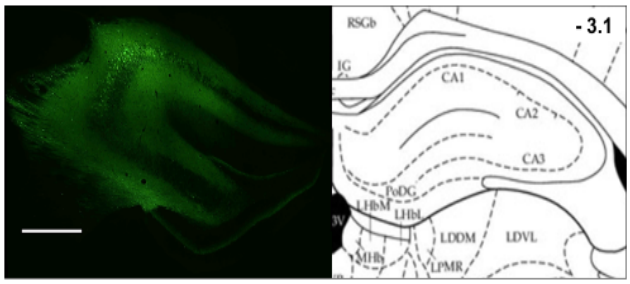
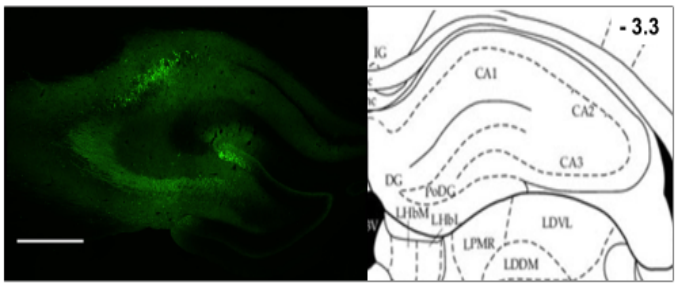
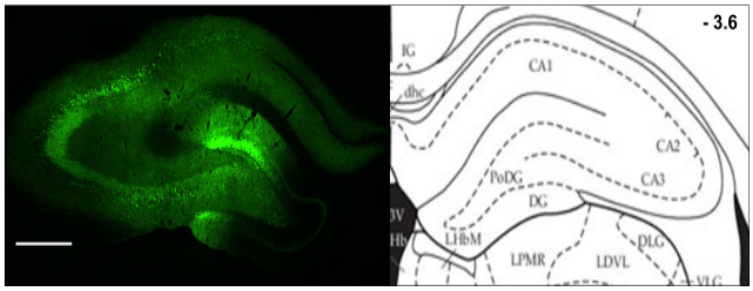


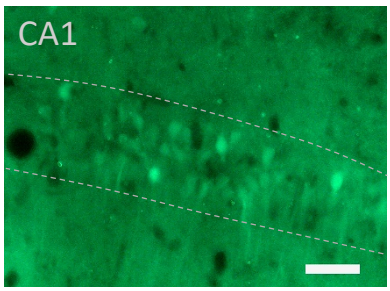
Figure 2.5: Gq-DREADD expression along the AP axis of the dorsal hippocampus.

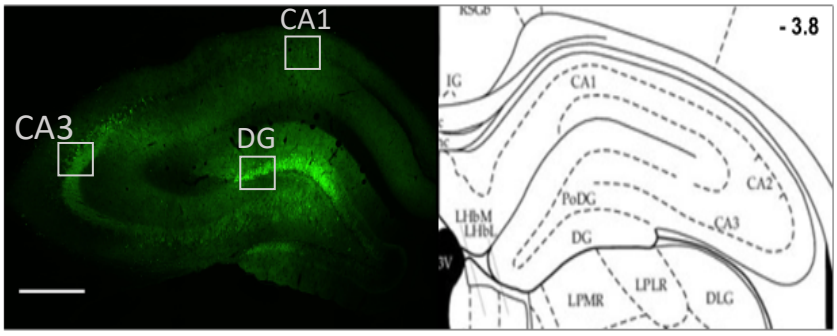
Fluorescent confocal stacks showing the spread of mCherry (red) tagged Gq-DREADD throughout the dorsal hippocampus of one single animal and corresponding illustration of the sections at the specific AP positioning. Numbers in the top right corner are AP coordinates measured from bregma (Paxinos & Watson, 2007). Scale bar = 500 µm. Confocal images were taken using a 10x objective and 5x5 fields with 20% overlap were stitched together. High magnification insets from the CA1, CA3 and DG areas are shown on the right. Fluorescent images were taken from one slice as indicated by the white boxes. Pyramidal (CA regions)/granule (DG) cell layer is delineated by the white dotted line in the insets. Scale bar = 50 µm.

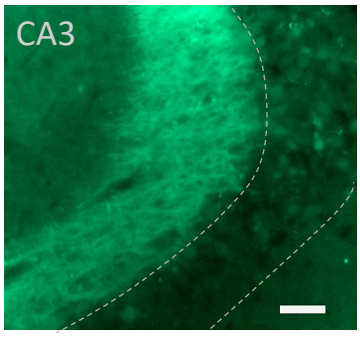

RSGb
- 3.1
IG
CA1
CA2
CA3
PoDG
LHbM
LHbl
LDDM
LDVL
MHb
LPMR

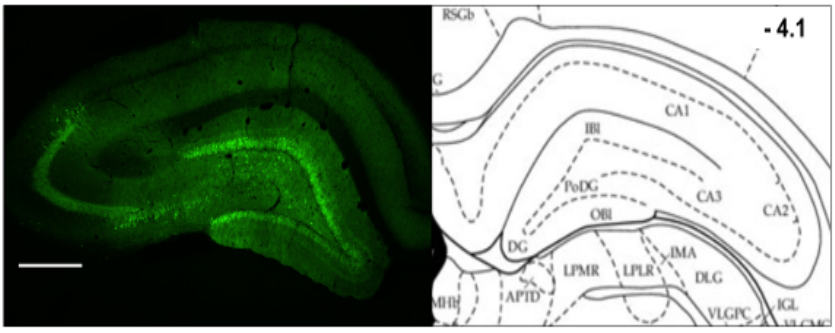

- 3.3
IG
CA1
CA2
CA3
DG
PoDG
LHbM
LHbl
LDVL
LPMR
LDDM

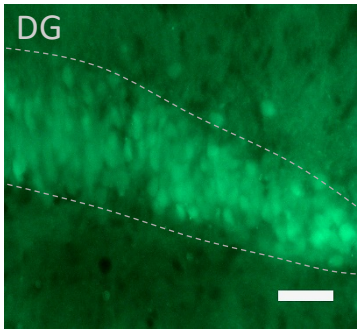

- 3.6
IG
CA1
dhc
CA2
PoDG
CA3
DG
LHbM
LPMR
LDVL
DLG


CA1


CA1
CA3
DG
RSGb
- 3.8
IG
CA1
CA2
PoDG
CA3
LHbM
LHbl
DG
LPLR
LPMR
DLG


CA3


RSGb
- 4.1
CA1
IBI
PoDG
CA3
CA2
OBI
DG
LPMR
LPLR
IMA
DLG
APTD
IGL
VLGPC


DG

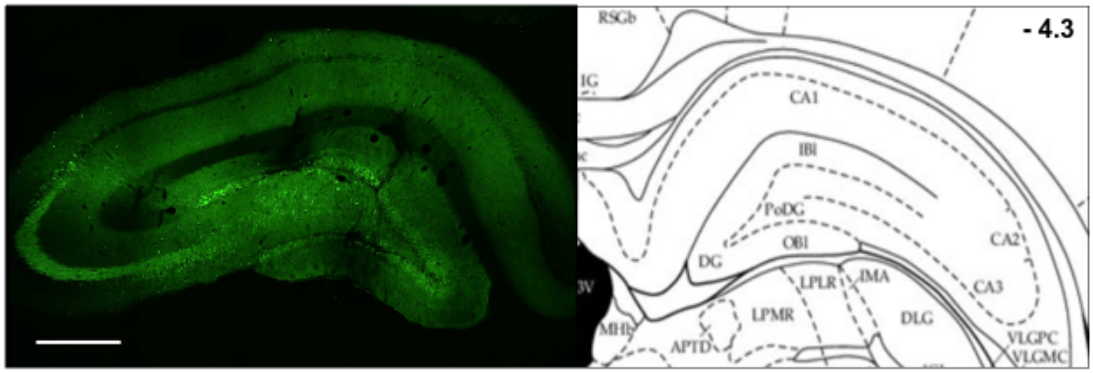


Figure 2.6: EGFP-control expression along the AP axis of the dorsal hippocampus.

Fluorescent confocal stacks showing the spread of an EGFP (green) tagged control construct throughout the dorsal hippocampus of one single animal and corresponding illustration of the sections at the specific AP positioning. Numbers in the top right corner are AP coordinates measured from bregma (Paxinos & Watson, 2007). Scale bar = 500 µm. Confocal images were taken using a 10x objective and 5x5 fields with 20% overlap were stitched together. High magnification insets from the CA1, CA3 and DG areas are shown on the right. Fluorescent images were taken from one slice as indicated by the white boxes. Pyramidal (CA regions)/granule (DG) cell layer is delineated by the white dotted line in the insets. Scale bar = 50 µm.

Confocal stacks were acquired for the qualitative assessment of the expression of DREADDs in the dorsal hippocampus. As illustrated in **Figures 2.4-2.6**, there was a different pattern of viral expression between animals. This variability prevented the quantification and estimation of a percentage of hippocampal pyramidal cells transfected by the viral constructs. Furthermore, spill-over of the viral construct in the cortex just above the hippocampus was occasionally observed (data not shown). Despite variability of the spread between rats, the transfection was mainly restricted to the CA1 pyramidal layer and mossy fibres of the stratum lucidum (Slu) of CA3 where CaMKIIa is abundantly expressed (Wang et al., 2013). The main sites of injection were the CA1 and CA3 regions, however many rats also showed transfection of the granule cells of the DG. Given its positioning between CA1 and CA3, the CA2 region was also transfected in most of the rats that showed expression at the sites of injection. Generally, the viral constructs seemed to spread for approximately ± 0.5 mm from the sites of injection (see **Figures 2.4-2.6**). Some animals displayed unilateral expression or no expression at all. These rats were usually excluded from analysis unless stated otherwise.

The successful CaMKIIa promoter driven expression of DREADDs to the dorsal hippocampus allowed for further investigation into the cell-specificity of the expression.

2.3.2 Cellular localisation of CaMKIIa promotor driven Gi-DREADD in hippocampus

Pyramidal cells

In order to selectively target excitatory neurons of the dorsal hippocampus, a CaMKIIa promoter was chosen as it has previously been shown to be specific in driving the gene expression in this neuronal population (Dittgen et al., 2004; López et al., 2016; Mayford et al., 1996; White et al., 2011).

To confirm that the expression of a CaMKIIa promoter driven Gi-DREADD was restricted to CaMKIIa expressing neurons, 2 coronal dorsal hippocampal sections were taken from 2 Gi-DREADD expressing rats and immunolabeled with a CaMKIIa primary antibody (**Figure 2.7**).

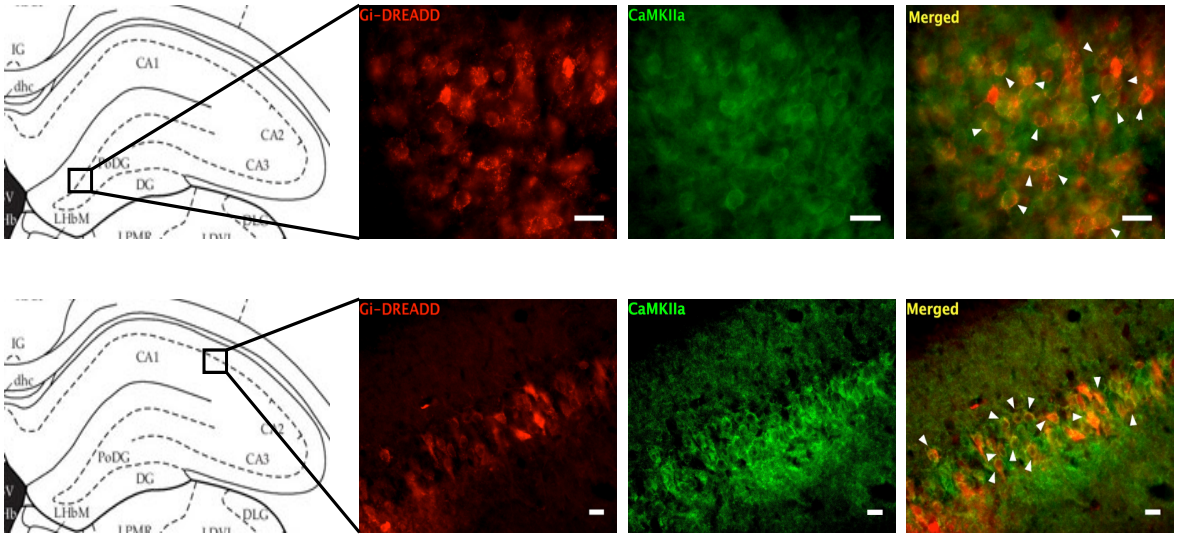


Figure 2.7: DREADD transfection of CaMKIIa expressing neurons in the CA1 and DG regions of the dorsal hippocampus

Example epi-fluorescent images showing the co-expression (merged, yellow) of CaMKIIa (green) with mCherry tagged Gi-DREADD (red) driven by a CaMKIIa promoter. Scale bar = 25 μm. White arrowheads indicate double-labelled neurons.

Epifluorescence images were collected, and a qualitative assessment confirmed the co-localisation of the mCherry tagged Gi-DREADD (red) with the CaMKIIa positive cells (green) in the regions where the Gi-DREADD was expressed. This suggests that the CaMKIIa promoter is indeed mainly expressed in excitatory neurons in the dorsal hippocampus. However, this was a small study that did not offer much information about the specificity of the construct which can also be achieved by assessing the spread of fluorophore tagged viral construct in the pyramidal layer. Therefore, it was of interest to assess whether the constructs were also transfected to hippocampal interneurons. This was an important consideration in order to interpret the outcomes of the functional studies on DREADD expression.

Interneurons

A potential caveat of using the CaMKIIa promoter is that the promoter drives gene expression in both excitatory and inhibitory neurons (Nathanson et al., 2009; Scheyltjens et al., 2015). To check for the possible transfection of interneurons, hippocampal sections were collected from rats previously injected with either an inhibitory (hM4Di-mCherry) or an excitatory (hM3Dq-mCherry) DREADD under the control of a CaMKIIa promoter. An *in situ* hybridisation study confirmed the co-expression of the two probes, mCherry (red) and GAD1 (blue), a pan-GABAergic interneuronal marker in the DG hilus (**Figure 2.8**) and in the CA1 region, albeit less than in the DG hilus (**Figure 2.9**). This suggested that the CaMKIIa promoter driven construct was not entirely restricted to pyramidal neurons and it also transfected to interneurons in the hippocampus. The colour images shown for each example confirm that the blue labelling observed in the pyramidal layer (mostly DG) in the fluorescent images is background from the strong mCherry signal that leaks into the blue channel.

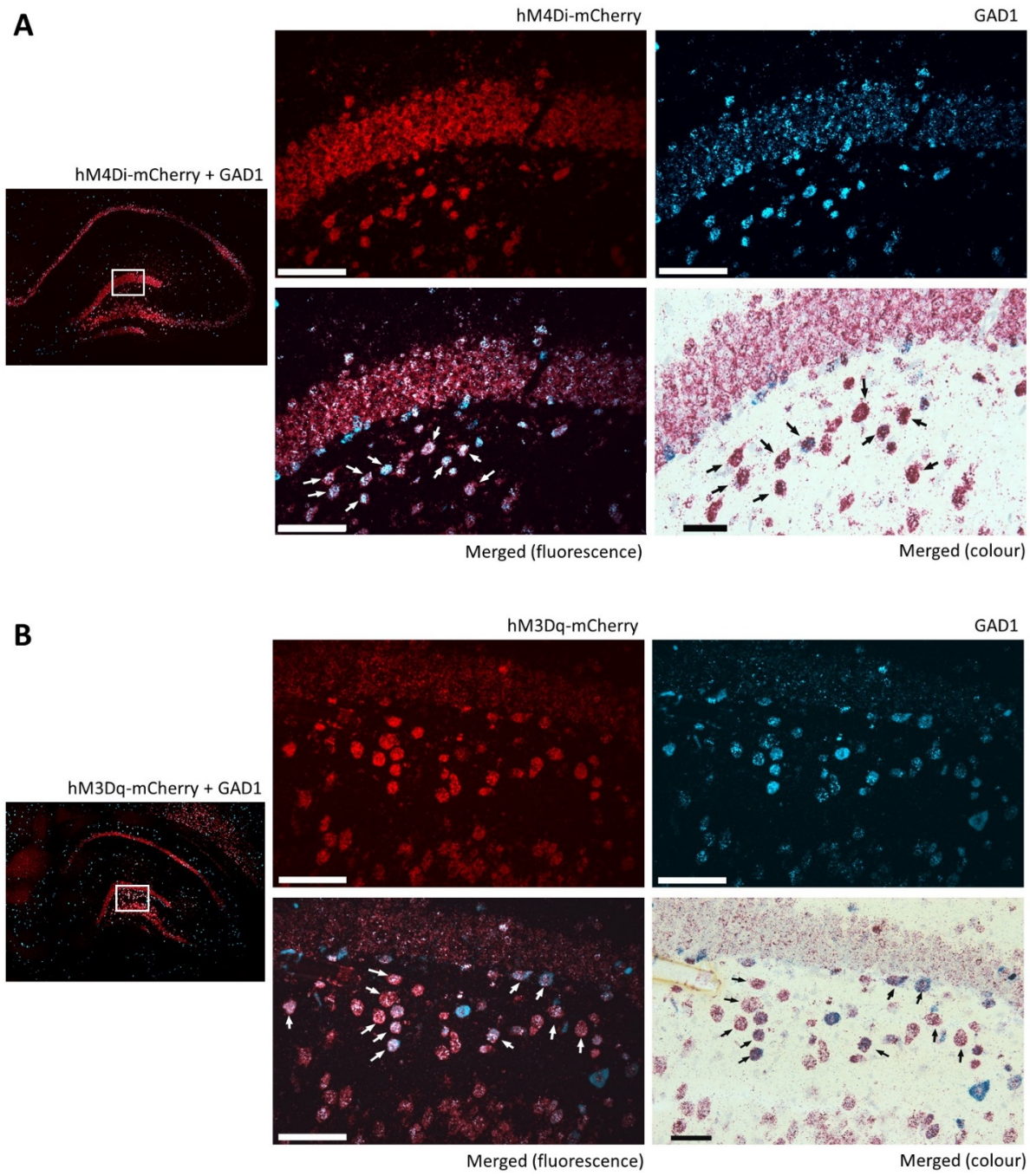


Figure 2.8: Transfection in GABAergic interneurons of the DG hilus by CaMKIIa promoter driven inhibitory and excitatory DREADDs

Example confocal stacks (fluorescence) or brightfield images (colour immunoreactivity) showing the co-expression (merged) of mCherry (red) with GAD1 (blue). Both hM4Di (A) and hM3Dq (B) constructs were under the control of a CaMKIIa promoter. Fluorescence and brightfield images were taken on different microscopes, such that the area shown differs slightly. Scale bar = 100 µm (white) or 50 µm (black). Arrows indicate double-labelled neurons.

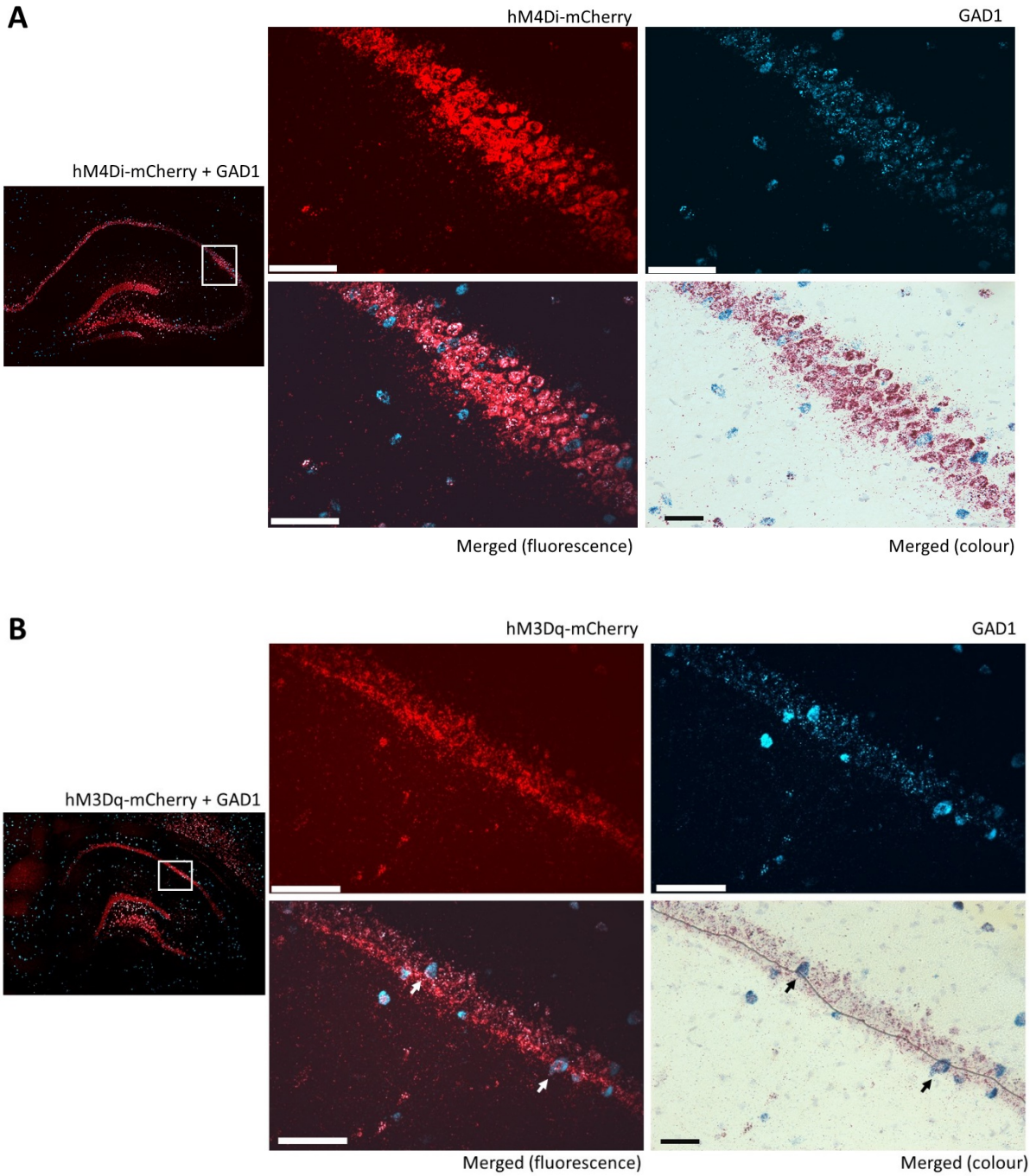


Figure 2.9: Transfection of a CaMKIIa promoter driven inhibitory and excitatory DREADD in GABAergic interneurons of the CA1 region

Example confocal stacks (fluorescence) or brightfield images (colour immunoreactivity) showing the co-expression (merged) of mCherry (red) with GAD1 (blue). Both hM4Di (A) and hM3Dq (B) constructs were under the control of a CaMKIIa promoter. Fluorescence and brightfield images were taken on different microscopes, such that the area shown differs slightly. Scale bar = 100 µm (white) or 50 µm (black). Arrows indicate double-labelled neurons.

The data from this *in situ* study suggest that DREADD (or EGFP) expression under the control of the CaMKIIa promoter is restricted to the CA1 and CA3 principal layers of the rat dorsal hippocampus where glutamatergic neurons are in abundance. A quantification of the number of GAD1 positive cells in the CA1 and the DG hilus regions as delimitated by the white boxes in Figures 2.8 and 2.9 confirmed the transfection of both a Gi and Gq-DREADD construct to GAD1 positive cells. Specifically, in the DG hilar region, from an average of 12.8 GAD1 positive cells per rat, 8.8 (counted from one slice from n = 6 rats) were also expressing mCherry in sections from Gq-DREADD expressing rats. Based on this quantification, 68.8% of GAD1 positive cells in the hilar area of Gq-DREADD expressing sections also expressed mCherry. In the case of Gi-DREADD expressing rats, from an average of 11.6 GAD1 positive cells per rat, 6.8 (counted from one slice from n = 5 rats) were also expressing mCherry (58.6% GAD1/mCherry co-localisation). Conversely, in the CA1 region, the same quantification revealed that in Gq-DREADD expressing slices, from an average of 6.3 GAD1 positive cells per slice/rat, 1.8 (counted from one slice from n = 6 rats) were also expressing mCherry (28% GAD1/mCherry co-localisation). In the case of sections from Gi-DREADD expressing rats, from an average of 9 GAD1 positive cells (counted from one slice from n = 5 rats), 1.4 of these also expressed mCherry (15% GAD1/mCherry co-localisation). Therefore, while the number of glutamatergic cells expressing the construct seems to be far greater than the number of interneurons expressing the DREADD constructs, it is unknown whether this non-specific labelling will have a significant impact on hippocampal function. Thus, investigators should be aware of this pitfall when using a CaMKIIa promoter driven construct.

2.3.3 Electrophysiological effect of CNO in Gi- and Gq-DREADD-expressing hippocampal slices

Once the cellular expression of the DREADD constructs was established, the functionality of the constructs was tested. *Ex vivo* MEA recordings were performed on dorsal hippocampal

slices taken from rats expressing one of the DREADDs (Gi, or Gq and EGFP-control). CA1 fEPSPs were evoked upon stimulation of Schaffer collaterals. A stimulating voltage giving 40-50% of the maximum response of an I-O curve was chosen. Once a stable baseline was achieved, CNO (10 μM) was added to the bath and fEPSPs were recorded for another 30 min. CNO induced activation of Gi-DREADD was expected to cause presynaptic inhibition, leading to synaptic silencing of excitatory neurons and a consequent decrease in fEPSPs. The opposite effect was expected of CNO in the presence of Gq-DREADD, due to elevated intracellular calcium leading to neuronal depolarisation (Roth, 2016). Since CNO is thought to be DREADD-selective (Armbruster et al., 2007), no changes in fEPSPs were expected in the presence of the EGFP-control.

In the presence of Gi-DREADD, a reproducible, robust and pronounced decrease in fEPSP slope was observed within 5 min of CNO application, and no marked effect was detected in EGFP-control slices. Surprisingly, CNO had a similar inhibitory effect in Gq-DREADD expressing slices (**Figure 2.10A**). Examples of fEPSP traces pre-CNO and post-CNO application are shown in **Figure 2.10E**.

A Kruskal-Wallis analysis with viral construct type as between subject factor revealed a significant effect of construct type on fEPSP slope at T49 (49 min from the beginning of the recording) between the 3 groups ($P<0.0001$). Dunn's multiple comparison post hoc test revealed a significant decrease in fEPSP slope at T49 of Gi-DREADD and Gq-DREADD expressing slices compared to control slices (EGFP-control *vs.*, Gi-DREADD, $P < 0.0001$; EGFP-control *vs.*, Gq-DREADD, $P = 0.0032$) and no differences between the Gi and Gq-DREADD expressing slices ($P = 0.4463$). In order to compare the effect drug application had on the fEPSP to baseline, T49 values were statistically analysed against one value of 100%, representing baseline value. All groups displayed significantly reduced fEPSP slope in the

presence of CNO as revealed by one sample t-test analysis against baseline values (100%) (EGFP-control: $t(18) = 2.112$, $P = 0.049$; Gi-DREADD: $t(18) = 12.16$, $P < 0.0001$; Gq-DREADD: $t(17) = 6.909$, $P < 0.0001$). (**Figure 2.10B**). The statistical significance in decreased fEPSP compared to baseline in the EGFP group can be explained by natural time dependent decay in fEPSP signal.

Raw baseline data from the three groups used in this experiment and the following one (experiment 1 and 2) were analysed to assess whether viral transfection *per se* affected synaptic transmission. A baseline average value was calculated for each slice. A one-way ANOVA of the raw baseline values with construct type as a between subject factor was used (**Figure 2.10C**). The results revealed no significant differences overall ($F(2, 68) = 0.4767$, $P = 0.623$). This result was also confirmed by the I-O curve that is a measure of synaptic strength (**Figure 2.10D**). Thus, a repeated measures 2-way ANOVA with stimulus intensity as a within-subject factor and construct type as a between subject factor, revealed a significant change with stimulus intensity as expected from an I-O curve ($F(12, 816) = 263.2$, $P < 0.0001$), no effect of construct type ($F(2, 68) = 0.8697$, $P = 0.4237$) or the interaction construct*stimulus ($F(24, 816) = 1.049$, $P = 0.3988$). This suggested there were no differences overall in basal synaptic strength based on the type of viral construct expressed. Overall, these data indicate that CNO decreased excitatory synaptic transmission in the presence of Gq and Gi-DREADD but had little to no effect in EGFP controls.

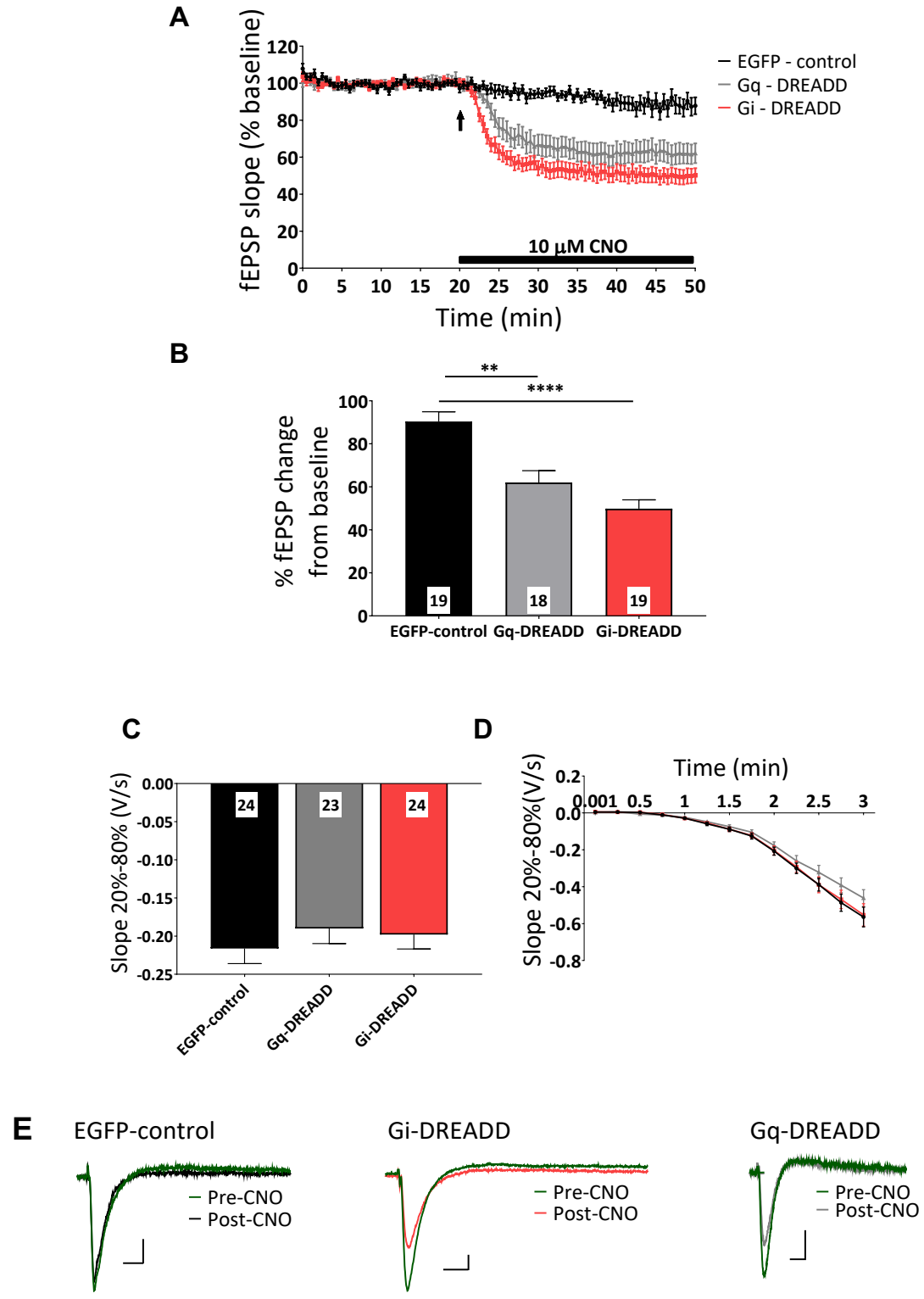


Figure 2.10: Electrophysiological effect of CNO in Gi- and Gq-DREADD expressing hippocampal slices

(A) Data showing time course effect of CNO application decreased fEPSP slope in Gi (red) and Gq-DREADD (grey) expressing hippocampal slices. Data are baseline-normalised and expressed as mean ± SEM values from n=18-19 slices obtained from N=6 rats. (B) Change in slope fEPSP at T49, before ending the recording. Data expressed as mean + SEM values (n=18-19 slices from N=6 rats) ****P<0.0001, **P=0.0032 (Kruskal-Wallis with Dunn's multiple

comparison post-hoc). (C) Baseline fEPSP slope raw data. (D) I-O voltage curve, data expressed as mean ± SEM values (n=23-24 slices from N=6 rats). (E) Example fEPSP traces from EGFP-control (black, left), Gi-DREADD (red, middle), Gq-DREADD (grey, right) before (green) and after CNO application (black, red or grey). A, B, C and E were obtained at a stimulation intensity that induced 40-50% of the maximal response obtained from I-O curve. Calibration: 0.1 mV, 10 ms.

2.3.4 Electrophysiological effect of clozapine in Gi- and Gq-DREADD-expressing hippocampal slices

CNO is a metabolite of clozapine but was proposed as a suitable DREADD agonist because it was thought to be otherwise pharmacologically inert, whereas clozapine itself has high affinity for M_3 receptors as well as a range of other receptors (Armbruster et al., 2007). However, CNO has previously been shown to be reverse metabolised to clozapine in guinea pigs and humans (Jann et al., 1994), and more recently in mice and rats (Gomez et al., 2017; MacLaren et al., 2016). Because of the latter findings, we assessed whether clozapine is also an activator of the DREADDs.

In a subset of slices expressing one of the three constructs (Gi, Gq-DREADD or EGFP-control) effect of clozapine (1 µM) on fEPSP was tested. As with CNO, bath application of clozapine decreased fEPSPs in both Gi-DREADD and Gq-DREADD expressing slices but not EGFP-control slices (**Figure 2.11A**). Representative fEPSP traces before and after clozapine application can be found below (**Figure 2.11C**). A one-way ANOVA with viral construct type as between subject factor revealed a significant effect of construct type on fEPSP slope at T49 (49 min from the beginning of the recording) between the 3 groups ($F(2,11) = 11.3$, $P = 0.0021$). Tukey's multiple comparison post hoc test revealed a significant decrease in fEPSP slope at T49 of Gi-DREADD and Gq-DREADD expressing slices compared to control slices (EGFP-control *vs*., Gi-DREADD, $P = 0.0036$; EGFP-control *vs.*, Gq-DREADD, $P = 0.0065$) and no differences between the Gi and Gq-DREADD expressing slices ($P = 0.8386$). In order

to compare the effect drug application had on the fEPSP to baseline, T49 values were statistically analysed against one value of 100%, representing baseline value. One value from a Gi-DREADD slice could not be included as recording post clozapine application was ended at T45. Slices from the Gi and Gq-DREADD groups displayed significantly reduced fEPSP slope in the presence of clozapine as revealed by one sample t-test analysis against baseline values (100%) (Gi-DREADD: $t(3) = 6.217$, $P = 0.0084$; Gq-DREADD: $t(4) = 3.818$, $P = 0.0188$). No change compared to baseline was found in the EGFP-control group ($t(4) = 0.9335$, $P = 0.4034$) (**Figure 2.11B**).

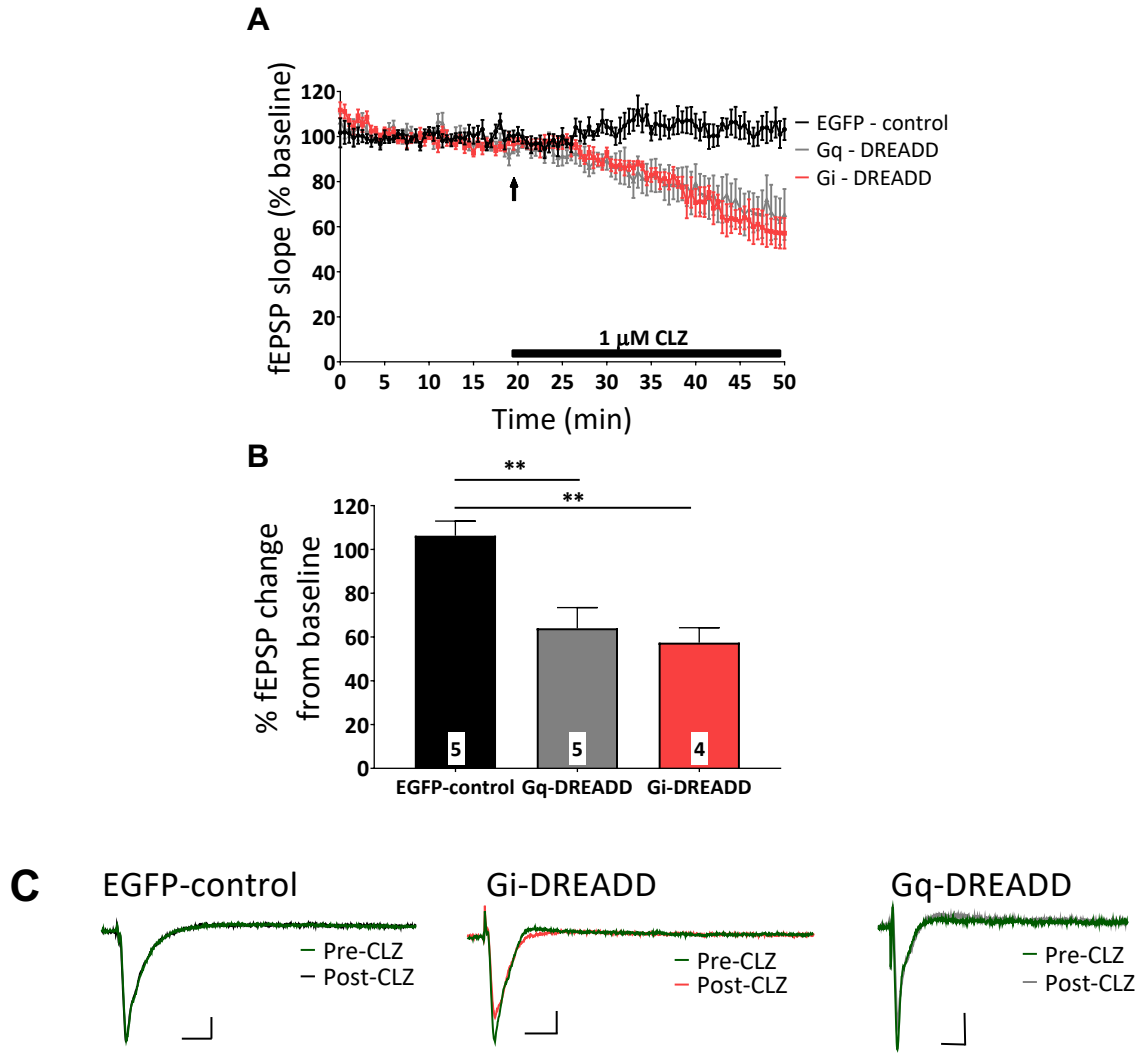


Figure 2.11: Electrophysiological effect of clozapine in the presence of Gi and Gq DREADDs

(A) Data showing time course effect of clozapine application decreased fEPSP slope in Gi (red) and Gq-DREADD (grey) expressing hippocampal slices. Data are baseline-normalised and expressed as mean ± SEM values from n=5 slices obtained from N=2 rats. (B) Change in slope fEPSP at T49, before ending the recording. Data expressed as mean + SEM values (n=4-5 slices from N=2 rats) **P=0.0036 (EGFP-control vs. Gi-DREADD), **P=0.0065 (EGFP-control vs. Gq-DREADD) (One way ANOVA and Tukey's multiple comparison post hoc test) (C) Example fEPSP traces from EGFP-control (black, left), Gi-DREADD (red, middle), Gq-DREADD (grey, right) before (green) and after clozapine application (black, red or grey). A, B, and C were obtained at a stimulation intensity that induced 40-50% of the maximal response obtained from I-O curve. Calibration: 0.1 mV, 10 ms.

2.3.5 Effect of GABA receptor blockade on CNO-induced inhibition in Gq-DREADD-expressing hippocampal slices

The paradoxical inhibitory effect of CNO and clozapine on fEPSPs in Gq-DREADD expressing hippocampal slices was investigated further. This inhibitory effect could potentially be explained by the results from the *in situ* study (see **2.3.2**) which show expression of CaMKIIa promoter driven DREADDs (Gi and Gq) in GAD1 positive neurons of the dorsal hippocampus. Thus, CNO (and clozapine) may inhibit transmission by activating GABAergic neurons. To test this scenario, recordings of CNO effect were made in the presence of GABAergic inhibitors. It was hypothesised that GABAergic blockade will prevent the CNO induced fEPSP decrease observed in Gq-DREADD slices.

Therefore, in a follow-up experiment once the slices had reached equilibrium in the well with normal aCSF, GABAergic transmission was blocked with a $GABA_A$ blocker, picrotoxin (100 µM) and a $GABA_B$ antagonist, CGP52432 (2 µM) prior to administration of CNO. GABAergic blockade was confirmed by the epileptiform activity seen in the fEPSPs (**Figure 2.12D**) as predicted considering that $GABA_A$ blockers are a pharmacological tool that has been used to cause and study epileptiform activity in slices (Avoli & Jefferys, 2016). Despite the presence of the GABA antagonists, CNO was still able to cause a decrease in the fEPSP slope in Gq-DREADD expressing slices, compared to baseline (**Figure 2.12A**). There were no changes in fEPSP slope in EGFP-control slices compared to baseline, as expected. Representative fEPSP traces before and after CNO application can be found below (**Figure 2.12D**). An unpaired t-test revealed a trend but not a statistically significant differences in fEPSP slope at T49 between the control group and the Gq-DREADD group in the presence of CNO ($t(10) = 1.928$, $P = 0.0827$). In order to compare the effect drug application had on the fEPSP to baseline, T49 values were statistically analysed against one value of 100%, representing baseline value. Gq-DREADD expressing slices displayed significantly reduced fEPSP slope

in the presence of CNO as revealed by one sample t-test analysis against baseline values (100%) ($t(7) = 2.532$, $P = 0.0096$) while was no change compared to baseline was found in the EGFP-control group ($t(3) = 2.472$, $P = 0.0899$).

Raw baseline data from the two groups were analysed to assess whether GABAergic blockade affected baseline synaptic transmission differently based on construct expressed. An unpaired t-test revealed no significant differences ($t(10) = 1.231$, $P = 0.2466$) between Gq DREADD expressing slices and control slices (**Figure 2.12C**).

Taken together these data indicate that the CNO-evoked decrease in glutamatergic transmission observed in Gq-DREADD expressing slices is not attributed to the activation of inhibitory transmission.

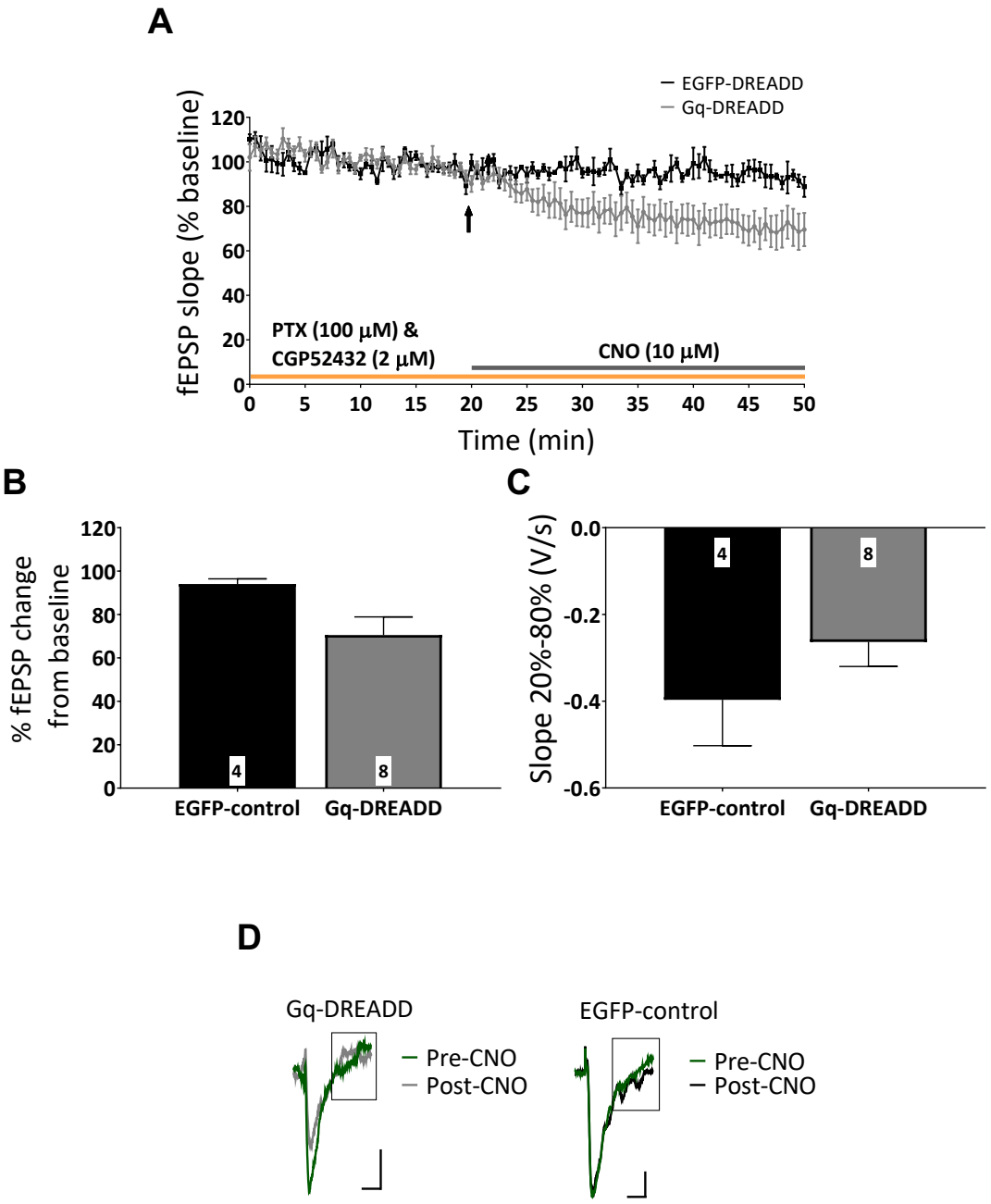


Figure 2.12: Effect of GABAergic blockade on the inhibitory effect of CNO in Gq-DREADD expressing slices

(A) Data showing time course effect of CNO application decreased fEPSP slope in Gq-DREADD (grey) expressing hippocampal slices. Data are baseline-normalised and expressed as mean ± SEM values from n=4-8 slices obtained from N=2-3 rats. $GABA_A$ and $GABA_B$ blockers were applied throughout the recordings. (B) Change in slope fEPSP at T49, before ending the recording. Data expressed as mean + SEM values (n=4-8 slices from N=2-3 rats) (C) Baseline fEPSP slope raw data. Data expressed as mean + SEM values (n=4-8 slices from N=2-3 rats). (D) Example fEPSP traces in the presence of GABA blockers from EGFP-control (black, right), and Gq-DREADD (grey, left) before (green) and after CNO application (black or grey). Black rectangles indicate epileptiform activity. A, B, C and D were obtained at a stimulation intensity that induced 40-50% of the maximal response obtained from I-O curve. Calibration: 0.1 mV, 10 ms.

2.3.6 Effect of metabotropic glutamate receptor blockade on CNO-induced inhibition in Gq-DREADD-expressing hippocampal slices

The $mGlu_{2/3}$ receptor is a metabotropic glutamate receptor that causes presynaptic inhibition. Another explanation for the inhibitory effect of CNO in Gq-DREADD expressing hippocampal slices is increased release of glutamate that activates $mGlu_{2/3}$ receptors to decrease excitatory transmission. To test this idea, the effect of CNO was examined in the presence of a potent and selective $mGluR_{2/3}$ antagonist, LY341495 (10 nM) (the GABA antagonists were also present).

Despite the presence of the $mGluR_{2/3}$ antagonist, CNO still decreased the fEPSP slope in Gq-DREADD expressing slices, compared to baseline and EGFP-control slices. However, there was also a decrease in fEPSP slope in EGFP-control slices **(Figure 2.13A, B)**. Representative fEPSP traces before and after CNO application are presented below (**Figure 2.13D**).

An unpaired t-test revealed a significant decrease in fEPSP slope in Gq-DREADD expressing slices compared to the control group in the presence of CNO ($t(15) = 3.332$, $P = 0.0045$). In order to compare the effect drug application had on the fEPSP to baseline, T49 values were statistically analysed against one value of 100%, representing baseline value. Both groups displayed significantly reduced fEPSP slope in the presence of CNO as revealed by one sample t-test analysis against baseline value (100%) (EGFP-control: ($t(5) = 2.901$, $P = 0.0338$; Gq-DREADD: $t(10) = 10.27$, $P < 0.0001$).

Raw baseline data from the two groups were analysed to assess whether GABAergic and $mGlu_{2/3}$ receptor blockade affected baseline synaptic transmission differently based on construct expressed. An unpaired t-test revealed a strong trend for decreased basal

transmission in Gq-DREADD slices, but no significant differences (t(15) = 1.946, P = 0.0707) between Gq DREADD expressing slices and control slices (**Figure 2.13C**)

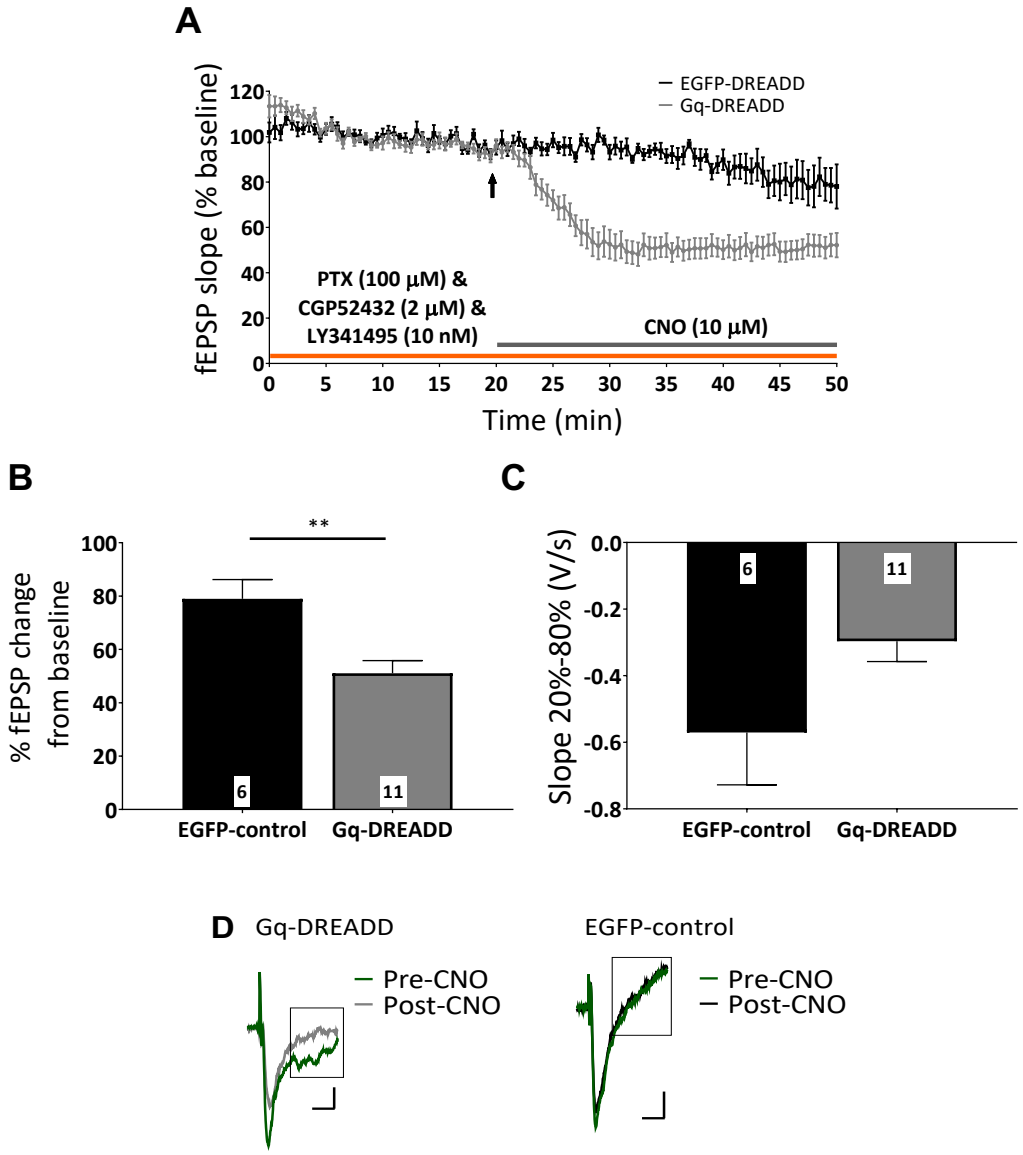


Figure 2.13: Effect of $mGluR_{2/3}$ blockade on the inhibitory effect of CNO in Gq-DREADD expressing slices

(A) Data showing time course effect of CNO application decreased fEPSP slope in Gq-DREADD (grey) expressing hippocampal slices. Data are baseline-normalised and expressed as mean ± SEM values from n=6-11 slices obtained from N=2-4 rats. $GABA_A$ and $GABA_B$ and $mGluR_{2/3}$ blockers were applied throughout the recordings. (B) Change in slope fEPSP at T49, before ending the recording. Data expressed as mean + SEM values (n=6-11 slices from N=2-4 rats). **P=0.0045 (unpaired t-test). (C) Baseline fEPSP slope raw data. Data expressed as mean + SEM values (n=6-11 slices from N=2-4 rats). (D) Example fEPSP traces in the presence of GABA and $mGluR_{2/3}$ blockers from EGFP-control (black, right), and Gq-DREADD (grey, left) before (green) and after CNO application (black or grey). Black rectangles indicate epileptiform activity. A, B, C and D were obtained at a stimulation intensity that induced 40-50% of the maximal response obtained from I-O curve. Calibration: 0.1 mV, 10 ms.

Overall, these data suggest that neither GABA receptors or $mGlu_{2/3}$ receptors are involved in the CNO-evoked decrease in excitatory transmission seen in Gq-DREADD expressing slices.

A final issue addressed statistically was whether the baseline treatment (i.e. aCSF only, GABAergic blockers or GABAergic and $mGlu_{2/3}$ blockers) affected synaptic transmission differently in slices expressing an EGFP-control compared to Gq-DREADD slices. The results suggested that baseline treatment increased fEPSP transmission step-wise in the EGFP slices while this increase was not seen in Gq-DREADD expressing slice (**see Figures 2.10C, 2.12C and 2.13C**) Specifically, the more inhibitory transmission was blocked, the bigger the fEPSP slope was in control slices. A 2-way ANOVA analysis with construct type and treatment as between subject factors revealed a significant effect of the construct type ($F(1, 70) = 9.745$, $P = 0.0026$), the treatment ($F(2, 70) = 12.32$, $P < 0.0001$) and the interaction treatment*virus construct ($F(2, 70) = 3.421$, $P = 0.0382$) on the raw fEPSP baseline values.

2.3.7 Effect of duration of application on CNO-induced inhibition in Gq-DREADD-expressing hippocampal slices

A final issue investigated was whether the decreased synaptic transmission induced by CNO in the presence of Gq-DREADD was reversible upon CNO washout. To answer this question, slices were prepared from a subset of Gq-DREADD expressing rats, and the inhibitory effect of brief (5 min) application of CNO (10 μM) was tested.

Brief application of CNO caused the characteristic decrease in fEPSP slope and this effect lasted for the remainder of the recording despite CNO being removed from the perfusion medium after the brief exposure (**Figure 2.14**). A one sample t-test analysis of values at T89

against baseline value (100%) revealed a significant decrease in fEPSP slope compared to baseline ($t(7) = 3.743$, $P = 0.0072$).

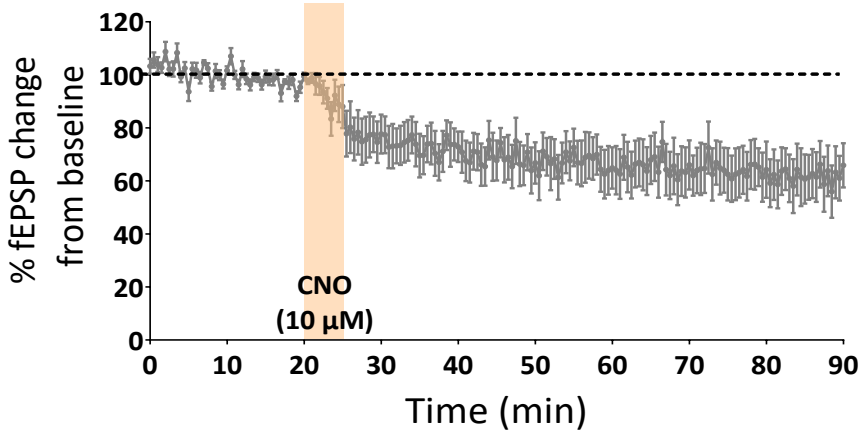


Figure 2.14: Duration of CNO-induced inhibition in Gq-DREADD-expressing hippocampal slices after short-term exposure

Data showing time course effect of brief CNO application induced a decrease in the fEPSP slope in Gq-DREADD expressing hippocampal slices. Data are baseline-normalised and expressed as mean ± SEM values from n=8 slices obtained from N=3 rats. Dotted line represents 100% baseline-normalised level.

2.3.8 Electrophysiological effect of CNO in interneuron-targeted, Gq-DREADD-expressing hippocampal slices

A final set of experiments tested whether it was possible to inhibit synaptic transmission using a novel Gq-DREADD targeted to interneurons. Recently, a Gq-DREADD construct driven by an hDlx promoter was shown to have restricted expression in GABAergic interneurons (Dimidschstein et al., 2016). Therefore, the prediction was that CNO-induced activation of this construct would evoke a decrease in the fEPSP slope similar to that observed using the CaMKIIa driven Gi-DREADD. If so, the construct could serve as another useful tool *in vivo* to inhibit hippocampal function.

In hippocampal slices obtained from rats receiving delivery of the hDlx promoter driven Gq-DREADD, CNO (10 μM) evoked the characteristic decrease in fEPSP seen in slices expressing CaMKIIa driven Gi-DREADD (**Figure 2.15A, C**). Representative fEPSP traces before and after CNO application can be found below (**Figure 2.15B**). To statistically confirm an effect of CNO on the hDlx-construct fEPSP, the values at T49 were compared to the values from the EGFP group presented in the first experiment (experiment 1) at the same time point (T49).

A Mann-Whitney U analysis revealed a significant decrease in fEPSP slope in hDlx-Gq-DREADD expressing slices compared to the control group in the presence of CNO ($P = 0.0031$). In order to compare the effect drug application had on the fEPSP to baseline, T49 values were statistically analysed against one value of 100%, representing baseline value. The results revealed significantly reduced fEPSP slope in the presence of CNO in hDlx-Gq-DREADD expressing slices ($t(11) = 7.761$, $P < 0.0001$).

Raw baseline data from the two groups were analysed to assess whether viral transfection *per se* affected baseline synaptic transmission differently based on construct expressed. A Mann-Whitney U analysis revealed a significant decrease in baseline fEPSP slope in the hDlx-Gq-DREADD slices compared to control slices ($P = 0.0071$) (**Figure 2.15D**)

This indicates that an overall decreased tone of excitatory transmission in the hippocampus can also be achieved using the DREADD approach to activate GABAergic interneurons despite decreased baseline synaptic strength displayed by the hDlx-Gq-DREADD slices.

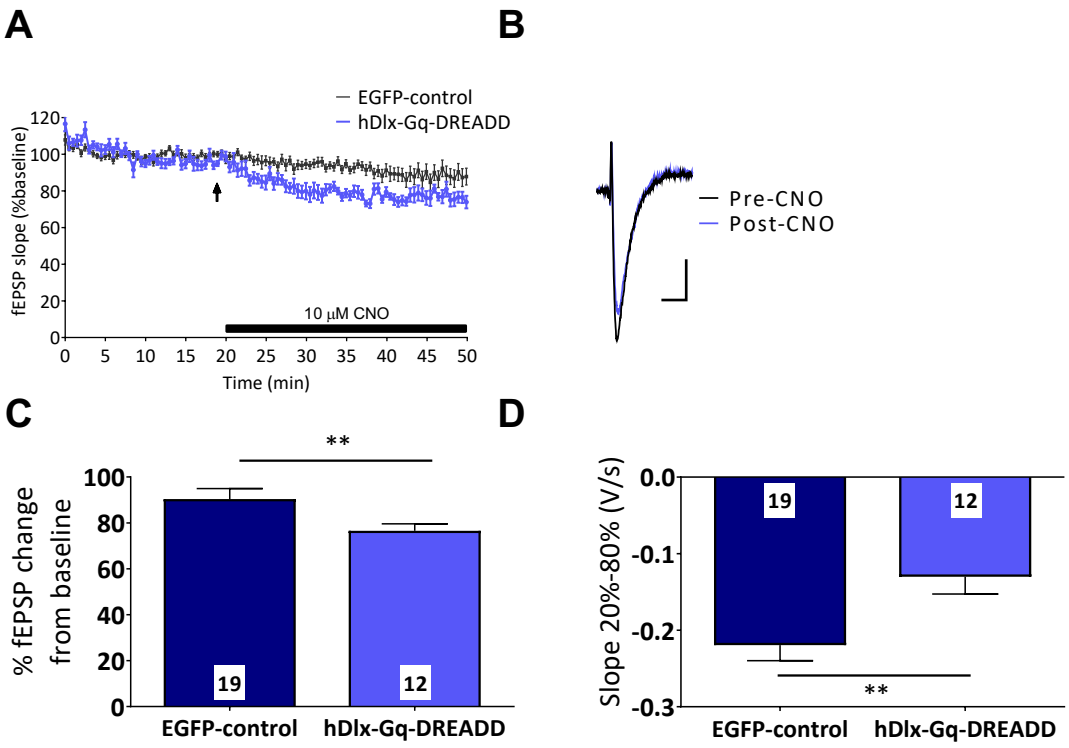


Figure 2.15: Effect of CNO in interneuron-targeted, Gq-DREADD-expressing hippocampal slices

(A) Data showing time course effect of CNO application decreased fEPSP slope in hDlx Gq-DREADD expressing hippocampal slices (blue). Data are baseline-normalised and expressed as mean ± SEM values from n=12 slices obtained from N=4 rats. (B) Example fEPSP traces from hDlx-Gq-DREADD before (black) and after CNO application (blue). (C) Change in slope fEPSP at T49, before ending the recording. Data expressed as mean + SEM values (n=12 slices from N=4 rats). **P=0.0031 (Mann-Whitney U). (D) Baseline fEPSP slope raw data. Data expressed as mean + SEM values (n=12 slices from N=4 rats). **P=0.0071 (Mann-Whitney U). A, B, C and D were obtained at a stimulation intensity that induced 40-50% of the maximal response obtained from I-O curve. Calibration: 0.1 mV, 10 ms.

2.4 Discussion

Experiments in this chapter aimed to develop and validate protocols for the viral delivery of DREADD constructs to the rat hippocampus before proceeding to *in vivo* studies. To this end, Gi- and Gq-DREADDs were targeted to excitatory neurons in the rat dorsal hippocampus using viral vectors containing a CaMKIIa promoter. Transfection of the DREADDs to the dorsal hippocampus was achieved by stereotaxic intracerebral delivery using multiple injection sites. DREADD was expressed in a significant number of principal neurons although experiments also revealed off-target expression in small numbers of GAD1-positive interneurons in the hilar region of hippocampus. Experiments revealed some inter-animal variability in the level of DREADD expression and its spread, with some animals exhibiting different expression patterns, unilateral expression or no expression at all. This emphasises the importance of post hoc confirmation of expression after each experiment involving DREADDs.

Electrophysiological experiments using hippocampal slices tested the functionality of the DREADD constructs, from which several observations were made. Firstly, these experiments confirmed that the DREADD agonist CNO inhibited excitatory transmission in the presence of Gi-DREADD, with EGFP controls showing no effect. Clozapine itself also acted as DREADD agonist in these experiments. Unexpectedly, CNO and clozapine also inhibited excitatory transmission in the presence of Gq-DREADD. Follow up experiments revealed that this decrease in transmission as seen in Gq-DREADD expressing slices was not attributed to transfection of the Gq-DREADD to GAD1-positive neurons. Pharmacological experiments ruled out the involvement of GABA and $mGluR_{2/3}$ receptors but further studies are necessary to establish the mechanism.

2.4.1 DREADD delivery to the dorsal hippocampus

When deciding the type of DREADD construct to use, two important considerations are the virus serotype and the gene promoter. The serotype will control the spread and efficacy of transfection while the promoter of choice will dictate the tropism of the virus. All viral constructs used in this thesis were of serotype AAV5/2 (widely referred to as AAV5). This means that the genome of serotype 2 is packaged into the capsid of serotype 5. Commercially available viral constructs have mixed the genome of one serotype with the capsid of another in order to improve efficiency of transfection. Serotype 5 was chosen based on its CNS transfection efficiency and tropism. In the present study it was found, based on observations, that the DREADD expression produced by the AAV5 constructs was typically distributed ±0.5 mm from the injection site, sometimes over greater distances (**Figures 2.4-2.6**), although there was some inter-animal variability in the distribution of expression.

In accordance with the present findings, Burger et al. (2004) showed that AAV5/2 constructs spread throughout the rat hippocampus and were largely transfected into principal cells of the CA regions, as opposed to AAV2/2 that was restricted to the hilar region of the DG. Additionally, the latter study found that AAV5/2 spreads over greater distances in the hippocampus compared to AAV2/2 but also that serotype 5 showed retrograde transport in hippocampal neurons (Burger et al., 2004). The greater distribution of AAV5 was also confirmed by a later study (Watakabe et al., 2015) that estimated the spread of an AAV5 construct in the marmoset cerebral cortex to be 1.3 ± 0.3 mm from the injection site. This is similar to the findings in the current study, where AAV5 constructs were typically distributed ±0.5 mm from the injection site, sometimes beyond that.

Nevertheless, a caveat of stereotaxic delivery of viral constructs is the inter-animal expression variability. Thus, upon post-hoc confirmation of DREADD expression, rats that showed no

expression or unilateral expression were excluded from analysis (unless stated otherwise). Based on results from post-hoc confirmation of viral expression in the cohorts from behavioural studies described later in the thesis, a high viral transfection success rate of 88.6% of all the rats injected was achieved, with 3.8% of the unsuccessful transfection being characterised by unilateral viral expression. The lack of expression in some animals was mostly explained by technical issues such as a blocked needle or potentially insufficient volume of viral construct left in the needle for the contralateral hemisphere. Rats that displayed successful DREADD transfection showed expression in the CA1 and CA3 regions where the viral construct was injected, but also CA2 due to its localisation between the two regions. Interestingly, high levels of expression were observed in the DG region of most rats despite it not being a direct site of injection.

2.4.2 Specificity of the CaMKIIa promoter

All but one experiment described in this chapter used viral constructs under the control of a CaMKIIa promoter to target excitatory neurons in the dorsal hippocampus. This promoter has been shown previously to be specific in driving the transfection of viral constructs into excitatory neurons (Dittgen et al., 2004; López et al., 2016; Mayford et al., 1996; White et al., 2011). In the present study, immunohistochemical analysis using a CaMKIIa antibody confirmed that the expression of CaMKIIa-driven DREADDs was mainly restricted to CaMKIIa positive neurons. The high expression of CaMKIIa-driven DREADDs in the granule cells of the DG and the mossy fibres of the CA3 stratum lucidum (Slu) is consistent with evidence that CaMKIIa is abundantly expressed in these cells (Wang et al., 2013). It was also found that the DREADD constructs under the control of the CaMKIIa promoter were expressed in GAD1-positive cells, specifically in the hilus of the DG and the CA1. This observation concurs with other studies that have also reported CaMKIIa driven AAV constructs being transfected to interneurons in the mouse somatosensory cortex and visual cortex (Nathanson et al., 2009;

Scheyltjens et al., 2015) and to parvalbumin-positive cells in the marmoset (Watakabe et al., 2015).

Basket cells are GABAergic hippocampal interneurons (Müller & Remy, 2014) that project and innervate the pyramidal cell somata and modulate their synchronised firing by doing so (Cobb et al., 1995). It is estimated that one basket cell can innervate somewhere between 1500-2000 CA1 pyramidal cells (Sik et al., 1995). Thus, despite the seemingly small number of GAD1-positive cells also expressing a DREADD construct, the potential functional effect that manipulation of these cells could have should not be overlooked.

The *in situ* study also showed evidence of DREADD construct in cells that were not GAD1-positive, but were located outside of the pyramidal layer of the CA regions or the granule layer of the DG, specifically in the hilar region of the DG. In the DG, other than the granule cells, mossy cells are also excitatory and are located in the hilar region (Scharfman, 2016). More so, a recent study used a CaMKII-driven AAV construct and validated its specificity for the DG mossy cells (Yeh et al., 2018). This suggests that perhaps a population of mossy cells in the DG hilar region are also targeted by the DREADD constructs used in this thesis.

Taking into consideration the above, the current data confirm the successful targeting of Gi- and Gq- DREADD constructs to glutamatergic neurons in the rat dorsal hippocampus.

2.4.3 CNO as a DREADD agonist *ex vivo*

Next, the functionality of the DREADDs was assessed using electrophysiological measurement of synaptic transmission in hippocampal slices. fEPSPs were evoked in the CA1

region of the rat dorsal hippocampus upon stimulation of Schaeffer collaterals. It was found that bath application of CNO (10 μM) led to a reproducible, rapid-onset decrease in the fEPSP slope to 50% below baseline response in slices expressing Gi-DREADD without having a pronounced effect in EGFP-control expressing slices. These results are in line with previous studies on the effect of CNO on neurons expressing DREADD constructs. Thus, with a similar preparation to that used here, López et al. (2016) showed that CNO (5 μM) decreased the fEPSP slope in Gi-DREADD expressing mouse slices, and no effect in control slices - the effect of CNO in the latter study was not as large and rapid onset as observed here (15% versus 50% below baseline), but this might be due to the lower CNO concentration used, inter-species differences or amount of viral transfection (López et al., 2016). Also it was found that in rat retrosplenial cortex, CNO (10 μM) decreased firing frequency of principal cells neurons expressing an hSyn-hM4Di construct (Robinson et al., 2014) and hyperpolarised these neurons in CaMKIIa-hM4Di double transgenic mice (Zhu et al., 2014). Similarly, CNO (5 μM) induced hyperpolarisation and reduced epileptiform activity in organotypic hippocampal slice cultures expressing a Gi-DREADD (Avaliani et al., 2016).

Contrary to expectations, CNO evoked a decrease in fEPSP slope in Gq-DREADD expressing hippocampal slices. The effect was reproducible, and the magnitude of the decrease was comparable to that observed in Gi-DREADD slices. A PCR quality control confirmed the viral constructs were in the correctly labelled tubes and excluded the possibility of a mix-up between the Gi/Gq-DREADD constructs (Tau Benned-Jensen, personal communication). In contrast, other studies report an excitatory effect of CNO in neurons expressing a Gq-DREADD. For example, CNO (10 μM) increased neuronal firing of mouse hippocampal neurons expressing a Gq-DREADD (Zou et al., 2016), and depolarised and evoked burst firing in neurons of the dorsal subiculum in mice expressing a Gq-DREADD (Cordella et al., 2018). CNO (20 μM) was reported to have an excitatory effect on hippocampal pyramidal cells (Sudarov et al., 2018), but also at lower concentrations (500 nM) in mouse hippocampal cells

expressing a CaMKIIa-hM3Dq construct (Alexander et al., 2009). Thus, the present experiments found that CNO induced a predicted inhibition of transmission in the presence of the Gi-DREADD but a paradoxical inhibitory effect in the presence of Gq-DREADD.

2.4.4 Investigation of inhibitory effect of CNO in the presence of Gq-DREADD

Interestingly, in accord with the current data, Lopez and colleagues (2016) found that CNO decreased fEPSP slope in Gq-DREADD expressing mouse hippocampal slices. In this case, Gq-DREADD expression was driven by the general neuron-specific promoter hSyn, leading the authors to conclude that the inhibitory effect of CNO was a consequence of presynaptic activation of GABAergic terminals. Indeed, when Gq-DREADD was driven by a CaMKIIa promoter, CNO evoked an increase in fEPSPs (López et al., 2016). Nevertheless, the current observation of transfection of the Gq-DREADD in GAD1-positive interneurons raised the possibility that increased GABA release underpinned the inhibitory effect of CNO observed here. However, this mechanism is unlikely as CNO also decreased fEPSPs in Gq-DREADD expressing slices in the presence of the $GABA_A$ and $GABA_B$ receptor antagonists, picrotoxin and CGP52432, respectively.

Next, it was considered whether activation of $mGluR_{2/3}$ by excess glutamate leads to decreased fEPSP. Group II metabotropic glutamate receptors ($mGluR_{2/3}$) are predominantly located pre-synaptically on hippocampal pyramidal neurons (Wright et al., 2013) where they inhibit glutamate release (Niswender & Conn, 2010). Post-synaptically, $mGluR_{2/3}$ enhance NMDAR function (Trepanier et al., 2013) and dampen glutamate excitation by induction (Nicoletti et al., 2011) and maintenance of LTD (Anwyl, 1999; Manahan-Vaughan, 1997). It was found however that in the presence of the selective $mGluR_{2/3}$ antagonist LY341495 CNO evoked a pronounced decrease in fEPSP.

Raw baseline data (see **Figures 2.10C**, **2.12C and 2.13C**) suggest a ceiling effect of basal synaptic transmission in Gq-DREADD expressing slices that is missing from EGFP-control slices. While this does not explain the inhibitory effect observed on excitatory transmission, it can explain the absence of increased fEPSP. A potential mechanism by which CNO could inhibit transmission in Gq-DREADD slices is through increased endocannabinoid production and activation of inhibitory CB1 receptors. Thus, activation of a Gq-coupled pathway is likely to enhance endocannabinoid production through mobilisation of internal calcium stores (Alger et al., 2014). In support of this scenario, a recent study found that CNO decreased synaptic transmission in Gq-DREADD targeted to GABA neurons in the bed nucleus stria terminalis, and the effect was reversed by a CB1 antagonist (Mazzone et al., 2018). In the light of these findings an attempt was made to test whether the same CB1 antagonist (SR141716A) would reverse the inhibitory effect of CNO in Gq-DREADD expressing hippocampal slices, but it proved unsuccessful because of the inability to dissolve the compound in aCSF so the experiment had to be abandoned.

'Activating' a cell population by means of DREADDs entails activating a signalling cascade that can generate irreversible downstream changes. This is supported by the absence of washout of CNO effect observed. The present study found that in Gq-DREADD hippocampal slices, a brief (5 min) application of CNO (10 μM) was sufficient to cause a long-lasting inhibition of transmission. This is in agreement with other studies that found CNO to produce effects that out-lasted the period of washout (López et al., 2016; Mazzone et al., 2018; Smith et al., 2016; Zhu et al., 2014). As such, it is possible that on binding to the Gq-DREADD, CNO generates long-lasting downstream signalling changes that underpin the inhibition of synaptic transmission, that do not involve the 'canonical' Gq signalling pathway (Urban et al., 2007). Interestingly it is now well recognised that many G protein coupled receptors signal via G-protein independent mechanisms, and this might also be the case for DREADDs. This would open up the possibility for biased agonism by CNO, whereby the drug is not acting via the

classical Gq coupled excitatory phosphoinositide pathway. Additionally, CNO might be acting as an inverse agonist of the Gq-DREADD and thereby reducing constitutive signalling to decrease excitatory transmission.

2.4.5 Clozapine as DREADD agonist *ex vivo*

Initial studies selected CNO as a DREADD agonist with the view that it was otherwise pharmacologically inert, readily crosses the BBB and was not reverse metabolised to clozapine (Armbruster et al., 2007). However, during experiments described in this thesis, a pivotal study reported evidence that CNO is back-metabolised to clozapine which crosses the BBB to activate DREADDs (Gomez et al., 2017). Although clozapine was known to have nM affinity for Gq-DREADD (Armbruster et al., 2007), its efficacy at DREADDs was unknown. Interestingly, the current study found that in Gi-DREADD transfected hippocampal slices, bath applied clozapine (1 μM) decreased fEPSP slope in a comparable manner to CNO. This effect was specific in that clozapine had no effect on fEPSP in EGFP-control hippocampal slices, although the effect was slower in onset than with CNO. These data are consistent with clozapine being a DREADD agonist. To our knowledge, this was the first study to assess and confirm this. Therefore, if CNO is reverse metabolised to clozapine, some of the CNS effects of systemically administered CNO may indeed be mediated by clozapine. This issue is investigated further in Chapter 4.

Some of the electrophysiology experiments presented in this chapter had small sample sizes of 2 rats, from which multiple slices were used to record from. Slices were chosen as the unit because the DREADD expression and spread was varied throughout the AP and DV axes of the hippocampus such that even within the same rat, responses could be different depending on the level of transfection in the particular slice and thus be a representative of a population.

Nonetheless, even using a small number of rats, it was enough to reach statistical significance suggesting the effect was strong and reproducible between slices.

2.4.6 Interneuron activation as an alternative approach to pyramidal neuron silencing

A final experiment investigated the possibility of using DREADDs to inhibit pyramidal neurons by targeting hippocampal GABAergic interneurons. These experiments used a Gq-DREADD viral construct driven by a hDlx promoter which specifically targets interneurons (Dimidschstein et al., 2016). It was found that CNO evoked a suppression of fEPSP in hippocampal slices expressing hDlx promoter-driven Gq-DREADD with a magnitude of effect comparable to that of CNO in Gi-DREADD expressing slices. Although small, this study suggests that hDlx driven Gq-DREADD could be a useful tool *in vivo* to inhibit hippocampal function either alone or complementary to the application of a CaMKIIa promoter driven Gi-DREADD.

2.4.7 Conclusions

Data presented in this chapter show the successful delivery of Gi- and Gq-DREADDs to principal neurons in the rat dorsal hippocampus using CaMKIIa promoter driven AAV vectors. Moreover, electrophysiological measurements of synaptic transmission in hippocampal slices confirmed the functionality of the Gi-DREADD construct, and that not only CNO but also clozapine acted as agonists. The latter observation reinforces recent evidence that any reverse metabolism of CNO to clozapine may lead to DREADD effects triggered by clozapine. Interestingly, under the present conditions, the Gq-DREADD construct was also found to exert an inhibitory effect on synaptic transmission when activated by CNO. Pharmacological experiments ruled out an involvement of either $GABA_{A/B}$ and $mGluR_{2/3}$ receptors in this paradoxical effect, and the possible role of cannabinoid and even non-canonical Gq-coupled

mechanisms is discussed. Overall, these experiments emphasise the importance of carrying out studies of DREADD expression and function at the cellular level prior to embarking on *in vivo* investigations, which are reported in the next chapter of this thesis.

Chapter 3

DREADDs as tools to modulate learning and memory behaviour

3.1 Introduction

Experiments in the previous chapter presented evidence for functionality of an inhibitory DREADD, whereby the Gi-DREADD decreased excitatory transmission in hippocampal slices upon CNO and clozapine application. No changes were observed in slices expressing a control construct. Thus, the current chapter interrogates hippocampal function *in vivo* at the behavioural level. DREADDs have been used to deconstruct neural circuitry of various behaviours such as feeding (Atasoy et al., 2012; Carter et al., 2013; Kong et al., 2012; Krashes et al., 2011; Zhan et al., 2013), modulation of circadian rhythms (Brancaccio et al., 2013; Sasaki et al., 2011) but also to investigate the neural basis of cognition, memory or emotions (Giannotti et al., 2019; Li et al., 2013; Silva et al., 2013; Tipps et al., 2018; Tuscher et al., 2018). While DREADDs have proven to be a useful tool to study brain function in basic research, from a translational perspective, the use of a suitable behavioural task answering the scientific question is as important as the chemogenetic tool asking the question.

3.1.1 Hippocampal dependent cognitive tasks

In humans the hippocampus is thought to be important for episodic memory formation and processing (Bird & Burgess, 2008), while in rodents the hippocampus is widely regarded as the origin of the 'cognitive map' that aids the animal to spatially navigate its environment (Moser et al., 2008; O'Keefe & Dostrovsky, 1971). However, this is an overly simplified, textbook description of its function. Although the hippocampus is involved in some types of memory, it is widely recognised that it also plays a role in emotional processing (Bannerman et al., 2003; Fanselow & Dong, 2010). Specifically, the dorsal hippocampus is mostly involved

in spatial functions, while the ventral hippocampus has also been implicated in aspects of emotionality - lesions of the ventral hippocampus decreased anxiety but did not impact performance on spatial memory tasks (Bannerman et al., 2003).

Generally, the spatial memory domain of the hippocampus is tested in variations of either an open field water maze or in radial mazes (Bannerman et al., 2014). Both tasks provide a measure of spatial reference memory (SRM), also regarded as long-term memory but both mazes can also be adapted to assess spatial short-term/working memory (SWM). SRM is traditionally tested in the Morris water maze (MWM), where the animals are forced to swim to find a sub-merged platform the animal having to form spatial cue associations to guide itself to the platform. The platform is removed in a subsequent probe trial when the animals are expected to spend more time exploring the quadrant where the platform was initially positioned. SRM can also be tested on radial mazes when the animal is trained to follow the same rule, trial after trial and creating a 'reference memory' by doing so (Deacon & Rawlins, 2006).

However, these tasks can be adapted to test SWM. In the context of dry-land, appetitively motivated mazes, the animal is trained to refrain from going into a previously visited arm (i.e. win-shift mazes). This is motivated by rewards and a trial is made up of a sample and choice run. For example, in the reward alternation T-maze task, the rat is forced to collect the reward in one arm during the sample phase. After an intra trial interval (ITI), the rat is returned to the start arm and allowed to make a choice between the two goal arms, only the previously unvisited (novel) arm being rewarded (Deacon & Rawlins, 2006). In the spatial novelty preference Y-maze task, the rat is only motivated by novelty (i.e. by exploration and foraging behaviour), the task being based on spontaneous alternation which is an innate rodent behaviour. Specifically, the animal is allowed to explore two arms of the maze during a sample phase. Following an ITI, the animal is returned to the maze and allowed to explore all three

arms. Thus, the animal is expected to spend more time exploring the previously unvisited arm (novel) (Barkus et al., 2014). The ITI represents the short-term memory component in the spatial novelty preference Y-maze or the 'working memory' component of the rewarded alternation T-maze, where animals must keep the newly acquired information on-line, and make their next decision based on their previous choice. As a result, increasing the ITI will subsequently increase the difficulty of the task. In rewarded alternation tasks, the animals are usually tested in blocks of several trials. Depending on the number of trials in one block, the memory acquired from a recent trial that is not relevant anymore can lead to errors and subsequently makes the task more difficult (Deacon & Rawlins, 2006). Rewarded alternation T-maze tasks could also be solved on the basis of relative familiarity as described more below.

While these tasks and SRM tasks are sensitive to hippocampal lesions (Deacon et al., 2002; Sanderson & Bannerman, 2012), they might not always be sensitive enough to detect a more subtle manipulation of hippocampal function at the behavioural level. For example, *Gria1* KO animals (AMPA deficient GluA1 subunit) which exhibit impaired hippocampal LTP (Zamanillo et al., 1999) show normal SRM but impaired SWM (Reisel et al., 2002). A task that allows for adaptations and increasing levels of difficulty is the reward alternation T-maze task which also has the potential to detect more subtle changes in hippocampal function, as shown by Bannerman *et al*., (1999) who reported higher sensitivity to hippocampal lesions in terms of effect sizes on the T-maze task compared to the water maze for example (Bannerman *et al*., 1999). Evidence from muscimol micro-infusion studies in the dorsal hippocampus also showed chance performance on the rewarded alternation T-maze task compared to sham rats (McHugh et al., 2008). Taken together, these reports suggest that the rewarded alternation T-maze task is a hippocampal sensitive task that could detect subtle changes in hippocampal function.

3.1.2 Short-term habituation, novelty and the hippocampus

Historically, habituation has been described as the 'simplest form of learning' (Thompson & Spencer, 1966) and it is considered to be the ability to ignore old stimuli that one has been exposed to and instead focus on newer stimuli that might provide new information. For rodents in the wild, this new information can be vital as it can come in the form of food, mate or predators. Specifically, spatial stimuli in a new environment will elicit a response in the animal that will lead to increased exploration. After a period of time in which the stimuli remain the same, the exploratory behaviour will decline as the animal gets habituated to the surroundings. More recently, Sanderson and Bannerman have proposed alternating behaviour seen in rodents as a form of short term habituation to spatial stimuli (Sanderson & Bannerman, 2012).

In the context of a reward alternation T-maze task, whilst the two alternating arms become gradually more familiar across trials, for a short period of time, during the ITI, one arm will be more familiar relative to the other. This implies that the animal is more habituated to the most recently visited arm and when allowed a free choice, it will choose to explore the previously unvisited arm. Thus, while alternation can be viewed as a form of working memory by which the animal has to actively hold the memory of the information over a short period of time and base their next decision on this prior information (analogous to human working memory), it could also be solved on the basis of relative familiarity through short-term habituation processes (Sanderson & Bannerman, 2012). In a novel environment, it may be more likely that the task is solved based on relative familiarity, with the animal solving the task more like a novel object recognition (NOR) task. To this end, rats with dorsal hippocampal deficits may be expected to show impaired performance in the novel room even if the performance in a familiar room is intact.

Hippocampal lesioned rats perform poorly in spatial working memory tasks and show novelty induced hyperactivity and deficits in novelty preference (Bannerman et al., 1999; Rawlins & Olton, 1982) while rats with muscimol infusions in the dorsal hippocampus also show chance performance in a working memory task (McHugh et al., 2008). Animals lacking the GluA1 subunit of the AMPA receptors which results in decreased fEPSPs and impaired hippocampal LTP (Romberg *et al*., 2009) are also hyperactive in a novel environment (Bannerman et al., 2004), have impaired alternating behaviour but in contrast to lesioned animals, associative spatial learning is spared (Zamanillo et al., 1999). Based on the above phenotypes as a consequence of different hippocampal manipulations, we hypothesised that rats expressing an inhibitory DREADD in excitatory neurons of the dorsal hippocampus might have impaired SWM on the T-maze.

3.1.3 Chapter 3 experimental aims

Experiments in this chapter aimed to investigate the involvement of hippocampal excitatory transmission in spatial working memory while assessing the functionality of an inhibitory DREADD *in vivo* in response to CNO or clozapine administration. Rats were tested on a rewarded alternation task, a novelty preference task and novelty induced hyperlocomotion was also assessed under various conditions.

3.2. Materials and Methods

All experiments described in this chapter have been carried out at the University of Oxford.

3.2.1. Animals

All animal experiments performed were in compliance with the UK Home Office Animals (Scientific Procedures) Act of 1986, and a Local Ethical Review Committee at The University of Oxford. Male Lister Hooded rats (Envigo, Bicester, UK), weighing between 250-300g on arrival were kept under environmentally controlled temperature (20 ± 2ºC) with *ad libitum* access to food and water unless stated otherwise. Rats were allowed to acclimatise for at least a week following arrival to the animal facility and were housed in open top polycarbonate cages with wire lids and kept on a 12h light/dark cycle (lights on at 07:00). Sawdust was used as bedding and cages were environmentally enriched with a cardboard house.

3.2.2 Viral constructs

For the experiments described in this chapter, the DREADDs were originally created by Bryan Roth and were purchased from UNC Vector Core (University of North Carolina) for the rewarded alternation T-maze cohort, and from Addgene for the spatial novelty preference Y-maze cohort. More details can be found in the table below (**Table 3.1**).

Name	Supplier	Experimental cohort	Number of rats injected (used after exclusions)	Titre (vector genomes /ml)
AAV5-CaMKIIa-mCherry	UNC Vector Core	Reward alternation T-maze & LMA	n=7 (7)	≥3 x 10^{12} vg/ml
AAV5-CaMKIIa-hM4D(Gi)-mCherry	UNC Vector Core	Reward alternation T-maze & LMA	n=7 (4)	≥3 x 10^{12} vg/ml
AAV5-CaMKIIa-EGFP	Addgene (#50469)	Spatial novelty preference Y-maze & LMA	n=8 (8)	4.3 x 10^{12} vg/ml
AAV5-CaMKIIa-hM4D(Gi)-mCherry	Addgene (#50477)	Spatial novelty preference Y-maze & LMA	n=8 (8)	4.4 x 10^{12} vg/ml

Table 3.1: Experimental details for the viral constructs used at The University of Oxford (LMA: locomotor activity)

3.2.3 Intracerebral viral injection

Delivery of the viral construct to the neuronal population of choice in the dorsal hippocampus was performed as described in Chapter 2 (see **2.2.3**). Briefly, anaesthesia was induced and maintained throughout the surgery with isoflurane. The skull was exposed and 4 small holes were drilled above the dorsal hippocampus to enable intracranial injections at the following stereotaxic coordinates relative to brain surface (i, ii) AP -3.6 mm, ML ±3 mm, DV -3 mm, iii, iv) AP -3.6 mm, ML ±3 mm, DV -2.2 mm, v, vi) AP -3.6 mm, ML ± 2 mm, DV -2.0 mm). A maximum on 1 µl of viral construct was injected per hemisphere using an injection pump (Micro 4, Microsyringe Pump Controller, World Precision Instruments), evenly distributed between

the 6 sites of injection. The scalp was sutured, and rats were administered peri and post-operative care as described in the previous chapter (see **2.2.3**). Rats were allowed to recover for at least a week before being placed on food restriction (reward alternation T-maze cohort). All experiments were done 2-3 weeks post-stereotaxic injection to allow for an appropriate level of expression of the DREADDs.

3.2.4 Drugs

Both CNO and clozapine (Tocris Biosciences, Bristol, UK) were freshly prepared on the experimental day. CNO (3 mg/kg) was dissolved in sterile saline solution and administered i.p. in a 1 ml/kg volume. Clozapine, 0.1 or 0.5 mg/kg was dissolved in sterile saline and 0.3% or 4% DMSO respectively (VWR International) with continuous vortexing. Once dissolved, it was administered i.p. in a 1 ml/kg volume. Vehicle was saline solution with the respective percentage of DMSO required for dissolving clozapine.

Drug doses used were chosen based on previous studies. Specifically, to avoid any risk of back metabolism to clozapine, CNO was recommended to be used in rats and mice in doses of up to 3 mg/kg. In addition to this, the dose of 3 mg/kg was chosen based on studies that have successfully used CNO as a DREADD agonist in rat (Ferguson et al., 2011; Yau & McNally, 2015). Clozapine (0.1 mg/kg) was used as suggested by a study that reported no non-DREADD specific effects of this specific low dose of clozapine in rats in a locomotor activity task (in comparison to 1 mg/kg) (Gomez et al., 2017). The higher dose of clozapine (0.5 mg/kg) was chosen based on the results obtained using 0.1 mg/kg clozapine.

3.2.5 Reward alternation T-maze

The task described below was done under the guidance of Dr. Chris Barkus and was based on the task described here (Deacon & Rawlins, 2006). SWM was tested on a rewarded alternation T-maze task in the presence of CNO or vehicle. The apparatus was a grey wooden elevated (approximately 1 m from the ground) plus maze with one arm blocked so it became a T-maze (all arms were open, 3 cm height of the edges, 61 cm length of arms, 10 cm width). The maze was wiped clean after each run to prevent the animals from using olfactory cues. A trial was made up of one sample and one test run. During the sample run, one arm of the maze was blocked and the rat was forced to run out of the start arm and into the open arm to collect the condensed milk reward (Nestlé®), 1:1 volume in drinking water, in small metal wells. For the test run, the divider was removed, the rat was placed on the start arm facing away from the maze and was allowed a free choice but only the 'novel' arm (the previously unvisited arm) was rewarded. A correct trial was marked when the rat entered the novel arm first with all four paws. The number of correct trials and latency to centre (choice point) and latency to reward were recorded using an event timer. The task consisted of a few stages described below: handling, food deprivation, habituation, training (pre-surgery), surgery, training (post-surgery), testing, re-training, testing.

Rats were handled for 1-2 weeks prior to the beginning of the experiment to minimise stress. During this time rats were also habituated to the reward in the home cage. This was repeated until the rats were comfortably eating the reward. Next, rats were placed on food restriction and kept at 85-90% of their free feeding weight. Rats were then habituated to the maze, first in groups followed by individual exposure. During this phase, all arms were rewarded, and rats were left on the maze until they ate from all the wells but for no longer than 3 min. Rats were then trained on the maze for 1-2 weeks for as many days as necessary until they achieved

approximately 80% correct performance. Over the training period, each animal had a total of at least 50 trials on the maze.

Animals were placed back on free food, before the intracerebral viral injection and until they recovered before putting them back on food restriction. For surgeries involving the hippocampus, it was important to re-train the rats and ensure that performance had not changed as a consequence of intrahippocampal injections. Thus, rats were re-trained, in blocks of 10 trials, to make it comparable to the test day design, alternating between two littermates and until their performance reached the same level as before the surgery. Once this was achieved, testing began. The goal arm identity on the sample run was counterbalanced with an equal number of left/right directions per session and not more than 3 consecutive runs in the same direction. Rats were paired (one Gi-DREADD and one mCherry-control) and were injected with CNO (3 mg/kg, i.p.) 30 minutes prior to testing. The rats in the pair were then tested in alternation and in blocks of 10 trials (sample + test run), meaning the time between trials was approximately 2 minutes while the intra-trial interval (ITI) was of approximately 30s – the time it took to remove the block and clean the maze. During the ITI the rats were placed in an empty temporary cage. Finally, after each testing day there was a washout re-training day to ensure performance has returned to baseline, followed by a pre-drug training day, again to ensure optimal performance before further testing. Using the same protocol, the rats were also tested in a novel room with a new set of extramaze spatial cues, to assess whether they exhibit similar performance to the familiar room. As the scoring of the rats' performance was done by an experimenter during the task, it was important that the experimenter was blinded to treatment and construct type the rats were expressing in order to minimise bias. Thus, the experimenter was handed syringes filled with either CNO or saline, that were not distinguishable were directly labelled with the rat number by a colleague in the morning of each experimental day.

3.2.6 Spatial novelty preference Y-maze

The task described below was done under the guidance of Dr. Chris Barkus and followed a similar protocol to the one described here (Sanderson et al., 2009). Spatial short-term memory was tested on a transparent Plexiglass Y-maze (50 cm length of arms, 17 width, 30 cm height of walls) placed on the ground in a room with prominent distal extra-maze cues. The bottom of the maze was covered with a mixture of clean and dirty sawdust from unfamiliar rats to promote exploratory behaviour. In the sample phase, one arm was blocked and the rats were allowed to explore for 5 min, timed from when the rat has left the start arm. The allocation of novel *vs.* familiar arm was counterbalanced between rats, but the start arm was kept constant. Hereinafter, the familiar arm was considered the one choice arm that the rat was allowed to explore during the sample phase (other than the start arm). After the sample phase, the rat was removed and temporarily placed in an empty cage for a few seconds while the divider was removed, and the sawdust mixed around the maze to prevent rats from using these olfactory cues. The rat was then returned to the start arm, facing the investigator and allowed access to all arms for 2 min. The movement of the rat was tracked with ANY-maze (Stoelting Co, Ireland) but scoring was done manually using an event timer. The preference for the novel arm was calculated as a discrimination index - the ratio between the time spent in the novel arm divided by the total time spent in the novel and familiar arms. The number of entries in each arm was also recorded. A rat was considered to have entered an arm if all four paws were in the specific arm. Rats expressing a hippocampal Gi-DREADD or EGFP-control were injected with clozapine (0.1 mg/kg i.p.) or vehicle 30 min prior to testing. A washout period of 72h was allowed between drug/vehicle injections and re-testing of the rats on the Y-maze. The investigator was blinded to treatment, and to construct type expressed by the rats, as described above for the rewarded alternation T-maze task (see **3.2.5**).

3.2.7 Novelty-induced locomotor activity

The task described below was done under the guidance of Dr. Chris Barkus and followed a similar protocol to the one described here (Bygrave et al., 2019). To check for novelty-induced hyperactivity in the Gi-DREADD expressing rats upon injection of either CNO or clozapine, rats were placed in transparent plastic photocell cages (43 cm length x 22 cm width x 20 cm height) 20 min post i.p. injection. The bottom of the cages was covered with clean sawdust and the number of infrared beam breaks was recorded automatically over 2 h in 5-min time bins (San Diego Instruments, San Diego, USA). Rats were tested on two days to allow for within-subject drug effect comparisons with a minimum of 48h between injections for washout. The time of day, the order of injection and the test boxes were counterbalanced. As above, to reduce bias, the experimenter was blinded to treatment and type of construct expressed by the subjects. This was achieved by a colleague preparing the syringes containing either treatment or vehicle and numbering them with the rat number each treatment was assigned to.

3.2.8 Histology

At the end of the experiments, the rats were transcardially perfused with PBS followed by PFA 4% to confirm the presence, extent and location of the viral construct post-hoc. The brains were dissected and kept in PFA 4% solution over night at 4ºC. Brains were then transferred to a 30% sucrose solution to ensure cryoprotection before slicing them on a cryostat (Bright Instruments, UK) at -20ºC. Free-floating (30 µm) hippocampal sections were collected in PBS. Sections were then mounted onto slides and cover-slipped using Vectashield (Vector Labs, USA). Slides were imaged and the expression of mCherry or EGFP was visualised using an epifluorescent microscope (DM-500B, Leica Microsystems, Wetzlar, Germany). Acquired images were exported into Image J (NIH) for further processing. Rats showing unilateral or no expression were excluded from the behavioural analysis, with the exception of one control rat

from the T-maze cohort that displayed unilateral expression of the mCherry-control construct. As these constructs lack the mutated receptor that binds CNO, no effect of the viral construct *per se* was expected, so the data from the rat was included in the analysis.

3.2.9. Statistical analysis

All data in this chapter were analysed using GraphPad Prism 7 (GraphPad Software, Inc., San Diego, CA) or SPSS Statistics. Ordinary and repeated measures 2-way ANOVAs were used to analyse the locomotor activity and the behavioural data from the mazes. One sample t-test against a fixed ratio of 0.5 was used to assess the performance against chance levels in the T-maze and Y-maze. Significance was set at a P value of $p<0.05$.

3.3 Results

3.3.1 Spatial working memory in Gi-DREADD expressing rats in a familiar room

The spatial working memory of Gi-DREADD expressing rats was tested on a rewarded alternation T-maze task in the presence of CNO (3 mg/kg). The experimental design is illustrated in **Figure 3.1 A, B.** The rats were trained on the maze before and after stereotaxic viral injection to confirm normal hippocampal function post-injection. Task performance was expected to be submaximal (around 80-90%) on the rewarded alternation task. This was confirmed by the pre and post-surgery training (**Figure 3.1C**).

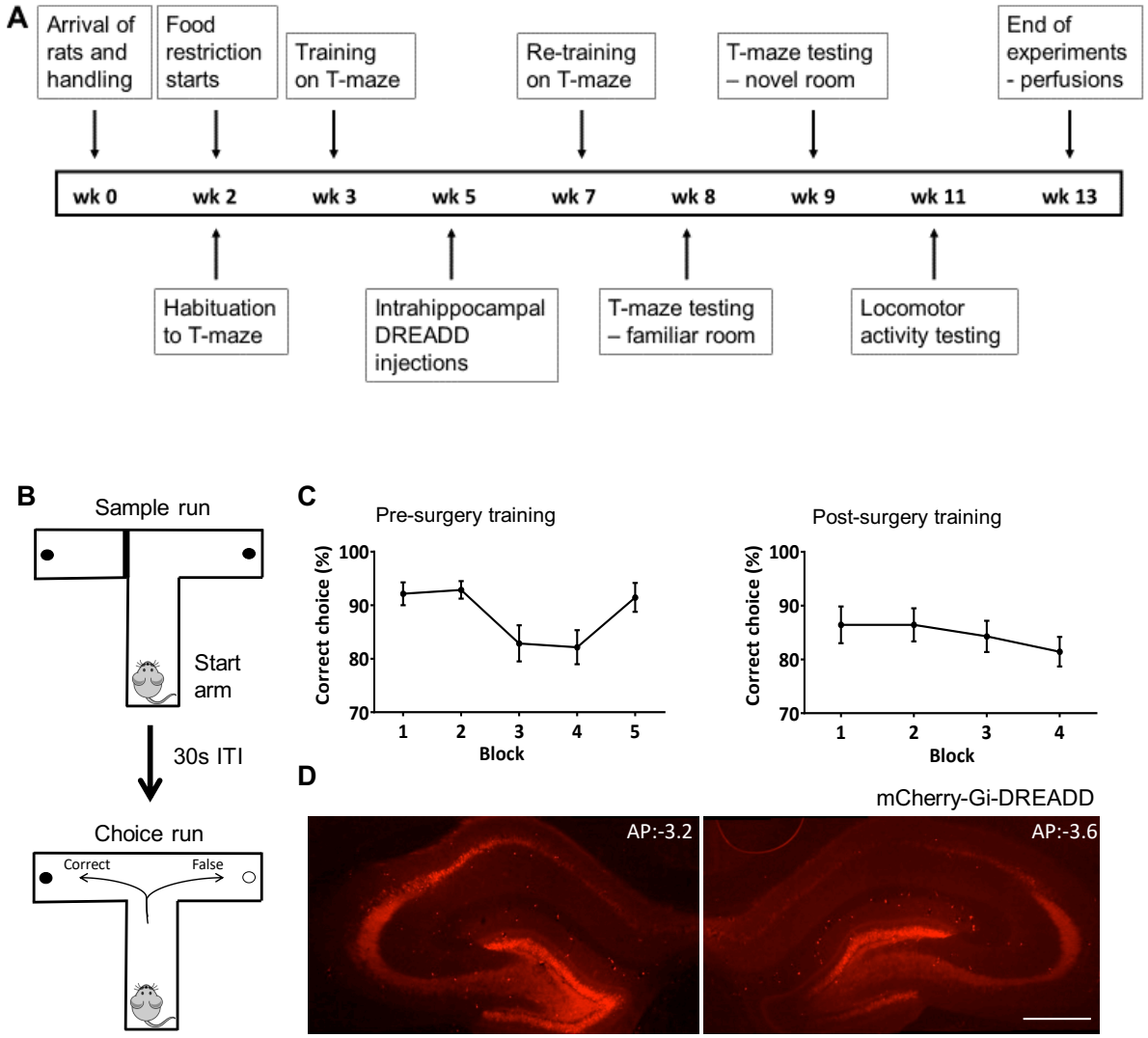


Figure 3.1: Reward alternation T-maze experimental design.

(A) Experimental design and timeline used for the T-maze cohort (B) Typical trial structure during the reward alternation T-maze task (ITI: intra-trial interval). (C) Pre-surgery training (left) and post-surgery training on the T-maze (right). Data shown as mean of 10 trials per block ± SEM values. Chance performance represents 50%. (D) Representative epi-fluorescence images of mCherry-Gi-DREADD (red) expression and spread in the dorsal hippocampus from one rat of the cohort. Scale bar = 500 µm.

The results showed normal working memory in a familiar room, regardless of treatment or viral construct expressed as revealed by the statistical analysis (**Figure 3.2**). A percentage of correct choices out of each block of 10 was calculated for the test days. A two-way ANOVA with construct type as a between subject factor and treatment (CNO, 3 mg/kg or saline) as a within-subject factor revealed no significant effect of the construct type ($F(1, 9) = 3.369$, $P = 0.0996$), the treatment ($F(1, 9) = 0.1519$, $P = 0.7058$) or the interaction, construct*treatment

(F(1, 9) = 0.3284, P = 0.5806) on the task performance (**Figure 3.2A**). All but one group (Gi-saline) displayed performance levels that were significantly above chance levels as revealed by one sample t-test analysis against chance performance (50% correct) (EGFP-saline: t(6) = 5.667, P = 0.0013; EGFP-CNO: t(6) = 5.435, P = 0.0016; Gi-saline: t(3) = 2.121, P = 0.124; Gi-CNO: t(3) = 7.833, P = 0.0043). This may be explained by the amount of variance observed in the Gi-saline group.

Latency to reward was also recorded (in deciseconds) but no changes in locomotor behaviour were observed in the presence of CNO in the two groups. Two-way ANOVA with construct type as the between subject factor and treatment as a within-subject factor revealed no significant effect of the construct type (F(1, 9) = 0.0006864, P = 0.9797), the treatment (F(1, 9) = 0.2852, P = 0.6063) or the interaction construct*treatment (F(1, 9) = 2.129, P = 0.1786) on the latency to collect the reward (**Figure 3.2B**).

The data suggest that silencing a population of excitatory neurons in the dorsal hippocampus does not affect task performance on a rewarded alternation T-maze task. The results also confirm that CNO (3 mg/kg) *per se* does not cause any off-target effects in the EGFP-control group.

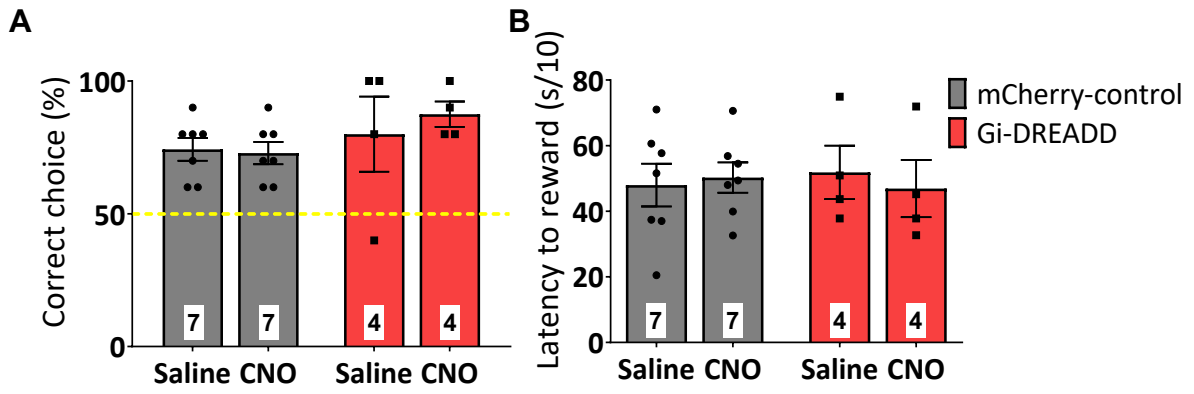


Figure 3.2: Rewarded alternation behaviour of Gi-DREADD expressing rats upon CNO administration in a familiar room

(A) Percentage of correct choices from a block of 10 trials on the T-maze in a familiar environment. Results were analysed from n=7 mCherry-control rats (grey) and n=4 Gi-DREADD expressing rats (red) upon CNO (3 mg/kg) or saline injection i.p., in a within-subject control design. Dotted yellow line represents chance performance level. Data are shown as mean ± SEM values (B) Latency to reward in the test phase is expressed in deciseconds (s/10). Data expressed as mean ± SEM values.

3.3.2 Spatial working memory in Gi-DREADD expressing rats in a novel room

Next, performance on the same task (same apparatus) was measured in a novel room. As rats had been extensively trained in the familiar room, they may have been highly efficient at attending to the appropriate spatial cues in the familiar environment. Thus, to increase the difficulty of the task, SWM was assessed in the context of a novel room. The hypothesis was that Gi-DREADD expressing rats will now exhibit decreased task performance on the maze in a novel room in the presence of CNO despite normal performance in the familiar room.

Contrary to expectations, both groups performed similarly and above chance on the task in a novel room regardless of treatment. A two-way ANOVA with construct type as a between subject factor and treatment as a within-subject factor revealed no significant effect of the construct type ($F(1, 9) = 0.05861$, $P = 0.8141$), the treatment ($F(1, 9) = 0.01494$, $P = 0.9054$) or the interaction, construct*treatment ($F(1, 9) = 3.361$, $P = 0.1$) on task performance (**Figure 3.3A**). All groups displayed performance levels that were significantly above chance levels as

revealed by one sample t-test analysis against chance performance (50% correct trials) (EGFP-saline: t(6) = 15.88, P < 0.0001; EGFP-CNO: t(6) = 6.935, P = 0.0004; Gi-saline: t(3) = 13, P = 0.001; Gi-CNO: t(3) = 9.798, P = 0.0023).

Latency to reward was recorded (in deciseconds) but no changes in locomotor behaviour were observed in the presence of CNO in the two groups in the novel room. A two-way ANOVA with construct type as a between subject factor and treatment as a within-subject factor revealed no significant effect of the construct type (F(1, 9) = 2.434, P = 0.1513), the treatment (F(1, 9) = 0.1158, P = 0.7414), but a significant interaction of construct*treatment (F(1, 9) = 6.594, P = 0.0303) on the latency to collect the reward (**Figure 3.3B**). A Sidak's post hoc test did not reveal any further significant differences based on treatment or group.

Nevertheless, overall these data give no indication of deficits in short-term working memory in Gi-DREADD expressing rats upon CNO injection and indicate a different effect of treatment on the latency to reward of the two groups depending on viral construct expressed.

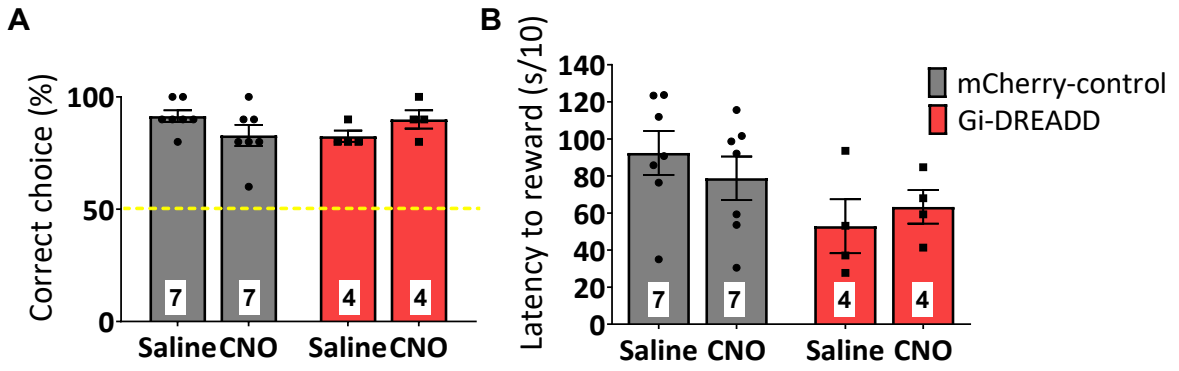


Figure 3.3: Rewarded alternating behaviour of Gi-DREADD expressing rats upon CNO administration in a novel room

(A) Percentage of correct choices from a block of 10 trials on the T-maze in a novel environment. Results were analysed from n=7 CTRL-DREADD rats (grey) and n=4 Gi-DREADD expressing rats (red) upon CNO (3 mg/kg) or saline injection i.p., in a within-subject control design. Dotted yellow line represents chance performance level. Data are shown as mean ± SEM values (B) Latency to reward in the test phase expressed in deciseconds (s/10). Data expressed as mean ± SEM values.

Finally, the rats were tested for novelty induced hyperactivity as this in itself can be a measurement of hippocampal dysfunction. No changes in locomotor activity were recorded upon CNO administration in any of the groups. A repeated measures 2-way ANOVA with viral construct as the between subject factor and time and treatment as within-subject factors revealed no effect on the number of beam breaks based on viral construct expressed ($F(1, 9) = 0.081$, $P = 0.783$), the treatment ($F(1, 9) = 2.377$, $P = 0.158$) or the interaction of construct*treatment ($F(1, 9) = 3.48$, $P = 0.095$). The number of beam breaks decreased significantly over time ($F(23, 207) = 76.119$, $P<0.0001$) but there was no significant effect of construct*time interaction ($F(23, 207) = 1.173$, $P = 0.273$), treatment*time interaction ($F(23, 207) = 1.027$, $P = 0.433$) or construct*treatment*time interaction ($F(23, 207) = 0.618$, $P = 0.914$; **Figure 3.4**). These data show that reducing the pyramidal neuron excitability in the dorsal hippocampus does not alter locomotor activity compared to control rats.

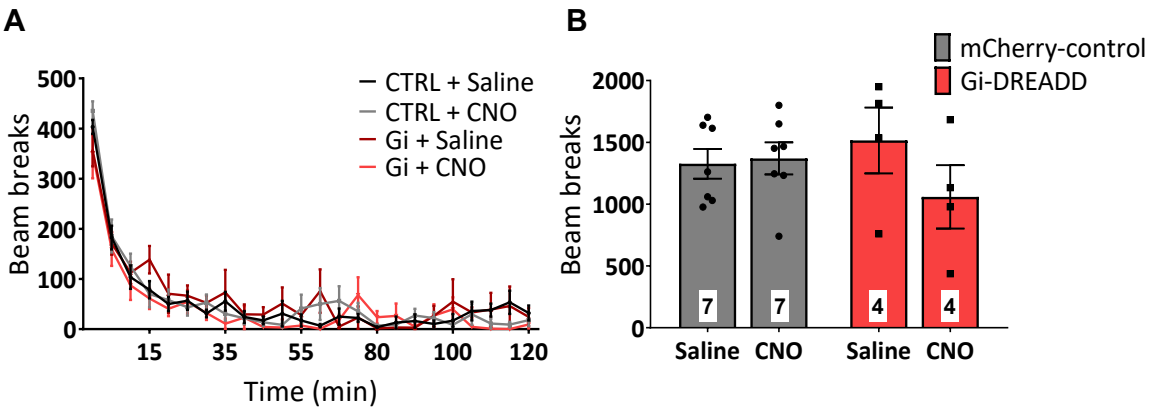


Figure 3.4: CNO induced activation of hippocampal Gi-DREADD does not alter locomotor activity

(A) Locomotor activity presented in 5-min time bins over 2h, as means ± SEM values of n=7 CTRL-DREADD rats (grey and black) and n=4 Gi-DREADD (red and dark red). (B) Total beam breaks over 2h for each treatment group. Data shown as mean ± SEM values.

3.3.3 Spatial novelty preference in Gi-DREADD expressing rats in the presence of clozapine

Short-term memory was also assessed in a spatial novelty preference Y-maze task. The task was based on the innate preference of rats for novelty and required no prior familiarisation (see experimental design in **Figure 3.5A, B**). To this end a new cohort was injected with either Gi-DREADD or a control construct bilaterally in the dorsal hippocampus as described previously. The literature at the time of the experiments was suggesting that CNO is not brain permeable and in fact it is clozapine that crosses the BBB and readily activated the DREADDs. As slice experiments presented in the previous chapter demonstrated that clozapine is indeed a DREADD activator, the ability of clozapine to modulate hippocampal function *in vivo* was assessed rather than CNO. A sub-threshold dose of clozapine (0.1 mg/kg) was used, as suggested by Gomez and colleagues who reported no non-DREADD specific effect of clozapine in a locomotor activity task (Gomez et al., 2017).

The results showed no differences in novelty preference between the two groups independent of treatment, although performance levels on the task overall were low. A two-way ANOVA with construct type as a between subject factor and treatment (CLZ 0.1 mg/kg or vehicle) as a within-subject factor revealed no significant effect of the construct type ($F(1, 14) = 0.01827$, $P = 0.8944$), the treatment ($F(1, 14) = 1.343$, $P = 0.2659$) or the interaction, construct*treatment ($F(1, 14) = 0.1373$, $P = 0.7165$) on the novelty preference over the 2 min test phase (**Figure 3.5C**).

None of the groups, including the control group, displayed a significant preference for the novel arm and performed at chance levels as revealed by one sample t-tests against chance performance (ratio of 0.5) (EGFP-vehicle: $t(7) = 0.7971$, $P = 0.4516$; EGFP-clozapine: $t(7) = 1.908$, $P = 0.0981$; Gi-vehicle: $t(7) = 0.7759$, $P = 0.4632$; Gi-clozapine: $t(7) = 1.727$, $P = 0.1277$).

Thus, an analysis of only the first minute of exploration in the test phase was performed, to check whether the novelty preference had diminished after the first minute of exposure.

The analysis for the first minute confirmed that the vehicle treated control group did now display above chance levels of performance as shown by a one sample t-test against chance (ratio of 0.5) performance ($t(7) = 3.858$, $P = 0.0062$). The other groups did not display novel arm preference ratios significantly above chance performance level (EGFP-clozapine: $t(7) = 2.166$, $P = 0.067$; Gi-vehicle: $t(7) = 0.2643$, $P = 0.7992$; Gi-clozapine: $t(7) = 1.474$, $P = 0.184$). In the first minute of analysis the results showed that the EGFP-control group performed significantly better compared to the Gi-DREADD group (independent of treatment) as revealed by a statistical analysis. A two-way ANOVA with construct type as a between subject factor and treatment as a within-subject factor revealed a significant effect of construct type ($F(1, 14) = 13.24$, $P = 0.0027$), but no effect of the treatment ($F(1, 14) = 0.1533$, $P = 0.7013$), nor the interaction of construct*treatment ($F(1, 14) = 0.6897$, $P = 0.4202$) on the novelty preference task over the first minute of test phase (**Figure 3.5D**). To check whether the effect of construct was due to carry-over effects from the first injection given the within-subjects design, an analysis of the first day of the experiment only was carried out that revealed a similar performance profile (Gi-DREADD + vehicle performance at chance level, data not shown). Thus, Gi-DREADD injected animals were significantly impaired on the Y-maze spatial novelty preference task, but this was independent of whether they had been injected with either vehicle or clozapine.

Finally, as locomotor activity during the exposure phase can impact on task performance in the test phase, an analysis of the distance travelled during the 5 min sample period was performed. However, no differences were found between the groups. A two-way ANOVA with construct type as the between subject factor and treatment as the within-subject factor

revealed no significant effect of the construct type ($F(1, 14) = 1.051$, $P = 0.3226$), treatment ($F(1, 14) = 2.925$, $P = 0.1093$) or the construct*treatment interaction ($F(1, 14) = 4.431$, $P = 0.0538$) on the distance travelled during the sample phase (**Figure 3.5E**).

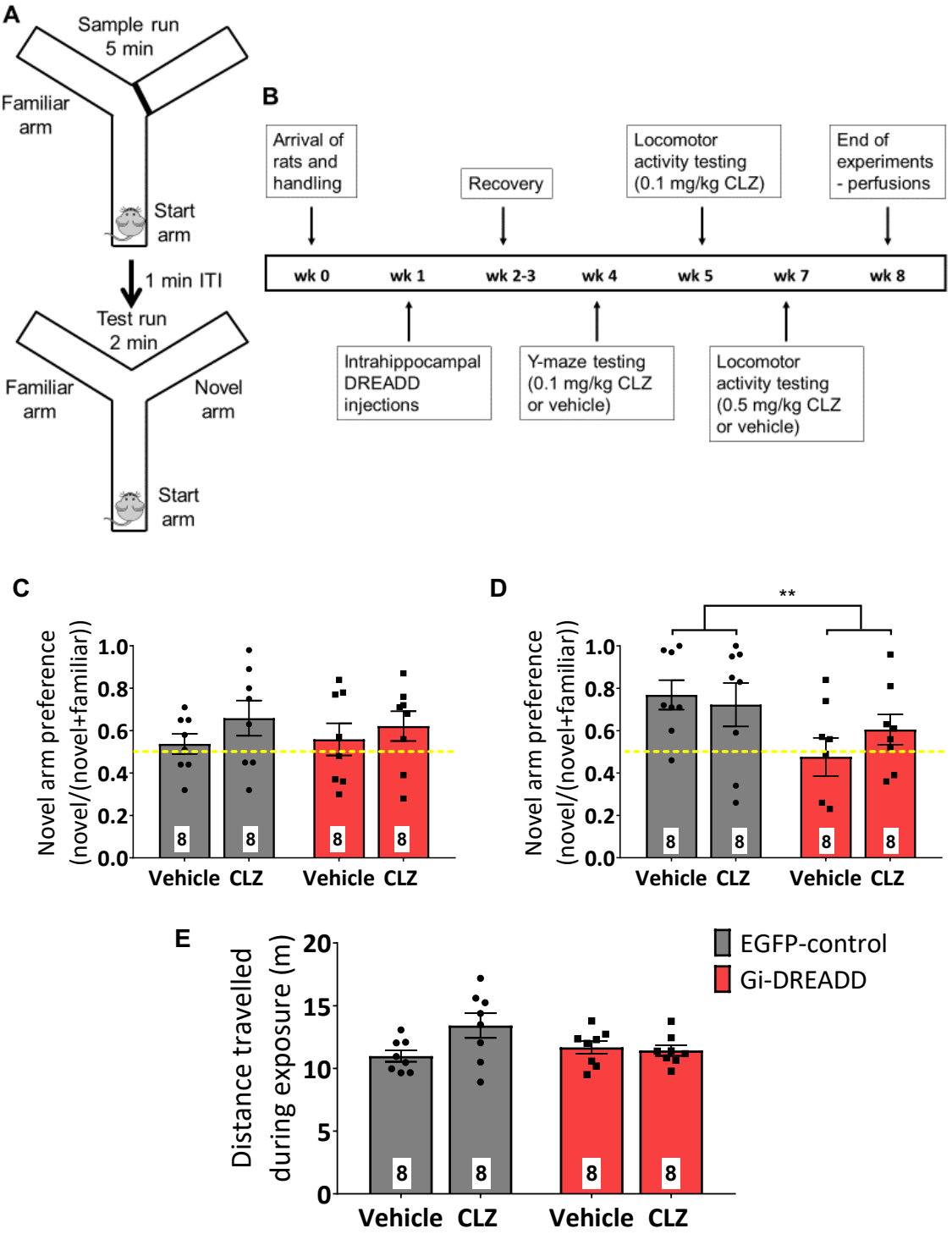


Figure 3.5: Spatial working memory in Gi-DREADD expressing rats in the presence of clozapine

(A) Experimental design for spatial novelty preference Y-maze (ITI: intra-trial interval) (B) Experimental timeline for the Y-maze cohort (CLZ: clozapine) (C) Novel arm preference ratio (time spent in novel arm/(time spent in familiar arm + time spent in the novel arm) over 2 min test phase (D) Novel arm preference ratio (time spent in novel arm/(time spent in familiar arm + time spent in the novel arm) over the first minute of test phase. **P=0.0027 (2-way ANOVA). Dotted yellow line represents chance performance level. (E) Total distance travelled during the exposure phase (5 min). Data are shown as means ± SEM values (n=8 per group).

3.3.4 Novelty induced locomotor activity in the presence of clozapine

The novelty induced locomotor activity of this cohort was also assessed in response to clozapine. No changes in locomotor activity were recorded upon clozapine administration in any of the groups. A repeated measures 2-way ANOVA with viral construct as the between subject factor and time and treatment as within-subject factors revealed no effect on the number of beam breaks based on the viral construct expressed ($F(1, 14) = 0.097$, $P = 0.76$), the treatment ($F(1, 14) = 1.339$, $P = 0.267$) or the interaction of construct*treatment ($F(1, 14) = 0.001$, $P = 0.978$). The number of beam breaks decreased significantly over time ($F(23, 322) = 126.464$, $P<0.0001$) and there was a significant effect of treatment*time interaction ($F(23, 322) = 2.727$, $P<0.0001$) but no effect of construct*time interaction ($F(23, 322) = 1.108$, $P = 0.334$) or treatment*time*construct interaction ($F(23, 322) = 0.829$, $P = 0.694$). This suggests that the decrease in locomotor activity was different over time based on clozapine or vehicle treatment (**Figure 3.6**).

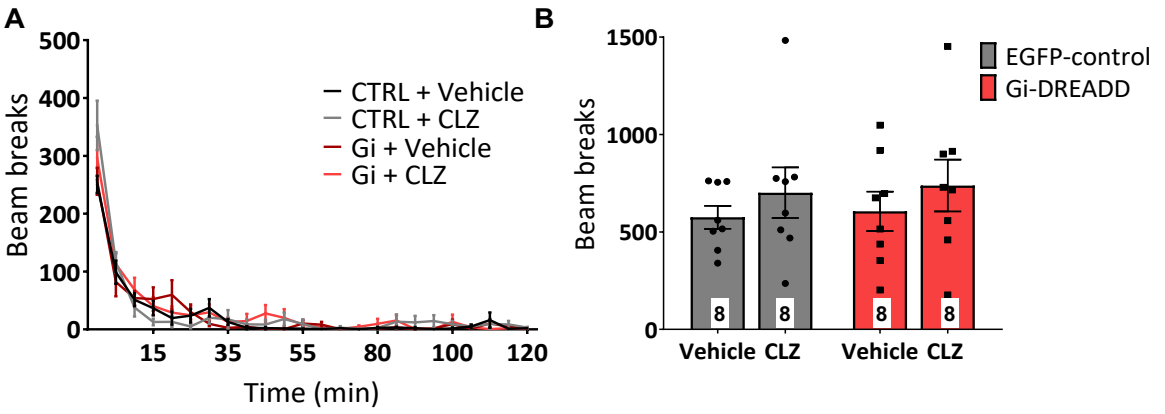


Figure 3.6: Locomotor activity of Gi-DREADD expressing rats in the presence of clozapine (0.1 mg/kg)

(A) Data showing time course effect of clozapine application on locomotor activity. Data presented as a mean ± SEM values of n=8 CTRL-DREADD rats (grey and black) and n=8 Gi-DREADD (red and dark red). (B) Total number of beam breaks over 2h for each treatment group. Data shown as mean ± SEM values (CLZ: clozapine).

As no marked effects were observed in this experiment with a very low dose of clozapine, in a follow-up experiment, the dose of clozapine was increased to 0.5 mg/kg i.p. and the

locomotor activity was measured once more. The results were similar to the previous experiment in that no differences in locomotor activity were observed between groups. A repeated measures 2-way ANOVA with viral construct as the between subject factor and time and treatment as within-subject factors revealed no effect on the number of beam breaks based on viral construct expressed ($F(1, 14) = 1.682$, $P = 0.216$), the treatment ($F(1, 14) = 0.131$, $P = 0.723$) or the interaction, construct*treatment ($F(1, 14) = 0.083$, $P = 0.778$). The number of beam breaks decreased significantly over time ($F(23, 322) = 115.293$, $P<0.0001$) and there was no significant effect of treatment*time interaction ($F(23, 322) = 0.649$, $P = 0.893$), construct*time interaction ($F(23, 322) = 1.031$, $P = 0.425$) or construct*treatment*time interaction ($F(23, 322) = 0.375$, $P = 0.997$; **Figure 3.7**).

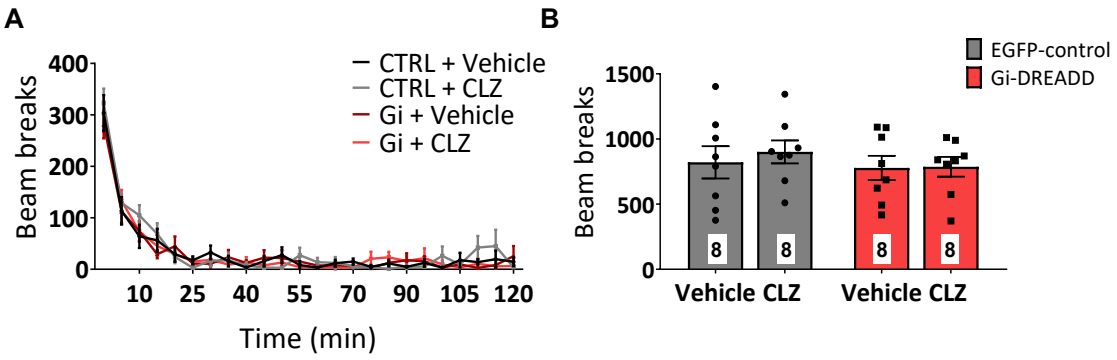


Figure 3.7: Locomotor activity of Gi-DREADD expressing rats in the presence of clozapine (0.5 mg/kg)

(A) Data showing time course effect of clozapine application on locomotor activity. Data presented as a mean ± SEM values of n=8 CTRL-DREADD rats (grey and black) and n=8 Gi-DREADD (red and dark red). (B) Total number of beam breaks over 2h for each treatment group. Data shown as mean ± SEM values (CLZ: clozapine).

Taken together, the behavioural data suggest that Gi-DREADD activation by either CNO or clozapine does not alter working memory in a rewarded alternation T-maze, or spatial short-term memory as assessed on a novelty preference Y-maze. Moreover, no differences in locomotor activity were observed in any of the groups.

3.3.5. Post-hoc histological validation

At the end of each experiment, histological validation of viral expression was required. From the two cohorts used in this chapter, 3 Gi-DREADD expressing rats from the first cohort were excluded from the analysis. This was done based on lack of DREADD transfection (1/3 rats excluded) or unilateral expression (2/3 rats excluded). The remainder of rats showed transfection in all of the principal layers, specifically around the injection sites in CA1 and CA3 (as illustrated in **Figure 3.1D**) and in the neighbouring cells as illustrated by the lighter shades of red. Across the AP axis the construct was transfected for a minimum of ± 0.5 cm as reported in the previous chapter. **Figure 3.8** shows a schematic representation of the viral transfection at the site of the injection (AP: -3.6 mm). The statistical analyses presented in this chapter are for groups after exclusions.

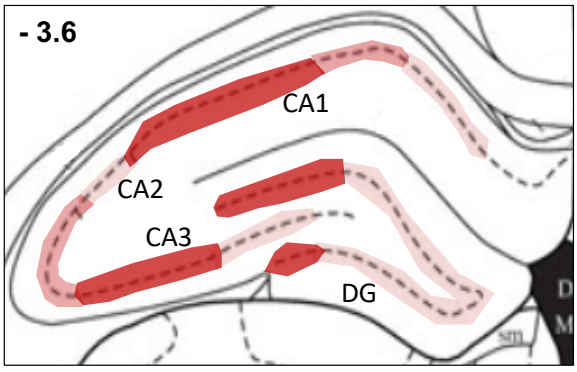


Figure 3.8. Schematic representation of viral transfection

Schematic illustration of viral transfection efficacy at the site of injection superimposed on a corresponding illustration of the sections at the specific AP position taken from The Rat Brain Atlas. Number in the top left corner represents AP coordinate measured from Bregma (Paxinos & Watson, 2007). Dark red represents the spread in the majority of the animals and coincides with the sites of injection (CA1 and CA3). Lighter shading suggests transfection in the area is not seen in all animals.

3.4 Discussion

Experiments in this chapter aimed to investigate changes in spatial short-term and working memory upon CNO-induced activation of a Gi-DREADD construct expressed in excitatory neurons of the dorsal hippocampus and at the same time test the functionality of the construct *in vivo*. Silencing a population of excitatory neurons in the hippocampus is a refined method of modulating hippocampal function and it enables a cell-specific investigation of behaviour arising from it. To this end, the current experiments assessed the hippocampal-dependent behavioural phenotype of Gi-DREADD expressing rats in the presence of CNO and clozapine. Contrary to expectations based on findings from Chapter 2 that showed evidence of decreased glutamatergic transmission in Gi-DREADD expressing slices, the rats displayed normal spatial short-term/working memory compared to control rats on a rewarded alternation and a novelty preference task. Additionally, there were no changes in locomotor activity in photocell activity cages regardless of construct type.

3.4.1 SWM on a rewarded alternation T-maze task in a familiar room in Gi-DREADD expressing rats

Normal brain function requires a balanced excitatory/inhibitory (E/I) synaptic transmission throughout the brain. Impairments in either of the transmitter systems that maintain this balance can lead to psychopathologies such as schizophrenia (Beasley & Reynolds, 1997; Fung et al., 2010; Lisman et al., 2008), autism (Fatemi et al., 2009) or epilepsy (Fukata & Fukata, 2017; Wong, 2010). Learning and memory dysfunctions are also associated with an E/I imbalance (Nanou et al., 2018). In the hippocampus, impaired excitatory transmission as seen in *Gria1* KO mice as decreased fEPSPs (Romberg *et al*., 2009), thereby reflecting reduced pyramidal cell excitability, behaviourally manifests as normal SRM but impaired SWM (Reisel et al., 2002). In a different model, muscimol induced hippocampal inactivation caused impaired performance in a novel object recognition task (NOR) (Cohen et al., 2013). The same

study suggested that discrimination in a NOR task engages hippocampal activity and subsequently causes a significant increase in glutamate levels during the task in naïve mice. While there were no positive controls in the current experiment, published data from our lab showed that hippocampal micro-infusions of muscimol caused deficits in performance on the rewarded alternation T-maze task in rats (McHugh et al., 2008). Based on the above studies and results in the previous chapter we hypothesised that CNO-induced activation of Gi-DREADD in hippocampal pyramidal neurons would decrease performance on this hippocampal-dependent memory task. Surprisingly, the results showed no differences between the Gi-DREADD and the control group when CNO was injected 30 min prior to testing. Both groups performed well above chance levels regardless of CNO or saline systemic administration.

DREADDs have not been widely used to investigate hippocampal-dependent behaviour despite their extensive use in neuroscience research. Still, a few studies have reported altered phenotypes in response to CNO-induced Gi-DREADD activation in the hippocampus. For example, Varela et al., (2016), targeted the ventral and dorsal hippocampus of mice using a pCB promoter driven Gi-DREADD and tested contextual fear memory and spontaneous alternation behaviour on a T-maze task upon CNO injection (5 mg/kg i.p.). The study reported that CNO blocked retrieval of a recent but not distant fear memory and reduced performance on the spontaneous alternation T-maze task to chance levels in Gi-DREADD expressing mice (52%) compared to above chance for saline treated mice (59%), in marked contrast to the rewarded alternation T-maze result in the present study (Varela et al., 2016). The study fails to describe the neural mechanism underlying the phenotype, by targeting both dorsal and ventral hippocampus that have dissociable roles (discussed earlier) and using a ubiquitous promoter that does not discriminate between neuronal subtypes.

A different study (López et al., 2016) examined the behavioural phenotype of mice expressing a Gi or Gq-DREADD in the dorsal hippocampus in response to CNO (3 mg/kg i.p.) injection. Using two different promoters, hSyn (non-specific neuronal promoter) and CaMKIIa (specific to excitatory neurons), the investigators inject CNO 40 min before training the mice on an object location and object recognition task in an attempt to block encoding. The results showed that CNO-induced activation of a Gq-DREADD transforms sub-threshold training into long term memory (LTM) in the object location but not object recognition task regardless of promoter gene. In contrast, Gi-DREADD expression blocked LTM formation in an object location but not object recognition task (López et al., 2016). Finally, in a more recent study, (Tuscher et al., 2018), used female mice expressing a CaMKIIa driven Gi-DREADD in the dorsal hippocampus. The study showed evidence of impaired object placement performance but intact object recognition performance in Gi-DREADD mice, regardless of ITI (4h and 24h) and CNO doses used (2, 4, 8 mg/kg i.p.) (Tuscher et al., 2018).

Considering the above, the lack of effect of CNO induced activation of a Gi-DREADD in the rewarded alternation T-maze task in the current study could be attributed to a few factors. Firstly, a drawback of using chemogenetics is that a certain transfection rate must be achieved for detection of behavioural changes. However, the virus titration cannot be changed once delivered to the area of interest, the only adjustable variable being the dose of CNO (Urban & Roth, 2015). The success of transfection (or lack of) is only confirmed *post-mortem*. Therefore, chemogenetics use requires brain and cell specific validation and characterisation to ensure that any behavioural readout is interpreted appropriately. In the current study viral expression was generally localised to the CA1 and CA3 subfields. Secondly, there is the possibility of inter-species differences. Specifically, the studies mentioned above have been done in mice, and have used similar (1-1.2 µl) volumes of viral construct per injected hemisphere as were used in the experiments in this thesis (1 µl). Thus, using the same volume in the smaller mouse brain will lead to higher percentage viral transfection of the hippocampus. Finally, considering

that the rats were well trained it is possible that the short ITI duration used has not made the task challenging enough.

3.4.2 SWM on a rewarded alternation T-maze in a novel room in Gi-DREADD expressing rats

The rats were then tested on the same task set-up, using the same protocol but in a novel room. Surprisingly, again CNO-induced Gi-DREADD activation did not alter the performance in the novel room either. There was however a statistically significant construct type*treatment interaction on the latency to reward. The data suggests that saline treatment increased latency to reward in the control group compared to the Gi-DREADD group (albeit not statistically significant). The only potential explanation for this result would be that CNO caused carry-over effects in the Gi-DREADD group and despite saline treatment the group performed similarly to the Gi-DREADD/CNO group. This is however, highly unlikely as there was a minimum of 72 h between doses, the treatment was counterbalanced and effects of CNO induced DREADD activation are not thought to last beyond 12 h (Alexander et al., 2009).

Novelty-induced hyperactivity is a characteristic of *Gria1* KO mice (Bannerman et al., 2004; Fitzgerald et al., 2010; Vekovischeva et al., 2001) and hippocampal lesions (Bannerman et al., 1999) and serves as a measure of hippocampal dysfunction in its own right. To this end, locomotor activity was recorded in a novel set-up in 5-min time bins over 2h. No differences were detected between groups regardless of construct type expressed or treatment over the 2h. The lack of deficits in hippocampal function could suggest that changes in glutamatergic transmission as a consequence of pyramidal neuron activity suppression are not comparable to GLUA1 knockout (including in the hippocampus) or to the extent lesions affect hippocampal function and that perhaps muscimol hippocampal micro-infusions are a better comparison.

In a recent study Aitta-Aho et al. (2019) used the *Gria1-/-* mouse in combination with a CaMKIIa-Gi-DREADD expressed in the dorsal hippocampus. The study shows reversal of novelty-induced hyperactivity in *Gria1-/-* mice upon CNO (3 mg/kg i.p.) induced Gi-DREADD activation. The study showed no evidence of behavioural changes in wild-type Gi-DREADD expressing mice upon CNO induced activation (Aitta-Aho et al., 2019). This result in WT mice is in line with the current findings and suggests a potential floor effect of Gi-DREADDs. Specifically, it is possible that the functionality of a Gi-DREADD *in vivo* can be demonstrated only when there is a pre-existing network hyperactivity that can be reduced by CNO binding to the Gi-DREADD. This idea is also potentially supported by studies in which epileptiform activity was reduced by CNO-induced activation of Gi-DREADDs (Avaliani et al., 2016; Zhou et al., 2019).

Another potential explanation for the lack of effects seen in this cohort could be the small sample size in the Gi-DREADD group, and the potential that the study wass underpowered. For DREADD studies in general, exclusion of animals is done post-hoc upon confirmation of viral expression. In this specific cohort, 3 of the Gi-DREADD animals showed either bilateral or no expression and had to be excluded from analysis. However, the reward alternation T-maze task is considered to be sensitive enough to detect hippocampal deficits in individual animals (Deacon & Rawlins, 2006). As there was no evidence of a SWM impairment in any of the 4 subjects, the sample size was not increased and further directions, that were less time-consuming and could also give an indication of hippocampal function impairment, were explored instead.

3.4.3 Short-term memory on a spatial novelty preference Y-maze task in Gi-DREADD expressing rats

While experiments were being undertaken, a study suggesting that CNO is back-metabolised to clozapine, that subsequently crosses the BBB, and ultimately activates the DREADDs was published (Gomez et al., 2017). While this did not explain the lack of deficits seen in the rewarded alternation task in the current study, it prompted the assessment of clozapine as a DREADD agonist *in vivo*. Thus, in a different cohort, spatial memory was tested in a spatial novelty preference Y-maze task with clozapine (0.1 mg/kg i.p.) as a DREADD agonist. The same dose as used by Gomez and colleagues was chosen as the study showed evidence of decreased locomotor activity in rats expressing a Gi-DREADD in the accumbens upon injection of 0.1 mg/kg clozapine, an effect comparable to the decrease caused by 10 mg/kg CNO. Additionally, the investigators found decreased locomotor activity following 1 mg/kg clozapine in non-DREADD expressing rats suggesting 0.1 mg/kg clozapine as a more appropriate dose that lacks non-DREADD specific effects.

In the current study, the results showed poor levels of novelty preference during the 2 min test phase in all animals. Thus, the analysis was carried out for the first minute of behaviour on the test run. This time the results showed above chance performance in the control group independent of clozapine or vehicle treatment and an overall significant effect of viral construct regardless of treatment, characterised by chance performance in the Gi-DREADD group independent of saline or CNO treatment. This floor effect would also occlude the chance to see any further deterioration in the clozapine/Gi-DREADD group. The experiment was carried out on two different days to allow for within-subject comparisons of treatments with a 72h washout period. It seems unlikely that clozapine caused an irreversible downstream effect on the Gi-DREADD group on the first day that would carry over to the second day of testing.

3.4.4 Novelty induced locomotor activity in response to clozapine

In two follow-up experiments, locomotor activity was recorded over 2h following clozapine systemic administration. There were no differences in locomotor activity after either 0.1 or 0.5 mg/kg clozapine treatment between groups and independent of treatments, except for a significant time by treatment interaction after 0.1 mg/kg clozapine. This is in contrast to other studies that have reported clozapine-induced locomotor decreases at different doses. For example Gomez et al., reported decreased locomotor activity after 1 mg/kg clozapine in wild type rats (Gomez et al., 2017) while Ilg and colleagues show evidence of decreased locomotor activity in wild type rats upon injection of clozapine at doses as low as of 0.05 mg/kg, 0.1 mg/kg and 1 mg/kg (Ilg et al., 2018). A different report found a dose-dependent decrease in locomotor activity in wild-type rats using doses of clozapine from 1 mg/kg and up to 30 mg/kg (McOmish et al., 2012). As clozapine displays a complex pharmacology and binds to a variety of receptors with different affinities, it is possible that behavioural effects would differ dose-dependently. Specifically, clozapine was reported to occupy histamine (H1) receptors at doses as low as ED_{50} = 0.15 mg/kg, α1 adrenergic receptors at ED_{50} = 0.58 mg/kg and 5-HT_2 receptors at ED_{50} = 1.3 mg/kg (Schotte et al., 1993). However, this does not explain the different results seen in the Gomez (Gomez et al., 2017) and the current study and the Ilg report (Ilg et al., 2018).

Finally, the post-hoc histological analysis showed similar levels of transfection in most of the animals. Still there are two explanations for the lack of behavioural deficits. Firstly, it is possible that the level of transfection was not sufficient to cause changes in behaviour, as discussed more in the general discussion (Chapter 6). Secondly, there is the possibility that despite neurophysiological changes as a consequence of DREADD activation in the slice electrophysiology experiments, this does not translate into changes at the behavioural level.

This indicates that the interpretation of drug induced behavioural modifications should be accompanied by neurophysiological readouts.

3.4.5 Conclusions

Data presented in this chapter revealed no indications of deficits in spatial short-term/working memory in rats expressing a Gi-DREADD in the excitatory neurons of the dorsal hippocampus, upon binding of either CNO (3 mg/kg) or low-dose clozapine (0.1 mg/kg). Additionally, experiments in this chapter provide no evidence for non-DREADD specific effects of CNO or clozapine. Moreover, despite the electrophysiological validation presented in the previous chapter, the functionality of the hippocampal Gi-DREADD *in vivo* was brought into question. Specifically, the data presented call for a more in depth understanding of DREADD function at the cellular and network level in vivo. Finally, the pharmacokinetics of CNO must be re-evaluated in the context of its apparent pharmacological inertness.

Chapter 4

Bioavailability of CNO and clozapine in relation to DREADD function

4.1 Introduction

Experiments in the previous chapter found that after systemic administration of either CNO or clozapine, rats expressing a CaMKIIa-targeted inhibitory DREADD in hippocampus performed similar to controls in hippocampal-dependent behavioural tasks. This prompted experiments reported in the current chapter which re-evaluated the functionality of the DREADD construct by using c-Fos expression as a marker of neuronal activity. At the same time the bioavailability of CNO and clozapine was investigated.

4.1.1 c-Fos as marker of neuronal activity

Following early experiments which showed induction of the immediate early gene (IEG) c-Fos in certain brain areas following epileptic seizure (Morgan et al., 1987), c-Fos expression became widely used as a marker of neuronal activity and a tool for neuroanatomical mapping of the effects of pharmacological or physiological stimuli (Dragunow et al., 1989; Hoffman et al., 1992; Bullitt *et al* , 1990; Lyons & West, 2011; Morgan & Curran, 1991). Basal levels of c-Fos are typically low because auto-repression reduces constitutive transcription by the protein (Lyons & West, 2011), but expression is increased when an external stimulus elevates intracellular calcium to then activate multiple signalling pathways. For example, in the case of strong stimuli c-Fos expression can be induced by the MAPK pathway which phosphorylates CREB and Elk-1, two transcription factors that bind to the nuclear c-Fos promoter and lead to c-Fos mRNA and protein expression (Chung, 2015, Ghosh et al., 2014). The expression of c-Fos can be detected quickly after stimulation, with peak c-Fos mRNA being found 30 min after stimulation and c-Fos protein levels peaking 90-120 min post stimulus (Kovacs et al., 1998).

4.1.2 c-Fos use in functional DREADD validation

Expression of c-Fos can be used as a marker of increased neuronal activity following activation of an excitatory DREADD. For example, it was found that activation of a Gq-DREADD by CNO increased c-Fos signal in the areas expressing the viral construct (Yuan & Grutzendler, 2016, Sengupta et al., 2016, Keenan et al., 2017, Yau & McNally, 2015). However, in order to probe the ability of a Gi-DREADD to silence neuronal activity, basal levels of c-Fos expression need to be elevated. For example, Ferguson et al. (2011), used amphetamine to drive c-Fos expression in the rat striatum, and found that CNO reduced this response in rats expressing Gi-DREADD in this region. In a different study (Lopez et al., 2016), investigators administered CNO to Gi-DREADD expressing mice exposed to a novel environment. Although the novel environment increased c-Fos expression, unexpectedly, a further increase in c-Fos expression was found in the Gi-DREADD expressing mice potentially due to the use of a non-specific (hSyn) promoter. Other studies have been more successful in using c-Fos expression to test the functionality of a Gi-DREADD. For example, one study found decreased numbers of c-Fos cells in the anterior cingulate cortex (ACC) of mice after fear conditioning training, upon administering CNO continuously for 3 days prior to fear conditioning in the drinking water (Vetere et al., 2017). To elevate the numbers of c-Fos such that Gi-DREADD function can be tested, other studies have made use of the circadian rhythm of the animals, when expressing a Gi-DREADD in orexin neurons (Sasaki et al., 2011) or phetylenetetrazole, a $GABA_A$ antagonist in the dorsal anterior cingulate cortex (dACC) of mice (Koike et al., 2016). Thus, c-Fos detection serves as a suitable tool for molecular validation of DREADDs *post mortem*.

Experiments in this chapter tested the functionality of Gi-DREADD targeted to principal cells in the dorsal hippocampus by elevating basal c-Fos in this region through novel context exposure (VanElzakker *et al*, 2009). To avoid confounding effects of other sensory stimuli

such as handling that might trigger c-Fos expression, animals were habituated to handling prior to the beginning of the experiment.

4.1.3 CNO, designer drug or pro-drug?

The clozapine metabolite CNO was initially proposed as a useful DREADD activator on the basis of its bioavailability in humans and rodents, and lack of affinity for M_3 receptors, and the assumption that it was not back-metabolised to clozapine which has high affinity at a range of transmitter receptors (Armbruster et al., 2007). However, the original study also disclosed evidence that show clozapine has nM affinity for DREADDs. Moreover, the back conversion of CNO to clozapine had been previously documented in guinea pigs (Jann et al., 1994) and in humans (Chang et al., 1998), although there was little data on the metabolism of CNO in rodents.

In a pivotal study published whilst the current thesis work was in progress Gomez et al. (2017) described the *in vivo* mechanism of CNO as DREADD agonist. The report found no CNO but high clozapine binding in DREADD expressing in HEK 293 cells, mouse or rat brain tissue. Furthermore, PET scans from striatal Gq-DREADD expressing rats revealed no CNO brain uptake in contrast to high clozapine uptake after CNO intravenous injection. Behaviourally, the investigators reported similar locomotor activity effects as a result of nucleus accumbens Gi-DREADD activation by both clozapine (0.1 mg/kg) and CNO (10 mg/kg) (Gomez et al., 2017). Thus, the results suggested that CNO is back metabolised to clozapine which then penetrates the CNS and activates the DREADDs. Moreover, data in the paper indicated that clozapine might accumulate over time and that its peak effect on the DREADDs could be beyond the 2 h experimental window that most studies used to conduct behavioural testing. On the basis of their findings, the investigators recommended the use of low doses of clozapine (i.e. 0.1 mg/kg in rats) to induce preferential DREADD-mediated effects (Gomez et

al., 2017). Prior to this study however, two other reports investigated the 'pharmacological inertness' of CNO. A study performed in rats showed that CNO (5 mg/kg but not 1 or 2 mg/kg i.p.) decreased amphetamine-induced hyperlocomotion, and also showed reverse metabolism of CNO to clozapine in plasma (MacLaren et al., 2016). In rhesus monkeys, Raper and colleagues assessed the pharmacokinetic properties of CNO (3 and 10 mg/kg s.c.) and found evidence of back conversion of CNO to clozapine in the plasma and CSF (Raper et al., 2017). All in all, these studies emphasise the importance of employing appropriate controls in DREADD studies and query the mechanisms by which CNO generates its effects.

4.1.4 Chapter 4 experimental aims

One set of experiments in this chapter aimed to use c-Fos as a marker of changes in neuronal activity induced by CNO in DREADD transfected rats. A second set of experiments aimed to examine the exposure of rat brain and plasma to different doses of CNO and clozapine at various time points following systemic administration.

4.2 Materials and Methods

The first two c-Fos studies (Study 1 and 2) described in this chapter were carried out at the University of Oxford. The third c-Fos study (Study 3) and the LC-MS/MS exposure study were performed at H. Lundbeck A/S.

4.2.1 Animals

Experiments performed at the University of Oxford were in compliance with the UK Home Office Animals (Scientific Procedures) Act of 1986, and local ethical review. Experiments performed at H. Lundbeck A/S Copenhagen were carried out in accordance with the Danish legislation regulating animal experiments; Law and Order on Animal experiments; Act No. 474 of 15/05/2014 and Order No. 12 of 07/01/2016, and with the specific license for these experiments issued by the National Authority

Male Lister Hooded rats (Charles River, Germany or Envigo, Bicester, UK) weighing between 250-300g on arrival were kept under environmentally controlled temperature (20 ± 2ºC) and humidity (50 ± 20%) with *ad libitum* access to food and water. Rats were group housed until viral injections when they were separated and housed individually until the end of the experiment (at H. Lundbeck A/S) or paired with a littermate (University of Oxford). Rats were housed in open Makrolon polycarbonate cages with wire lid and kept in a ventilated scantainer in a 12h light/dark cycle (lights on at 06:00 and at 07:00, University of Oxford). Sawdust was used as bedding and cages were environmentally enriched with wooden chew blocks, a polycarbonate rectangular house (Rat Retreats™, Bio-Serv, Flemington, NJ, USA) or a cardboard house (University of Oxford).

4.2.2 Viral constructs

For all the experiments performed at H. Lundbeck A/S, viral constructs were purchased from the Viral Vector Facility (VVF) of the Neuroscience Centre Zurich (ZNZ). For the experiments performed at the University of Oxford, viral constructs were obtained from either UNC Vector Core (University of North Carolina) or Addgene, having been originally created by Bryan Roth. Details about the viral constructs used in this chapter are shown in Table 4.1.

Name	**Supplier**	**Experimental cohort**	**Number of rats**	**Titre (vector genomes/ml)**
AAV5-CaMKIIa-mCherry	UNC Vector Core	c-Fos analysis – CNO (3 mg/kg, study 2)	n=6	≥3 x 10^{12} vg/ml
AAV5-CaMKIIa-hM4D(Gi)-mCherry	UNC Vector Core	c-Fos analysis – CNO (3 mg/kg, study 2)	n=4	≥3 x 10^{12} vg/ml
AAV5-CaMKIIa-EGFP	Addgene (#50469)	i) c-Fos analysis – clozapine (0.5 mg/kg, study 2) ii) c-Fos analysis – CNO (3 mg/kg, study 2, unilateral design)	i) n=7 ii) n=5	4.3x10^{12} vg/ml
AAV5-CaMKIIa-hM4D(Gi)-mCherry	Addgene (#50477)	i) c-Fos analysis – clozapine (0.5 mg/kg, study 2) ii) c-Fos analysis – CNO (3 mg/kg, study 2, unilateral design)	i) n=8 ii) n=5	4.4x10^{12} vg/ml
ssAAV-5/2-CaMKIIa-hM3D(Gq)_mCherry-WPRE-hGHp(A)	VVF of ZNZ (V96-5)	c-Fos analysis – CNO (10 mg/kg, study 3)	n=6	4.7x10^{12} vg/ml
ssAAV-5/2-CaMKIIa-hM4D(Gi)_mCherry-WPRE-hGHp(A)	VVF of ZNZ (V102-5)	c-Fos analysis – CNO (10 mg/kg, study 3)	n=8	7.3x10^{12} vg/ml
ssAAV-5/2-CaMKIIa-EGFP-WPRE-hGHp(A)	VVF of ZNZ (V113-5)	c-Fos analysis – CNO (10 mg/kg, study 3)	n=6-8	7.5x10^{12} vg/ml

Table 4.1: Experimental details of the viral constructs used in this chapter.

4.2.3 Intracerebral viral injection

Viral delivery of CaMKIIa-driven expression of DREADD constructs to the dorsal hippocampus was performed as described in Chapter 2 (see **2.2.3**). Briefly, anaesthesia was induced and maintained with isoflurane. The skull was exposed and 4 small holes were drilled above the dorsal hippocampus. A total of 1 µl of viral construct was delivered using an injection pump to 3 injections sites per hemisphere, using the following stereotaxic co-ordinates: i, ii) AP -3.6 mm, ML ±3 mm, DV -3 mm, iii, iv) AP -3.6 mm, ML ±3 mm, DV -2.2 mm, v, vi) AP -3.6 mm, ML ± 2 mm, DV -2.0 mm. The scalp was then sutured, and rats were administered peri and post-operative care as described in the previous chapter (see **2.2.3**). All experiments were carried out 2-3 weeks post virus injection to allow for expression of the DREADDs, and animals recovered either singly housed (H. Lundbeck A/S) or group housed (University of Oxford).

For c-Fos studies, typically a within-subject control design was employed. Specifically, one hemisphere of the dorsal hippocampus was injected with a control construct (EGFP-control) while the contralateral hemisphere was injected with either an inhibitory (Gi-DREADD) or excitatory (Gq-DREADD) construct. This design does not account for callosal projections between the two hippocampi but has been used previously to validate DREADD functionality using c-Fos in the mouse hypothalamus (Zhou et al., 2018).

4.2.4 Drugs

CNO and clozapine (Tocris Biosciences, Bristol, UK) were freshly prepared on the experimental day. CNO was dissolved in saline solution and administered i.p. in a volume of 1-5 ml/kg. Clozapine was either dissolved in saline in 4% DMSO (VWR International) or in saline with HCl 1M added in small quantities to aid the dissolving process and then pH

adjusted to 4. Once dissolved, clozapine was administered i.p. in a 1 ml/kg volume. Vehicle was saline solution or saline with DMSO as appropriate.

4.2.5 Novel context-induced c-Fos activation

Study 1) Initially a pilot study was conducted to confirm whether novel context exposure elevated c-Fos levels in the dorsal hippocampus. A group of naïve rats was placed into a novel cage, in a novel room. The bottom of the cages was covered with clean sawdust in which was placed a novel object (typically a Duplo® brick). A second group of rats remained in their home cage and acted as controls. On the experimental day rats were placed into a novel environment for 2 h and administered a pentobarbitone overdose before transcardial perfusion with PBS followed by 4% PFA. The brains were placed in 4% PFA overnight prior to transfer to a 30% sucrose solution until preparation for immunohistochemical analysis. The rats from the control group were taken directly from the home cage and perfused as above.

Study 2) The aim of this set of experiments was to elevate the levels of c-Fos expression in the hippocampus using a novel environment, and then attempt to decrease it through CNO/clozapine-induced activation of CAMKII-driven Gi-DREADD expression. Three different cohorts were used for this study – the two cohorts that were used for behavioural experiments in Chapter 3, and a new cohort. Rats from the new cohort expressed a Gi-DREADD tagged by mCherry in one hemisphere of the dorsal hippocampus and an EGFP-control construct in the contralateral hemisphere and were handled for a minimum of 5 days prior to test day, when they were injected with CNO (3 mg/kg i.p.) and then placed in the novel environment as above. The other 2 cohorts were injected with either CNO (3 mg/kg i.p.). or clozapine (0.5 mg/kg i.p.) and placed in the novel environment. All three groups were administered a pentobarbitone overdose two hours later, before transcardial perfusion with PBS followed by

4% PFA. The brains were placed in PFA 4% overnight prior to transfer to a 30% sucrose solution until preparation for immunohistochemical analysis.

Study 3) This set of experiments followed on from experiments above but used a higher dose of CNO and also tested both CaMKIIa-driven Gi-DREADD and Gq-DREADD constructs. Rats were injected in one hemisphere of the dorsal hippocampus (as described above) with a mCherry tagged Gi or Gq-DREADD and an EGFP-control construct in the contralateral hemisphere. Rats were handled and habituated to i.p. (saline) injection for at least 5 consecutive days before the experimental day. On that day, rats were injected with CNO (10 mg/kg i.p.) and returned to the home cage. Post injection, Gi-DREADD expressing rats were returned to home cage for 30 min followed by 1 h exposure to a novel environment (novel cage, clean sawdust, plastic red mouse house as a novel object). Next, rats were killed by guillotine and brains were snap frozen until fluorescence *in situ* hybridisation (FISH) analysis. Gq-DREADD expressing rats were killed by guillotine 1 h after CNO injection and brains were snap frozen on dry ice until FISH.

4.2.6 Immunohistochemistry (c-Fos fluorescence and DAB staining)

For study 1 and 2 above (where two different fluorophores were expressed in the brain), brains were analysed for c-Fos expression using immunocytochemistry. Coronal sections (30 µm) were cut on a cryostat at -20ºC and free-floating slices were collected in PBS. Attempts to label c-Fos positive cells using a fluorophore that was neither red or green (i.e. avoiding cross-labelling with mCherry/EGFP-tagged DREADDs) were unsuccessful, therefore a DAB (3,3'-diaminobenzidine) protocol was optimised in conjunction with fluorescence. Sections were washed 3 times in PBS followed by 1 wash with 90% PBS-X, 10% methanol and 0.3% H_2O_2. Sections were then washed in 0.3% PBS-X 3 times followed by a 1 h blocking step in 90% PBS-X and 10% donkey serum. Next, sections were incubated overnight with rabbit anti-c-

Fos primary antibody (1:2500, Abcam, Cambridge UK) at room temperature with constant gentle agitation. This dilution was chosen based on optimization trials with higher concentrations that have displayed increased background staining. The following day, sections were washed 3 times in PBS, followed by 90 min incubation with biotinylated anti-rabbit secondary antibody (1:1000, Vector Labs, CA, USA) in 2% donkey serum and PBS-X solution. Next, the sections were washed 3 times with PBS-X and incubated for 1 h in VECTASTAIN® Elite® ABC HRP kit (Vector Labs, CA, USA) followed by a PBS wash. Brain sections were then incubated in DAB for 6 min with gentle agitation using a DAB peroxidase (HRP) substrate kit with nickel enhancement (Vector Labs, CA, USA). Finally, sections were washed in deionised water, moved from PBS onto poly-L-lysine coated slides and cover-slipped using Vectashield (Vector Labs, CA, USA). Controls used for the immunolabeling included slices without primary antibody and slices without the secondary antibody.

For one cohort (study 2), where both the control construct and the Gi-DREADD were tagged by the mCherry fluorophore, fluorescent antibody labelling was possible. Washing steps were carried out as described in section **2.2.4.** and were followed by overnight incubation with rabbit anti-c-Fos primary antibody (1:1000, Abcam, Cambridge UK) at 4ºC. Sections were then incubated for 2 h in a donkey anti-rabbit Alexa Fluor 488 (1:1000, Invitrogen, UK) secondary antibody in PBS-X and 2% donkey serum. Controls used for the immunolabeling included slices lacking the primary antibody and slices lacking the secondary antibody. Slides were imaged and expression of mCherry, EGFP and c-Fos positive cells was visualised under an epifluorescent and brightfield microscope (DM-500B, Leica Microsystems, Wetzlar, Germany). Acquired images were exported into Image J (NIH) for further processing.

Specificity of the primary c-Fos antibody has been previously established in our lab and characterised by others in the rat somatosensory cortex (Ohira et al., 2009) and arcuate

nucleus (Rajkumar et al., 2013). Additionally, as an internal control, in study 1, c-Fos expression was checked in the mPFC, that is known to be sensitive to acute stressors (Cullinan et al., 1995) and display increased levels of c-Fos expression as a result. This response was not quantified, but slices belonging to control rats showed very little if any c-Fos expression, and rats that had been exposed to a novel context showed visibly higher levels of c-Fos (data not shown).

4.2.7 Fluorescence *in situ* hybridisation

Fluorescence *in situ* hybridisation (FISH) was performed by Kirsten Jørgensen and Pia Møller Carstensen under the guidance of Dr. Camilla Stampe Jensen. For study 3 above, brains were analysed for c-Fos expression using FISH. Because of a lack of availability of an EGFP oligonucleotide probe, only mCherry and c-Fos oligonucleotide probes were used. The steps in this protocol are described in detail in Chapter 2 (see **2.2.5**). Briefly, FISH was performed using a ViewRNA ISH Tissue, 2-Plex Assay Kit 96 assay (Affymetrix, Santa Clara, USA) to examine c-Fos mRNA (Type 6 = Fast Blue probe or Type 1 = Fast Red probe) following CNO administration to rats with hippocampal mCherry-tagged DREADD constructs (Type 1, Fast Red probe). Brain sections (2 per microscope slide) were fixed in 4% PFA overnight at 4ºC. The following day sections were washed twice in PBS (1 min) and dehydrated in increasing concentrations of alcohol: 50%, 70%, 96%, 99% (10 min each). Next, sections were incubated with Protease QF 1:100 for 30 min. Prior to hybridisation sections were washed consecutively in PBS (1 min), PFA 4% (5 min) and PBS again twice (3 min). For hybridisation, sections were incubated overnight with 400 µl of the Probe Set Diluent containing 10 µl of each oligonucleotide probe (Type 1 and Type 6). The sections were incubated in PreAmplifier Mix QT for 30 min followed by 15 min incubation with Amplifier Mix QT. Label probe 6 was added to the sections for 1 h, followed by Fast Blue substrate for 45 min at room temperature in the dark. AP Stop QF was then added for 30 min before incubating the slices with oligonucleotide

probe 1 for 1 h at 40ºC. AP Enhancer was added for 5 min at RT followed by Fast Red substrate for 30 min. Finally, after a series of washes with PBS (1 min), PFA 4% (5 min), PBS (1 min) and deionised water, Hematoxylin (15 s at room temperature) and Hoechst (0.6 µl/ml, 3 min) reagents were added as a counterstain. Finally, sections were washed once more in PBS and deionised water and cover-slipped using CC/Mount (Sigma-Aldrich).

To quantify the number of c-Fos expressing cells, sections from each rat were stained for c-Fos mRNA only by using the Type 1, Fast Red oligonucleotide probe, to avoid leakage of the red (mCherry labelled) channel into the blue (c-Fos labelled) channel and subsequent false negatives. To visualise the signals of hybridised mRNA, confocal images were acquired (Nikon Eclipse Ti confocal microscope) using Volocity software (PerkinElmer, USA). Three z-slices (0.2 µm step size) images were taken and 4 x 4 fields with 20% overlap were stitched in Volocity, and contrast was enhanced using the same settings for all of the images captured.

4.2.8 Quantification of c-Fos positive cells

The number of c-Fos immuno-positive cells was counted using 20X magnification of a fluorescence microscope (DM-500B, Leica Microsystems, Wetzlar, Germany), or images were captured by either a fluorescent or brightfield (for DAB stained cells) microscope and then imported into Image J (NIH, USA) where c-Fos positive cells were counted from the pyramidal cell layer of the CA and DG region using the Cell Counter plugin (study 2). An average of c-Fos numbers from at least two sections per animal was calculated. As indicated on each graph, the quantification was either bilateral and the numbers of c-Fos cells was presented per slice (**Figure 4.4**) or unilateral and the data was presented per hemisphere (**Figure 4.5**). During quantification the experimenter was blind to treatment or type of construct expressed to minimise bias.

For study 1 only, c-Fos positive cells were stereologically counted using the Stereo Investigator software (MBF Biosciences, VT, USA). C-Fos cells were counted from both hemispheres and only from the pyramidal layer of the CA region and the DG. For this specific study, 3 slices per animal were counted, and an average of c-Fos positive cells per slice per rat was calculated. The pyramidal layer of the dorsal hippocampus can be visualised under a microscope without a counterstain such that it was used as a natural delimitation for the area where c-Fos cells were counted from. The data are shown as the number of counted cells rather than the number of cells per area.

Fluorescent hybridised mRNA (study 3) was visualised in cells using a confocal microscope (Nikon Eclipse Ti). Confocal images were acquired using Volocity software (PerkinElmer, USA). Three z-slice (0.2 µm step size) images were taken and 4 x 4 fields with 20% overlap were stitched in Volocity, and then contrast was enhanced using the same settings for all images. Quantification was performed automatically using the 'Measurements' tab of the Volocity software. The analysis was carried out using a pre-set threshold intensity that was kept constant for all images once the region of interest (ROI) was selected. Here, the ROI was drawn around the entire dorsal hippocampus of one hemisphere. As very little to no background was detected outside the hippocampal principal layers, the ROI selection should not have impacted the results of the quantification.

It is important to note that because the method of quantification and immunolabeling of c-Fos cells was different in each of these studies, the numbers of c-Fos cells are not comparable between studies. However, the results are similar between studies, suggesting that the outcome is replicable, regardless of the analysis done. Additionally, these studies were used as a method of comparison between groups or hemispheres to assess DREADD functionality

and they should not serve as a determinant in assessing the absolute number of c-Fos cells in the hippocampus in each condition.

4.2.9 CNO/clozapine exposure study (LC-MS/MS)

To assess the extent to which CNO enters the brain and the extent to which it is back converted to clozapine, plasma and brain concentrations of clozapine and CNO were measured in a cohort of rats (n = 60) following administration of either CNO (3 or 10 mg/kg i.p.) or clozapine (0.1 or 0.5 mg/kg i.p.). Brain tissue and blood were collected 5, 30, 60, 120 and 240 min post injection. Blood samples were collected in EDTA-coated tubes followed by centrifugation at 3300 g for 15 min at 4ºC. Plasma was then separated and kept at -80ºC until further analysis. Brains were quickly dissected, cut in half, weighed and kept at -80ºC until further analysis.

Quantitative analysis of CNO and clozapine was performed using liquid chromatography coupled to tandem mass spectrometry (LC-MS/MS). LC-MS/MS analysis was performed by Hossein Armandi under the guidance of Dr. Line Rørbæk Olsen. Brain samples were homogenised with deionised water (1:4, v/v) for 3 min on the Covaris E220X ultasonicator (Covaris, Inc., MA, USA). Next, 25 µl of brain or plasma sample was precipitated with 100 µl acetonitrile containing the internal standard. Samples were then centrifuged followed by transfer to a new plate of 50 µl of supernatant mixed with 150 µl acetonitrile (25:75 v/v in water). Samples were centrifuged once more before being ready for LC-MS/MS analysis.

Substances were separated on a Waters Acquity UPLC HSS C18 SB column (1.7 µm particles, 30 mm x 2.1 mm; Waters, MA, USA) using a mobile phase gradient of 0.1% formic acid in water and acetonitrile that was pumped through the column at a rate of 0.6 ml/min. MS/MS

was performed using a Waters Xevo Triple Quadrupole Spectrometer-2 (TQS-2) (Waters, MA, USA) operated in electrospray MS/MS mode (multiple reaction mode, MRM). The XEVO TQS was controlled by Mass Lynx software version 4.1 (Waters, MA, USA) that was used for data acquisition and analysis. To detect clozapine and CNO the mass to charge (*m/z)* ratio was 327.13>270 and 343>270, respectively. Elution peak area correlated linearly with the concentration in the range of 1–1000 ng/ml in plasma and brain for both analytes. **Figure 4.1** and **4.2** show the calibration curves for plasma and brain clozapine and example of peaks of clozapine and internal standards in plasma and brain samples.

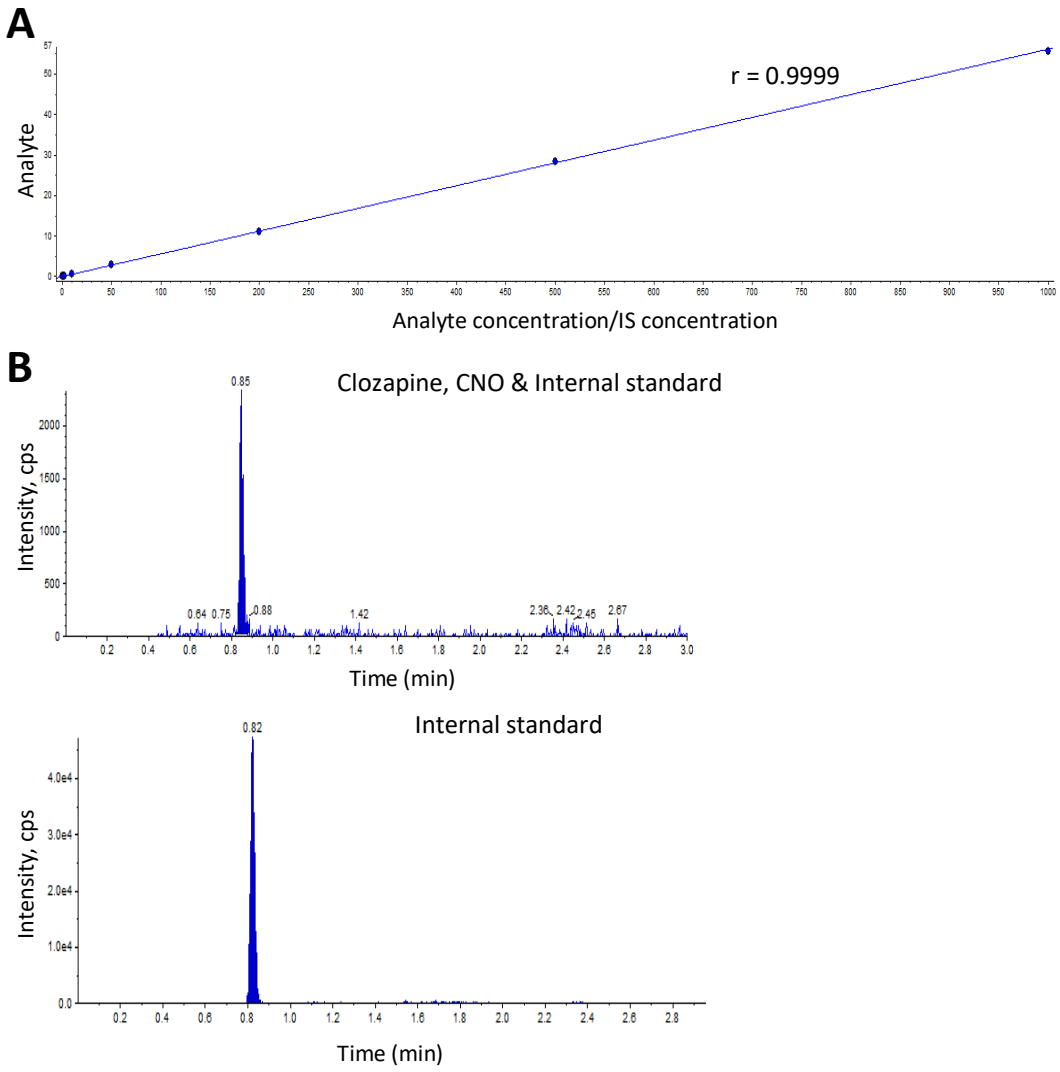


Figure 4.1: Plasma calibration curve and chromatogram lower limit of quantification

(A) Clozapine and internal standard (IS) plasma calibration curve and (B) peaks of clozapine, CNO and internal standard and the internal standard on its own from a plasma sample.

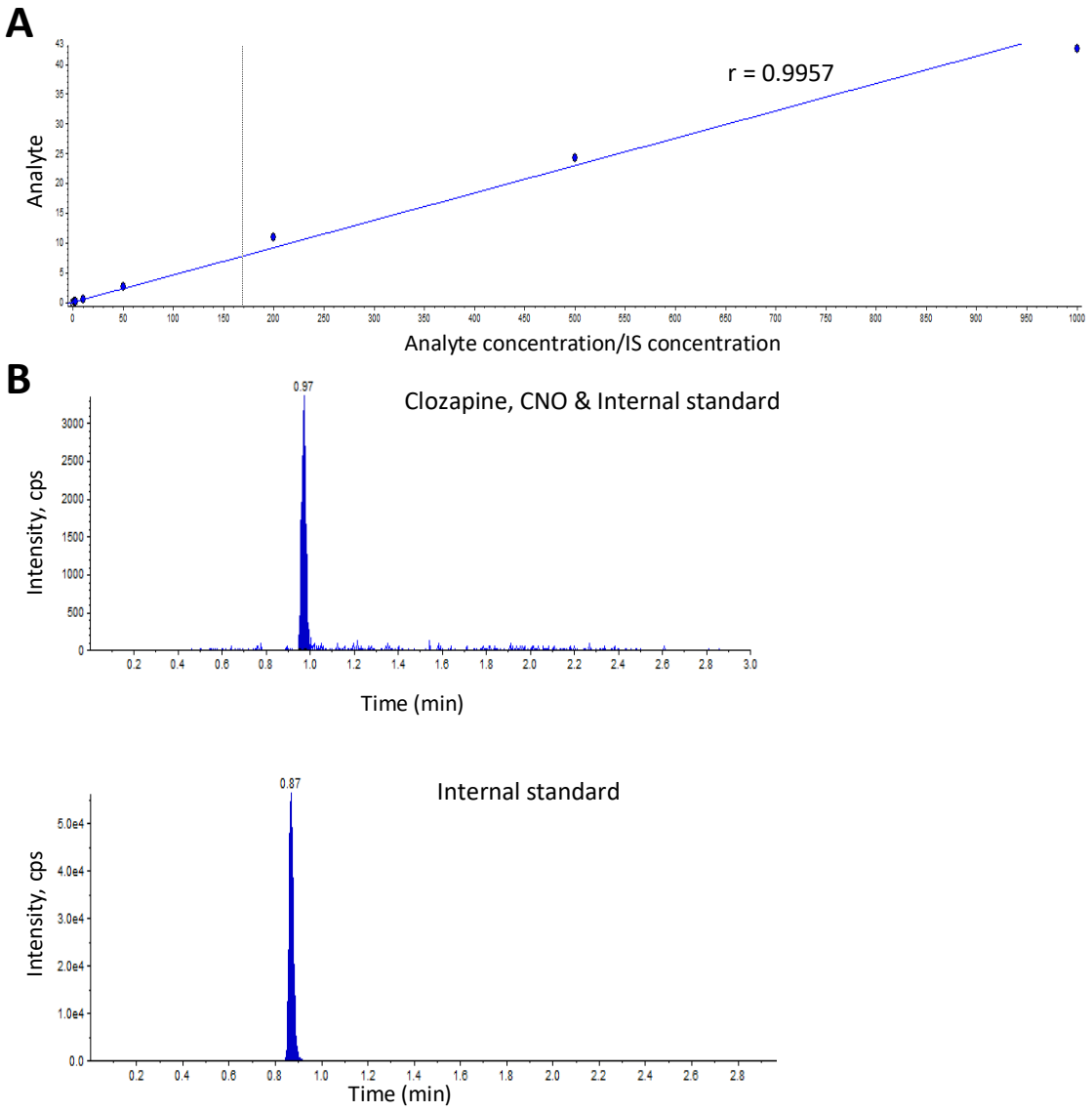


Figure 4.2: Brain calibration curve and chromatogram lower limit of quantification

(A) Clozapine and internal standard (IS) brain calibration curve and (B) peaks of clozapine, CNO and internal standard and the internal standard on its own from a brain sample.

4.2.10 Statistical analysis

All data in this chapter were analysed using GraphPad Prism 7 (GraphPad Software, Inc., San Diego, CA). Data was tested for normality by using a Shapiro-Wilk analysis. Paired t-test were used for experiments where a within-subject control design was employed. Otherwise,

unpaired t-tests or Mann Whitney-U tests were used. Significance was set at a P value of $p<0.05$.

The results of the CNO/clozapine exposure study were not analysed statistically, firstly because of the small samples size, n = 3 per group and secondly because this was an exploratory study rather than hypothesis-driven. The data presented for this study are mean values of n = 3 replicates.

4.3 Results

4.3.1 Effect of novel environment on c-Fos expression in hippocampus (Study 1)

Under resting state conditions, c-Fos expression in the hippocampus is low (Ryabinin et al., 1997). To facilitate c-Fos studies aimed to measure DREADD functionality in hippocampus, a pilot study was carried out in an attempt to elevate hippocampal c-Fos expression to measurable levels by exposing rats to a novel environment containing a novel object. Control animals remained in their home cage.

Stereological analysis of c-Fos immunopositive cells in hippocampus revealed a trend for increased number of c-Fos expression in hippocampus of rats exposed to novelty (mean ± SEM: 199.5 ± 6.3) compared to the control group (mean ± SEM: 130.2 ± 16.07) although the effect was not statistically significant (Mann-Whitney U, P = 0.1320) (**Figure 4.3**). Closer inspection of the data revealed elevated c-Fos levels in two control rats that were the last ones of their cage to be perfused, suggesting stress associated with separation from littermates may have been a confounding factor.

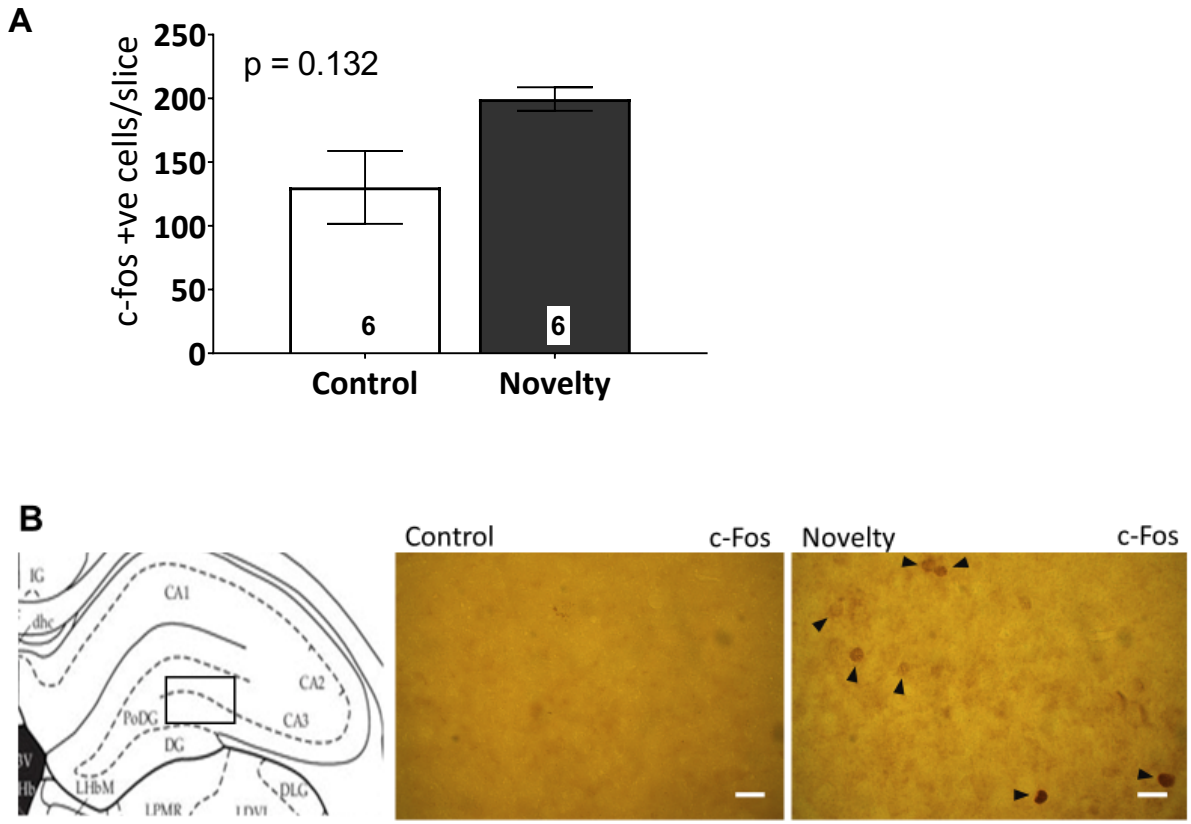


Figure 4.3: Effect of novelty on c-Fos expression in dorsal hippocampus.

(A) Stereological quantification of c-Fos positive cells in hippocampus of rats exposed to novelty (n=6, black) versus control rats (n=6, white). Data are represented as mean ± SEM values (Mann-Whitney U, P = 0.1320) (B) Example brightfield images showing c-Fos immunopositive muclei as indicated by black arrowheads in the CA3 area of a rat that has been exposed to novelty (right) versus control rat (left). Scale bar = 25 µm.

4.3.2 Effect of CNO or clozapine on c-Fos in hippocampus with Gi-DREADD (Study 2)

The functionality of CaMKIIa-driven expression of Gi-DREADD was tested in three cohorts. First, two groups of rats expressing a control construct (EGFP or mCherry tagged) and two groups expressing a Gi-DREADD were injected with either CNO (3 mg/kg, i.p.) or clozapine (0.5 mg/kg i.p.) and then placed in a novel environment for 2 h before perfusion to elevate the otherwise low resting state levels of c-Fos expression (see above). It was hypothesised that CNO or clozapine induced activation of the Gi-DREADD would decrease the elevated levels of c-Fos in response to novel environment exposure.

It was found that after 3 mg/kg i.p. CNO, the number of c-Fos positive cells in the Gi-DREADD expressing rats (71.75 ± 1.18) was not significantly different compared to the control group (67.83 ± 8.22) (t(8) = 0.3796, P = 0.7141, unpaired t-test; **Figure 4.4A**). Similarly, after 0.5 mg/kg i.p. clozapine the number of c-Fos positive cells in the Gi-DREADD expressing rats (88.19 ± 14.85) was not different from that in the control group (93.29 ± 9.39) (t(13) = 0.2803, P = 0.7836, unpaired t-test; **Figure 4.4B**).

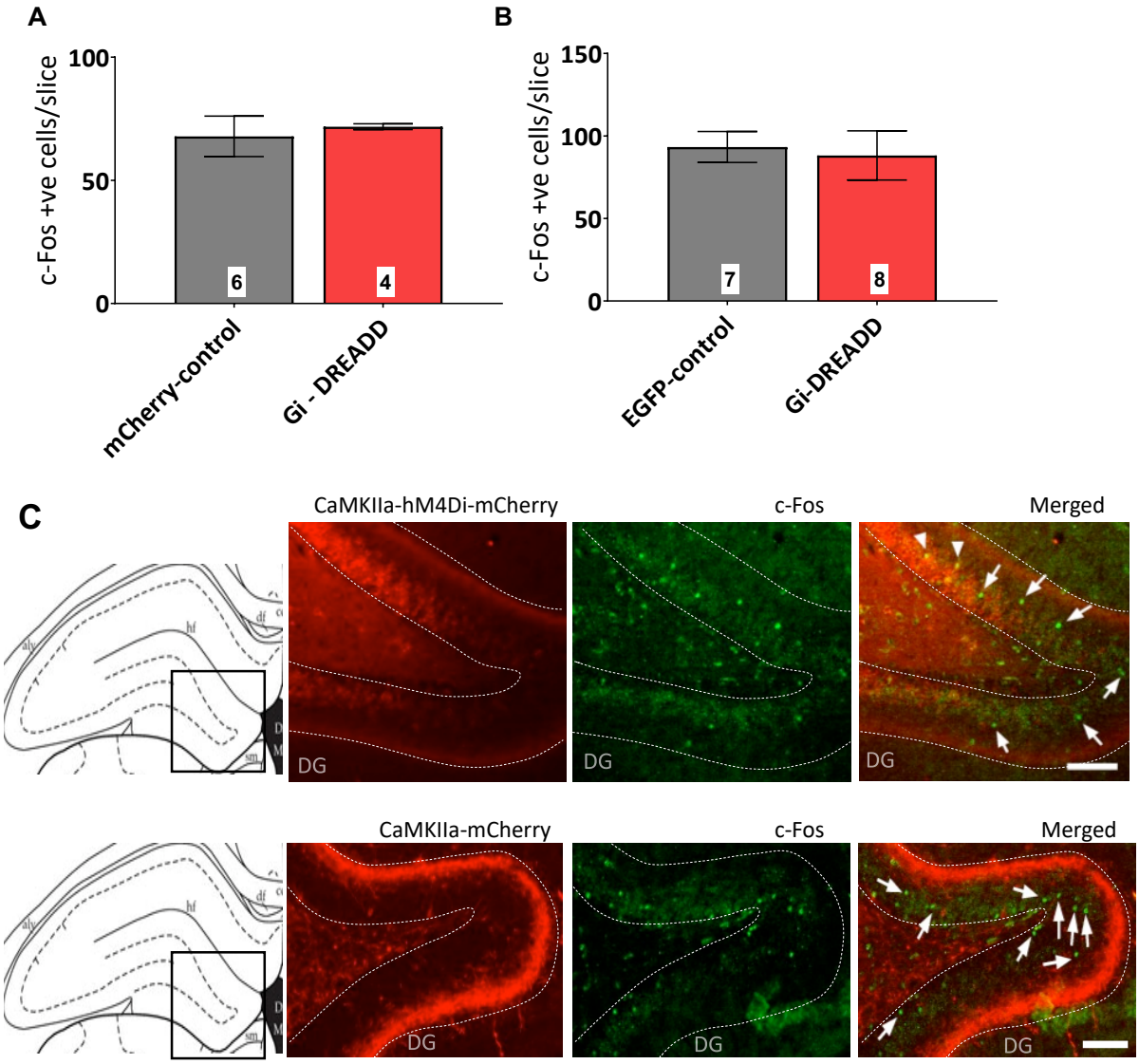


Figure 4.4: Effect of CNO or clozapine on c-Fos expression in hippocampus expressing CaMKIIa-driven expression of Gi-DREADD (hM4Di).

c-Fos positive cells in control or Gi-DREADD expressing rats following administration of (A) 3 mg/kg i.p. CNO (mCherry control, grey n=6; Gi-DREADD, red n=4) and (B) 0.5 mg/kg i.p. clozapine (EGFP control, grey n=7; Gi-DREADD, red n=8). (C) Examples of fluorescent images showing c-Fos labelling (green) in dentate gyrus with mCherry tagged Gi-DREADD (red, top) and mCherry-tagged control (red, bottom). Data are shown as mean ± SEM values. Scale bar = 100 µm. Arrows indicate c-Fos immunopositive nuclei.

In a third cohort a within-subject control design was employed by which one hippocampus expressed a mCherry tagged Gi-DREADD and an EGFP control construct was expressed in the contralateral hemisphere. All rats were injected with CNO (3 mg/kg i.p.) and placed in a novel environment for 2 h followed by perfusion. It was found that after 3 mg/kg i.p. CNO, the number of c-Fos positive cells in the Gi-DREADD expressing hippocampus (39.5 ± 8.29) was not significantly different compared to the control hemisphere (39.4 ± 5.99) ($t(4) = 0.02064$, $P = 0.9845$, paired t-test; **Figure 4.5**). Quantification was done in the CA3 area only where all rats displayed viral expression.

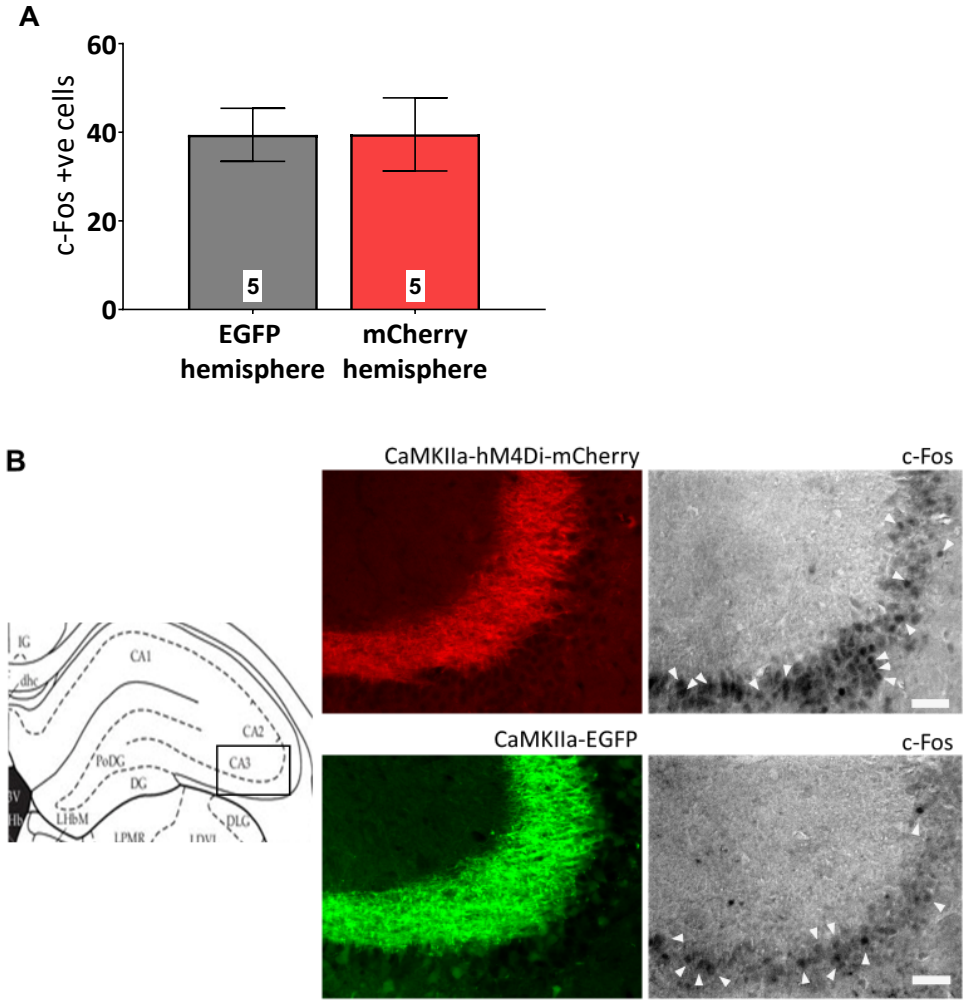


Figure 4.5: CA3 c-Fos levels in response to CNO induced Gi-DREADD activation.

(A) Control or Gi-DREADD expressing hippocampus following administration of 3 mg/kg i.p. CNO (mCherry control, grey n=5; Gi-DREADD, red n=5). (B) Example of fluorescent images (middle panels) showing mCherry tagged Gi-DREADD (red, top) and EGFP tagged EGFP-control (green, bottom) and DAB colour staining images (right panels) showing c-Fos labelling (black, right) in CA3. Data are shown as mean ± SEM values. Scale bar = 50 µm. Arrowheads indicate c-Fos immunopositive nuclei.

The above experiments failed to detect evidence of a decrease in c-Fos expression following administration of either CNO or clozapine to rats expressing CaMKIIa-driven Gi-DREADD in hippocampus. However, as in the case of the behavioural experiments, this lack of effect might be attributed to CNO not entering the brain (Gomez et al., 2017) or the CNO dose being too low. Additionally, the timing of the novel context exposure experiments in conjunction with CNO injection could be another explanation for the lack of effect. However, this does not explain the lack of effects observed with clozapine. To address this, in a final study (Study 3 below), the dose of CNO was increased to 10 mg/kg and rats were placed in the novel environment 30 min after injection.

4.3.3 Effect of higher dose CNO on c-Fos in hippocampus with Gi-DREADD or Gq-DREADD (Study 3)

The dose of CNO was increased for a final c-Fos study in both Gi and Gq-DREADD expressing rats in a within-subject design as described above. All rats were injected with CNO (10 mg/kg i.p.) and returned to the home cage, followed by 1 h novel environment exposure for the Gi-DREADD group. It was found that after 10 mg/kg i.p. CNO, the number of c-Fos positive cells in the Gi-DREADD expressing hippocampus was not significantly different compared to the control hemisphere ($t(7) = 0.02146$, $P = 0.9835$, paired t-test; **Figure 4.6**)

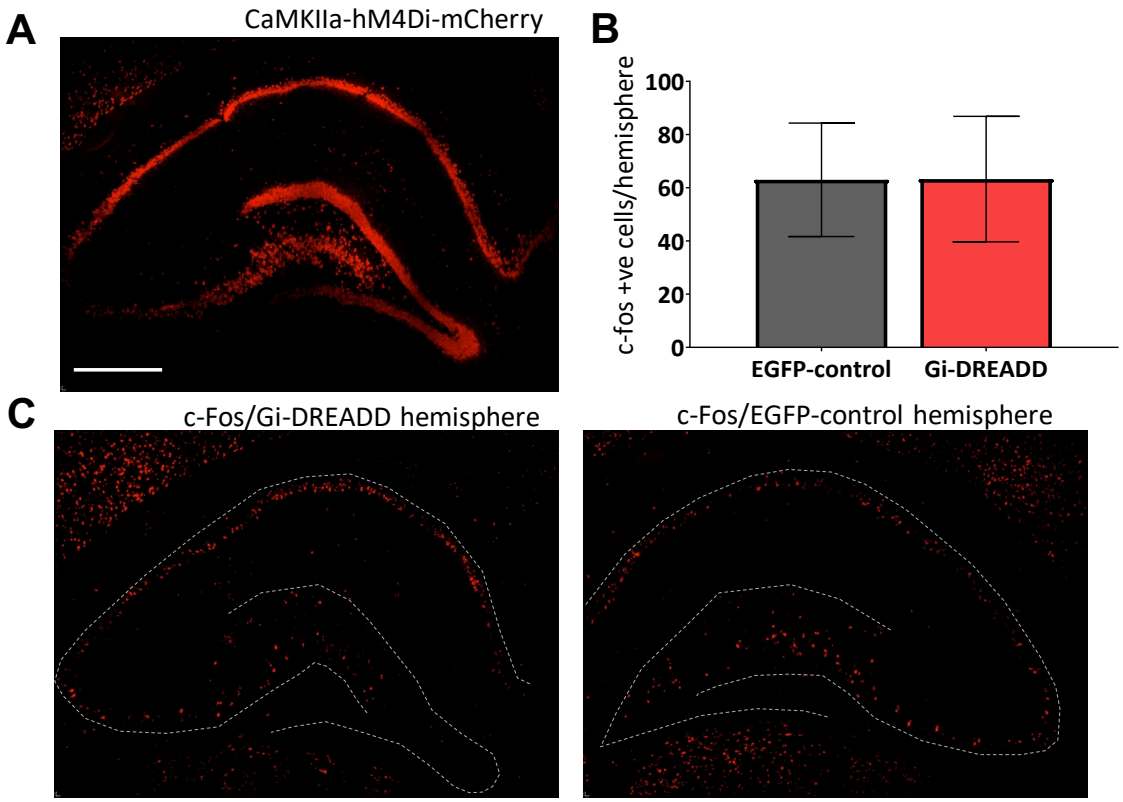


Figure 4.6: c-Fos expression pattern upon CNO (10 mg/kg) induced activation of a hippocampal inhibitory DREADD

(A) Example FISH image showing mCherry tagged Gi-DREADD (red) in the dorsal hippocampus. (B) c-Fos positive cells in an EGFP-control hemisphere (grey, n=8) or a Gi-DREADD hemisphere (red, n=8). (C) Example of FISH images showing c-Fos labelling (red) in dorsal hippocampus hemisphere expressing a mCherry tagged Gi-DREADD (left) and EGFP-control (right). Data are shown as mean ± SEM values**.** Scale bar = 500 µm.

Finally, rats expressing a Gq-DREADD in one hippocampal hemisphere and a control-DREADD in the contralateral hemisphere were injected with 10 mg/kg i.p. CNO and returned to home cage. It was found that after 10 mg/kg i.p. CNO, the number of c-Fos positive cells in the Gq-DREADD expressing hippocampus was significantly higher compared to the control hemisphere ($t(5) = 3.356$, $P = 0.0202$, paired t-test; **Figure 4.7**) This increase in c-Fos mRNA expression seems to be more pronounced in the areas where the viral construct was also expressed. Thus, this confirms the *in vitro* functionality of a Gq-DREADD upon CNO systemic administration.

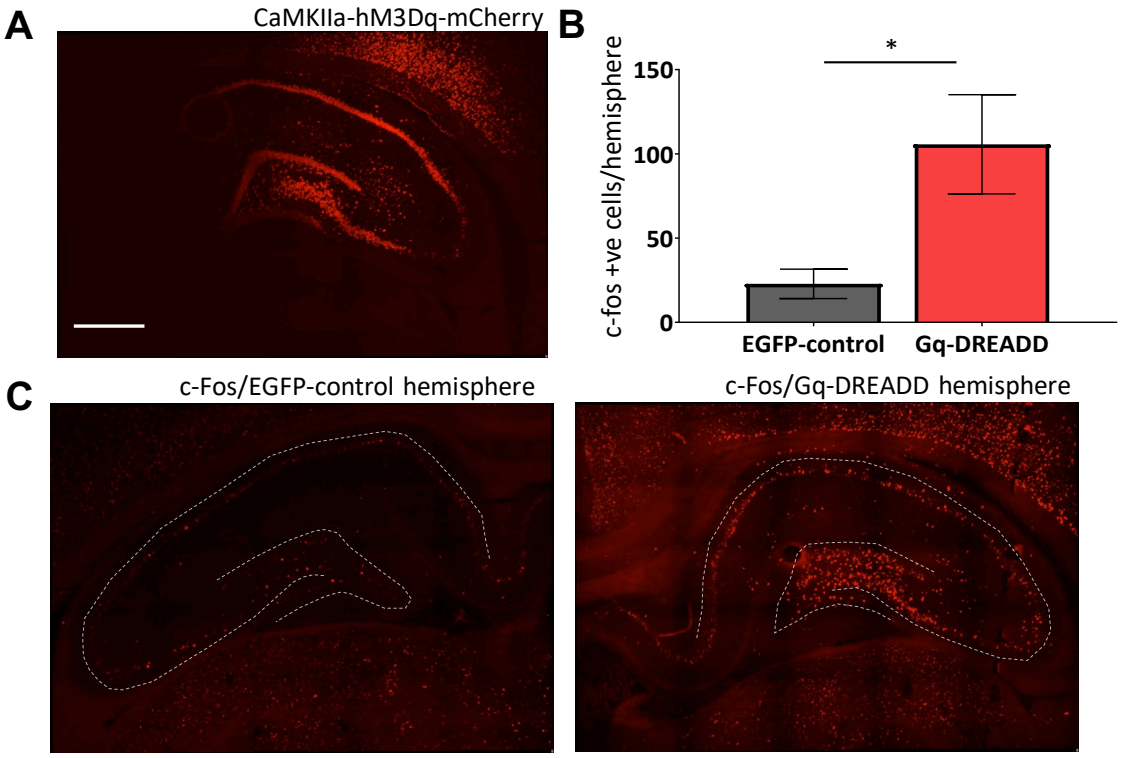


Figure 4.7: c-Fos expression pattern upon CNO (10 mg/kg) induced activation of a hippocampal excitatory DREADD

(A) Example FISH image showing mCherry tagged Gq-DREADD (red) in the dorsal hippocampus. (B) c-Fos positive cells in an EGFP-control hemisphere (grey, n=6) or a Gi-DREADD hemisphere (red, n=6), *P = 0.0202, paired t-test. (C) Example of FISH images showing c-Fos labelling (red) in dorsal hippocampus hemisphere expressing a mCherry tagged Gq-DREADD (right) and EGFP-control (left). Data are shown as mean ± SEM values. Scale bar = 500 µm.

Collectively, these data found no evidence of a decrease in c-Fos expression following administration of CNO (3 or 10 mg/kg) or clozapine (0.5 mg/kg) to rats expressing CaMKIIa-driven Gi-DREADD in hippocampus. There was however evidence of increased c-Fos activity following CNO (10 mg/kg) administration in Gq-DREADD expressing rats, thus providing proof of concept evidence for the excitatory DREADD.

4.3.4 Plasma levels of clozapine and CNO following systemic administration of clozapine and CNO

Results presented thus far showed no effect of CNO/clozapine on behaviour or on c-Fos expression, unsuitable dose or timing of drugs administration being a potential reason for these outcomes. Additionally, it was important to assess how concentrations of CNO/clozapine that inhibit transmission in the slice experiments compare to brain concentrations after systemic administration. Thus, in the light of the above and a report published whilst this thesis was in progress (Gomez et al., 2017), a study measuring the exposure of brain and plasma to CNO (3 or 10 mg/kg i.p.) and clozapine (0.1 or 0.5 mg/kg i.p.) was conducted. The first aim was to assess whether CNO reached the brain and if it was back metabolised to clozapine. The second aim was to establish a time-dependent profile of tissue exposure to the two compounds. To this end, brain tissue and plasma were collected 5, 30, 60, 120 and 240 min post injection.

The results showed that i.p. injection of CNO caused a dose-related increase in plasma concentrations of CNO which peaked within 30 min of administration (768.3 ng/ml after 3 mg/kg CNO; 1836.7 ng/ml after 10 mg/kg CNO) and decrease to undetectable levels within 2 h (**Figure 4.8B**). Interestingly, i.p. injection of CNO also caused a dose-related rise in plasma levels of clozapine which showed a similar time course as CNO itself, although clozapine levels were around 2 orders of magnitude lower (4.7 ng/ml after 3 mg/kg CNO; 12.8 ng/ml after 10 mg/kg CNO) (**Figure 4.8A**). The latter data are evidence of that at the doses used there is back conversion of CNO to clozapine.

In comparison, i.p. injection of clozapine caused a variable but dose-related increase in plasma concentrations of clozapine without a clear peak over the time course tested (**Figure 4.8A**). There was no detectable increase in plasma levels of CNO within 4 h of clozapine

injection, (**Figure 4.8B**), suggesting the lack of metabolism of clozapine to CNO at the doses tested.

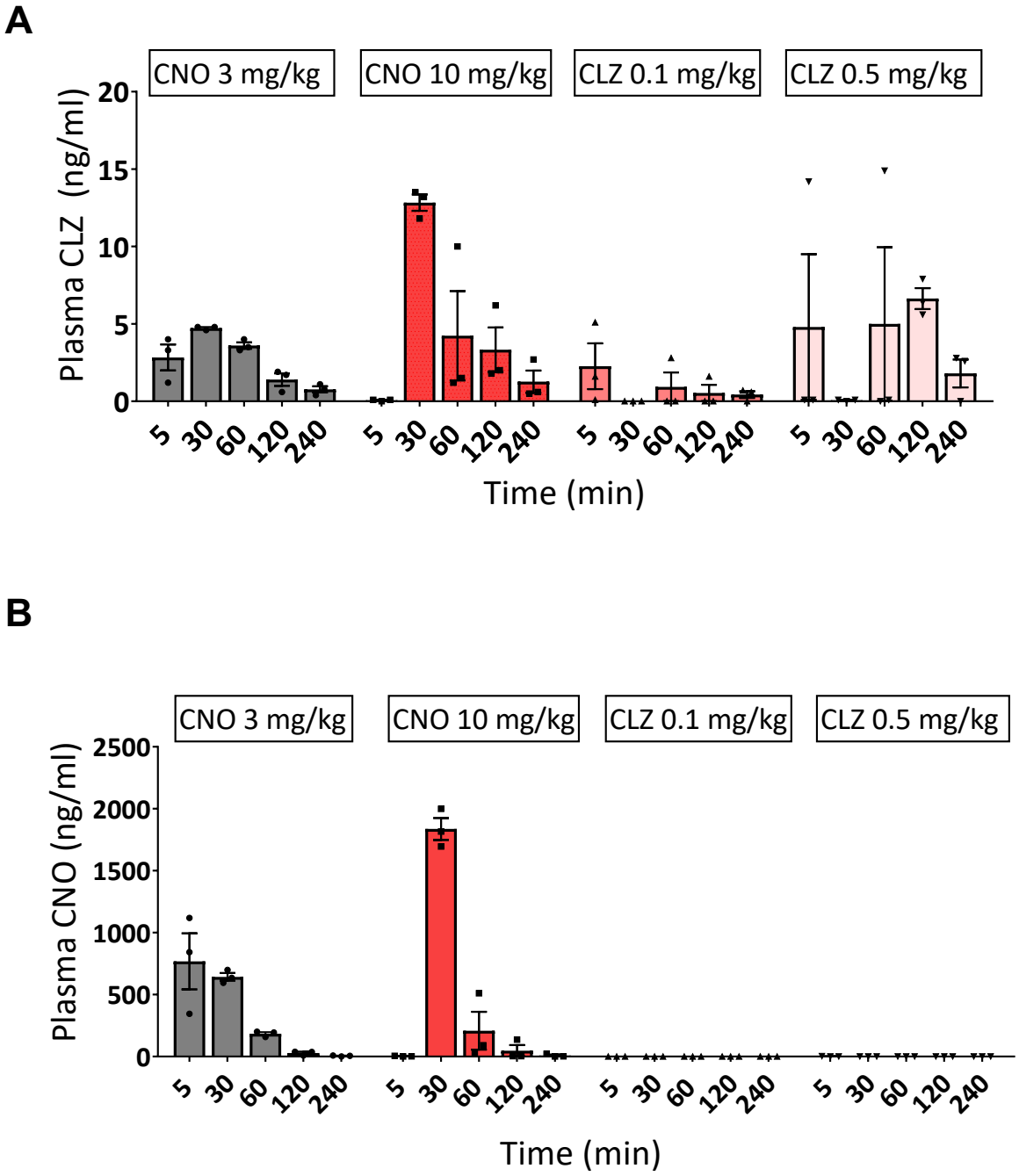


Figure 4.8: Changes in plasma levels of clozapine and CNO at different time points following systemic administration of these agents.

Plasma concentrations of clozapine (A) and CNO (B) were measured in rats injected with either CNO (3 or 10 mg/kg i.p.) or clozapine (0.1 or 0.5 mg/kg i.p.). Individual values from each rat are shown together with mean ± SEM values (n=3).

4.3.5 Brain levels of clozapine and CNO following systemic administration of clozapine and CNO

Next, brain levels of CNO and clozapine were analysed following administration of these agents. CNO evoked a dose-related increase in brain levels of CNO, which followed a similar time-course to plasma CNO levels (**Figure 4.9B**). At the highest dose tested CNO (10 mg/kg) increased brain CNO levels to around 25 ng/g. Interestingly, systemic administration of CNO also generated the presence of clozapine in the brain with levels peaking around 30-60 min and being around 5-10 times higher than brain levels of CNO (e.g. 188 ng/g clozapine 30 min post 10 mg/kg i.p. CNO; 70.8 ng/g clozapine 60 min post 3 mg/kg i.p. CNO) (**Figure 4.9A**).

Injection of clozapine also caused an increase in brain levels of clozapine, which was dose-related and followed a similar time course to plasma clozapine levels. (**Figure 4.9A**). There was no detectable CNO in the brain over the 4 h post-clozapine period (**Figure 4.9B**), suggesting the lack of metabolism of clozapine to CNO at the doses tested. The latter result suggests that clozapine was not metabolised to CNO, in accordance with the above plasma data.

Overall, these data suggest that while there is a high concentration of CNO in the plasma following CNO systemic administration, very little of it enters the brain. To further test this idea, brain/plasma (B/P) ratios were plotted for CNO (**Figure 4.10B**) and clozapine (**Figure 4.10A**). These plots illustrate that CNO and clozapine lead to a time-dependent increases in the B/P clozapine ratio, suggesting that both agents elevate the brain concentration of clozapine to a degree higher than that for plasma. Interestingly, the plots for the B/P CNO ratios suggest that whilst administration of CNO elevates CNO levels in plasma, very little enters the brain.

In summary, the above data on CNO exposure suggest that the 3 mg/kg dose used in the behavioural and c-Fos studies generates a low level of clozapine in the brain but little or no CNO itself. However, a higher dose of 10 mg/kg CNO produces brain clozapine concentrations similar to that of a low dose of clozapine (0.5 mg/kg).

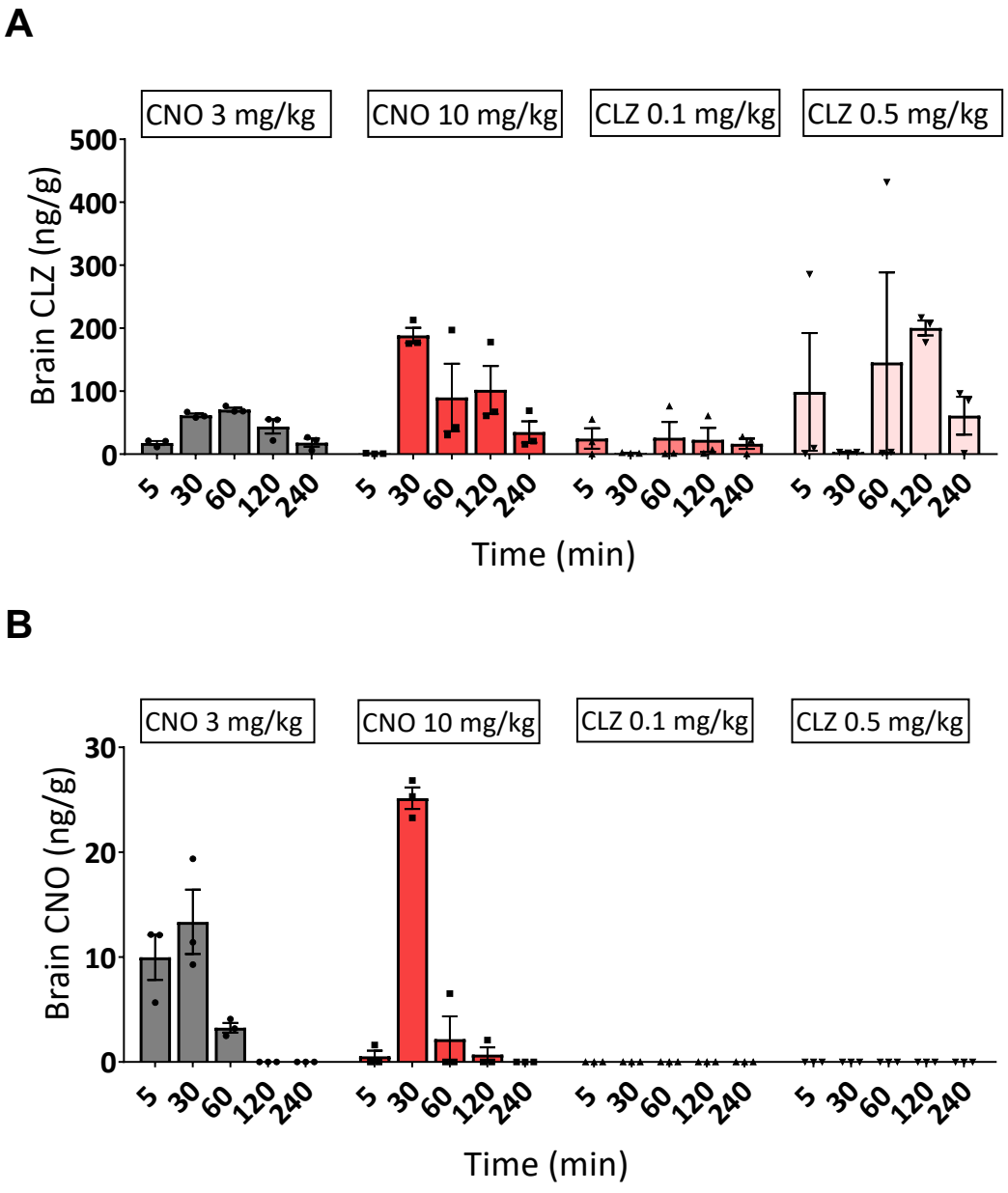


Figure 4.9: Changes in brain levels of clozapine and CNO at different time points following systemic administration of these agents.

Whole brain concentrations of clozapine (A) and CNO (B) were measured from rats injected with either CNO (3 or 10 mg/kg i.p.) or clozapine (0.1 or 0.5 mg/kg i.p.). Individual values from each rat are shown together with mean ± SEM values (n=3).

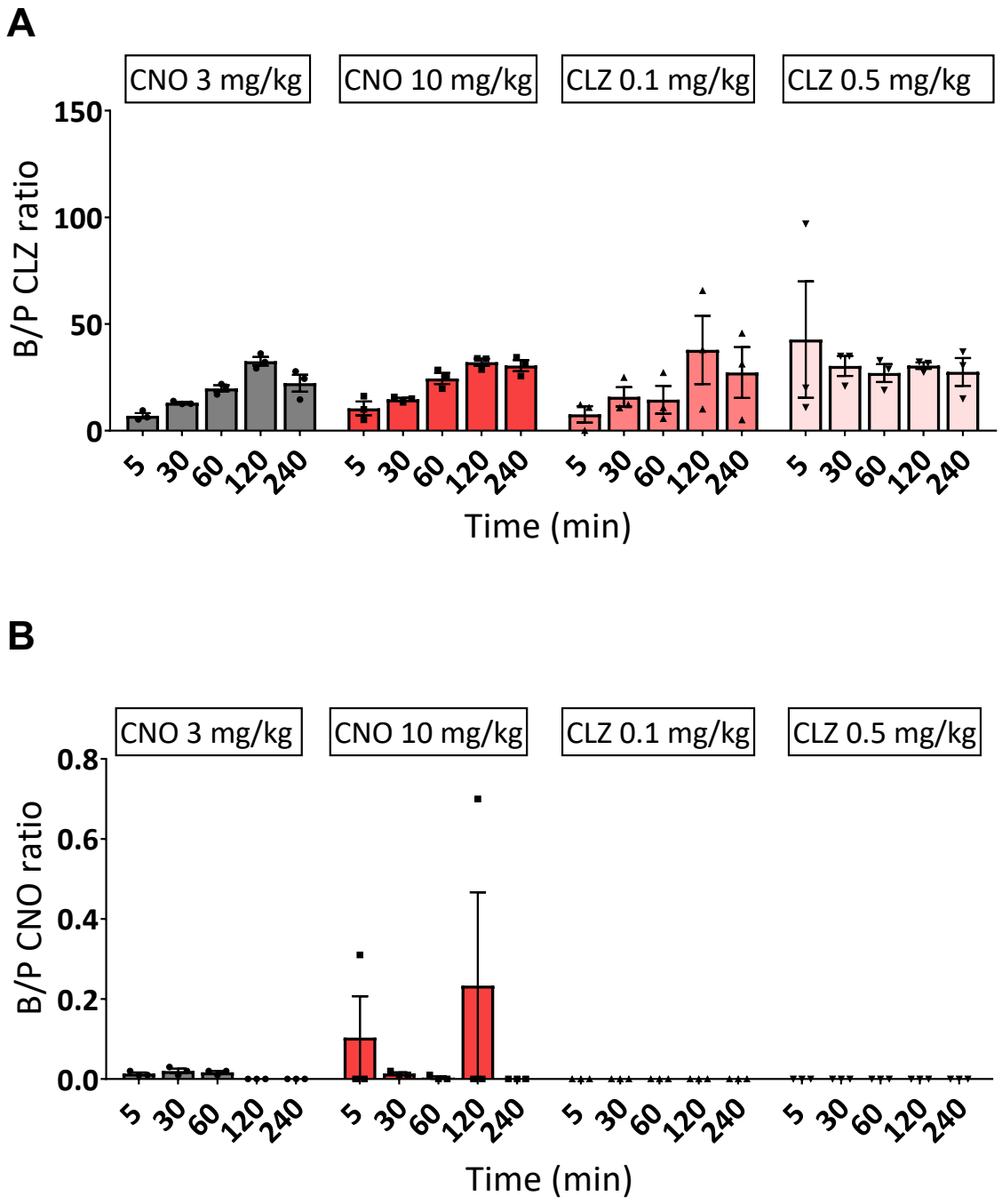


Figure 4.10: Brain/plasma ratio of clozapine and CNO at different time points following systemic administration.

Brain/plasma ratios for clozapine (A) and CNO (B) in rats injected with either CNO (3 or 10 mg/kg i.p.) or clozapine (0.1 or 0.5 mg/kg i.p.). Individual values from each rat are shown together with mean ± SEM values (n=3).

4.4 Discussion

Experiments in this chapter aimed to investigate the lack of behavioural effect of CNO administered to rats expressing CaMKIIa-driven Gi-DREADD in hippocampus observed in chapter 3. Specifically, one set of experiments investigated the functionality of Gi-DREADD using c-Fos expression as a marker of neural activity. A second set of experiments investigated the exposure of the brain to systemically administered CNO. The main findings were as follows.

A pilot study showed that hippocampal c-Fos expression showed a tendency to be activated by environmental manipulation (novel environment). Using this model it was found that CNO (3 mg/kg i.p.) did not inhibit c-Fos expression in hippocampus despite the expression of Gi-DREADD in this region. Clozapine (0.5 mg/kg i.p.), another putative DREADD agonist, was similarly ineffective in this model. The CNO exposure study revealed that the dose of CNO used in the c-Fos study (3 mg/kg i.p.) generated measurable amounts of CNO in plasma but very low if detectable levels of CNO in the brain. Interestingly, it was found that CNO (3 mg/kg i.p.) increased brain levels of clozapine, with a higher dose of CNO (10 mg/kg i.p.) producing brain levels of clozapine similar to that of clozapine (0.5 mg/kg i.p.) alone. The latter finding is consistent with emerging evidence that CNO has poor brain penetrance and that any DREADD-mediated effects of CNO are likely to be mediated by back metabolism to clozapine which enters the brain to act as a DREADD agonist. In the light of these findings a final c-Fos experiment with Gi-DREADD expressing rats was carried out using an increased dose of CNO (10 mg/kg i.p.). Although at this higher dose CNO still did not inhibit c-Fos expression in hippocampus, it increased c-Fos expression in a separate experiment using rats expressing Gq-DREADD.

4.4.1 Effects of CNO and clozapine on c-Fos after DREADD expression

Neither CNO nor clozapine decreased c-Fos expression in the presence of Gi-DREADD in hippocampus. The number of c-Fos positive cells in hippocampus was low under resting conditions but nevertheless measurable and tended to increase in response to exposure to a novel environment, as previously reported (VanElzakker *et al*, 2009). Thus, it is unlikely that the lack of effect of CNO and clozapine on c-Fos expression was simply caused by a floor effect that masked inhibitory effects of CNO/clozapine. Moreover, these experiments were sufficiently powered in the sense that a within-subject design was utilised, with measurements of c-Fos expression in a Gi-DREADD transfected hippocampus being compared with a control viral construct transfected in the contralateral side. The experiment was replicated in a different cohort to eliminate the interference prior experience of novelty might have had on c-Fos levels, as c-Fos in known to decrease with repeated exposure to novelty and subsequent habituation (Papa et al., 1993), and similar results were achieved.

An interesting finding was that whilst the current study did not detect an effect of CNO on hippocampal c-Fos expression in the presence of CaMKIIa-driven Gi-DREADD, the drug evoked a clear-cut increase in c-Fos in the presence of CaMKIIa-driven Gq-DREADD. This result was expected on the basis of previous studies demonstrating that CNO increases c-Fos expression in Gq-DREADD transfected brain regions. For example, in mice, CNO (0.5 mg/kg) was reported to increase c-Fos expression in the cortex in the presence of a Gq-DREADD (Yuan & Grutzendler, 2016). Also in mice, CNO administered in eye-drops increased c-Fos levels in the hippocampus in a dose dependent manner 90 min after administration, with less than 10% of Gq-DREADD cells also expressing c-Fos after saline, 0.001 and 0.01 mg/kg CNO, 26% of cells showing co-labelling after 0.1 mg/kg CNO and more than 95% of Gq-DREADD cells being co-expressed with c-Fos after 1 mg/kg CNO (Keenan et al., 2017). In rats, it was reported that c-Fos levels were tripled in the doubled labelled c-Fos/Gq-DREADD population

in the dmPFC after 3 mg/kg CNO (Yau & McNally, 2015). Lastly, at the same CNO dose (3 mg/kg) Sengupta et al., (2016) found in a within-subject design that was also used in the current study, that c-Fos was increased in the basolateral amygdala of rats expressing a Gq-DREADD, 150 min after CNO injection, compared to the control hemisphere (Sengupta et al., 2016). Still, the increased c-Fos levels in the current experiment are somewhat surprising considering the results in Chapter 2 that found that CNO decreased neuronal activity in hippocampal slices expressing a Gq-DREADD. However, there is the possibility that the decrease in excitatory transmission observed in the electrophysiological experiments comes about as a consequence of increased neuronal activity (see Chapter 6 for discussion).

The current unaltered c-Fos expression in the Gi-DREADD expressing slices is also in contrast to the results in Chapter 2 that found decreased excitatory transmission in slices in the presence of CNO but also other studies that have used different techniques to elevate c-Fos levels followed by subsequent decrease in response to CNO induced Gi-DREADD activation. For example, as mentioned above, one study pharmacologically increased c-Fos levels in the mouse dACC by using phetylenetetetrazole, a $GABA_A$ antagonist (Koike et al., 2016). Another study, where KORD – a different type of inhibitory DREADD – was used instead of a Gi-DREADD, a similar experimental design as described in this chapter was used. Specifically, agonist binding to the KORD decreased novelty-induced c-Fos expression in neurons expressing the DREADD in the ventral subiculum of rats (Marchant et al., 2016).

A number of factors could explain the lack of c-Fos changes as a consequence of CNO binding to Gi-DREADD. Firstly, one cannot be certain that decreased neuronal activity is correlated with decrease c-Fos expression, as evidence from the slice experiments in Chapter 2 showing opposite effects in excitatory transmission to the results in the c-Fos experiments presented here in both Gi and Gq-DREADD expressing hippocampal cells. Secondly, there is the

possibility that the Gi-DREADD is expressed in interneurons in which case the effects targeted to CaMKIIa expressing neurons would be missed. As shown in earlier experiments (Chapter 2), DREADDs were transfected in a population of GABAergic interneurons. Future experiments could address this issue by assessing the extent of c-Fos expression in interneurons. Thirdly, there is the possibility that there is a short-lasting inhibition of pyramidal cells but then there is recovery/adaptation, such that the net effect on c-Fos is minimal, which could indicate that the c-Fos approach does not have the temporal resolution required to assess Gi-DREADD function. Lastly, the exposure data addresses the issue of the CNO dose used, and shows that high dose of CNO (10 mg/kg) increases brain levels of clozapine (0.58 μM) to concentrations likely to interact with the DREADDs (1 μM), as confirmed in the slice *ex vivo* experiments in Chapter 2. Moreover, this dose was shown to be effective in activating c-Fos in Gq-DREADD expressing rats which could indicate an issue with the Gi-DREADD/c-Fos pairing. Thus, this rules out the possibility of insufficient agonist binding to the Gi-DREADD.

Finally, the current result observed in the Gi-DREADD slices are in line with the lack of behavioural changes presented in Chapter 3, which might suggest that there might not be enough inhibition of glutamatergic transmission to cause changes in neuronal activation or lead to behavioural deficits.

4.4.2 CNO and clozapine pharmacokinetics

At the time of the current study, the literature regarding the ability of CNO to act as a DREADD agonist had been brought into question by reports showing back conversion of CNO to clozapine in mice, rats and rhesus monkeys, and the absence of CNO in the brains of rats and mice following CNO exposure (MacLaren et al., 2016; Raper et al., 2017; Gomez et al., 2017). The results from the current exposure study have strengthen the notion that CNO is poorly brain penetrant by providing some of the first data on brain concentrations of CNO after

systemic administration. In particular, it was found that systemic administration of CNO failed to produce detectable levels of CNO in the brain despite increasing plasma CNO levels, suggesting poor CNS penetrance. Moreover, the same doses of CNO which failed to generate significant brain levels of CNO, caused clear-cut increases in brain levels of clozapine, likely through reverse metabolism. All this is in keeping with the idea that any DREADD agonist effects of systemically administered CNO are mediated by clozapine entry into the brain.

A number of very recent studies have also addressed the pharmacokinetics of CNO. Jendryka and colleagues (2019) have reported a detailed analysis of the pharmacokinetics of CNO, clozapine and Compound 21, a novel DREADD agonist, in mice. In line with the current findings, this study demonstrated evidence of the back metabolism of CNO to clozapine (Jendryka et al., 2019). A recent report using a drug discrimination procedure found that rats and mice were not able to discriminate based on interoceptive effects between 1.25 mg/kg clozapine and 10 mg/kg CNO, but not lower doses of CNO (Manvich et al., 2018).

Data from the current study revealed similar levels of clozapine in the brain after 10 mg/kg CNO or 0.5 mg/kg clozapine injection (0.58 μM *vs*. 0.61 μM respectively). This is interesting as clozapine (1 μM) was shown to be an agonist at both the Gi and Gq-DREADD in the *ex vivo* slice electrophysiology experiments presented in Chapter 2 (see **Figure 2.10**). Thus, this provides evidence that clozapine is mediating the effects of systemic CNO in the context of DREADD activation.

Clozapine itself binds with high affinity to a multitude of receptors (serotoninergic, dopaminergic, muscarinic, adrenergic) (Ashby & Wang, 1996; Roth et al., 2004) so there is a risk of off-target effects at endogenous receptors. However, CNO was also shown to competitively inhibit binding of ligands at < 0.1 μM concentrations (i.e. 5-HT2A, 5-HT2B and

H1 receptors) (Jendrkya et al., 2019). Still, as results in the current exposure study showed the highest concentration of CNO in the brain after 10 mg/kg CNO was 73 nM, the chance for off-target effects of CNO is minimal.

It is unclear where in the body back metabolism of CNO to clozapine takes place. As seen in the current exposure study, after systemic administration of CNO most of the CNO remains in the plasma while clozapine is mostly found in the brain. This suggests that back metabolism of CNO to clozapine is unlikely to take place in significant amounts in either the plasma or brain. One possibility is that the back conversion happens at the blood brain barrier (BBB) where it is aided by BBB enzymes. An alternative explanation for the low concentrations of CNO in the brain is that the drug is a substrate for p-glycoprotein efflux pump that prevents molecules from crossing the BBB (Schinkel et al., 1996). Interestingly, clozapine is not a substrate for the p-glycoprotein efflux pump (Raper et al. 2017, Gomez et al., 2017), thereby making it readily available for BBB entry.

A potential drawback of the current drug exposure measurements is that whole brain tissue extracts may not provide an accurate indicator of compound concentrations because of the likelihood that molecules remain bound to the tissue (Jandryka et al., 2019). Further, it is proposed that drug levels in cerebrospinal fluid (CSF) may give a better measure of BBB penetration and drug levels in the brain. However, the efflux pump that limits the permeability into the brain is located at the BBB while blood and CSF are separated by the choroid plexus that is known to be leakier than the BBB and allows most compounds in the blood to enter the CSF, (Partridge, 2011; Bickel, 2005). As a result, drug CSF levels are indeed a good indicator of unbound drug levels but should not be used as a measure of the ability of molecules to enter the brain *via* the BBB.

Lastly, a few solutions are available to bypass the risk of back conversion of CNO to clozapine. Firstly, CNO micro infusions to the site of DREADD expression could be used instead of injections (Stachniak et al., 2014). Alternatively, different DREADD agonists could be used. Compound 21 has gained a lot of attention in the light of the Gomez report, with a few groups validating its agonistic properties at the DREADDs and assessing its promising pharmacokinetics (Thompson et al., 2018; Jendryka et al., 2019). However, based on the numerous studies that have successfully used CNO as a DREADD agonist, CNO should not be discarded and deemed useless prematurely. Most importantly, investigators should use appropriate controls, for both viral construct and for the agonist of choice in order to avoid any misinterpretation of the data.

4.4.3 Conclusions

Experiments in this chapter aimed to use a c-Fos approach to assess DREADD function in the hippocampus. The results however suggested that while Gq-DREADD functionality is straightforward to achieve using c-Fos as a marker of neuronal activation, Gi-DREADD function as predicted from experiments in Chapter 2 was not established by using this technique. Additionally, an exposure study strengthened the notion that CNO is poorly brain penetrant and that *in vivo*, its DREADD agonist effects are likely mediated by back metabolism to clozapine which readily penetrates the brain. *In vivo* electrophysiological recordings in the next chapter were aimed at investigating the paradoxical effects reported in these first chapters.

Chapter 5

DREADDs as tool to study cortical mechanisms of cognition

5.1 Introduction

Experiments in the previous chapters provided evidence for functionality of a hippocampal inhibitory DREADD in a slice electrophysiology experiment. The decreased excitatory transmission observed in slices was not however translated into c-Fos or behavioural changes. Surprisingly, similar decreased excitatory transmission was observed in slices expressing an excitatory DREADD. Paradoxically, this was manifested by increased c-Fos expression upon CNO administration. Thus, *in vivo* electrophysiological recordings could provide insights into whether the glutamatergic decrease causes changes at the network level and if these changes are sufficient to alter behaviour.

5.1.1 *In vivo* electrophysiological recordings

Local field potentials (LFP) are electrical signals measured extracellularly in deep brain structures. LFP recordings are enabled by the implantation of a metal or glass electrode into the brain causing minimal damage. The changes in voltage in the brain region around the electrode are detected and recorded in respect to a reference electrode or screw. The major contributor to the LFP signal is synaptic current, however any transmembrane flow of ions or excitable cell causing voltage changes will contribute to the LFP (Buzsaki et al., 2012).

Electrocorticography (ECoG) uses skull implanted stainless steel electrodes above the brain region of interest. The electrical activity is therefore recorded directly from the surface of the dura mater and minimises the interference created by the skull upon EEG recordings from the scalp (Buzsaki et al., 2012).

Voltage fluctuations in the LFP represent a summation of coordinated neuronal activity that gives rise to rhythmic oscillations at different frequencies. Here, brain oscillations were separated into the following frequencies: theta (4-10 Hz), beta (10-30 Hz), low gamma (30-50 Hz), high gamma (50-90 Hz) and high frequency oscillations (HFO, 90-150 Hz).

5.1.2 Hippocampal oscillations

Theta, θ

Hippocampal theta rhythms are low frequency brain waves known to occur during rapid eye movement (REM) sleep and active exploration (Vanderwolf, 1969; Colgin, 2013), but also during freezing in a fear conditioning task (Seidenbecher et al., 2003). Medial septum (MS) parvalbumin (PV) interneurons projecting to the principal layers of the dorsal hippocampus act as 'pacemakers' of the theta rhythm (Freund & Antal, 1988), with evidence from MS inactivation studies showing disruption of theta generation (Mizumori et al., 1990, Brandon et al., 2005, 2011). Functionally, theta rhythms are present during exploratory behaviour with theta power being increased during learning and memory retrieval, in short-term memory tasks (Vertes, 2005) and absent during periods of immobility (Buzsaki, 2002).

Beta, β

The role of beta waves in the hippocampus is yet unclear but it is thought that beta rhythmic oscillations play a role in processing of meaningful cues. Increased beta oscillations have been reported in olfactory discrimination tasks in the DG and CA1. Increased beta was correlated with decreased theta oscillations upon anticipation of an outcome based on external cues (Rangel et al., 2015).

Gamma, γ

Gamma oscillations (30-90 Hz) can be separated into two frequency bands, slow and fast gamma (Colgin, 2016), based on their origin. Slow gamma in the CA1 was shown to be phase locked to CA3 gamma oscillations whilst fast gamma in the CA1 is driven by input from the medial entorhinal cortex (Colgin, 2009). However, more recently researchers have described three types of gamma osillations, slow, mid-frequency and fast based on their origin from the CA3, entorhinal cortex or CA1 respectively (Schomburg et al., 2014; Lasztoczi & Klausberger, 2016). For clarity, in this thesis gamma oscillations have been divided into two frequency bands and will be referred to hereinafter as low gamma (30-50 Hz) and high gamma (50-90 Hz). Gamma generation requires coordinated activity between excitatory and inhibitory neuronal ensembles with evidence from perisomatic inhibition of pyramidal neurons by parvalbumin basket cells as generator of brain oscillations at a gamma frequency (Buzsaki & Wang, 2012). Further evidence comes from optogenetic studies showing decreased cortical gamma power upon optogenetic silencing of parvalbumin interneurons (Sohal et al., 2009), or increased gamma oscillations upon optogenetic activation (Cardin et al., 2009). Additionally, blockade of AMPA receptors abolished gamma activity suggesting dependence of gamma rhythm on excitatory tone from pyramidal neurons (Mann et al., 2005). Failure in gamma regulation is a marker of neurological disorders and is thought to be at the root of cognitive deficits in schizophrenia (Gandal et al., 2012).

Sharp wave ripples (SWR)

Sharp waves are high amplitude oscillations recorded from the CA1 stratum radiatum being originally generated in the CA3 (Buszaki et al., 1983). The ripple component of the SWR is a ‘short-lived fast oscillatory pattern’ in the range of 110-200 Hz that can be observed in the LFP of hippocampal recordings (Buszaki, 2015). SWR are associated with awake behaviour in the rat and appear during periods of theta rhythm absence (O’Neill et al., 2006). Specifically, while

theta occurs during exploratory behaviour, SWR occur during awake immobility or regular non-exploratory behaviour such as eating or drinking. SWR are also seen in non-REM sleep recordings (O'Neill et al., 2006). It is believed that SWR play a role in memory consolidation by occurring during non-REM sleep. In support of this Girardeau et al. (2009) showed that in the absence of SWR during sleep after learning a task on a radial maze, rats performed worse compared to controls (Girardeau et al., 2009). The presence of SWR was not investigated in this thesis as this was beyond the scope of these studies.

5.1.3 DREADDs as tools to study hippocampal oscillations

Based on their ability to modulate specific neuronal populations, DREADDs can be a useful tool to study brain oscillation in relation to behavioural output. Alexander et al., (2009) showed dose-dependent increase in high gamma power in LFP signal recorded from hippocampus in response to CNO induced activation of a Gq-DREADD in mice. The investigators suggest that the gamma oscillations are a consequence of pyramidal excitatory transmission mediating interneuron activation (Alexander et al., 2009). More recently, a different study reported suppression of sharp wave ripples (SWR) in mouse CA1 during LFP awake head fixed recordings upon CNO activation of a Gi-DREADD targeted to the excitatory neurons of the olfactory bulb (Liu et al., 2017). DREADDs were also used to manipulate CA2 excitatory neurons. Results from this study showed decreased low-gamma power and increased SWR upon inhibition of CA2 pyramidal neurons in the hippocampus and neurons in the prefrontal cortex. The opposite effect was observed on low-gamma power and SWR activity upon CNO mediated excitation of CA2 pyramidal neurons (Alexander et al., 2018).

Based on the above and data presented in previous chapters, we predicted that Gi-DREADD expression in the pyramidal neurons of the dorsal hippocampus will cause decreased gamma power in LFP recorded from the site of DREADD expression. CNO induced supressed

excitatory transmission from the pyramidal neurons would lead to a subsequent decreased excitatory tone onto the interneurons that are responsible for gamma oscillations generation through perisomatic inhibition of the pyramidal neurons. Furthermore, hippocampal-dependent memory deficits would be expected as a consequence of reduced gamma power. The opposite effect would be anticipated from Gq-DREADD expressing rats. However, based on electrophysiological results from Chapter 2, decreased gamma power in Gq-DREADD rats would not be surprising.

Resting state recordings were carried out in the experiment described in this chapter. Unlike resting state in humans that is preferred for EEG or fMRI studies and is characterised by awake immobility to avoid movement artefacts (Jobert et al., 2012), resting state in rodents is described and used in the context of this thesis as free movement that mimics home cage exploratory activity in the absence of external stressors (Hansen et al., 2019). The aim of this chapter was to assess the functionality of DREADDs *in* vivo and assess whether the effects seen in slice electrophysiology can be translated to an *in vivo* electrophysiology model. Thus, the rationale behind recording resting state activity was to have a rat model in which any other stimuli or factors that could influence oscillatory activity were eliminated by habituating the rat to the test box and set-up such that it carried on with natural home cage behaviour and the effect of DREADD activation on oscillatory activity was thus isolated.

5.1.4 Chapter 5 experimental aims

Experiments in this chapter aimed to assess whether Gi or Gq-DREADD mediated modulation of hippocampal excitatory cells caused changes in power in different frequency bands. This was an important assessment considering the lack of behavioural results observed in Chapter 3, despite the apparent functionality of the Gi-DREADD in Chapter 2. To this end, resting state ECoG/LFP (rsECoG/LFP) recordings in the hippocampus and PFC of Gi and Gq-DREADD

expressing rats were made upon CNO or clozapine systemic injection. Moreover, experiments attempted to establish whether changes in brain oscillations were associated with changes in short-term memory on hippocampal dependent behavioural tasks.

5.2 Materials and Methods

All experiments described in this chapter were performed at H. Lundbeck A/S.

5.2.1 Animals

All experimental procedures were carried out in accordance with the Danish legislation regulating animal experiments; Law and Order on Animal experiments; Act No. 474 of 15/05/2014 and Order No. 12 of 07/01/2016, and with the specific license for these experiments issued by the National Authority.

Male Lister Hooded rats (Charles River, Germany), weighing between 250-300g on arrival were kept under environmentally controlled temperature (20 ± 2ºC) and humidity (50 ± 20%) with *ad libitum* access to food and water. Rats were group housed until the viral injections when they were separated and housed individually until the end of the experiment. Rats were housed in open Makrolon polycarbonate cages with wire lid and kept in a ventilated scantainer in a 12h light/dark cycle (lights on at 06:00) unless states otherwise. Sawdust was used as bedding and cages were environmentally enriched with wooden chew blocks and a polycarbonate rectangular house (Rat Retreats™, Bio-Serv, Flemington, NJ, USA). For the second rsECoG/LFP study, all rats were placed on reversed light cycle (lights off at 06:00) once the rats have recovered from the electrode implantation surgery and until the end of the experiments. Reversal of light cycle in this case was in order to test the rats during their active phase, such that they do not go to sleep during resting state ECoG/LFP recordings.

5.2.2 Viral constructs

For all the experiments in this chapter the viral constructs were purchased from the Viral Vector Facility (VVF) of the Neuroscience Centre Zurich (ZNZ) having originally been created by Bryan Roth. Details about the viral constructs used to produce the experiments described in this chapter can be found in the table below (**Table 5.1**).

Name	**Abbreviation**	**Description**	**Identifier**	**Titre (vector genomes /ml)**
ssAAV-5/2-CaMKIIa-hM3D(Gq)_mCherry-WPRE-hGHp(A)	Gq-DREADD	Pyramidal excitatory DREADD	V96-5	4.7×10^{12} vg/ml
ssAAV-5/2-CaMKIIa-hM4D(Gi)_mCherry-WPRE-hGHp(A)	Gi-DREADD	Pyramidal inhibitory DREADD	V102-5	7.3×10^{12} vg/ml
ssAAV-5/2-CaMKIIa-EGFP-WPRE-hGHp(A)	EGFP-control	Pyramidal control construct	V113-5	7.5×10^{12} vg/ml

Table 5.1: Viral constructs used in this chapter. All purchased from Viral Vector Facility (VVF) of the Neuroscience Centre Zurich (ZNZ)

5.2.3 Intracerebral viral injections

Stereotaxic delivery of the viral construct to the glutamatergic cells in the dorsal hippocampus was performed as described in Chapter 2 (see **2.2.3**). Briefly, anaesthesia was induced and maintained throughout the surgery with isoflurane. The skull was exposed and 4 small holes were drilled above the dorsal hippocampus (i, ii) AP -3.6 mm, ML ±3 mm, DV -3 mm, iii, iv) AP -3.6 mm, ML ±3 mm, DV -2.2 mm, v, vi) AP -3.6 mm, ML ± 2 mm, DV -2.0 mm). A total of 1 µl

of viral construct was injected per hemisphere using an automatic injection pump, evenly distributed between the 6 injection sites. The scalp was then sutured, and rats were administered peri and post-operative care as described in the previous chapter (see **2.2.3**). Rats were single housed post intracerebral injection and allowed 1-2 weeks to recover prior to the electrode implantation surgery.

5.2.4 Stereotaxic electrode implantation

Anaesthesia was induced and maintained with a mixture of Hypnorm (fentayl/fluanisone, Skandeborg Apotek, Skandeborg, Denmark) and Dormicum (midazolam, B. Braun, Frederiksberg, Denmark) injected in a 2.5 ml/kg volume (s.c.). All rats were given prophylactic treatment with an antibiotic 1 ml/kg s.c. (150 mg Amoxicillin/ml, Noromox Prolongatum Vet., ScanVet, Fredensborg, Denmark) and a non-steroidal anti-inflammatory drug (NSAID), 5 mg/kg s.c. (Norodyl (carprofen), Scan Vet, Fredensborg, Denmark). Once anaesthesia was induced, the scalp was shaved and the rat was placed in the stereotaxic frame (Kopf Instruments). Eye gel was applied (Neutral Ophtha Eye Gel, Teva Pharmaceuticals) to prevent dryness and the scalp was sterilised prior to injection of a local anaesthetic (2 mg/kg s.c., Marcain Polyamp Steripack 0.5% AstraZeneca, UK). The temperature of the rat was kept constant at 37 ºC by a homeothermic heating blanket. The skull was exposed and six holes were drilled as illustrated in **Table 5.2**. Depth electrodes were placed in the left dorsal hippocampus and left medial prefrontal cortex (E363/20 series, Plastics One, Roanoke, VA, USA). Screw electrodes (E363/1 series, Plastics One, Roanoke, VA, USA) were placed above the right dorsal hippocampus and the right medial prefrontal cortex and two additional ones were used as a ground and a reference. The reference screw was placed very anterior on the frontal bone in order to attempt a neutral EEG signal (Liu et al., 2015). Once all six electrodes were fitted, dental cement (RelyX™ Unicem, 3M, Minnesota, US) was used to secure them into place. A six-channel pedestal was then lowered into place and the six electrodes were

inserted into each of their pre-allocated channels. Next, the set-up was secured with pedestal cement to soften any sharp edges (GC Fuji PLUS®, GC America Inc., Alsip, IL, US). The scalp was then sutured and the rat was placed in a clean cage under a heating lamp to recover for a minimum of 2h. Recovering rats were single housed, monitored, weighed and administered post-operative care with Noromox and Norodyl or BLT's (Bacon Lover Treats with Norodyl/Rimadyl 2mg/Tablet, Bio-Serv, Flemington, NJ, USA) daily for 5 consecutive days post-surgery.

Electrode	AP (from bregma)	ML (from midline)	DV (from dura)
mPFC	- 2.7 mm	- 0.7 mm	- 3.0 mm
dHipp	- 3.6 mm	+ 2.5 mm	- 2.5 mm
mPFC surface	+ 2.7 mm	- 0.7 mm	n/a
dHipp surface	+ 3.6 mm	+ 2.5 mm	n/a
Reference	+ 8.0 mm	+ 2.0 mm	n/a
Ground	- 5.0 mm	- 5.0 mm	n/a

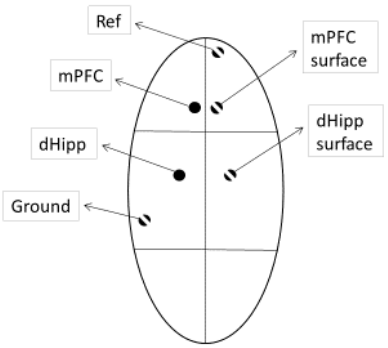


Table 5.2: Brain coordinates (Paxinos and Watson, 2007) used for electrode placement and illustration (right). n/a: not applicable

5.2.5 Drugs

CNO (3 and 10 mg/kg) (Tocris Biosciences or made in house) was freshly dissolved in saline on the day of the experiment. Clozapine (0.5, 1 and 3 mg/kg) (Tocris Biosciences) was dissolved in saline solution (with HCl 1M added to enable the dissolving process). All drug solutions were adjusted to a pH of 4 and injected in a 5 ml/kg volume. Vehicle was saline solution with a pH of 4.

5.2.6 Resting state ECoG/LFP recordings (study I and II)

Two different cohorts were tested on the rsECoG/LFP setup. The second experimental design was refined based on the results from the first study. Rats from the second cohort also underwent behavioural testing once recordings were finished. All rats were tested in clean Plexiglas cages (30 cm width x 45 cm length x 55 cm height), similar to the holding cages, covered with clean saw dust within a Faraday, sound-proof box (90 cm width x 55 cm length x 65 cm height). During a typical testing day, rats were connected to a six-pin recording wire attached to a rotating swivel and a plastic spring that attenuated the weight of the wire and allowed for unobstructed movement of the rat. Analog LFP/ECoG brain signals were amplified 1000x (Precision Model 440, Brownlee, CA, USA) and converted to digital at a sampling rate of 1 kHz (CED Power 1401, Power 1 (625 kHz, 16bit) and CED Expansion ADS16, CED, Cambridge, England). All recording wires had accelerometers (Analog Devices, MA, US) attached that allowed for detection of changes in locomotor state. LFP/ECoG signals were band-pass filtered at 0.1-300 Hz. Spike 2 (CED, Cambridge, England) was used for data acquisition of LFP/ECoG signals and accelerometer data.

Accelerometers were mounted on each recording cable enabling the differentiation between locomotor states. This also allowed the assessment of locomotor activity based on percentage of time spent active *vs.* inactive. LFP/ECoG data from the active and inactive state was pooled and analysed regardless of locomotor state as no striking differences in specific band powers were observed based on locomotor state. Data from the dorsal hippocampal depth electrode is presented in the results section as that was the site of injection of the Gi-DREADD where changes in LFP were predicted to be detected. Data from the mPFC depth electrode and the dHipp and mPFC screw recordings is not shown for Study I as explained below and can be found in the appendix (Chapter 7) for Study II.

Study I) All recordings of the first experiment were done during the light phase of the light/dark cycle. Rats expressing either a Gi-DREADD or an EGFP-control construct were habituated to the testing box and to being tethered a week prior to the beginning of experiments. During the testing day, rats were connected to the recording cable and habituated for 45 min to 1h. This was to ensure that the rats are settled and in a 'resting state' before recordings started. Baseline was then recorded for 1h. Rats were injected i.p. with CNO (3 and 10 mg/kg), clozapine (0.5, 1 and 3 mg/kg) or vehicle while they were tethered and then returned to the testing cage for a further 4h of recording post-drug (**Figure 5.1**). Rats received all conditions according to within-subject design in a fully counterbalanced order of treatment that was determined by a Latin square. As all data analysis was done automatically using the MatLab script available, it was not necessary for the experimenter to be blind to treatment or the type of viral constructs the rats were expressing. Rats did not have access to food or water while in the test box.

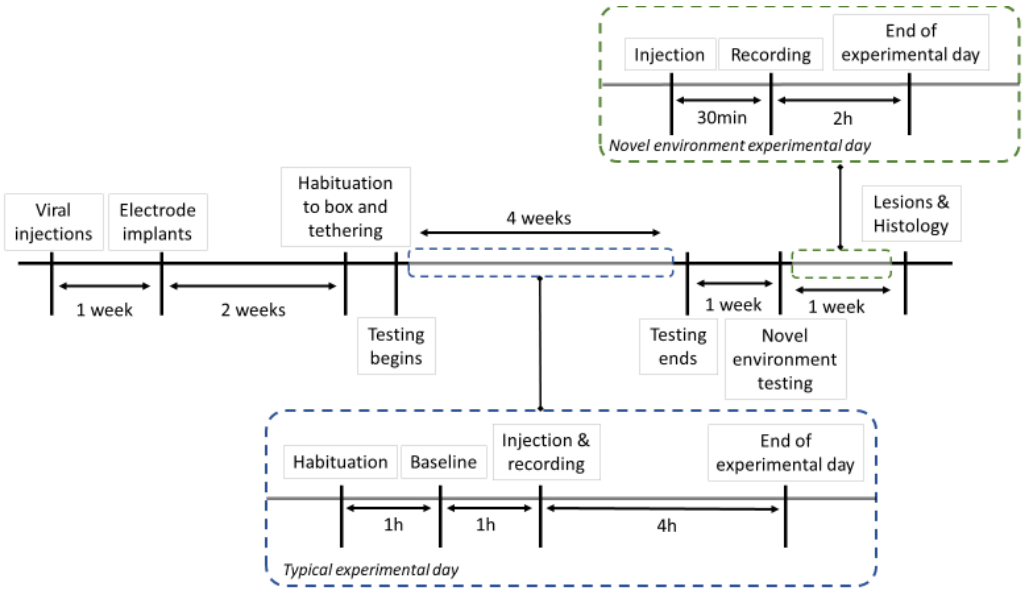


Figure 5.1: Experimental timeline of the first rsECoG/LFP study

Rats from this cohort were also recorded in a novel environment. This was done to assess whether hippocampal deficits were enhanced in a novel environment. To this end, all rats were injected with CNO (10 mg/kg i.p.) and returned to the home cage for 30 min. Next, they were placed in the testing box and LFP/ECoG signals recorded for 2h. In order to create a novel

environment, rats were tested in different labs and at a different time of day. All boxes had wallpaper (3 orange walls and one black and white striped wall) added to the walls so they were no longer transparent. The saw dust was changed, Cellu-Dri® Soft and one scoop of PAPERCHIP® animal bedding with pelleted texture (both Shepard Specialty Paper, Watertown, TN, US) was used instead. A novel plastic object (Mouse Igloo™, Bio-Serv, Flemington, NJ, USA) was introduced. At the end of each experimental day rats were returned to their home cages.

Study II) Based on results from the first study that suggested that the animals went to sleep during the recording, in order to achieve a resting state defined by natural home-cage exploration, all recordings took placed during the dark phase of the light/dark cycle, during the active phase of the rats. To this end rats (Gi or Gq-DREADD and EGFP-control) were placed on a reversed light cycle a week after the electrode implant surgery and were kept on reversed light cycle until the end of experiments. Rats were habituated to the test box, to being tethered and to i.p. injections for a week prior to the beginning of recordings, as it has been shown that by the fourth exposure to restraint stress, levels of c-Fos in all brain regions (except hippocampus) return to baseline, indicating habituation (Melia et al., 1994). During testing day, rats were connected to the recording cable and habituated for 45 min. Baseline was then recorded for 45 min. Rats were injected i.p. with CNO (10 mg/kg) or vehicle while they were tethered and then returned to the testing cage for a further 2h of recording post-drug (**Figure 5.2**). Treatment dose and injection were determined by a Latin square. Rats did not have access to food or water while in the test box.

Prior to the ECoG/LFP experiment, a small pilot study was conducted, in which 3 Gq-DREADD expressing rats were systemically injected with CNO (10 mg/kg) and monitored for seizure activity for 2 h post injection. The rats in this pilot study were not part of any rsECoG/LFP

study. As there was no indication of seizure like behaviour and based on the results from the *ex vivo* slice electrophysiology study, a Gq-DREADD expressing group was introduced to this cohort to assess whether there was an indication of decreased excitatory transmission as observed in the electrophysiological studies (Chapter 2).

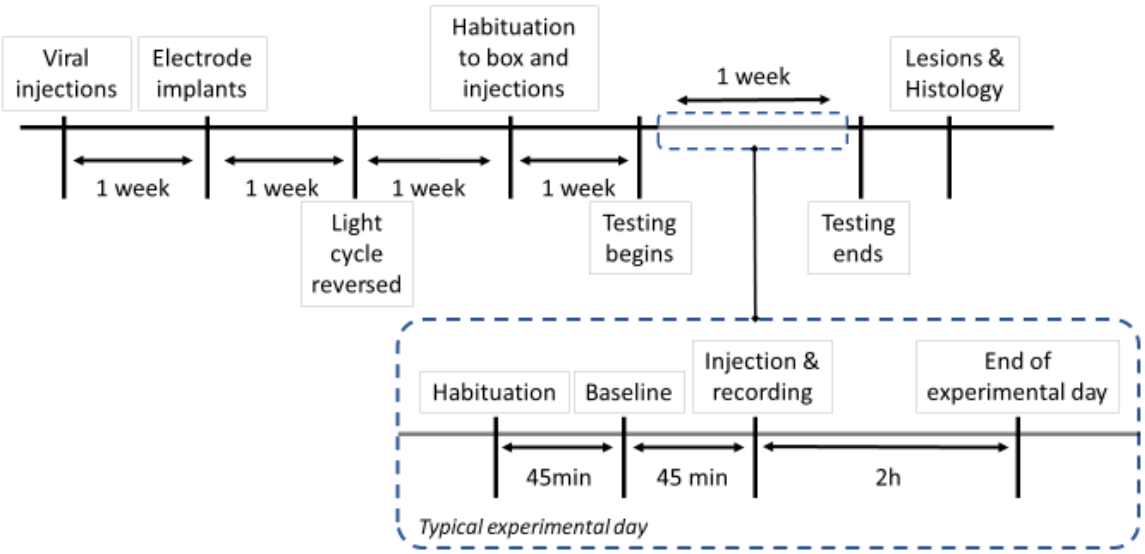


Figure 5.2: Experimental timeline of the second rsECoG/LFP study

5.2.7 Spatial novelty preference Y-maze

Spatial short-term memory was tested on a spatial novelty preference Y-maze to assess whether higher dose of CNO leads to hippocampal deficits in Gi-DREADD expressing rats. Only Gi-DREADD and EGFP-control rats were tested on the Y-maze. ECoG/LFP signals were not recorded during the behavioural tasks. The rats were tested in the dark phase of the dark/light cycle and injected under red light. However, testing was done under normal light to facilitate video tracking. The apparatus was a transparent Plexiglas Y maze (30 cm height of walls, 17 cm width of arms, 50 cm length of arms) placed on the ground. The bottom of the maze was covered with a mixture of clean and dirty sawdust from unfamiliar rats. The same protocol was followed as described in Chapter 3 (see **3.2.6**). In brief, rats were injected with CNO (10 mg/kg i.p) 30 min prior to testing. Rats were then brought to the testing room and

placed on the maze for a 5 min sample phase during which one arm was blocked. This was followed by a 1 min ITI while the block was removed and 2 min testing when all arms were opened. The novel arm was counterbalanced. As scoring was all done automatically by EthoVision XT 9 software (Noldus, Wageningen, Netherlands), the experimenter was not blinded to treatment or the type of viral construct the rats expressed. Because the centre-point was chosen as the top of the rat's head, entries in each arm were not based on the animal entering the arm with all four paws but with the centre-point instead. However, as the quantification was done automatically, through the EthoVision software, this excluded the possibility for human bias. The first arm choice, distance travelled, time spent in each arm and number of entries were recorded. The preference for the novel arm was calculated as a discrimination index - the ratio between the time spent in the novel arm divided by the total time spent in the novel and familiar arm.

5.2.8 Locomotor activity

As locomotor activity is a hippocampal function measure in itself and because the accelerometer used in ECoG/LFP recordings only gives an indication of time spent active *vs* inactive, Gi-DREADD and EGFP-control rats were tested on a locomotor activity task. Locomotor activity was recorded in the dark phase of the dark/light cycle and rats were injected under red light (CNO 10 mg/kg i.p. or vehicle). Rats were placed in transparent plastic cages (30 cm width x 45 cm length x 20 cm height) 30 minutes post injection. The bottom of the cages was covered with clean sawdust and the number of beam breaks was recorded automatically over 2 hours in 5-minute time bins (software built in house). Rats were tested on two days to allow for within-subject drug effect comparison with a minimum of 72h between injections to allow for drug washout. The order of injection and the test boxes were counterbalanced. The experimenter was not blinded to treatment and type of viral construct expressed, as the analysis was done automatically by the software.

5.2.9 Spontaneous recognition task with 4 objects

The task described below was designed by Dr. Eric Tam and Dr. Steve McHugh at the University of Oxford. The protocol for this task was kindly shared by Dr. Eric Tam (personal communication). As the literature on hippocampal dependence in a classical novel object recognition task is mixed (see Clark et al., 2003; Piterkin et al., 2008), the aim of this task was to assess the object recognition of Gi-DREADD and EGFP-control rats, in a task with increased memory load. This was based on evidence from a study reporting deficits in novel object discrimination in mice with dorsal hippocampal lesions when the memory load was increased (i.e. from one novel object to four) (Sannino et al., 2012).

The rats were tested during their dark phase of the dark/light cycle and injected under red light. However, habituation and testing were done under normal light in order to be able to facilitate video tracking. The apparatus was an open field with a Plexiglas floor (60 cm x 95 cm) and grey wooden walls (49 cm height). The apparatus was placed on top of a suction table (68 cm elevated from the floor) to minimise the risk of allergens. A white Plexiglas sheet was placed under the floor of the open field to reflect the infrared lights placed underneath that enabled the detection of the animal by the camera mounted above the testing arena and facilitate video tracking by EthoVision XT 9 software (Noldus, Wageningen, Netherlands). All rats were habituated for two consecutive days prior to the test day by placing them in the box for 10 min.

On the test day, rats were injected with CNO (10 mg/kg, i.p.) and returned to the home cage for 30 min. Next, the testing began as illustrated in **Figure 5.3**. Briefly, the rats were allowed to habituate to 4 objects for 10 min in a sample phase (T0). Following a 1 min ITI, rats were returned to the testing box for 4 consecutive trials (T1-T4) that each lasted 5 min. During each of the testing trials, a familiar object was replaced with a novel object. A battery of object was used, such as metal and plastic geometrical shapes or plastic figurines. Finally, the experiment

finished with a recency trial (T5) in which the rat was presented with the same objects as in the sample phase (T0) and was expected to explore the object presented longest ago. Thus, in the below example the rat was expected to explore the objects in the following preference order: A, C, D and B, with A being the object the rats were only exposed to during the sample phase, and B being the most recently explored object in T3. The time spent exploring each object was recorded and a Novel/Familiar ratio was calculated as the time spent exploring the novel object divided by the time spent exploring the rest of the objects. Chance performance was 0.25.

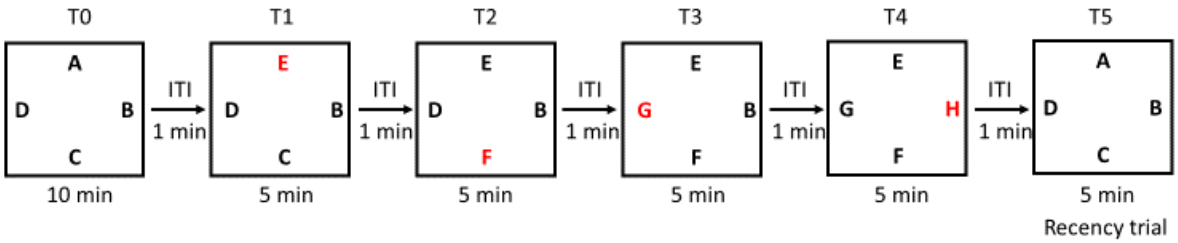


Figure 5.3: Spontaneous recognition task with 4 objects

T0 represents the sample phase and T5 the recency trial. Order of recency preference: A, C, D and B, with B being the object predicted to be explored the least as it has been seen most recently.

Due to the black and white colours of the Lister Hooded rats, the software could not accurately differentiate between the 'tail-point' and 'head-point' of the rat. Thus, the time spent exploring each object by the 'tail-point' and the 'nose-point' were added together and a novelty preference ratio was calculated based on the cumulative time. As the quantification was done automatically, through the EthoVision software, this excluded the possibility of human bias so the experimenter was not blind to the type of viral construct expressed by the rats. However, the novel object was not counterbalanced between rats which caused issues with the interpretation of the data as novelty preference ratio. Thus, the data was analysed as object exploration time disregarding the familiar/novel status of the object to avoid bias caused by counterbalancing issues.

5.2.10 Electrode placement confirmation and histology

Upon termination of experiments, positioning of the electrodes and viral expression was confirmed. Rats were anaesthetised with 10 ml/kg Avertin and lesions were made by stimulation of 0.1 mA current through the electrodes for 7 seconds (Stimulus Isolator A365, World Precision Instruments, Sarasota, FL, US). Next, rats were transcardially perfused with PBS followed by PFA 4%. Brains were kept at 4ºC in PFA 4% overnight followed by transfer to 30% sucrose solution until further analysis. 30 µm thick brain sections were cut on a cryostat (Leica CM3050, Leica Biosystems, IL, US) at -18ºC. Sections from the dorsal hippocampus and mPFC were mounted on slides and cover-slipped with Dako fluorescence mounting medium (Agilent, CA, US). Viral expression and electrode placement were visualised using brightfield and fluorescence microscope (Zeiss Scope.A1, Carl Zeiss). Images were acquired with a ZEISS Axiocam 506 Color camera (Carl Zeiss) and processed by the ZEN pro software (Carl Zeiss). Images were then imported in ImageJ (NIH, US) for further processing if required. Rats that showed misplacement or no electrode were excluded from the analysis. From Study I, 4 out of 34 electrodes were excluded based on location being too anterior or no viral expression in the electrode hemisphere. One rat showed unilateral DREADD expression on the electrode side. The rat was not excluded from the analysis as a potential Gi-DREADD induced effect would still be detectable in the LFP signal even upon unilateral expression. In study II, 5 out of 52 electrodes were excluded based on the same criteria. Two Gq-DREADD expressing rats showed epileptiform activity during the LFP recordings such that the experiment had to be terminated. The data collected from the two rats was excluded from ECoG/LFP analysis because the recording had to be stopped prematurely.

5.2.11 rsECoG/LFP data analysis

Development of MATLAB script for analysis and implementation has been done at H. Lundbeck A/S by Dr. Ulrike Richter and details can be found here (Amat-Foraster et al., 2019).

To reiterate, analysis of LFP signals was done in MATLAB (MathWorks, Natick, MA). For each LFP signal, a spectrogram with time resolution of 5 s and frequency resolution of 0.5 Hz, was acquired using the Fast Fourier transform (FFT). A spectrogram is a time series of power spectral densities and allows the detection of oscillatory activity in certain frequency bands, over time. Within every spectrogram, each power spectral density was normalised to the average power spectral density during the stable 45 or 60-min baseline period prior to injection. The spectrograms were then analysed in 4 frequency bands: theta (4-10 Hz), beta (10-30 Hz), low gamma (30-50 Hz) and high gamma (50-90 Hz). Artefact detection was performed in all channels, and 5 s segments in which data points exceeded ± 6 standard deviations (SD) from the mean were excluded from the analysis. A period of 75 s around the time of injection was also excluded. The spectral content was baseline-normalised and presented in decibel (dB), with +3 power (dB) representing double increase from baseline and -3 power (dB), half of baseline value. Spectrograms were analysed statistically at the pixel level compared to vehicle treatment using a paired mean comparison analysis.

For the statistical analysis, MATLABs *fitglme* function was used to fit each tested dataset with a generalised linear mixed-effects (GLME) model. Fixed-effect predictors were Time, Viral construct or Treatment and the interactions Time*Treatment, Time*Viral construct. A random-effects intercept for each animal was used to account for animal-specific variations. The overall effect of each fixed-effect predictor was determined performing an analysis of variance (ANOVA) with MATLABs *anova*-method for GLME models, which by using an F-test (marginal test) determines if all coefficients representing the fixed-effects term are equal to zero. Finally, the multiple comparison-corrected p-values for the individual interaction coefficients between Time and Treatment were determined post hoc by using Tukey's honest significant differences test.

5.2.12 Statistical analysis

All behavioural data was analysed using GraphPad Prism 7 (GraphPad Software, Inc., San Diego, CA) or SPSS Statistics. Repeated measures 2-way ANOVAs were used to analyse the novelty induced locomotor activity and the object exploration data. Y-maze data was tested for normality using a D'Agostino Pearson normality test followed by an unpaired t-test and using one sample t-test against a fixed ratio of 0.5 (novelty preference ratio). Significance was set at a P value of $p<0.05$.

5.3 Results

5.3.1 LFP profile of dorsal hippocampus Gi-DREADD expressing rats in the presence of CNO or clozapine – Study I

In an attempt to assess LFP changes in Gi-DREADD expressing rats, rats were implanted with one depth electrode in the mPFC and one in the dHipp where the DREADD was expressed and two screws were placed above the mPFC and dHipp to record ECoG. On test day, rats were habituated to the testing boxes, followed by 1h baseline recording. The rats were then injected i.p. with either CNO (3 and 10 mg/kg), clozapine (0.5, 1 and 3 mg/kg) or vehicle and returned to the testing cage for a further 4h recording. Data from the dorsal hippocampal depth electrode is presented as this was the site of injection of the Gi-DREADD where changes in LFP were predicted to be detected.

Locomotor activity data was collected by accelerometers mounted on each recording cable. The rats were injected at time point 0 as indicated by the arrows. The cables were not disconnected, and locomotor activity was recorded while the rats were injected, which is depicted on the graph as maximal active locomotor state. Additionally, locomotor data was grouped in 10-min time bins, and the values for each time point were connected by a line, such that it appears, as plotted on the graph that the rats were becoming more active as injection time approached, which was not the case. The results revealed no effect of CNO treatment on locomotor state in the two groups (EGFP-control: $F(2, 504) = 0.01$, $P = 0.9$; Gi-DREADD: $F(2, 504) = 0.16$, $P = 0.85$), a significant effect of time (EGFP-control: $F(23, 504) = 6.026$, $P < 0.0001$; Gi-DREADD: $F(23, 504) = 10.5$, $P < 0.0001$), but no interaction treatment*time (EGFP-control: $F(46, 504) = 0.5$, $P = 0.99$; Gi-DREADD: $F(46, 504) = 0.85$, $P = 0.75$; **Figure 5.4**). This suggests that locomotor activity decreased significantly over time in both groups regardless of treatment which can indicate that the rats were going to sleep and that the LFP results might be impacted by this.

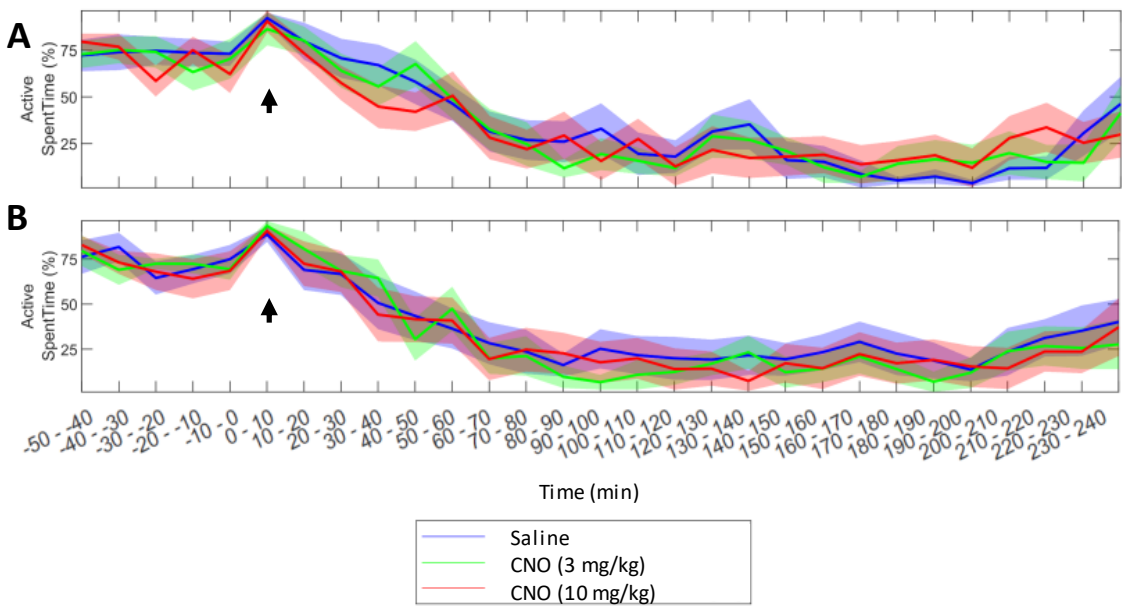


Figure 5.4: Resting state locomotor activity of Gi-DREADD and EGFP-control rats after CNO or vehicle injection

Percentage of time spent active presented in 10-min time bins over 4h after CNO (3 and 10 mg/kg) or vehicle injection in the presence of a Gi-DREADD (n=9) (A) or an EGFP-control (n=8) construct (B). Data is presented as mean ± SEM values. Arrows represent time of injection.

Despite predictions, and the plotted band powers suggesting decreased low and high gamma power in the Gi-DREADD group in the presence of CNO, the results showed no statistically significant differences between treatments in Gi-DREADD or control rats (see **Table 5.3**). Thus, there was no significant effect of treatment in the low gamma band ($F(2, 414) = 0.55$, $P = 0.58$) or high gamma ($F(2, 414) = 0.23$, $P = 0.79$) in the Gi-DREADD expressing group (**Figure 5.5C**), but a statistically significant effect of time in the EGFP-control group in the low gamma ($F(22, 414) = 2.02$, $P = 0.0045$) and high gamma band ($F(22, 414) = 2.07$, $P = 0.0032$). This decrease with time in band power is also illustrated by the band specific plots (**Figure 5.6C**) independent of treatment. While the statistical results did not reveal any marked differences between groups, or treatments, one noteworthy finding is the decrease in power in higher frequency band (> 80 Hz) after the initial baseline period and approximately 30 min into the recording. This decrease seems to correlate with the increased theta power that is missing from the baseline but also with the decreased locomotor activity (**Figure 5.4**). Thus, these data

could indicate that the rats are falling asleep in the first hour of recording. This is a possibility as the rats were tested during their light phase, were well habituated to the test boxes and were recorded for an extended period of time (4h). As a result, these results might not be an accurate indication of ‘resting state’.

Moreover, the same pattern of decreased power in the higher frequency bands was also observed in the mPFC depth electrode and dHipp and mPFC screws that were also used for recording LFP or ECoG signal respectively (data not shown). However, this study was focused on the dorsal hippocampus where the DREADDs are expressed such that only LFP hippocampal data is presenter hereinafter.

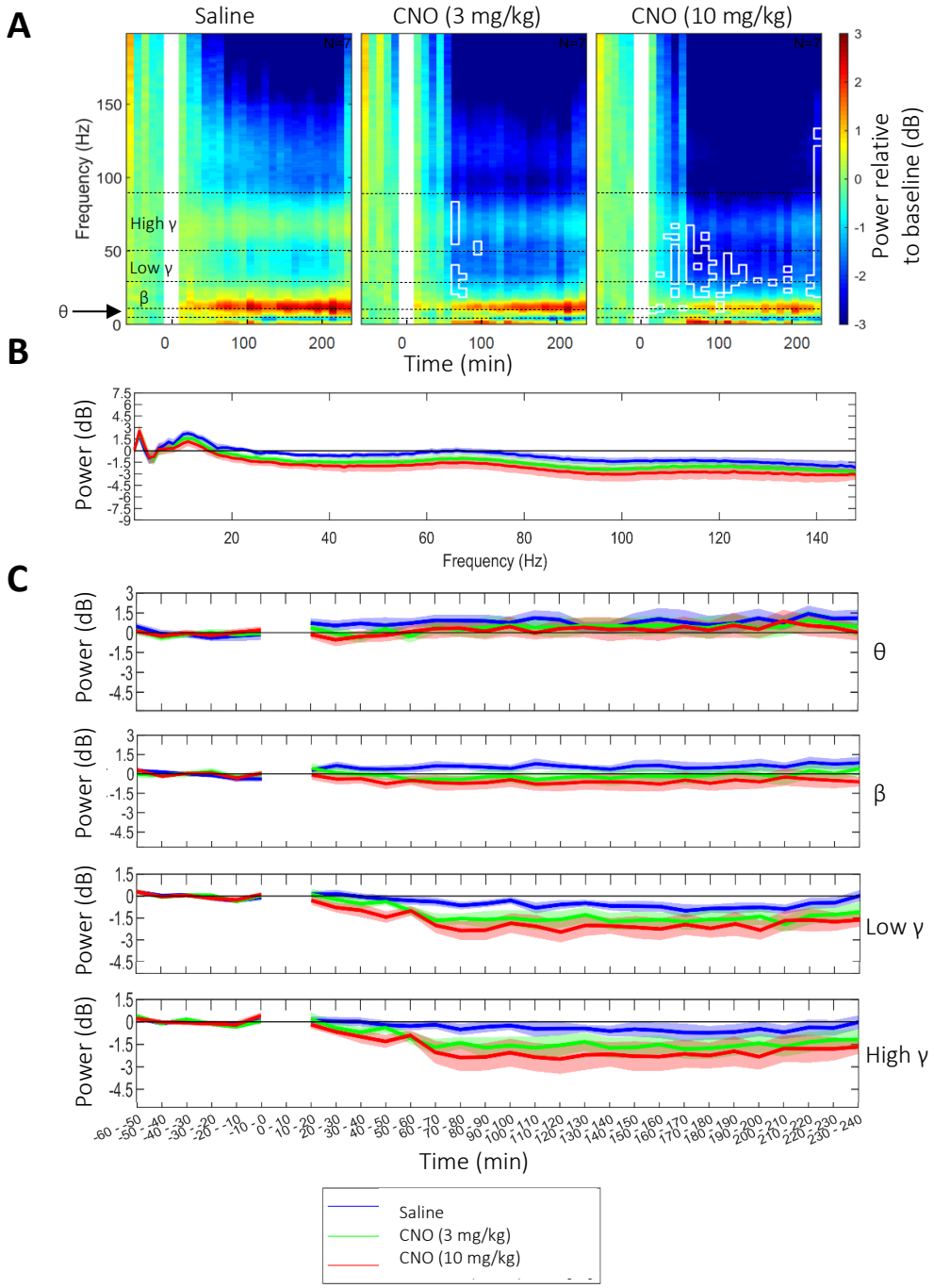


Figure 5.5: LFP profile of dHipp Gi-DREADD expressing rats in response to CNO

(A) Spectrogram of LFP signal recorded over 4h post injection from a depth electrode in the dHipp of rats expressing a Gi-DREADD after saline or CNO (3 and 10 mg/kg) treatment. Area within the white line represents statistical significance compared to saline treatment at pixel level. Time point of 0 represents time of injection. Frequency bands are separated by dotted lines: δ (1-4 Hz, bottom band not labeled), θ (4-10 Hz), β (10-30 Hz), low γ (30-50 Hz), high γ (50-90 Hz). (B) Power of brain oscillations (up to 150 Hz) in the 30-240 min time interval. (C) Band power separation (from top to bottom) for theta, beta, low and high gamma over 4h recording illustrated in 10-min time bins. Missing data represents time of injection (T0). All data are shown as mean ± SEM values from n=7 rats and are baseline normalised.

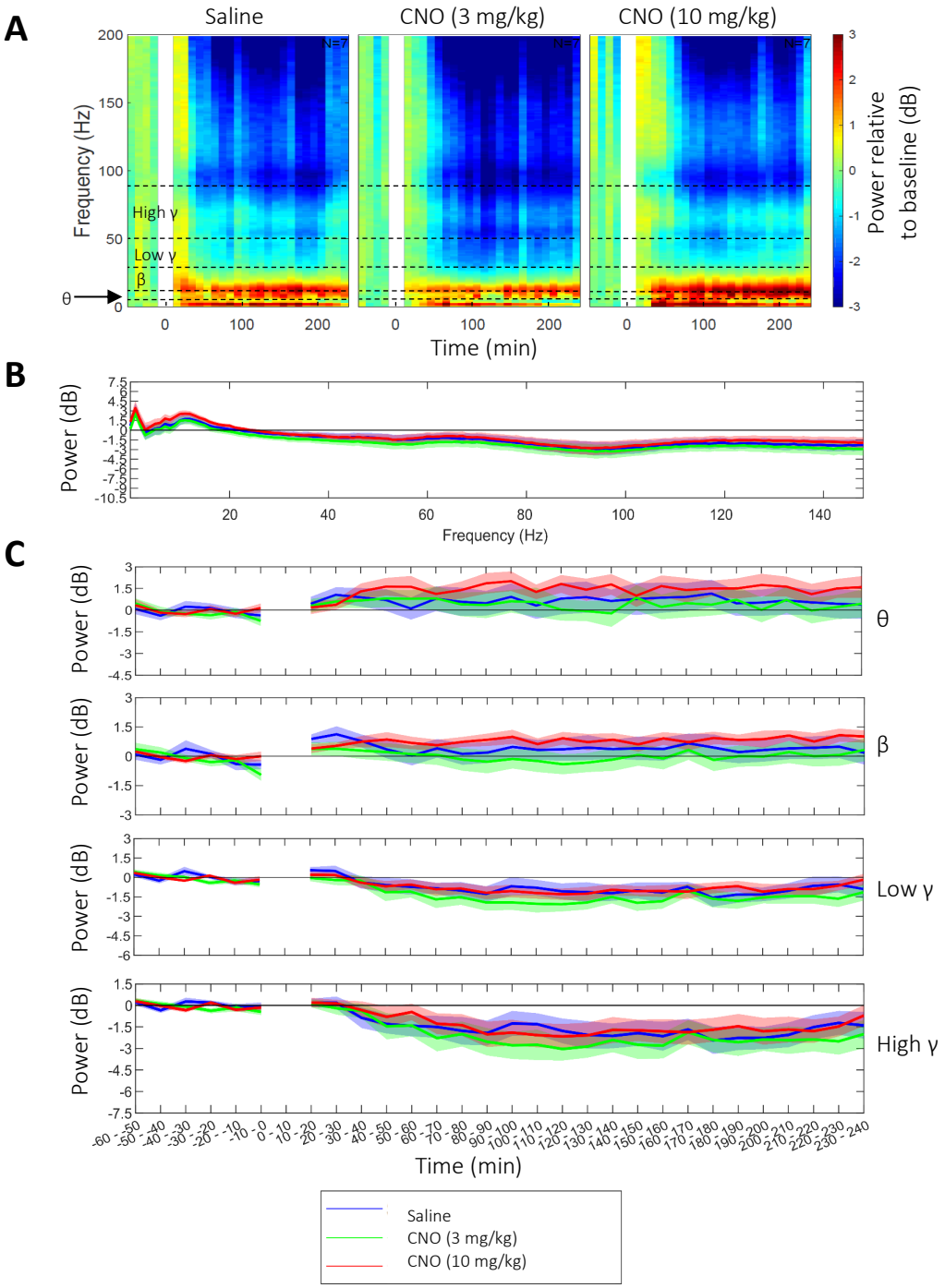


Figure 5.6: LFP profile of dHipp EGFP-control expressing rats in response to CNO

(A) Spectrogram of LFP signal recorded over 4h post injection from a depth electrode in the dHipp of rats expressing an EGFP construct after saline or CNO (3 and 10 mg/kg) treatment. Area within the white line represents statistical significance compared to saline treatment at pixel level. Time point of 0 represents time of injection. Frequency bands are separated by dotted lines: δ (1-4 Hz, bottom band not labeled), θ (4-10 Hz), β (10-30 Hz), low γ (30-50 Hz), high γ (50-90 Hz). (B) Power of brain oscillations (up to 150 Hz) in 30-240 min time interval. (C) Band power separation (from top to bottom) for theta, beta, low and high gamma over 4h recording illustrated in 10-min time bins. Missing data represents time of injection (T0). All data are shown as mean ± SEM values from n=7 rats and are baseline normalised.

	Gi-DREADD				EGFP-control			
	θ	**β**	**Low γ**	**High γ**	**θ**	**β**	**Low γ**	**High γ**
Treatment	F(2,414) = 1.83	F(2,414) = 1.08	F(2,414) = 0.55	F(2,414) = 0.23	F(2,414) = 0.11	F(2,414) = 1.2	F(2,414) = 0.69	F(2,414) = 0.0035
	P=0.16	P=0.34	P=0.58	P=0.79	P=0.89	P=0.3	P=0.5	P=0.99
Time	F(22,414) = 0.65	F(22,414) = 0.39	F(22,414) = 1.06	F(22,414) = 0.41	F(22,414) = 0.98	F(22,414) = 0.87	F(22,414) = 2.02	F(22,414) = 2.07
	P=0.89	P=0.99	P=0.38	P=0.99	P=0.98	P=0.64	**P=0.0045**	**P=0.0032**
Treatment* Time	F(44,414) = 0.47	F(44,414) = 0.5	F(44,414) = 0.54	F(44,414) = 0.5	F(44,414) = 0.96	F(44,414) = 0.7	F(44,414) = 0.44	F(44,414) = 0.44
	P=0.99	P=0.99	P=0.99	P=0.99	P=0.55	P=0.93	P=0.99	P=0.99

Table 5.3: Statistical table of LFP signals recorded from the dorsal hippocampus in the presence of CNO

ANOVA results for the fit generalised linear model with treatment and time as fixed-effect predictor, separated by band power and viral construct for data presented in Figures 5.5 and 5.6. Comparison was made between saline and CNO treatments and statistically significant p values are underlined and written in bold.

Next, a statistical analysis was done to establish whether CNO treatment affected the two groups differently. As data from the exposure study in Chapter 4 showed that CNO peaks 30 min after injection, the analysis was done for the 30-240 min time interval. The results showed a significant effect of the group in the theta band after CNO (10 mg/kg) injection ($F(1, 252) = 3.962$, $P = 0.0476$), a strong trend in the beta band ($F(1, 252) = 3.8617$, $P = 0.05049$) and a significant effect of time in the high gamma band after all treatments (saline: $F(20, 252) = 2.5$, $P = 0.00055$; CNO, 3 mg/kg: $F(20, 252) = 3.93$, $P < 0.0001$; CNO, 10 mg/kg : $F(20, 252) = 2.99$, $P < 0.0001$; **Table 5.4**). This suggests that at higher frequencies (and as seen in **Figures 5.5 and 5.6**), there was a decrease in power following all treatments and regardless of viral construct, but also that theta power is increased as a consequence of high dose CNO (10 mg/kg) in the control rats.

		EGFP - control – Gi - DREADD comparison					
Band power	**Treatment**	**Viral construct group**		**Time**		**Interaction**	
		F(dF1,dF2)	**p**	**F(dF1,dF2)**	**p**	**F(dF1,dF2)**	**p**
θ	Saline	F(1, 252) = 0.040902	0.84	F(20, 252) = 0.86696	0.62	F(20, 252) = 1.2538	0.21
	CNO 3mg/kg	F(1, 252) = 1.4072	0.24	F(20, 252) = 1.5289	0.072	F(20, 252) = 1.8289	**0.018**
	CNO 10mg/kg	F(1, 252) = 3.962	**0.0476**	F(20, 252) = 1.2631	0.2	F(20, 252) = 1.297	0.181
β	Saline	F(1, 252) = 0.4739	0.49	F(20, 252) = 1.0897	0.36	F(20, 252) = 1.2281	0.23
	CNO 3mg/kg	F(1, 252) = 0.24315	0.62	F(20, 252) = 1.1217	0.37	F(20, 252) = 0.74128	0.78
	CNO 10mg/kg	F(1, 252) = 3.8617	0.05049	F(20, 252) = 0.9156	0.57	F(20, 252) = 0.71499	0.81
Low γ	Saline	F(1, 252) = 0.2576	0.61	F(20, 252) = 2.6566	**0.04**	F(20, 252) = 0.66476	0.86
	CNO 3mg/kg	F(1, 252) = 0.15873	0.69	F(20, 252) = 2.3618	**0.001**	F(20, 252) = 0.78967	0.725
	CNO 10mg/kg	F(1, 252) = 0.67426	0.41	F(20, 252) = 1.3423	0.15	F(20, 252) = 0.65328	0.87
High γ	Saline	F(1, 252) = 0.99291	0.32	F(20, 252) = 2.4991	**0.00055**	F(20, 252) = 0.6147	0.9
	CNO 3mg/kg	F(1, 252) = 0.10557	0.74	F(20, 252) = 3.9346	**<0.0001**	F(20, 252) = 1.0487	0.4
	CNO 10mg/kg	F(1, 252) = 0.3909	0.54	F(20, 252) = 2.9915	**<0.0001**	F(20, 252) = 0.35678	0.99

Table 5.4. Between group statistical analysis of hippocampal band powers dependent on treatment

ANOVA results for the fit generalised linear model with viral construct and time as fixed-effect predictor, separated by band power and treatment for data presented in Figures 5.5 and 5.6. Comparison was made between the two groups after the same treatment dose. Statistically significant p values are underlined and written in bold.

Considering the limitation that CNO might be back-metabolised to clozapine that in turn is the activator of DREADDs, it was important to assess the effects of clozapine (0.5, 1 and 3 mg/kg) on dorsal hippocampal LFP and locomotor state in Gi-DREADD and control rats.

Analysis of locomotor activity revealed no differences in locomotor state in the two groups regardless of treatment. The results revealed no effect of treatment on locomotor activity in the two groups (EGFP-control: $F(3, 672) = 0.07$, $P = 0.57$; Gi-DREADD: $F(3, 672) = 0.322$, $P = 0.8$), a significant effect of time (EGFP-control: $F(23, 504) = 6.27$, $P < 0.0001$; Gi-DREADD: $F(23, 504) = 6.7$, $P < 0.0001$), a significant effect of interaction treatment*time in the control group (EGFP-control: $F(69, 504) = 1.47$, $P = 0.01$) but not in the Gi-DREADD group (Gi-DREADD: $F(69, 504) = 0.96$, $P = 0.57$; **Figure 5.7**). This suggests that rats were becoming significantly inactive over time in both groups regardless of treatment which once again suggests that the rats were going to sleep. The significant time treatment interaction in the control group suggests that the locomotor activity of rats in this group was impacted differently depending on clozapine treatment over the duration of recording, thus indicating the potential for non-DREADD specific effects of clozapine.

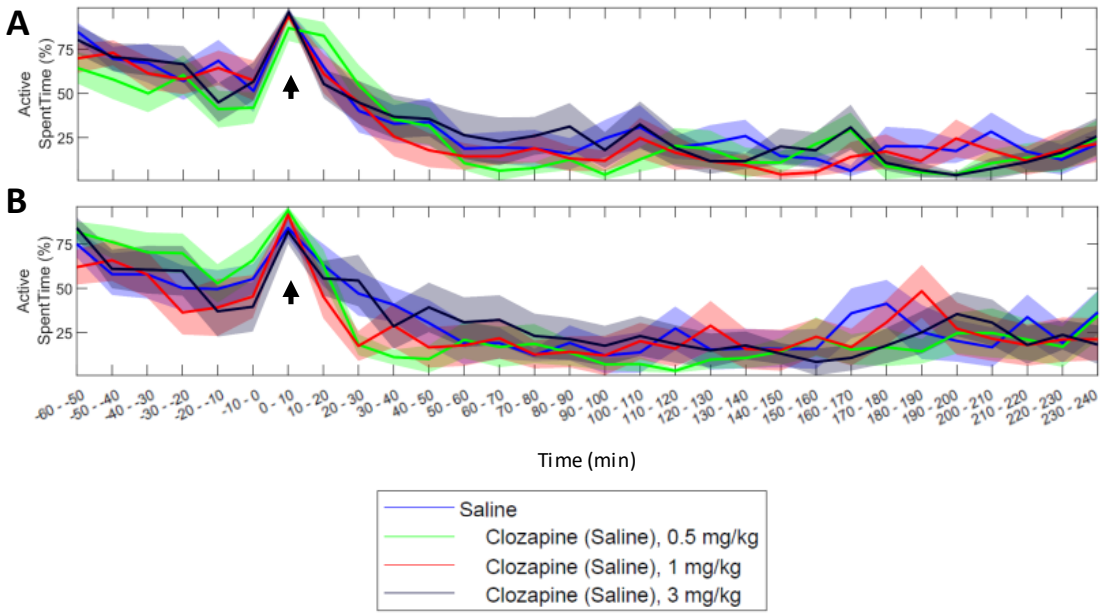


Figure 5.7: Locomotor state of Gi-DREADD and EGFP-control rats after clozapine or vehicle injection

Percentage of time spent active presented in 10-min time bins over 4h after clozapine (0.5, 1 and 3 mg/kg) or vehicle injection in the presence of a Gi-DREADD (n=9) (A) or an EGFP-control (n=8) construct (B). Data are presented as mean ± SEM values. Arrows represent time of injection.

Overall the results showed no conclusive marked differences between treatments in Gi-DREADD or control rats (see **Table 5.5**). However, a number of observations were made. Firstly, there was a significant effect of treatment in the Gi-DREADD group in the theta band ($F(3, 552) = 2.8811$, $P = 0.035$) that indicates decreased theta power in the presence of high dose clozapine (3 mg/kg) as shown by **Figure 5.8C**. Next, there was a significant effects of treatment in the control group in the beta ($F(3, 552) = 4.12$, $P = 0.0066$) and low gamma band ($F(3, 552) = 2.69$, $P = 0.045$; **Figure 5.9C**). Similarly to the recordings in the presence of CNO above, the same decrease in power in higher frequency bands (> 80 Hz) was observed after the initial baseline period and immediately after the injection. Again, the decrease appeared to correlate with the increased theta power that was absent in the baseline recordings but also with the decreased locomotor activity (**Figure 5.7**).

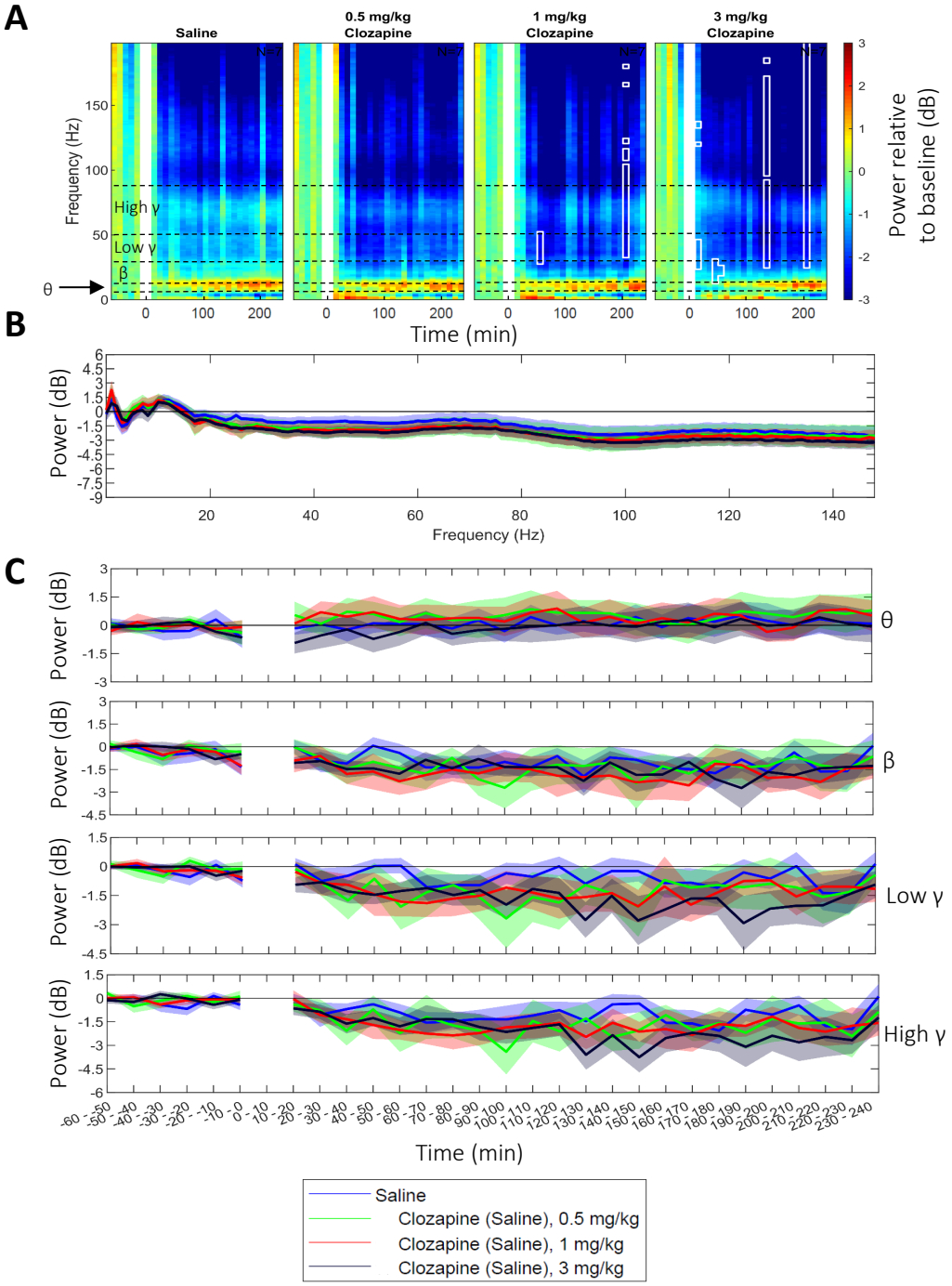


Figure 5.8: LFP profile of dHipp Gi-DREADD expressing rats in response to clozapine

(A) Spectrogram of LFP signal recorded over 4h post injection from a depth electrode in the dHipp of rats expressing a Gi-DREADD construct after saline or clozapine (0.5, 1 and 3 mg/kg) treatment. Area within the white line represents statistical significance compared to saline treatment at pixel level. Time point of 0 represents time of injection. Frequency bands are separated by dotted lines: δ (1-4 Hz, bottom band not labeled), θ (4-10 Hz), β (10-30 Hz), low γ (30-50 Hz), high γ (50-90 Hz). (B) Power of brain oscillations (up to 150 Hz) over the 30-240min time interval (C) Band power separation (from top to bottom) for theta, beta, low and high gamma over 4h recording illustrated in 10-min time bins. Missing data represents time of injection (T0). All data are shown as mean ± SEM values from n=7 rats and are baseline normalised.

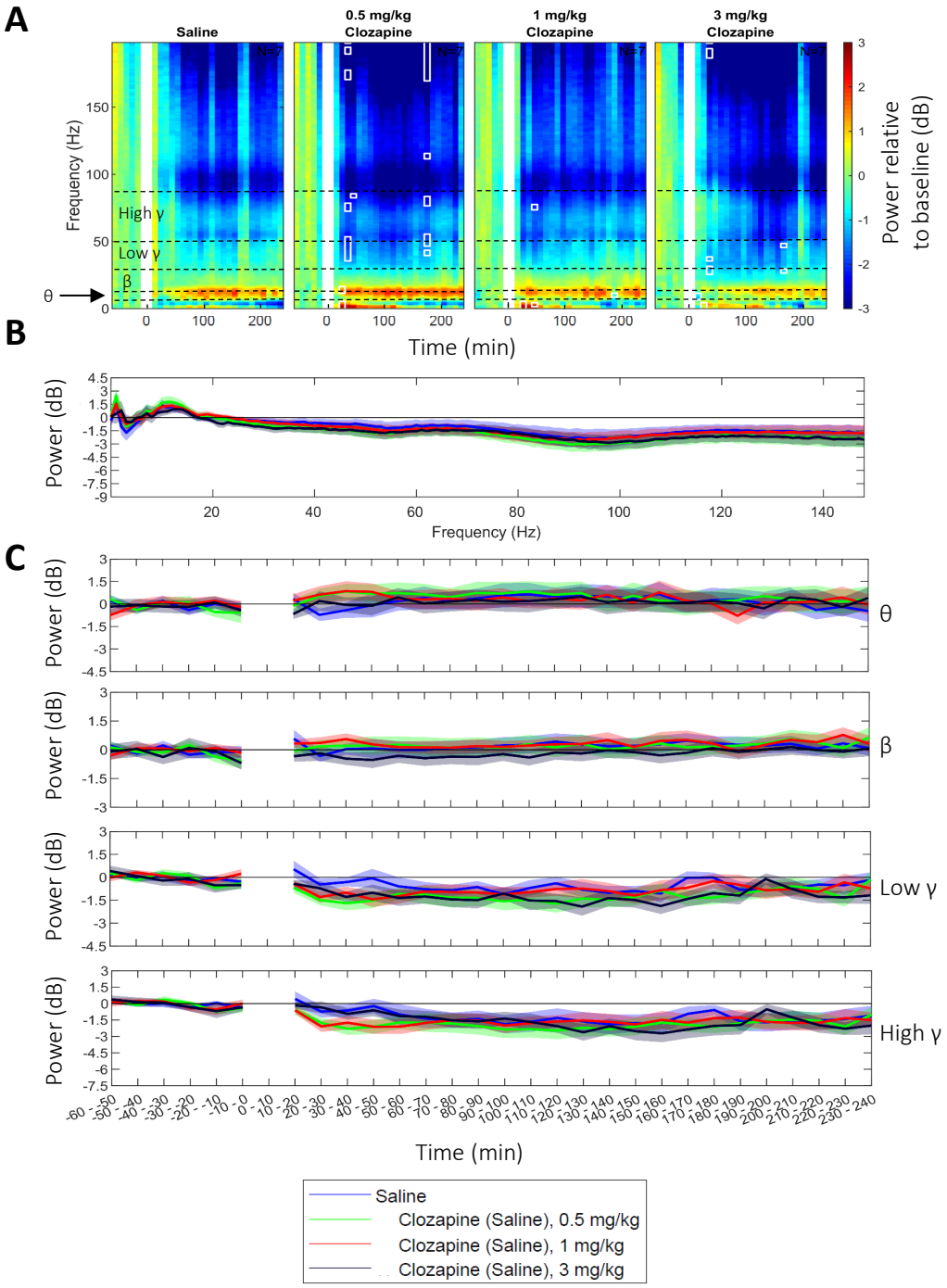


Figure 5.9: LFP profile of dHipp EGFP-control expressing rats in response to clozapine

(A) Spectrogram of LFP signal recorded over 4h post injection from a depth electrode in the dHipp of rats expressing an EGFP construct after saline or clozapine (0.5, 1 and 3 mg/kg) treatment. Area within the white line represents statistical significance compared to saline treatment at pixel level. Time point of 0 represents time of injection. Frequency bands are separated by dotted lines: δ (1-4 Hz, bottom band not labeled), θ (4-10 Hz), β (10-30 Hz), low γ (30-50 Hz), high γ (50-90 Hz). (B) Power of brain oscillations (up to 150 Hz) over the 30-240 min time interval. (C) Band power separation (from top to bottom) for theta, beta, low and high gamma over 4h recording illustrated in 10-min time bins. Missing data represents time of injection (T0). All data are shown as mean ± SEM values from n=7 rats and are baseline normalised.

	Gi-DREADD				EGFP-control			
	θ	**β**	**Low γ**	**High γ**	**θ**	**β**	**Low γ**	**High γ**
Treatment	F(3,552) = 2.8811	F(3,552) = 1.4876	F(3,552) = 1.8432	F(3,552) = 0.40663	F(3,552) = 1.67	F(3,552) = 4.12	F(3,552) = 2.6926	F(3,552) = 1.34
	P=0.035	P=0.22	P=0.14	P=0.75	P=0.17	**P=0.0066**	**P=0.045**	P=0.26
Time	F(22,552) = 0.37235	F(22,552) = 0.36046	F(22,552) = 0.62492	F(22,552) = 0.57927	F(22,552) = 1.22	F(22,552) = 0.9	F(22,552) = 1.5	F(22,552) = 1.98
	P=0.99	P=0.99	P=0.91	P=0.94	P=0.22	P=0.6	P=0.065	**P=0.0051**
Treatment* Time	F(66,552) = 0.4969	F(66,552) = 0.34261	F(66,552) = 0.5132	F(66,552) = 0.49038	F(66,552) = 0.79	F(66,552) = 0.70294	F(66,552) = 1.02	F(66,552) = 1.17
	P=0.99	P=1	P=0.99	P=0.99	P=0.87	P=0.96	P=0.43	P=0.18

Table 5.5: Statistical table of LFP signals recorded from the dorsal hippocampus in the presence of clozapine

ANOVA results for the fit generalised linear model with treatment and time as fixed-effect predictor, separated by band power and viral construct for data presented in Figures 5.8 and 5.9. Comparison was made between vehicle and clozapine treatments and statistically significant p values are underlined and written in bold.

Next a statistical analysis was done to establish whether different doses of clozapine treatment affected the two groups differently in the 30-240 min time interval. The results showed no effect of construct type on any band power after any of the four treatments. Interestingly, there was a significant effect of the interaction construct*time in the low gamma ($F(20, 252) = 2.1924$, $P = 0.003$) and high gamma band ($F(20, 252) = 1.6802$, $P= 0.037$; **Table 5.6**), after high dose of clozapine (3 mg/kg). This effect was not observed after smaller doses of clozapine. This indicates that the viral construct affects band power in the two gamma bands differently with time after clozapine (3 mg/kg) injection.

		EGFP - control – Gi – DREADD comparison					
Band power	**Treatment**	**DREADD group**		**Time**		**Interaction**	
		F(dF1,dF2)	**p**	**F(dF1,dF2)**	**p**	**F(dF1,dF2)**	**p**
θ	Saline	F(1, 252) = 0.053925	0.82	F(20, 252) = 1.634	**0.045**	F(20, 252) = 1.1684	0.28
	Clozapine 0.5 mg/kg	F(1, 252) = 0.014096	0.9	F(20, 252) =0.99047	0.47	F(20, 252) =0.69878	0.83
	Clozapine 1 mg/kg	F(1, 252) = 0.25015	0.62	F(20, 252) =2.2194	**0.0025**	F(20, 252) =1.7084	0.032
	Clozapine 3 mg/kg	F(1, 252) = 0.039795	0.84	F(20, 252) =0.85583	0.64	F(20, 252) = 1.04	0.42
β	Saline	F(1, 252) = 1.294	0.26	F(20, 252) = 0.48496	0.97	F(20, 252) =0.76557	0.75
	Clozapine 0.5 mg/kg	F(1, 252) = 0.98227	0.32	F(20, 252) =0.52325	0.96	F(20, 252) =0.86533	0.63
	Clozapine 1 mg/kg	F(1, 252) = 3.2492	0.073	F(20, 252) =1.0628	0.39	F(20, 252) =1.3272	0.16
	Clozapine 3 mg/kg	F(1, 252) = 1.0443	0.31	F(20, 252) =1.8449	**0.017**	F(20, 252) =0.98212	0.48
Low γ	Saline	F(1, 252) = 1.6166	0.2	F(20, 252) =1.4668	0.093	F(20, 252) =1.3327	0.16
	Clozapine 0.5 mg/kg	F(1, 252) = 0.096722	0.76	F(20, 252) =1.7693	**0.024**	F(20, 252) =1.1257	0.32
	Clozapine 1 mg/kg	F(1, 252) = 1.3287	0.25	F(20, 252) =0.78989	0.73	F(20, 252) =0.80117	0.71
	Clozapine 3 mg/kg	F(1, 252) = 0.43332	0.51	F(20, 252) =2.3589	**0.0012**	F(20, 252) =2.1924	**0.003**
High γ	Saline	F(1, 252) = 0.54128	0.46	F(20, 252) =1.9556	**0.0098**	F(20, 252) =1.5951	0.054
	Clozapine 0.5 mg/kg	F(1, 252) = 0.028899	0.87	F(20, 252) =1.3218	0.17	F(20, 252) =1.0574	0.4
	Clozapine 1 mg/kg	F(1, 252) = 0.0088198	0.93	F(20, 252) =0.38416	0.99	F(20, 252) =0.89213	0.6
	Clozapine 3 mg/kg	F(1, 252) = 0.46675	0.5	F(20, 252) =3.938	**<0.0001**	F(20, 252) =1.6802	**0.037**

Table 5.6. Between group statistical analysis of hippocampal band powers dependent on treatment

ANOVA results for the fit generalised linear model with viral construct and time as fixed-effect predictor, separated by band power and treatment for data presented in Figures 5.8 and 5.9. Comparison was made between the two groups after the same treatment dose. Statistically significant p values are underlined and written in bold.

Collectively these data suggest that an event taking place after baseline recording caused decreased power in higher frequencies and increased theta power in all groups independent of treatment of viral construct. Whether this event is a consequence of the stress associated

with the injection or the fact that the rats were going to sleep once they were injected, remains unknown. Still, the design was altered for a second study as described in the methods section above (see **5.2.6**). Before that however, the same cohort was tested in a novel room, to assess changes in hippocampal brain oscillations in a new environment.

5.3.2 Novel environment hippocampal LFP recordings

As no marked differences in brain oscillations were observed in the previous experiments where rats had been extensively habituated to the test cages, LFP recordings from the same cohort were carried out in a novel room. It was predicted that CNO induced Gi-DREADD activation could affect responses to novelty. Thus, increased novelty could lead to increased exploration followed by potentially stronger oscillatory signalling. To this end, all rats were administered CNO (10 mg/kg) and recorded in the novel test boxes for 2h. CNO was chosen over clozapine in this experiment due to its extensive use despite the known limitation of back-metabolism to clozapine.

The results showed no differences between the EGFP-control and Gi-DREADD group in locomotor activity after CNO injection. The results revealed no effect of construct ($F(1, 180) = 0.24$, $P = 0.62$), a significant effect of time ($F(11, 180) = 32.356$, $P < 0.0001$) but no interaction construct*time ($F(11, 180) = 0.79$, $P = 0.65$; **Figure 5.10A**). This suggests the lack of novelty induced hyper-locomotion in Gi-DREADD rats upon CNO injection, indicating normal short-term habituation.

Moreover, results showed that novel environment exposure did not affect band power differently in the control group compared to the Gi-DREADD group in the presence of CNO (10 mg/kg) as revealed by analysis of band power raw data (**Figure 5.10**). A statistical analysis

revealed significant effect of time on band power in the beta (F(10, 132) = 2.4261, P = 0.01), low gamma (F(10, 132) = 5.406, P < 0.0001) and high gamma (F(10, 132) = 5.571, P < 0.0001) range (**Table 5.7**). This suggests that power in those bands decreased significantly over the duration of the recording but this effect was observed in both the control and Gi-DREADD group.

		EGFP – Gi-DREADD comparison					
Band power	**Treatment**	**DREADD group**		**Time**		**Interaction**	
		F(dF1,dF2)	**p**	**F(dF1,dF2)**	**p**	**F(dF1,dF2)**	**p**
θ	CNO 10mg/kg	F(1, 132) = 0.33902	0.56	F(10, 132) = 1.8075	0.065	F(10, 132) = 0.92516	0.51
β	CNO 10mg/kg	F(1, 132) = 0.58827	0.44	F(10, 132) = 2.4261	**0.01**	F(10, 132) = 0.91558	0.52
Low γ	CNO 10mg/kg	F(1, 132) = 0.44882	0.5	F(10, 132) = 5.406	**<0.0001**	F(10, 132) = 0.88258	0.55
High γ	CNO 10mg/kg	F(1, 132) = 0.5384	0.46	F(10, 132) = 5.571	**<0.0001**	F(10, 132) =0.59261	0.82

Table 5.7. Between group statistical analysis of hippocampal band powers in a novel environment after CNO (10 mg/kg) injection

ANOVA results for the fit generalised linear model with viral construct and time as fixed-effect predictor, separated by band power and treatment for data presented in Figure 5.10. Comparison was made between the two groups after CNO (10 mg/kg) injection. Statistically significant p values are underlined and written in bold.

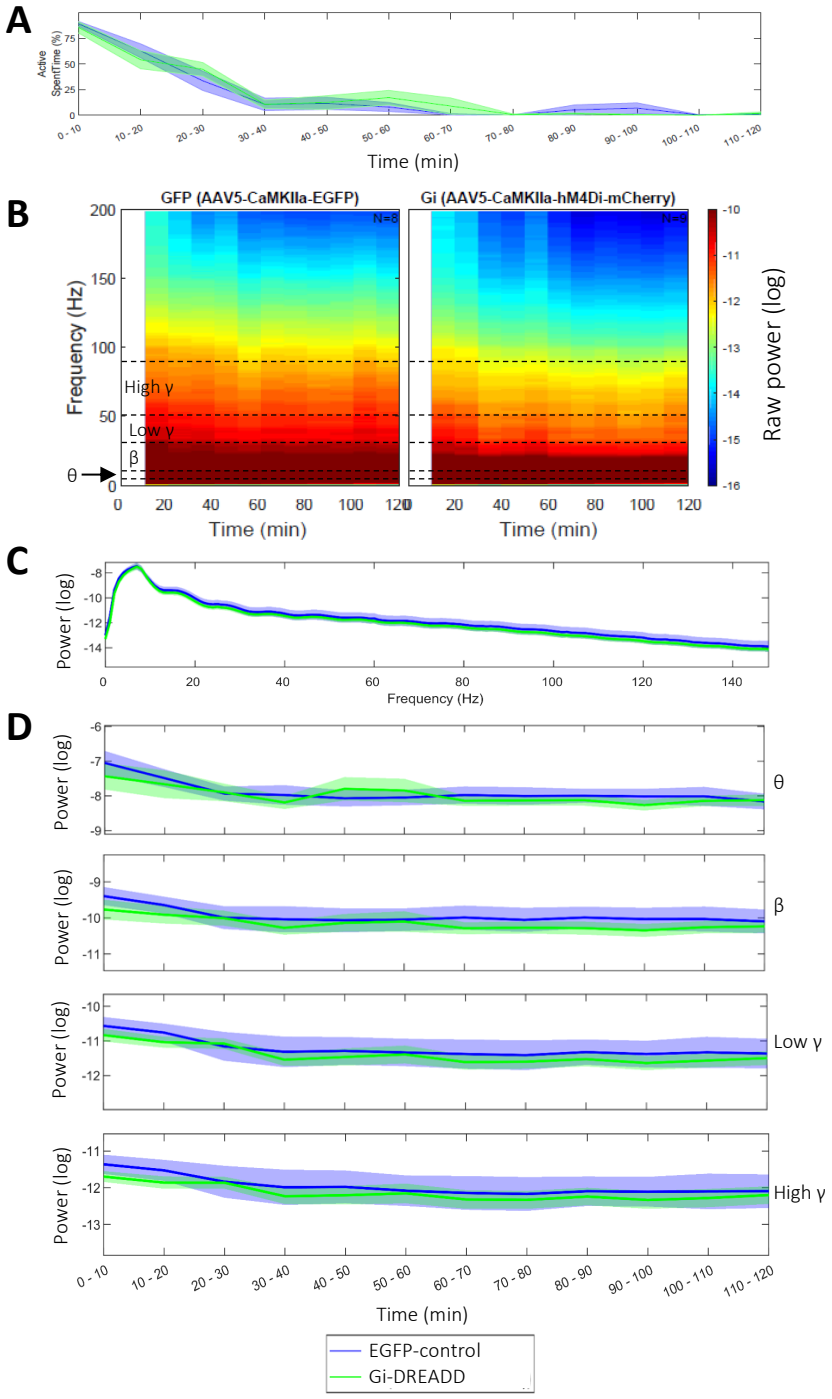


Figure 5.10 Hippocampal LFP and locomotor activity of Gi-DREADD and EGFP-control rats in a novel environment

(A) Percentage of time spent active presented in 10-min time bins over 2h after CNO (10 mg/kg) injection. (B) Raw baseline power spectrogram of EGFP-control (left) and Gi-DREADD expressing (right) rats upon CNO (10 mg/kg) activation over 2h. Frequency bands are separated by dotted lines: δ (1-4 Hz, bottom band not labeled), θ (4-10 Hz), β (10-30 Hz), low γ (30-50 Hz), high γ (50-90 Hz). (C) Power of brain oscillations (up to 150 Hz) for the duration of the recording. (D) Band power separation (from top to bottom) for theta, beta, low and high gamma over 2h recording illustrated in 10-min time bins.). All data are shown as mean ± SEM values.

5.3.3 Locomotor activity of Gi and Gq-DREADD and EGFP-control rats in the presence of CNO - Study II

Locomotor activity was recorded as above but during the dark phase of the animals to achieve a home-cage natural behaviour, with equal amount of time spent active *vs* inactive. Indeed, and as illustrated in **Figure 5.11**, the rats spent half of their times in the active state and half in the inactive state which indicates an appropriate readout of a 'resting state' locomotor profile of ECoG/LFP recordings. A statistical analysis revealed no effect of viral construct on locomotor state in the two treatment groups (Saline: $F(2, 252) = 2.31$, $P = 0.1$; CNO: $F(2, 252) = 0.76$, $P = 0.47$), a significant effect of time (Saline: $F(11, 252) = 5.01$, $P < 0.0001$; CNO: $F(11, 252) = 5.65$, $P < 0.0001$), but no interaction construct*time (Saline: $F(22, 252) = 0.9$, $P = 0.59$; CNO: $F(22, 252) = 1.004$, $P = 0.46$; **Figure 5.11**). This suggests neither saline nor CNO treatment impacted locomotor activity in any of the three groups.

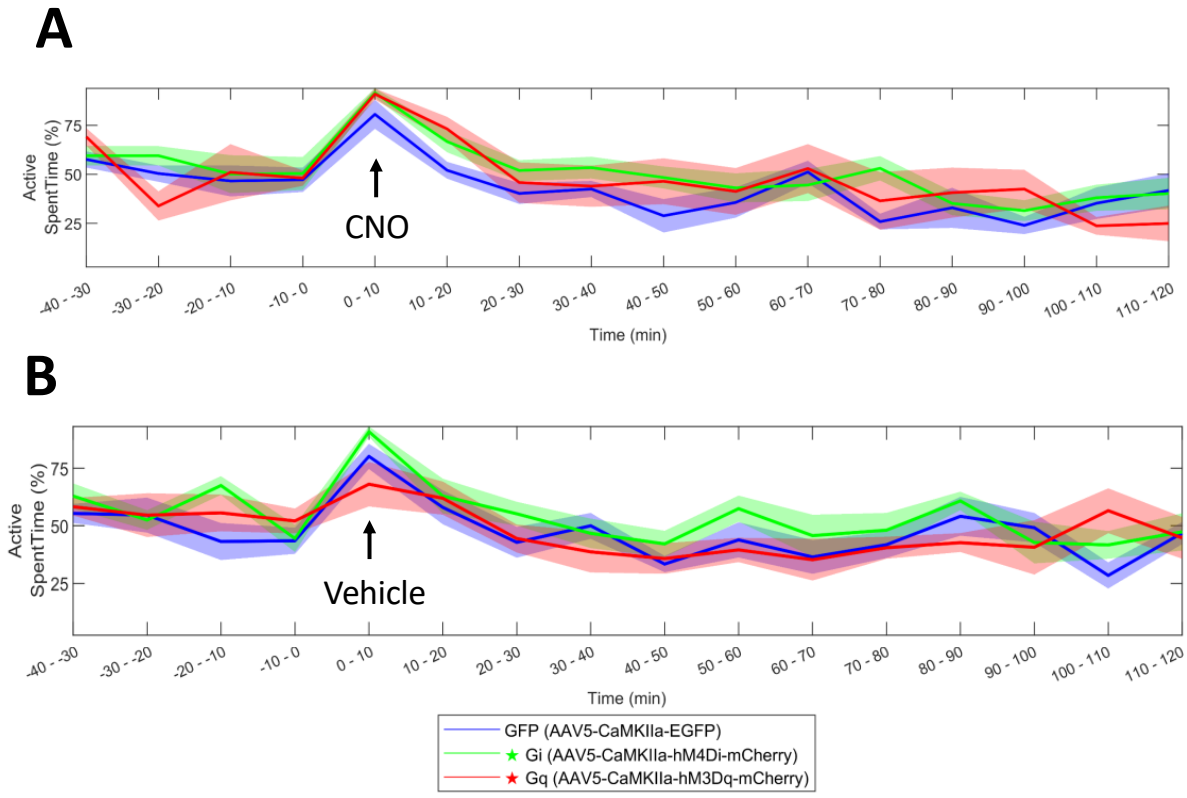


Figure 5.11: Locomotor activity of Gi and Gq-DREADD and EGFP-control rats after CNO or vehicle injection.

Percentage of time spent active presented in 10-min time bins over 2h after CNO (10 mg/kg) (A) or vehicle (B) injection. Data are presented as mean ± SEM values of n=9 EGFP-control rats (blue), n=10 Gi-DREADD (green) and n=5 Gq-DREADD rats (red). Arrow represents time of injection.

5.3.4 Resting state LFP profile of rats expressing an inhibitory or excitatory DREADD in the dorsal hippocampus – study II

Results in the previous study (see **5.3.1**) revealed decreased power compared to baseline in higher brain frequencies in both groups regardless of treatment, which could have hindered the detection of changes based on type of viral construct and/or treatment. Therefore, for the second cohort, changes were made to the experimental design (see **5.2.6**). Briefly, the rats were tested during the dark phase, were habituated to injections to avoid any interference of

stress with brain oscillations and only recorded for 2 h post injection to minimise the chance of rats going to sleep.

Overall the results showed decreased power in the 10-150 Hz range in the Gi-DREADD group in the presence of CNO (10 mg/kg). Gi-DREADD expressing rats showed significantly decreased power of beta, low and high gamma and HFO upon CNO injection as revealed by Tukey's post-hoc tests (**Figure 5.12C**, **Table 5.8**), and a significant effect of time*treatment interaction in the low gamma ($F(10, 198) = 3.2$, $P = 0.00076$), high gamma ($F(10, 198) = 3.32$, $P = 0.0005$) and HFO ($F(10, 198) = 2.31$, $P = 0.0014$) bands. This suggests that CNO treatment significantly decreased band power in ranges mentioned above. The decreased power was observed within 20 min of the injection but became statistically significant 40 min post CNO administration and was maintained throughout the recording period of 2h. **Figure 5.12B** shows the decreased power at all but one (theta) brain frequencies in the 30-120 min time interval. In the EGFP group. Data from the dorsal hippocampal depth electrode is presented as this was the site of injection of the Gi-DREADD where changes in LFP were predicted.

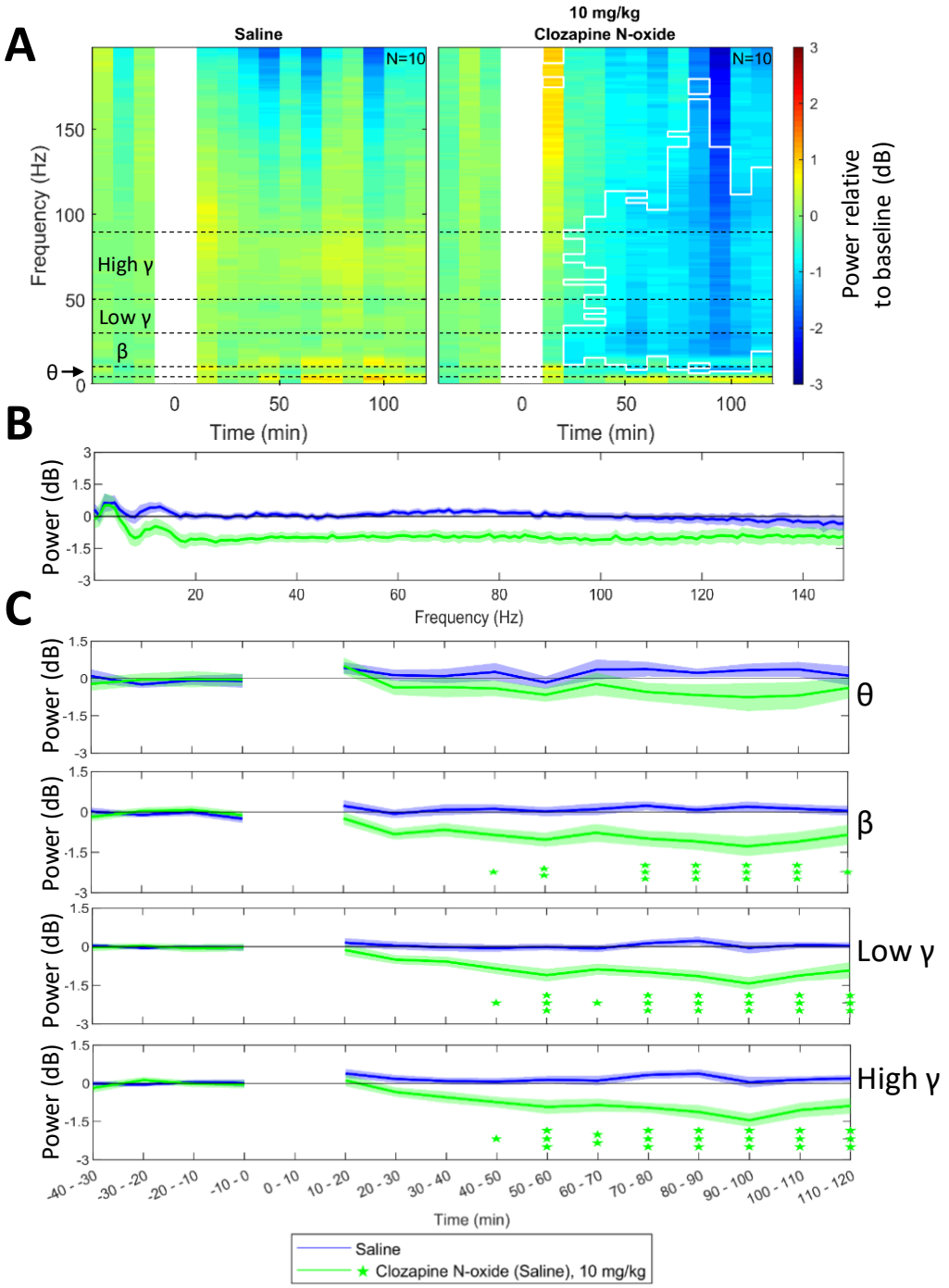


Figure 5.12: LFP profile of dHipp Gi-DREADD expressing rats in the presence of CNO

(A) Spectrogram of LFP signal recorded over 2h post injection from a depth electrode in the dHipp of rats expressing a Gi-DREADD after saline (left) or CNO (10 mg/kg) treatment (right). Area within the white line represents statistical significance compared to saline treatment at pixel level. Time point of 0 represents time of injection. Frequency bands are separated by dotted lines: δ (1-4 Hz, bottom band not labeled), θ (4-10 Hz), β (10-30 Hz), low γ (30-50 Hz), high γ (50-90 Hz). (B) Power of brain oscillations (up to 150 Hz) over the 30-120 min post injection time interval. (C) Band power separation (from top to bottom) for theta, beta, low and high gamma over 2h recording illustrated in 10-min time bins. Missing data represents time of injection (T0). All data are shown as mean ± SEM values from n=10 rats and are baseline normalised. *P<0.05, **P<0.01, ***P<0.001, fit of a generalised linear mixed effect model and multiple comparison tests with Tukey's honest significance difference.

Gq-DREADD expressing rats did not show any statistically significant differences compared to vehicle at any band power upon CNO injection (**Figure 5.13, Table 5.8**). However, two of the Gq-DREADD expressing rats developed seizures characterised by wet dog shakes during recording following CNO injection which prompted the termination of the experiment and culling the two rats on ethical grounds (see LFP/ECoG traces in **Figure 5.15D**). Wet dog shakes are considered to be a hallmark of kindling (Frush & McNamara, 1986), that is a consequence of progressive electrical stimulation of the hippocampus (in the current study) (Kandratavicius et al., 2014) and is used as a model of temporal lobe epilepsy (Leung & Shen, 2006). However, the Gq-DREADD expression could not be confirmed in the two rats that displayed seizures because the brains were not collected. Until that point and during the pilot study conducted before the current rsECoG/LFP study was initiated, no seizures had been observed in other Gq-DREADD expressing rats. Nevertheless, the Gq-DREADD group was no longer tested on follow up behavioural experiments. The lack of statistical significance in the Gq-DREADD group is most likely due to the high variability (**Figure 5.13**) observed in all frequency bands. However, the seizures in the two rats serve as direct evidence of Gq-DREADD functionality in the hippocampus. Moreover, the spectrograms suggest an increase in the low gamma power and a decrease in beta power in the Gq-DREADD group compared to vehicle. However, this observed effect was not statistically significant possibility because of the big variability in responses and the small sample size.

Finally, while there were no obvious effects of CNO treatment in the EGFP-control group (**Figure 5.14**), a statistical analysis revealed a significant effect of treatment ($F(1, 132) = 4.24$, $P = 0.041$), and time ($F(1, 132) = 2.37$, $P = 0.013$) but no effect of the interaction treatment*time ($F(10, 132) = 1.29$, $P = 0.24$) was observed in the low gamma band. Similarly, in the high gamma band there was a significant effect of treatment ($F(1, 132) = 4.39$, $P = 0.038$), and time ($F(1, 132) = 2.44$, $P = 0.0104$) but no effect of the interaction treatment*time ($F(10, 132) = 1.19$, $P = 0.3$). A post hoc analysis revealed no further statistical differences between the two

treatment groups in any of the frequency bands (**Table 5.8**). Wideband LFP/ECoG and accelerometer traces from example rats are shown in **Figure 5.15**.

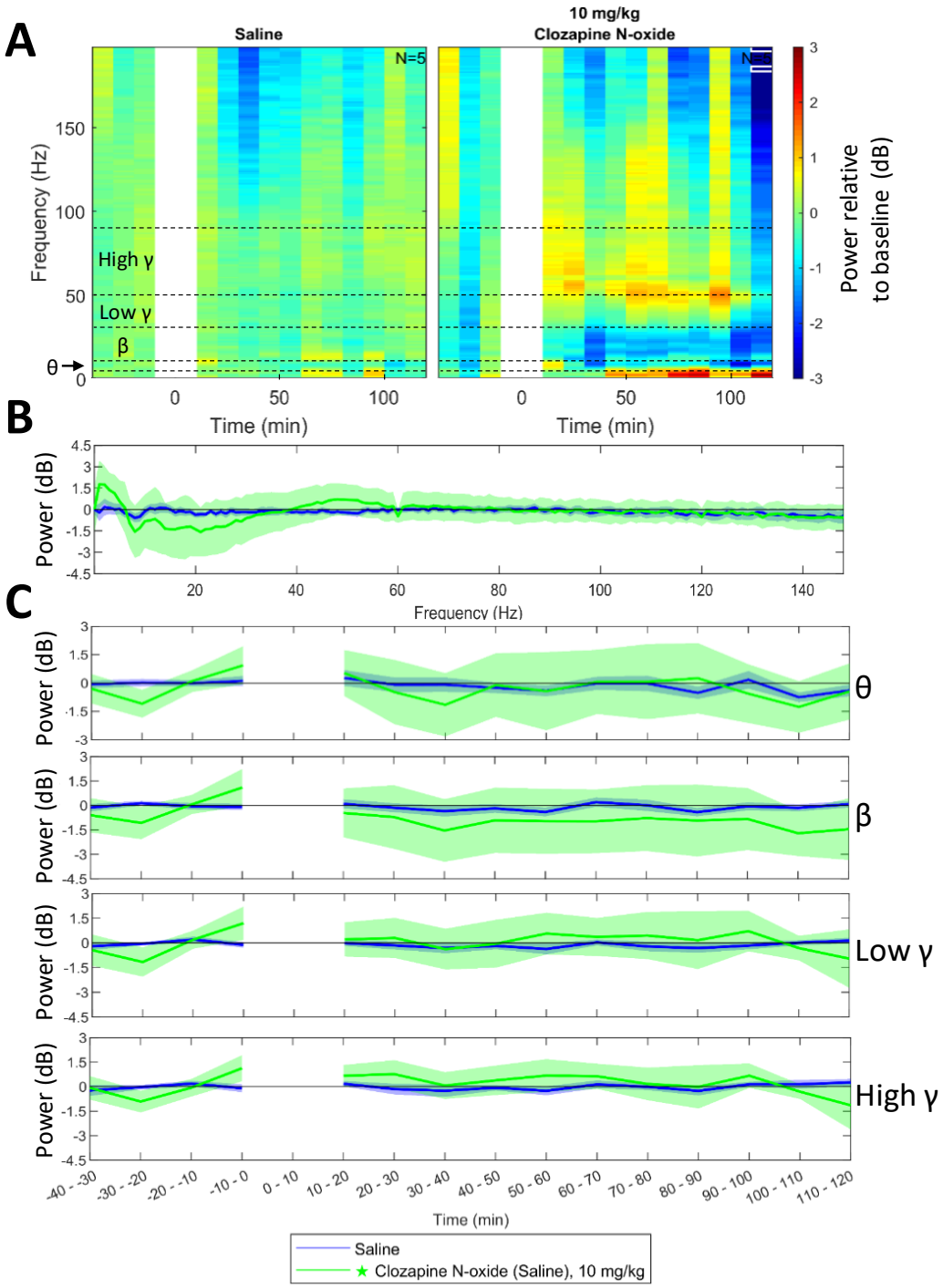


Figure 5.13: LFP profile of dHipp Gq-DREADD expressing rats in the presence of CNO

(A) Spectrogram of LFP signal recorded over 2h post injection from a depth electrode in the dHipp of rats expressing a Gq-DREADD after saline (left) or CNO (10 mg/kg) treatment (right). Area within the white line represents statistical significance compared to saline treatment at pixel level. Time point of 0 represents time of injection. Frequency bands are separated by dotted lines: δ (1-4 Hz, bottom band not labeled), θ (4-10 Hz), β (10-30 Hz), low γ (30-50 Hz), high γ (50-90 Hz). (B) Power of brain oscillations (up to 150 Hz) over the 30-120 min post injection time interval. (C) Band power separation (from top to bottom) for theta, beta, low and high gamma over 2h recording illustrated in 10-min time bins. Missing data represents time of injection (T0). All data are shown as mean ± SEM values from n=5 rats and are baseline normalised.

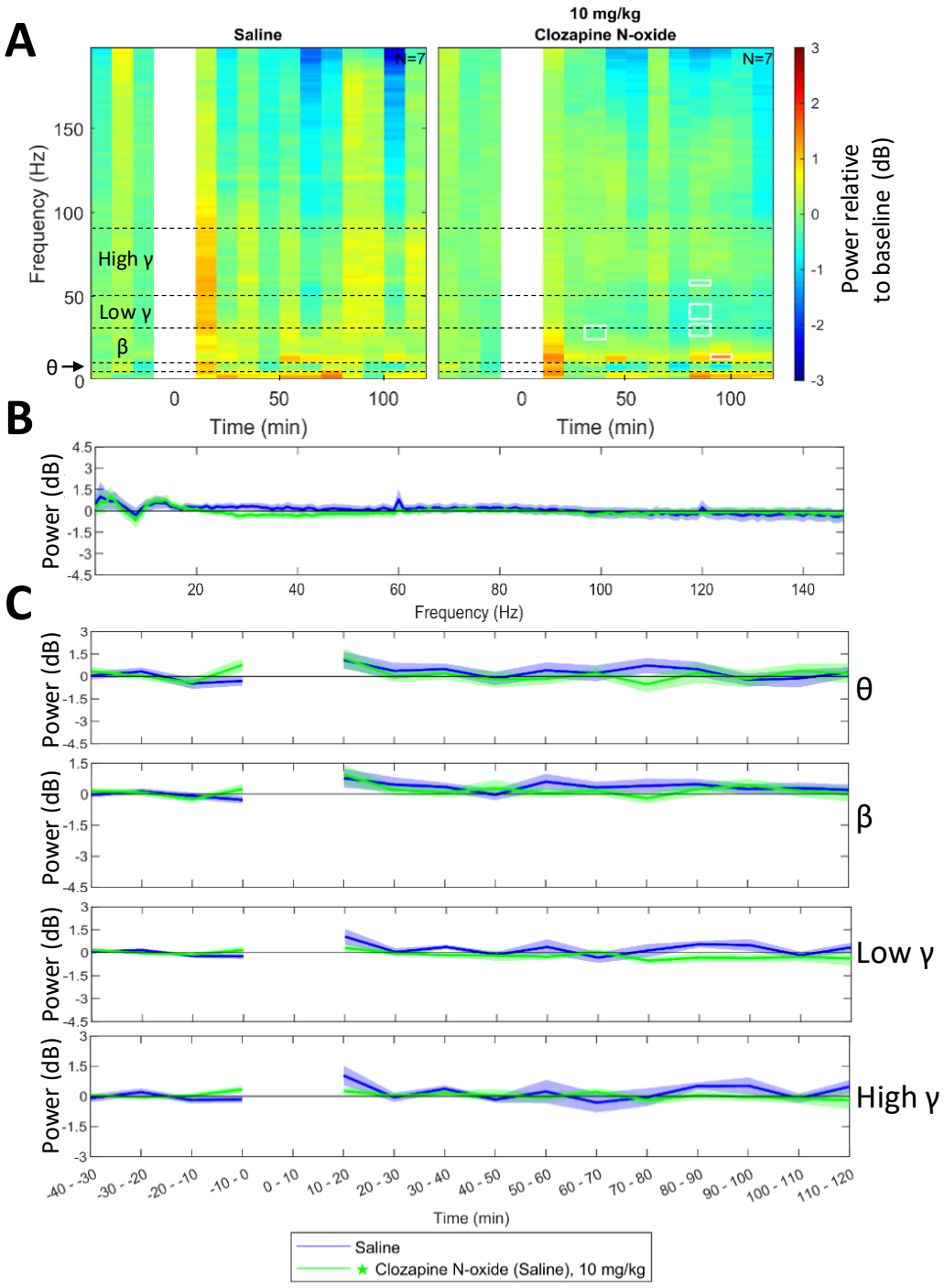


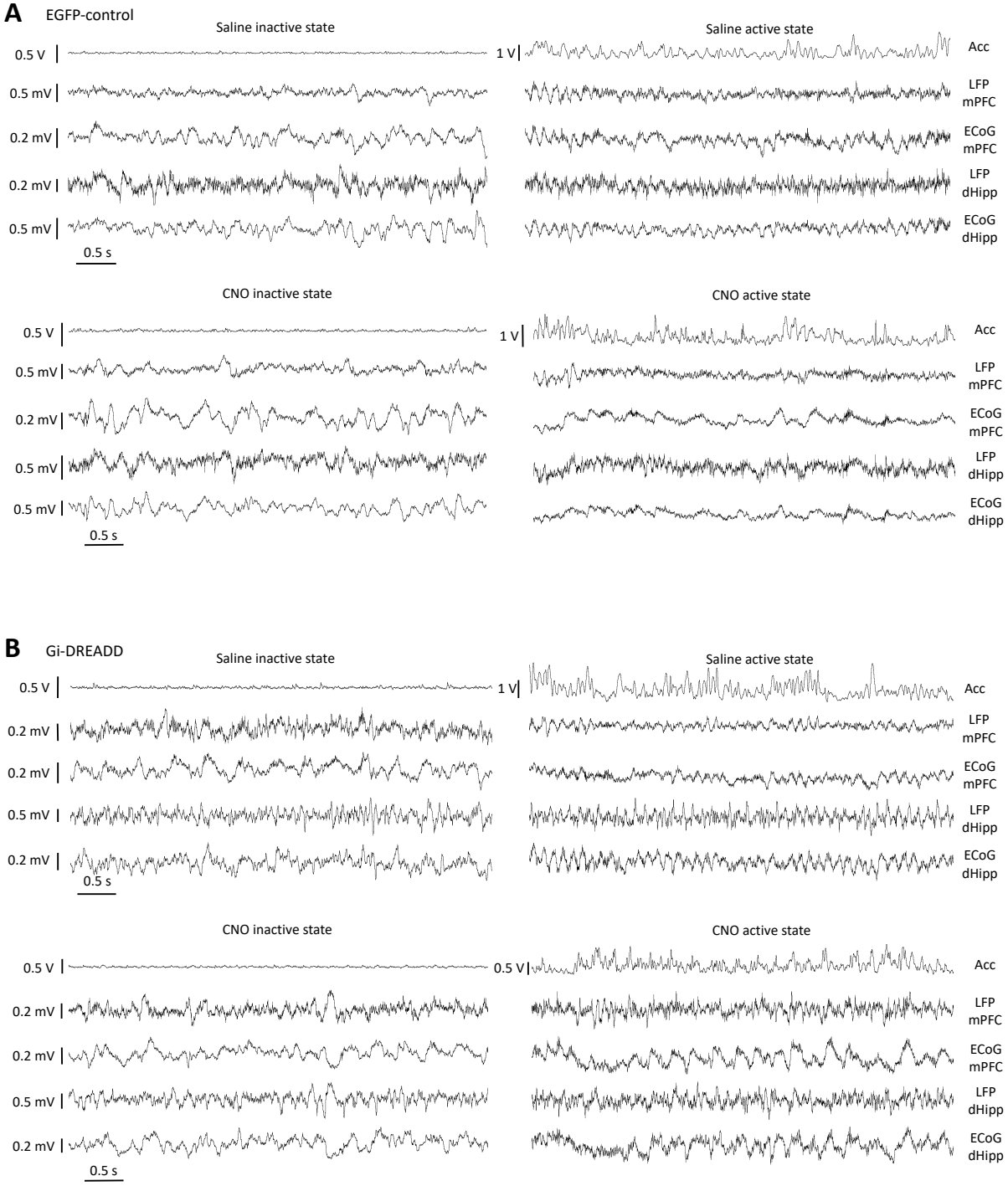
Figure 5.14: LFP profile of dHipp EGFP-control rats in the presence of CNO

(A) Spectrogram of LFP signal recorded over 2h post injection from a depth electrode in the dHipp of rats expressing an EGFP-control construct after saline (left) or CNO (10 mg/kg) treatment (right). Area within the white line represents statistical significance compared to saline treatment at pixel level. Time point of 0 represents time of injection. Frequency bands are separated by dotted lines: δ (1-4 Hz, bottom band not labeled), θ (4-10 Hz), β (10-30 Hz), low γ (30-50 Hz), high γ (50-90 Hz). (B) Power of brain oscillations (up to 150 Hz) over the 30-120 min post injection time interval. (C) Band power separation (from top to bottom) for theta, beta, low and high gamma over 2h recording illustrated in 10-min time bins. Missing data represents time of injection (T0). All data are shown as mean ± SEM values from n=7 rats and are baseline normalised.

Band power	Viral construct	Treatment		Time		Interaction		Post-hoc (p-values at different time bins post injection)								
		F(dF1,dF2)	p	F(dF1,dF2)	p	F(dF1,dF2)	p	T30	T40	T50	T60	T70	T80	T90	T100	T110
θ	Gi	F(1, 198) = 0.05	0.82	F(10, 198) =0.51	0.88	F(10, 198) =0.95	0.49	0.99	0.967	0.999	0.993	0.576	0.630	0.242	0.295	0.999
	Gq	F(1, 88) =0.06	0.81	F(10, 88) =0.15	0.99	F(10, 88) =0.99	0.99	1	1	1	1	1	1	1	1	1
	EGFP	F(1,132) =0.13	0.72	F(10,132) =2.15	**0.025**	F(10, 132) =1.39	0.19	1	1	0.99	1	0.2	1	1	0.99	1
β	Gi	F(1, 198) = 3.76	0.054	F(10, 198) =0.28161	0.98	F(10, 198) =1.36	0.2	0.26	**0.016**	**0.0054**	0.062	**0.00048**	**0.00073**	**0.00032**	**0.00046**	**0.048**
	Gq	F(1, 88) =0.2	0.65	F(10, 88) =0.058	0.99	F(10, 88) =0.1	0.99	1	1	1	1	1	1	1	0.99	0.99
	EGFP	F(1,132) =0.38	0.54	F(10,132) =1.24	0.27	F(10, 132) =1.15	0.33	1	0.99	0.95	1	0.89	1	1	1	1
Low γ	Gi	F(1, 198) = 1.98	0.161	F(10, 198) =0.47	0.91	F(10, 198) =3.2	**0.00076**	0.49	**0.018**	**0.0003**	**0.017**	**0.00032**	**0.00032**	**0.00032**	**0.00032**	**0.0008**
	Gq	F(1, 88) =0.068	0.88	F(10, 88) =0.07	0.99	F(10, 88) =0.45	0.92	1	1	0.99	1	1	1	1	1	0.99
	EGFP	F(1,132) =4.24	**0.041**	F(10,132) =2.37	**0.013**	F(10, 132) =1.29	0.24	0.99	1	0.98	1	0.98	0.78	0.827	1	0.959
High γ	Gi	F(1, 198) = 1.57	0.21	F(10, 198) =0.65	0.77	F(10, 198) =3.32	**0.0005**	0.36	**0.0496**	**0.0007**	**0.0036**	**0.00032**	**0.00032**	**0.00032**	**0.00033**	**0.00057**
	Gq	F(1, 88) =0.53	0.47	F(10, 88) =0.16	0.99	F(10, 88) =0.96	0.48	1	1	0.99	1	1	1	1	1	0.95
	EGFP	F(1,132) =4.39	**0.038**	F(10,132) =2.44	**0.0104**	F(10, 132) =1.19	0.3	1	1	1	0.99	1	0.99	0.99	1	0.98
90-150 Hz	Gi	F(1, 198) = 0.38	0.54	F(10, 198) =1.04	0.41	F(10, 198) =2.31	**0.014**	0.99	0.99	0.77	0.99	0.14	**0.0084**	**0.0057**	0.6	0.36
	Gq	F(1, 88) =0.12	0.73	F(10, 88) =0.44	0.92	F(10, 88) =1.42	0.19	1	1	0.99	1	1	1	1	0.99	0.68
	EGFP	F(1, 132) =0.59	0.442	F(10,132) =1.69	0.0882	F(10, 132) =1.08	0.382	1	0.99	1	0.99	1	1	1	0.99	0.99

Table 5.8: Statistical table of LFP signals recorded from the dorsal hippocampus in the presence of CNO

ANOVA results for the fit generalised linear model with treatment and time as fixed-effect predictor, separated by band power and viral construct for data presented in Figures 5.12-5.14. Comparison was made between vehicle and CNO treatments and statistically significant p values are underlined and written in bold.


A
EGFP-control
Saline inactive state
Saline active state
0.5 V
1 V
Acc
0.5 mV
LFP mPFC
0.2 mV
ECoG mPFC
0.2 mV
LFP dHipp
0.5 mV
ECoG dHipp
0.5 s
CNO inactive state
CNO active state
0.5 V
1 V
Acc
0.5 mV
LFP mPFC
0.2 mV
ECoG mPFC
0.5 mV
LFP dHipp
0.5 mV
ECoG dHipp
0.5 s
B
Gi-DREADD
Saline inactive state
Saline active state
0.5 V
1 V
Acc
0.2 mV
LFP mPFC
0.2 mV
ECoG mPFC
0.5 mV
LFP dHipp
0.2 mV
ECoG dHipp
0.5 s
CNO inactive state
CNO active state
0.5 V
0.5 V
Acc
0.2 mV
LFP mPFC
0.2 mV
ECoG mPFC
0.5 mV
LFP dHipp
0.2 mV
ECoG dHipp
0.5 s

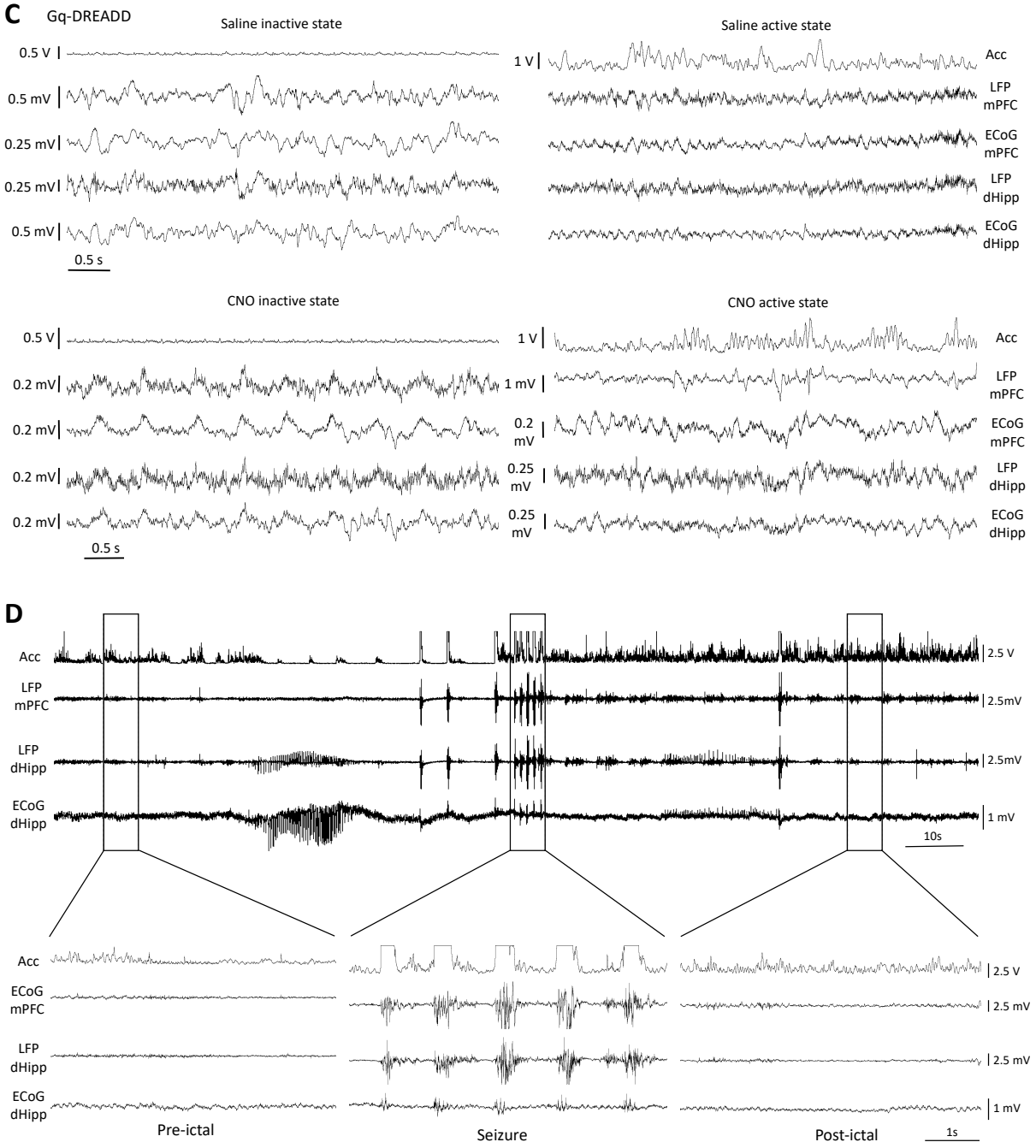


Figure 5.15: LFP and ECoG wideband traces from example animals.

Wideband LFP/ECoG and accelerometer data from example EGFP-control (A), Gi-DREADD (B) and Gq-DREADD (C) rats, during inactive (left) and active (states) as detected by the accelerometer. Data is shown for both drug conditions, saline and CNO (10 mg/kg) for the same rat as labelled on the diagrams (D) Example wideband traces from a rat that displayed seizures and was excluded from further analysis. mPFC: medial prefrontal cortex, dHipp: dorsal hippocampus, Acc: accelerometer.

A statistical analysis was done to establish whether CNO treatment affected the groups differently. As described in study I, the analysis was done from the 30 min time point when CNO/clozapine peak in the brain, in the 30-120 min time interval. The analysis revealed no effect of viral construct on band power after either saline or CNO (10 mg/kg) treatment, except for the beta band after saline treatment (F(2, 171) = 3.4817, P = 0.033; **Table 5.9**). These results are somewhat surprising based on within-group analysis, that shows clear decrease in a number of band powers in the Gi-DREADD group after CNO (10 mg/kg) treatment. However, this can be explained by the fact that the statistical analysis between viral construct group includes the Gq-DREADD group that shows great variability between the subjects.

		EGFP – Control – Gi & Gq – DREADD comparison					
Band power	**Treatment**	**Viral construct**		**Time**		**Interaction**	
		F(dF1,dF2)	**p**	**F(dF1,dF2)**	**p**	**F(dF1,dF2)**	**p**
θ	Saline	F(2, 171) = 0.82186	0.44	F(8, 171) = 2.0105	**0.048**	F(16, 171) = 1.3815	0.15
	CNO 10mg/kg	F(2, 171) = 0.74886	0.47	F(8, 171) = 1.0175	0.42	F(16, 171) = 1.4905	0.11
β	Saline	F(2, 171) = 3.4817	**0.033**	F(8, 171) = 1.5639	0.14	F(16, 171) = 1.422	0.14
	CNO 10mg/kg	F(2, 171) = 1.0387	0.36	F(8, 171) = 0.80134	0.6	F(16, 171) = 1.7052	**0.0496**
Low γ	Saline	F(2, 171) = 2.4271	0.091	F(8, 171) = 4.1727	**0.00014**	F(16, 171) = 2.0202	**0.014**
	CNO 10mg/kg	F(2, 171) = 0.17952	0.84	F(8, 171) = 0.33898	0.94	F(16, 171) = 1.6868	0.053
High γ	Saline	F(2, 171) = 1.6337	0.198	F(8, 171) = 2.8579	**0.005**	F(16, 171) = 1.4653	0.12
	CNO 10mg/kg	F(2, 171) = 0.98529	0.37	F(8, 171) = 0.26645	0.97	F(16, 171) = 1.6064	0.071

Table 5.9. Between group statistical analysis of hippocampal band powers dependent on treatment

ANOVA results for the fit generalised linear model with viral construct and time as fixed-effect predictor, separated by band power and treatment for data presented in Figures 5.12-5.14. Comparison was made between the 3 groups after the same treatment dose. Statistically significant p values are underlined and written in bold.

Collectively this study found evidence that CNO (10 mg/kg) did not alter the LFP profile of EGFP-control rats and that CNO treatment did not change locomotor state in Gi or Gq-

DREADD or EGFP-control rats. Interestingly, CNO-induced activation of a hippocampal Gi-DREADD led to decreased power in the beta, low gamma and high gamma bands. Recordings from the dHipp and mPFC ECoG screw and the mPFC depth electrode did not find such marked differences between groups or treatment and can be found in the appendix (Chapter 7).

5.3.5. Histology

Exclusions were made based on histological validation of electrode placement and confirmation of viral expression. In this study, data from two dorsal hippocampal electrodes from EGFP rats were excluded due to miscalculations during electrode implantation surgery that resulted in the electrode placement to be too superficial. LFP data from the dorsal hippocampus was also excluded from two Gq-DREADD expressing rats due to one electrode not being found in one rat and both rats showing unilateral viral expression on the contralateral side and not on the electrode hemisphere.

Figures **5.16-5.18** show the exact electrode positioning and viral spread around the area of the electrode in each rat from the study. The images indicate that the depth electrode was positioned above the CA3 region in the dorsal hippocampus (in 21 out of 22 rats that were used for recordings in the current study) (AP: -3.6 mm from bregma). Electrode placement was validated post-hoc with only one dorsal hippocampus electrode from the Gi-DREADD group and two from the Gq-DREADD group being placed more anterior than -3.6 mm (AP from bregma). In terms of viral expression, the majority of rats showed transfection of the construct around the injection sites in the CA1 and CA3 area but also the suprapyramidal and infrapyramidal blades of the DG. Histology for study I can be found in the appendix (Chapter 7).

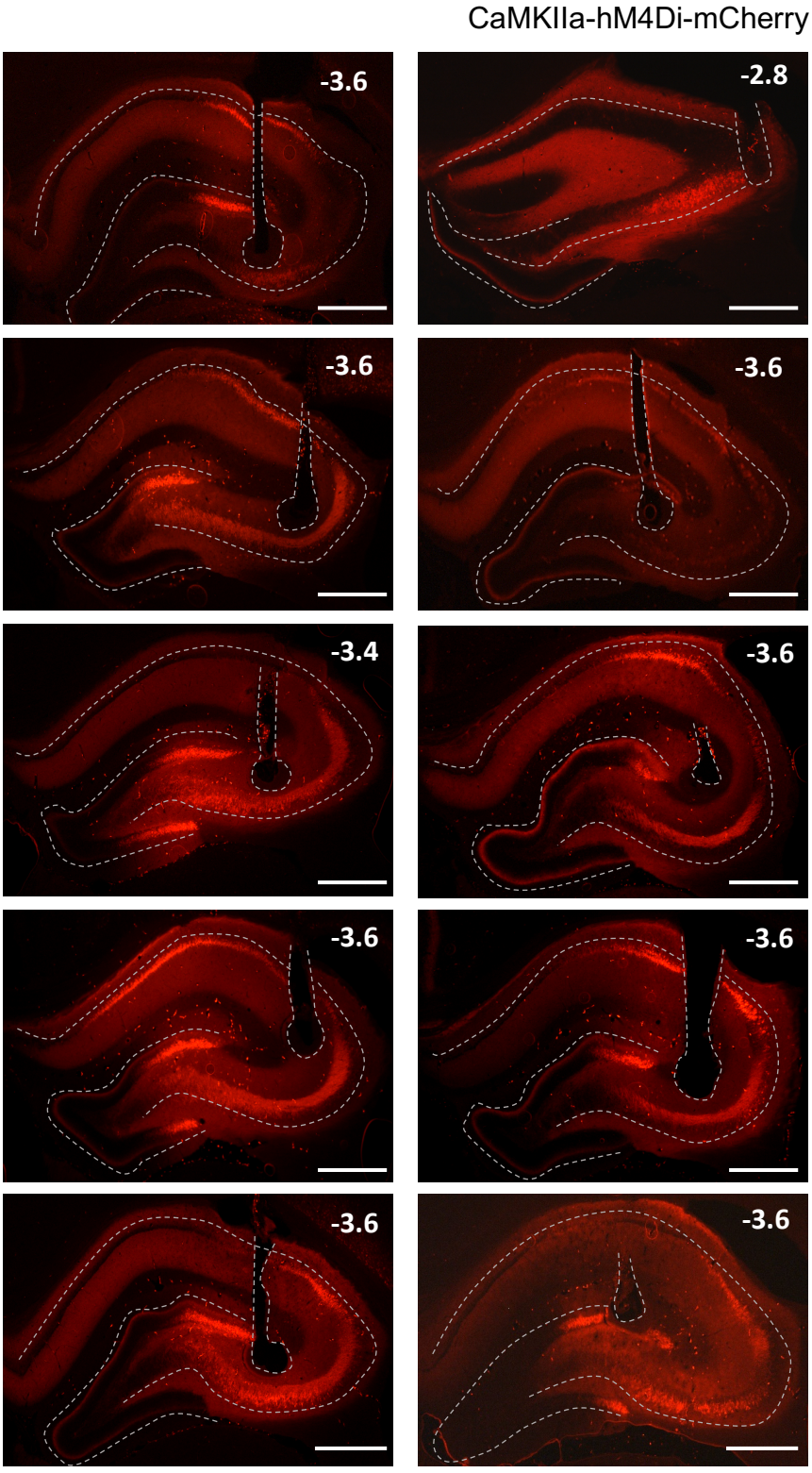


Figure 5.16: Electrode placement confirmation and Gi-DREADD expression validation

Epifluorescent images showing the expression of the mCherry tagged Gi-DREADD (red) in the area surrounding the recording electrode from all the rats in the LFP/ECoG Study II. Outside of pyramidal layer is outlined by white dotted line. Electrode positioning is highlighted by the white dotted line. Each image represents a different rat. Numbers represent approximate AP coordinates. Scale bar = 500 µm.

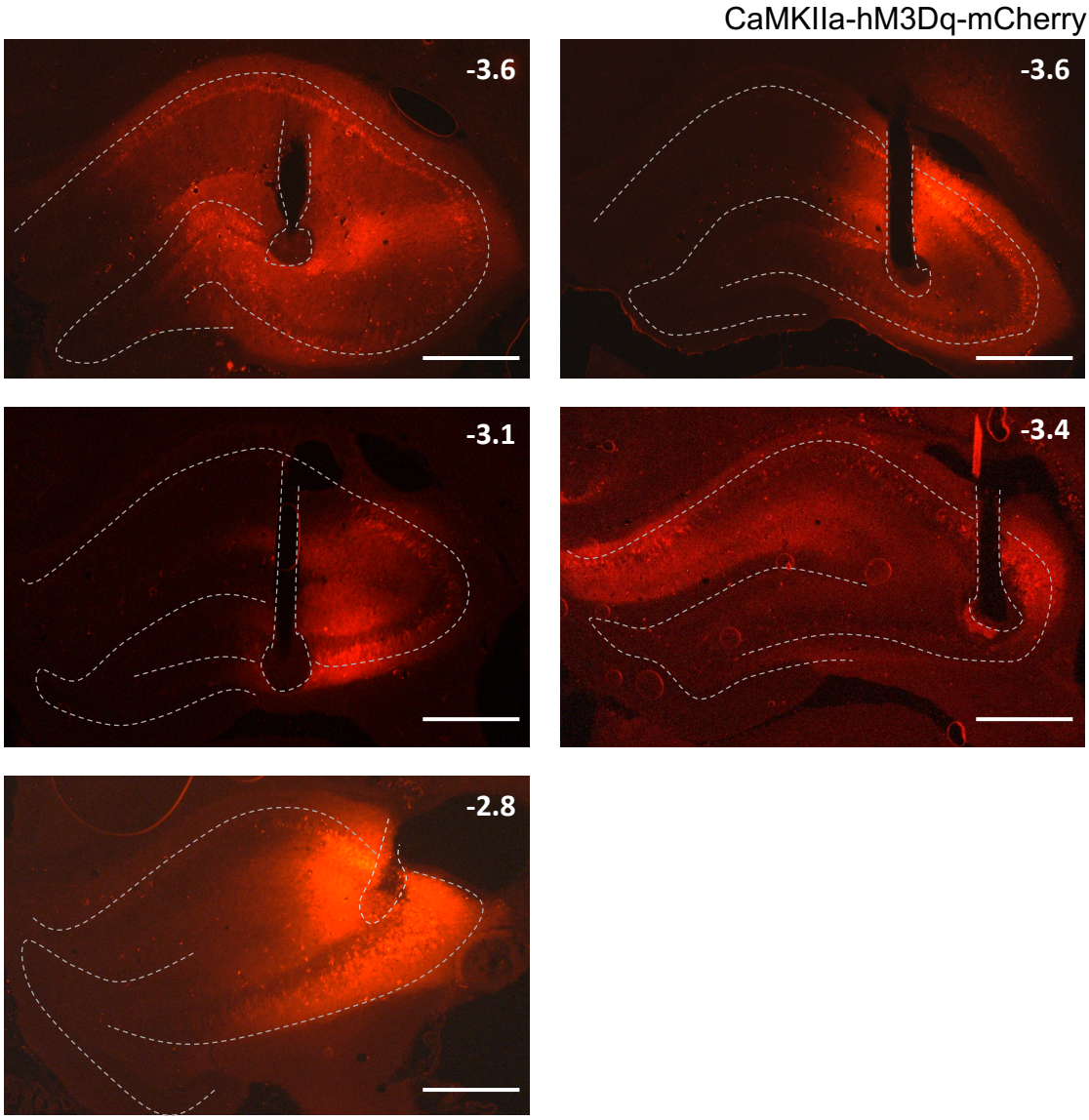


Figure 5.17: Electrode placement confirmation and Gq-DREADD expression validation

Epifluorescent images showing the expression of the mCherry tagged Gq-DREADD (red) in the area surrounding the recording electrode from all the rats in the LFP/ECoG Study II. Outside of pyramidal layer is outlined by white dotted line. Electrode positioning is highlighted by the white dotted line. Each image represents a different rat. Numbers represent approximate AP coordinates. Scale bar = 500 µm.

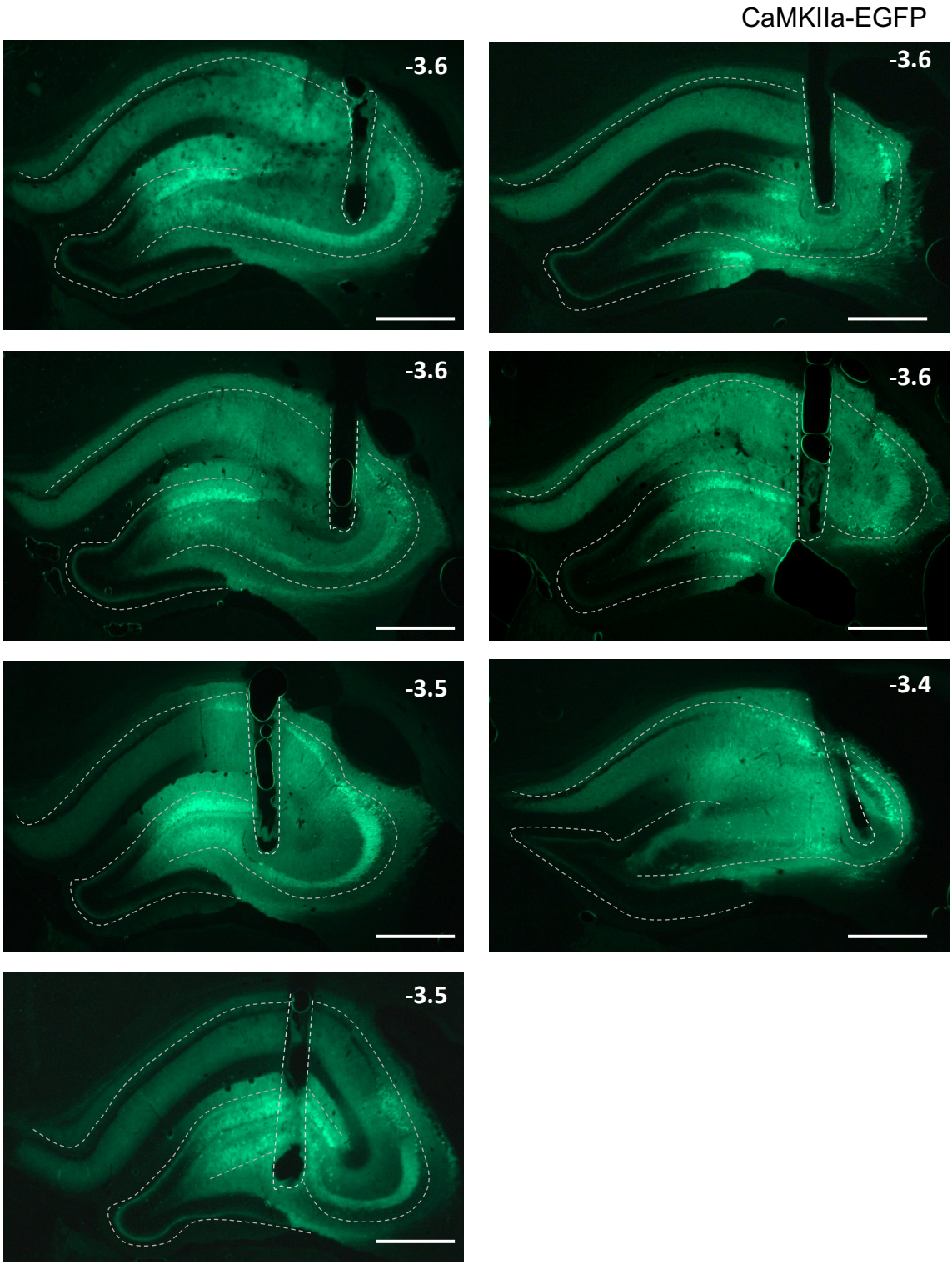


Figure 5.18: Electrode placement confirmation and EGFP-control expression validation

Epifluorescent images showing the expression of the EGFP tagged control construct (green) in the area surrounding the recording electrode from all the rats in the LFP/ECoG Study II. Outside of pyramidal layer is outlined by white dotted line. Electrode positioning is highlighted by the white dotted line. Each image represents a different rat. Numbers represent approximate AP coordinates. Scale bar = 500 µm.

5.3.6 Novelty induced locomotor activity of Gi-DREADD and EGFP-control in the presence of CNO

As the accelerometer measurements taken during the ECoG/LFP recordings are not a direct measure of locomotor activity, the rats were tested for novelty induced hyperlocomotion in a photocell set-up, using number of beam breaks as indicator of locomotor activity. A repeated measures 2-way ANOVA with viral construct as between subject factor and time and treatment as within-subject factor revealed no effect on the number of beam breaks based on viral construct expressed ($F(1, 17) = 1.06$, $P = 0.318$), the treatment ($F(1, 17) = 1.151$, $P = 0.298$) or the interaction, constructs*treatment ($F(1, 17) = 0.065$, $P = 0.802$). The number of beam breaks decreased significantly over time ($F(23, 391) = 69.374$, $P < 0.0001$) but there was no significant effect of treatment*time interaction ($F(23, 391) = 1.386$, $P = 0.112$). (**Figure 5.19**).

These data show that reducing the pyramidal neuron excitability in the dorsal hippocampus by means of Gi-DREADD in the presence of high dose CNO (10 mg/kg) does not alter locomotor activity.

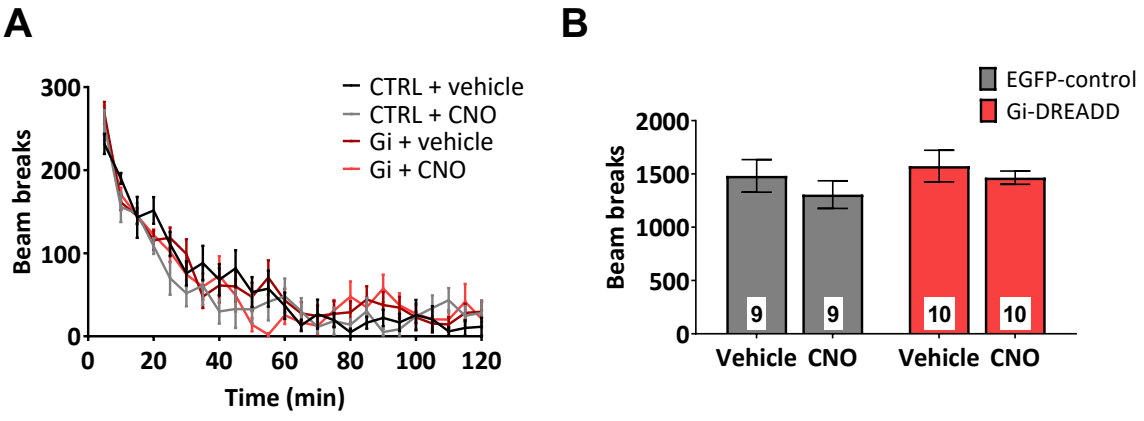


Figure 5.19: Novelty induced locomotor activity of Gi-DREADD and EGFP-control in the presence of CNO.

(A) Locomotor activity presented in 5-min time bins over 2h, as a mean ± SEM values of n=9 EGFP-control rats (grey and black) and n=10 Gi-DREADD (red and dark red). (B) Total number of beam breaks over 2h for each treatment group. Data shown as mean ± SEM values.

5.3.7 Short-term memory of Gi-DREADD and EGFP-control in the presence of CNO

In the light of the LFP study, the spatial short-term memory of Gi-DREADD expressing rats was re-assessed on the spatial novelty preference Y-maze upon increased CNO dose (10 mg/kg). The task was performed as previously described (see **3.2.6**). An unpaired t-test revealed no significant differences between the two groups ($t(17) = 1.693$, $P = 0.1088$) (**Figure 5.20A**). However, only the control rats revealed preference for the novel arm as revealed by one-sample t-tests against change performance (ratio of 0.5) ($t(8) = 9.924$, $P<0.0001$) in contrast to the Gi-DREADD rats that did not performed significantly above chance ($t(9) = 1.946$, $P = 0.0835$). Further, statistical analysis of the locomotor activity during the habituation phase revealed no significant differences between the EGFP-control group and the Gi-DREADD group ($t(17) = 0.1624$, $P = 0.829$; **Figure 5.20B**).

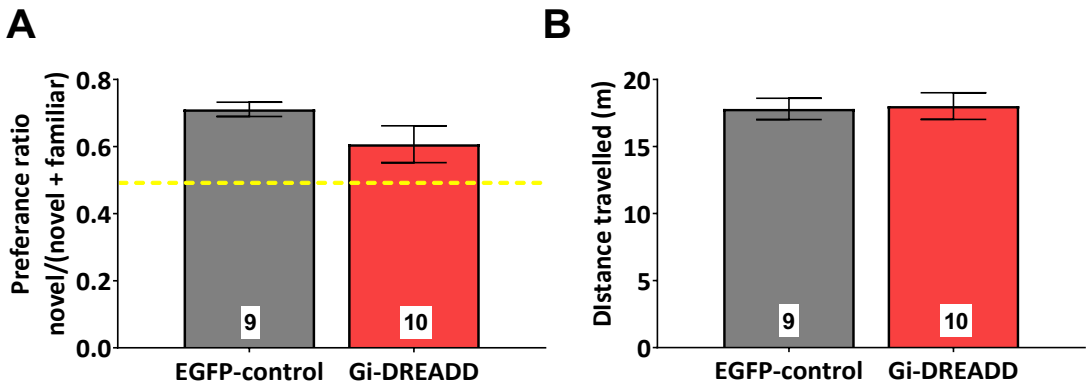


Figure 5.20: Spatial memory in Gi-DREADD expressing rats upon high dose of CNO administration

(A) Novel arm preference ratio (time spent in novel arm/(time spent in familiar arm + time spent in the novel arm) over 2 min of the test phase for the two groups (Gi-DREADD and EGFP-control) and treatments (vehicle and CNO 10 mg/kg. Dotted yellow line represents chance performance level. (B) Total distance travelled during the exposure phase (5 min) while one arm was blocked. Data are shown as means ± SEM values from Gi-DREADD (n=10) and EGFP-control (n=9) rats.

Finally, rats were tested on a spontaneous recognition memory task. Due to issues with counterbalancing of the novel object, the data was analysed and presented as object

exploration. No differences in object exploration were detected between groups as revealed by a repeated measures two way ANOVA statistical analysis with viral construct as between subject factor and trial as within-subject factor. There was no significant effect of the construct type ($F(1, 17) = 2.179$, $P = 0.1582$), a significant effect of the trial ($F(5, 85) = 59.63$, $P < 0.0001$) but no significant effect of the interaction, construct type*trial ($F(5, 85) = 0.8143$, $P = 0.5427$) on the object exploration time (**Figure 5.21**). These results suggest that both groups of rats exhibited similar object exploration time during each trial.

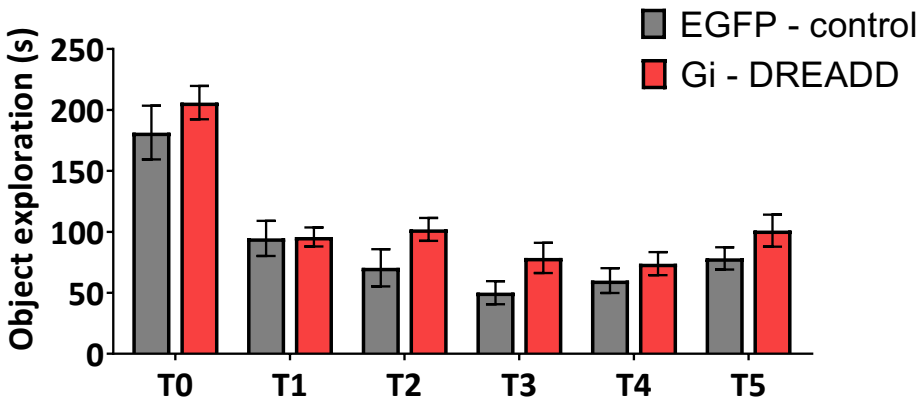


Figure 5.21: Object exploration upon CNO induced Gi-DREADD activation.

Time spent exploring all 4 objects in each trial in the presence of CNO (10 mg/kg). T0 was the exposure trial and lasted 10 min. All other trials lasted 5 min each. Data are shown as means ± SEM values from Gi-DREADD (n=10) and EGFP-control (n=9) rats.

All in all, these results suggest that decreased power in the 10-150 Hz frequency range in the dorsal hippocampus does not have an impact on locomotor activity, short term working memory or object exploration.

5.4 Discussion

Experiments in this final chapter aimed to establish whether Gi or Gq-DREADD dependent manipulation of excitatory transmission in the dorsal hippocampus caused changes in the LFP recorded from the site of viral injection and whether these changes impacted cognitive behaviour. To this end, two rsECoG/LFP studies were performed and dorsal hippocampal recordings were made.

For the first study, changes in brain oscillations in the presence of a Gi-DREADD were recorded in response to different doses of CNO and clozapine to establish the functionality of the inhibitory DREADD *in vivo*. The results showed tendency towards decreased gamma power in the dorsal hippocampus as a consequence of CNO (10 mg/kg) induced Gi-DREADD activation, albeit not statistically significant. Non-DREADD specific effects of high dose CNO were observed in control rats as increased theta and decreased beta power. While this first study has not provided any conclusive evidence regarding the function of the Gi-DREADD, it has enabled improvements in the experimental design of the second study. Thus, a few changes were made to the protocol. Firstly, to reflect 'resting state' – characterised here by free exploration of a familiar environment in the absence of external stressors – and to avoid them going to sleep, rats were placed on a reversed light cycle such that they were tested during their active phase once they had recovered from surgery. This allowed for all recordings to be made during the active phase of the rats. Secondly, the rats were habituated to i.p. injections prior to testing and recordings were only made for 2h post injection. Thirdly, based on the results from the first study, CNO (10 mg/kg) was chosen as agonist for DREADD activation. Lastly, a Gq-DREADD group was added to address the paradoxical effects observed in the slice electrophysiology experiments (Chapter 2).

Results of the second rsECoG/LFP study showed no changes in the theta power in any of the DREADD groups in response to CNO (10 mg/kg) injection. Decreased power was observed in the 10-150 Hz range in the presence of a Gi-DREADD in the dorsal hippocampus. No significant changes were recorded in the presence of a Gq-DREADD but this may be explained by an increased variability of responses in the group (discussed below). Furthermore, two of the Gq-DREADD expressing rats developed seizures and had to be culled. Thus, the Gq-DREADD group was terminated and no longer tested for behavioural changes. Finally, despite decreased power in a number of frequency bands, Gi-DREADD rats showed normal short-term memory, object exploration and locomotor activity.

5.4.1 LFP profile in response to CNO or clozapine Gi-DREADD activation – study I

This first study was designed to interrogate whether the decreased excitatory transmission observed *ex vivo* was also evident *in vivo*, in awake, behaving animals. In the present study it was hypothesised that CNO binding to Gi-DREADD will lead to decreased gamma power. Additionally, based on results from the exposure study (see **4.3.5**) it was predicted that CNO (10 mg/kg) and clozapine (0.5 mg/kg) will produce similar changes in the LFP. The results however, were inconclusive and no parallels between treatments could be drawn.

A caveat of the experiments was the marked decrease observed in frequencies over 60 Hz in the hippocampus but also the mPFC (data not shown) as recorded by a depth and screw electrode. This decrease was independent of viral construct or treatment, suggesting these changes are unlikely to be linked to DREADD expression or agonist treatment. However, this floor effect could have hindered any inhibitory effect of Gi-DREADD activation on brain oscillations. Still, the reason for this decrease is not fully understood.

Increased theta power 30 min into the recording was also detected in all recordings. Theta waves are known to be present during REM sleep (Vanderwolf, 1969) and during various behaviours. Generally, theta oscillations are not generated during immobile awake states (Buzsaki, 2002) with one exception being freezing during fear conditioning (Seidenbecher et al*., 2003)*. More recently it was suggested that theta power is also correlated with running speed, theta power being directly proportional to locomotor speed (Bender et al., 2015). In the current study, the aim was to record resting state activity. To this end the rats were habituated to the testing boxes a week prior. However, they had not been habituated to i.p. injections, the first testing day being the first time receiving i.p. injections. In addition, the rats were tested during their light phase. Thus, it is possible that the increased theta power independent of treatment or group was attributed to the rats going to sleep during the 4h recording. In support of this, the locomotor state recorded by the accelerometer shows < 25% time spent active 30 min post injection and throughout the remainder of the recording. The timing of the decreased locomotor activity is in line with the beginning of increased theta power observed. However, the correlation was not confirmed, as moment-by-moment analysis and evidence of slow wave activity would be required to establish a sleeping profile. Still, the presence of increased theta power independent of treatment or viral construct, rules out any effect (DREADD specific or non-specific) of CNO or clozapine treatment on theta oscillations. However, these results also indicated the lack of an appropriate 'resting state' model. To this end, a second refined rsECoG/LFP study was designed (see **5.4.3**).

5.4.2 LFP profile of Gi-DREADD expressing rats in a novel environment

Gria1$^{-/-}$ mice are known to be hyperactive in a novel environment due to deficits in short-term habituation (Wiedholz et al., 2008). More recently it was also shown that peak theta frequency was elevated in a novel environment in *Gria1*$^{-/-}$ mice (Bygrave et al., 2019). As *Gria1*$^{-/-}$ mice show impaired AMPA mediated glutamatergic transmission (Zamanillo et al., 1999), one could

expect that Gi-DREADD expressing rats will show increased theta power in response to CNO when recorded in a novel environment as a consequence of glutamatergic transmission suppression, hippocampal deficits and subsequent deficits in short-term habituation. To this end, all rats were injected with CNO (10 mg/kg) and returned to their home cage for 30 min. Next, they were placed in a novel environment (wallpapered cages, novel bedding and novel object) and LFP/ECoG and locomotor activity were recorded for 2h. The results showed no changes between the groups, in any frequency band. Similar to the previous study, the locomotor activity drastically decreased over the first 30 min of exposure to the novel context until it reached its minimum that was maintained for the rest of the recording. The decline in locomotor activity could indicate the loss of interest towards the novel context, that was potentially not stimulating enough for any of the groups. The data suggests that there were no deficits in short-term habituation in the Gi-DREADD rats.

5.4.3 LFP profile of Gq and Gi-DREADD rats in the presence of CNO – study II

In an attempt to reflect 'resting state' activity a few parameters (discussed above) were changed in the second study. Cortical PV interneurons are known to be involved in the generation of gamma oscillations (Buzsaki & Wang, 2012) with evidence from optogenetic studies showing suppression of gamma oscillations *in vivo* upon inhibition of PV interneurons (Sohal et al., 2009). Gamma oscillations require coordinated activity between excitatory and inhibitory neuronal ensembles. Specifically, excitatory drive from pyramidal neurons is required for activation of PV interneurons that in turn will regulate glutamatergic activity by perisomatic inhibition of pyramidal neurons (Buzsaki & Wang, 2012; Mann et al., 2005). This feedback mechanism is also known as the pyramidal-interneuron network gamma (PING) model (Whittington et al., 2000). Thus, chemogenetic silencing of dHipp pyramidal neurons was predicted to cause decreased gamma oscillations in the LFP. Indeed, the present results showed statistically significant decrease in both low and high gamma power in dHipp LFP in

rats expressing a Gi-DREADD. The decrease was gradual post CNO (10 mg/kg) injection, becoming significant 30 min later and remained constant throughout the recording, 2h post injection.

Assuming the PING model as the gamma generator in the CA3 and evidence from optogenetic studies showing increased gamma oscillations upon PV interneuron activation by means of principal cell activity (Sohal et al., 2009), an increase in gamma oscillations was also expected from Gq-DREADD rats. While the band separation analysis showed no statistically significant differences between treatment in the Gq-DREADD group, two rats displayed epileptiform activity – characterised by wet dog shakes at the behavioural level. In rodents, gamma oscillations have been detected before the onset of ictal activity and during epileptic activity (Bragin et al., 1999; Uhlhaas & Singer, 2010). The spectrograms indicate towards increased gamma power albeit not statistically significant. The lack of statistical significance may be due to the big response variability in the Gq-DREADD group. In line with this assumption, Alexander et al. (2009), provide evidence of CNO dose dependent increased gamma power in Gq-DREADD expressing mice and subsequent epileptiform activity. Elevated gamma oscillations were associated with increased interneuron firing that was likely a consequence of increased pyramidal neuron activity (Alexander et al., 2009).

The spectral analysis revealed no effects of CNO (10 mg/kg) on EGFP-control rats. Decreased power in low gamma was also detected and was statistically significant in the ECoG screw placed above the dorsal hippocampus. No further marked differences were observed between treatment groups in the mPFC ECoG or LFP or dHipp ECoG (see appendix, Chapter 7).

Taken together, these results suggest that the Gi-DREADD function in the hippocampus leads to decreased brain oscillations in the 10-150 Hz ranges. Gi-DREADD reduced power in a

number of frequency bands, suggesting a role of pyramidal neurons in regulating hippocampal oscillatory activity, likely through decreased excitatory output onto inhibitory interneurons. While Gq-DREADD mediated mechanisms remain inconclusive based on the LFP profile, the seizures exhibited by two rats are direct evidence of its functionality nonetheless. Future studies are needed to establish the mechanism underlying this phenotype in only a number of rats and the nature of the discrepancies seen in the *ex vivo* vs *in vivo* profiles.

It is difficult to establish what caused different responses in the two studies presented. A few factors could have contributed to this outcome. Firstly, it is possible that the circadian cycle could have had an influence on the activity of the rats, with rats being more active during the dark phase (Clemens et al., 2013), which in turn perhaps influenced their oscillatory responses, and led to a LFP profile similar to baseline in control groups. Secondly, there is the possibility that habituation to injections in the second study led to decreased stress (Melia et al., 1994), which could have also impacted on oscillatory activity. Lastly, the shorter recording period might have also played a role in decreasing the stress the rats were exposed to. It is likely that a combination of these factors has caused a more suitable control LFP profile in the second study that allowed for effects of DREADD/agonist manipulations to be detected.

Finally, there are a couple of considerations associated with the analysis that need to be taken into account. Firstly, the LFP data for the inactive and active state was pooled. This was done in the current study because the aim was to record natural home cage behaviour – and to assess any changes in power of diferent frequency bands as a consequence of DREADD activation – which involved both active and inactive behaviours. Additionally, the main findings (i.e. decreased gamma and beta power in the Gi-DREADD group in the presence of CNO) were observed in both states (data not shown). The active and inactive state could potentially be further characterised, as described by Lapray et al., (2012) into slow-wave and paradoxical

sleep, quiet wakefulness and movement. The same study also described how different hippocampal interneurons are involved in different behavioural states and associated oscillations (Lapray et al., 2012). However, in the case of the studies described in this chapter, the inactive state could not be separated into quiet wakefulness and sleep based on accelerometer data. In theory, one could further analyse the LFP and ECoG traces and separate quiet wakefulness from sleep (based on the parameters established by Lapray et al., (2012)) and further characterise the different behavioural states and associated changes in different frequency bands. However, characterising different sleep or movement states and correlating them with changes in band power was beyond the scope of this thesis. Secondly, the data collected during these studies hold potential for more discoveries that were perhaps masked by averaging the data for all animals in a group and by using a time resolution of 5 s for the spectrograms which would not detect changes in high frequency oscillations that are much faster and occurring at irregular intervals (Buzsaki, 2015). Nonetheless, the aim of assessing functionality of the DREADDs *in vivo* was achieved.

5.4.4 Behavioural readout of decreased brain oscillations

Finally, once the model of decreased excitatory transmission in the hippocampus was established and confirmed *in vivo*, the same cohort of rats was tested on hippocampal-dependent tasks. Despite predictions, but in line with previous behavioural experiments presented in Chapter 3, the rats showed no impairments in spatial memory and object exploration. These findings were somewhat surprising, considering disrupted gamma rhythm has been associated with cognitive deficits, such as working memory and attention, in schizophrenia (Uhlhaas & Singer, 2010; Lisman & Jensen, 2013) and decreased slow gamma was observed in Alzheimer's disease animal models (Malby & Colgin, 2018). Gamma power was found to be positively correlated with working memory load in humans (Howard, 2003).

In a final task, object exploration was assessed in Gi-DREADD and EGFP control rats in the presence of CNO (10 mg/kg). It was hypothesised that rats with hippocampal deficits will display increased object exploration due to memory impairment, as is the case with novelty induced hyperlocomotion as a result of deficits in short-term habituation (Bannerman et al., 1999; Rawlins & Olton, 1982). The current results showed no differences in object exploration in the two groups, between trials or as a total time spent exploring. This is in contrast to a previous study showing increased object exploration in rats with hippocampal lesions (Broadbent et al., 2009). Once more, the lack of behavioural deficits in the Gi-DREADD group could suggest that despite decreased brain oscillations at the LFP level, the viral transfection in a limited population of neurons in the dorsal hippocampus is not enough to impact behaviour.

5.4.5 Conclusion

Experiments in this final chapter aimed to build on prior knowledge from the previous chapters and assess DREADD function *in vivo*. Taken together, the data presented point towards an indirect mechanism of decreased excitatory transmission as a consequence of suppression of interneuron perisomatic inhibition on pyramidal cells upon CNO-induced activation of a Gi-DREADD. This in turn decreases gamma oscillations. However, decreased gamma or beta power was not associated with cognitive impairments. Furthermore, the functionality of Gq-DREADD was also established and CNO (10 mg/kg) was shown to not cause any changes in brain oscillation or behaviour in the absence of a DREADD.

Chapter 6

General discussion

The overall aim of this thesis was to capitalise on the potential of DREADDs as a tool to deconstruct behaviours in an attempt to investigate cortical and subcortical mechanisms of cognition. To this end, the dorsal hippocampus was chosen as the brain region of interest as it is known to be critical for cognitive functions (Olsen et al., 2012) and the excitatory pyramidal neurons as the target for chemogenetic manipulations, as they play an important role in integrating and transmitting the information to connected brain regions (Graves et al., 2012). Firstly, the DREADD constructs were stereotaxically delivered to the neuronal population of choice followed by immunohistochemical confirmation. Next, the DREADD functionality was assessed *ex vivo* in a series of slice electrophysiology experiments that confirmed the role of both CNO and clozapine as DREADD agonists. These experiments also revealed a paradoxical effect of an inhibitory (Gi-DREADD) and an excitatory (Gq-DREADD) construct in that they both decreased excitatory transmission (**Chapter 2**). Secondly, the functionality of the Gi-DREADD was tested *in vivo* in a short-term working memory and a spatial novelty preference task. Against predictions, results in this chapter showed that hippocampal Gi-DREADD dependent modulation did not alter cognition (**Chapter 3**). Thus, an investigation into the bioavailability of CNO and clozapine was triggered and a reassessment of DREADD functionality using a c-Fos molecular approach. Results provided evidence for back-metabolism of CNO to clozapine and deemed CNO as being poorly brain penetrant. In contrast to results presented in Chapter 2 that showed opposite effects of Gq-DREADD than expected, the c-Fos studies confirmed the functionality of a Gq-DREADD but not of the Gi-DREADD *in vitro* (**Chapter 4**). Lastly, DREADD functionality was assessed *in vivo* by means of ECoG/LFP recordings that showed that decreased power in brain oscillations in the 10-150 Hz range in a Gi-DREADD model has not caused cognitive impairments in a spatial memory task or object exploration (**Chapter 5**). The discussion following summarises the main findings and limitation of each chapter, addresses unanswered questions and suggests potential solutions.

6.1 Chapter 2 summary: DREADDs as tool to manipulate hippocampal function *ex vivo*

Experiments in this chapter were designed to establish the specificity and spread of CaMKIIa driven DREADDs to dorsal hippocampus. Immunohistochemical analysis revealed off-target expression in small numbers of GAD1-positive interneurons in the hilar region of hippocampus and inter-animal variability in the pattern of DREADD expression, with most, but not all, animals showing viral transfection restricted to the injection sites in the CA1 and CA3 subfields, but also the suprapyramidal blade of the DG. The lack of excitatory neuron specificity of the CaMKIIa promoter was somewhat surprising as its specificity has been documented prior (Dittgen et al., 2004; Mayford et al., 1996; White et al., 2011) with only a limited number of studies reporting expression of AAV constructs transfected to interneurons in the mouse (Nathanson et al., 2009; Scheyltjens et al., 2015).

A caveat of the present study was the stereotaxic delivery of the viral constructs that creates variability in itself during the stereotaxic injection. Specifically, using stereotaxic injection, it is likely impossible to ensure that the viral construct targets the same cells across animals in term of spatial location in the brain. Another sources of variability that prevents uniform transduction efficiency across subjects could also be viral diffusion amongst the animals (Atasoy & Sternson, 2018). Additionally, the specificity with which the viral construct is expressed specifically to pyramidal neurons without being transfected to interneurons is also a caveat of DREADDs use but a separate issue.

A way to improve specificity is by using Cre or Flp recombinases in transgenic models. For example, to improve cell specificity and isolating neuronal populations or projections, a dual-viral approach can be used by which AAV-Cre and a Cre-dependent DREADD are delivered to two brain areas such that DREADD expression will be restricted to projections between the

brain regions (Marchant et al., 2015). Cre-dependent DREADD mouse lines have also been developed to address this issue (Alexander et al., 2009; Zhu et al., 2016). Moreover, transgenic hM3Dq mice under the control of activity dependent *Fos* promoter have been used successfully to study context specific patterns of neuronal ensembles (Garner et al., 2012; Yoshii et al*.,* 2017). Specifically, by using this approach the expression of the hM3Dq DREADD is based on neuronal activation of ensembles in a context specific manner. The DREADD expression pattern can be reactivated in a different context by CNO. However, all these manipulations are only available in mice, with only a recently commercially available CaMKIIa-Cre rat. Still, a CaMKIIa-Cre rat would likely not bypass the issue of non-specific transfection of the DREADDs as the issue of the CaMKIIa promoter driving expression in interneurons will remain (Nathanson et al., 2009; Scheyltjens et al., 2015).

Next, electrophysiological experiments confirmed that the DREADD agonist CNO supressed excitatory transmission in the presence of Gi-DREADD, with EGFP-controls showing no effect. Clozapine itself also acted as DREADD agonist in these experiments. Unexpectedly, CNO and clozapine also inhibited excitatory transmission in the presence of Gq-DREADD. The decrease in transmission seen in Gq-DREADD expressing slices was not attributed to transfection of the Gq-DREADD to GAD1-positive neurons. Pharmacological experiments ruled out the involvement of GABA and $mGluR_{2/3}$ receptors.

Clozapine/CNO induced decreased excitatory transmission in Gi-DREADD slice was predicted based on previous reports (Lopez et al., 2016; Robinson et al., 2014; Zhu et al., 2014) showing similar results. Paradoxically, reduced excitatory transmission was also recorded in Gq-DREADD slices in the presence of both clozapine and CNO, contrary to expectations based on an extensive body of literature showing the opposite (Zou et al., 2016; Cordella et al., 2018; Lopez et al., 2016; Sudarov et al., 2018; Alexander et al., 2009).

Interestingly, a recent study published after these experiments were finalised, showed a similar outcome. Specifically, the investigators reported decreased fEPSP slope in hippocampal slices from Gq-DREADD transgenic mice. They suggested this is due to a dose-dependent effect and provided evidence from electrophysiological studies using a low concentration of CNO (1 μM) that showed no effect on fEPSP slope and higher concentrations (5-20 μM) that led to a prolonged decrease in fEPSP (Pati et al., 2019). The onset, magnitude and duration of the effect are consistent with findings reported in this thesis. At single cell level the investigators showed increased amplitude and frequency of spontaneous post synaptic currents after a low concentration CNO (1 μM) and decreased spontaneous activity following higher concentration of CNO (20 μM) (Pati et al., 2019). However, the investigators fail to provide a mechanism for this outcome.

Electrophysiological follow-up experiments presented in this chapter did not establish an underlying mechanism of this paradoxical effect. Single-cell recordings have previously established that CNO activation of Gq-DREADD in pyramidal cells caused depolarisation and elevated firing rate (Alexander et al., 2009). One possibility – albeit unlikely – is that the decreased excitatory response observed is a consequence of network hyperexcitation that could eventually lead to excitotoxicity and neuronal death. As $mGlu_{2/3}$ receptors block glutamate release on autoreceptors, an antagonist of the receptors would cause increased glutamate release. Thus, the enhanced fEPSP decrease observed as consequence of $mGlu_{2/3}$ receptors antagonism in Gq-DREADD slices would support the idea of excitotoxicity caused by excess glutamate as a consequence of CNO-induced Gq-DREADD activation. However, it is noteworthy that there was no evidence of this phenomenon in the slice electrophysiology experiments. Nonetheless, the hypothesis could be tested by reversing the Gq-DREADD induced effect. Mazzone et al., (2018) antagonised CNO binding to a Gq-DREADD targeted to GABA neurons in the bed nucleus stria terminalis using SR141716A, a CB1 antagonist (Mazzone et al., 2018). Finally, CNO might be acting as an inverse agonist of the Gq-

DREADD and thereby reducing constitutive signalling to decrease excitatory transmission or activate the DREADD in a pathway-dependent manner such that the drug is acting through β-arrestin mediated signalling (Rankovic et al., 2016).

6.2 Chapter 3 summary: DREADDs as a tool to manipulate hippocampal function *in vivo.*

DREADD function was tested *in vivo* using two hippocampal dependent short-term memory tasks, a reward alternation T-maze and a spatial novelty preference Y-maze. Surprisingly, there were no detectable impairments in rats expressing a Gi-DREADD in the presence of CNO (3 mg/kg) or clozapine (0.1 mg/kg). Locomotor activity was also unaltered by DREADD expression and agonist treatment.

These results were unexpected with evidence from chemogenetic studies using Gi-DREADDs in the hippocampus showing reduced performance on a spontaneous alternation T-maze in the presence of CNO (Varela et al., 2016), or impaired object-in-place memory but not object recognition (Lopez et al., 2016; Tuscher et al., 2018). One explanation for these contradictory results is likely to be inter-species differences. The studies mentioned above have all used mice, that have smaller hippocampal volume compared to rats, but similar volumes of viral constructs were injected per hemisphere. In addition, impaired excitatory transmission as seen in *Gria1* KO mice is known to cause a deficit in SWM but not SRM and also novelty induced hyperlocomotion (Reisel et al., 2002). Notably, a study published after the completion of the experiments presented in this chapter, used the Gi-DREADD/CNO pairing to reverse novelty induced hyperlocomotion in *Gria*$^{-1-}$ mice, and found no changes in locomotor behaviour in wild type Gi-DREADD expressing mice in the presence of CNO (Aitta-aho et al., 2019). This is in line with results presented in this chapter showing no changes in locomotor activity in Gi-DREADD expressing rats. Data from the same group also suggested that increased

glutamatergic transmission underlies the hyperlocomotion seen in *Gria*$^{-1-}$ mice (Maksimovic et al., 2014), which would explain the lack of changes in locomotor activity observed in the current study, where glutamatergic transmission was decreased by means of DREADD activation. Thus, there is a possibility that *in vivo* effects of Gi-DREADD activation in the model presented in this thesis are dependent on a prior state of increased neuronal activity. In support of this, recent reports have found that Gi-DREADD activation reduced epileptiform activity (Avaliani et al., 2016; Zhou et al., 2019).

The lack of cognitive deficits presented in this chapter is unlikely to be a consequence of CNO inability to silence pyramidal neurons as findings from experiments in Chapter 2 showed. One potential explanation could be insufficient spread and expression of the viral construct in pyramidal neurons. This could be improved by increasing the number of viral injection sites to maximise the viral expression. However, this imposes risks for animal wellbeing, such as increased surgery time and non-specific trauma or elevated risk of infection. It would be interesting to investigate the effects on cognitive behaviour of a combination of a CaMKIIa driven Gi-DREADD and an hDlx driven Gq-DREADD (targeted to interneurons). The previous chapter showed decreased fEPSP slopes in slices expressing each of these constructs in the presence of CNO. Thus, by using a combination of the constructs there could be a synergistic effect on excitatory transmission.

Finally, there is the possibility that the CNO dose used in this study (3 mg/kg) was insufficient for the DREADD activator (clozapine or CNO) to reach the brain, as suggested by the literature (Gomez et al., 2017; MacLaren et al., 2016, Raper et al., 2017). This issue was explored and discussed in more depth in Chapters 4 and 5.

6.3 Chapter 4 summary: CNO and clozapine bioavailability in relation to DREADD function

Experiments in this chapter re-assessed DREADD function using c-Fos as a marker of neuronal activity. Secondly, the literature around CNO bioavailability was challenged and re-evaluated in the rat. Results showed no changes in novelty induced c-Fos hippocampal expression in Gi-DREADD expressing rats in the presence of CNO (3 mg/kg or 10 mg/kg) or clozapine (0.5 mg/kg). There was a significant increase in c-Fos in Gq-DREADD expressing rats upon CNO (10 mg/kg) administration. In addition, the exposure study confirmed predictions about CNO being poorly brain penetrant and back-metabolism to clozapine in brain and plasma.

The lack of differences in the numbers of novelty induced c-Fos positive cells between the Gi-DREADD group and control group was again unexpected. Similar to the experiment in this chapter, Marchant et al., (2015) used novel context exposure to increase c-Fos activity. This was then decreased by SalB binding to a Gi-coupled kappa-opioid receptor DREADDD (KORD). Other studies have confirmed the ability of Gi-DREADDs to reduce the number of c-Fos positive cells that had been either elevated pharmacologically (Koike et al., 2016) or by making use of the circadian rhythms of the animals to activate c-Fos expression (Sasaki et al., 2011). In relation to data presented thus far, the current findings are in line with results presented in Chapter 3 but go against expectations on the basis of electrophysiological results in Chapter 2. Specifically, the Gi-DREADD functionality was validated in a slice electrophysiology model but this was not translated *in vivo* or explained at the level of c-Fos expression. Taken together, these data suggest that *in vivo* compensatory mechanisms could be potentially responsible for rectifying impairments that are only produced in an isolated network slice model, without being translated to the level of the organism. However, assuming this is true, the same compensatory mechanisms are not present in hippocampal lesions.

Specifically, rats with hippocampal lesions are able to perform as well as controls in a water maze after over-training, however the deficit is still present when they are tested on new tasks, suggesting the presence of different psychological processes used to solve the tasks instead of compensatory mechanisms (Morris et al., 1990).

The use of c-Fos as an indicator of Gq-DREADD activation is a tool that has been used reliably. For example, CNO injection (3 mg/kg) was reported to increase c-Fos numbers in Gq-DREADD expressing BLA rat neurons (Sengupta et al., 2016), and both Gq-DREADD expressing and neighbouring non-DREADD expressing cells of the rat dorsomedial PFC (Yau & McNally, 2015). Similarly, CNO eye-drops were used to induce c-Fos expression in the mouse hippocampus in the presence of Gq-DREADD (Keenan et al., 2017). These reports are in line with findings in the current study where CNO-induced activation of a Gq-DREADD resulted in increased c-Fos expression. It is noteworthy that despite similar decreased excitatory transmission in a slice electrophysiology model of a Gi and Gq-DREADD, rats belonging to the two groups show opposing c-Fos activity patterns in the presence of CNO. This might indicate that in the case of Gq-DREADD, the increased neuronal activation (marked by elevated c-Fos) precedes the long lasting decreased excitatory transmission observed in slices. However, the mechanism by which this could happen is not clear yet. Moreover, it is difficult to compare synaptic changes in an isolated system to changes at the level of the entire organism.

Next, the bioavailability of CNO and clozapine was assessed in brain and plasma. The findings were aligned with the literature, as discussed in Chapter 4 (Jendrkya et al., 2019, Manvich et al., 2018, Thompson et al., 2018, Gomez et al., 2017, MacLaren et al., 2016, Raper et al., 2017) and made a few important observations. Firstly, very low levels of CNO were found in the brain post CNO (3 and 10 mg/kg) injection. Secondly, there was evidence of back

metabolism of CNO to clozapine both in the brain and plasma. Lastly, clozapine concentration found in the brain post CNO (10 mg/kg) and clozapine (0.5 mg/kg) administration, was comparable to the concentration of clozapine that decreased excitatory transmission in the slice electrophysiology studies. These findings suggest that the lower CNO dose (3 mg/kg) used in the behavioural experiments might have been insufficient to reach the brain in the form of CNO or clozapine, despite other reports that have successfully used the same dose (Sengupta et al., 2016; Yau & McNally, 2015; Ferguson et al., 2011).

Finally, future studies are required to evaluate the levels of unbound CNO/clozapine in the brain and investigate where the CNO back-metabolism takes place in order to better describe the properties of CNO as DREADD agonist. In addition, in would be interesting to explore the role of Compound 21 as DREADD activator (Thompson et al., 2018, Jendryka et al., 2019).

6.4 Chapter 5 summary: DREADDs as a tool to study cortical mechanisms of cognition

Experiments in this chapter aimed to interrogate whether Gi or Gq-DREADD dependent manipulation of excitatory transmission in the dorsal hippocampus impacted LFP changes recorded from the dorsal hippocampus and mPFC, and whether this would ultimately modulate cognition.

The first rsECoG/LFP study did not provide conclusive evidence regarding the function of the Gi-DREADD, but it helped to improve the experimental design of the second study and pointed towards decreased gamma power in Gi-DREADD rats in the presence of CNO. Findings from the second study showed no changes in the theta power in any of the DREADD groups in response to CNO (10 mg/kg) injection. Gamma power was decreased in the presence of a Gi-

DREADD in the dorsal hippocampus upon CNO administration. Furthermore, CNO binding to Gi-DREADD decreased power in beta and higher frequencies up to 150 Hz in the dorsal hippocampus. No significant changes were recorded in the presence of a Gq-DREADD. However, two of the Gq-DREADD expressing rats developed seizures which could be a direct indicator of Gq-DREADD function *in vivo*. Finally, despite decreased power in a number of frequency bands, Gi-DREADD rats showed normal spatial memory and object exploration.

The mechanisms by which Gi-DREADD decreased gamma power indicate towards a pyramidal-interneuron network gamma (PING) model (**Figure 6.1**). Specifically, pyramidal neurons modulate the activity of interneurons through feedback excitation of interneurons. The interplay between the pyramidal-interneuron network will subsequently give rise to oscillations in the gamma range (Whittington et al., 2000). Integration of information in neuronal networks is thought to be a result of synchronised neuronal assemblies that in the case of PING are orchestrated by interneurons (Craig & McBain, 2016). Based on this scenario, disrupting pyramidal mediated transmission by Gi-DREADD activation would subsequently disrupt generation of gamma oscillations. Additionally, decreased gamma (and beta) power in the hippocampus of Gi-DREADD rats was expected to translate into cognitive impairments. In contrast, the results showed normal spatial memory on a Y-maze and similar patterns of object exploration compared to the control group.

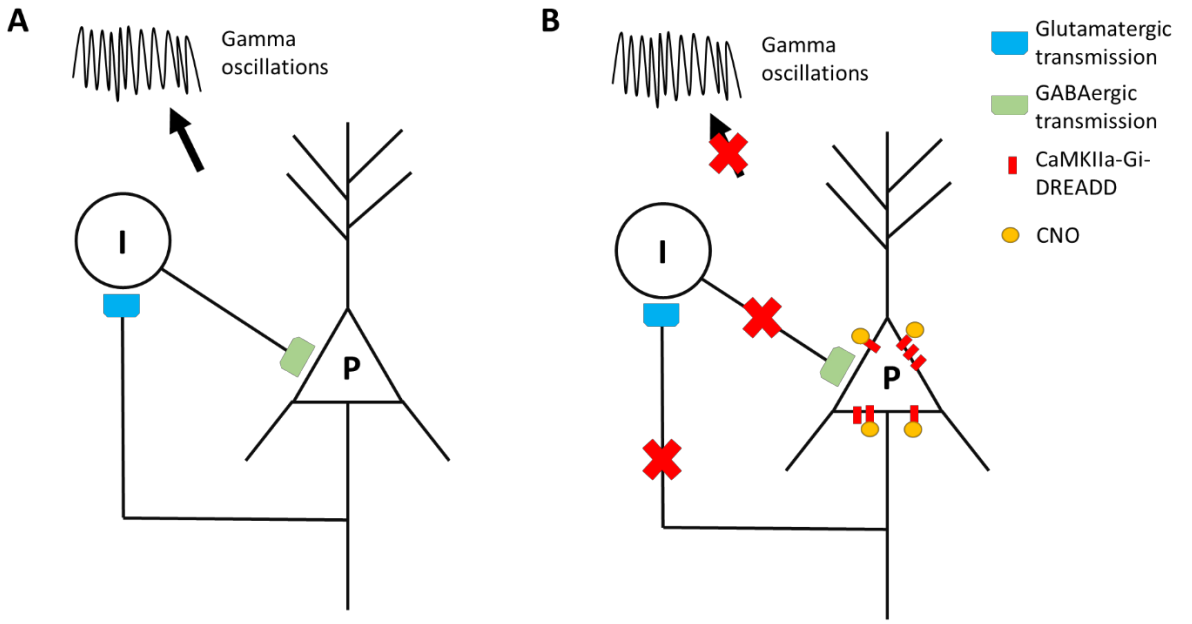


Figure 6.1: Pyramidal-interneuron network gamma (PING) model

(A) Gamma oscillations arise as a result of pyramidal (P) interneuron (I) interplay. Pyramidal cells will excite (blue) interneurons that in turn will regulate glutamatergic activity by perisomatic inhibition (green) of the pyramidal neuron (Buzsaki & Wang, 2012; Mann et al., 2005). (B) Assuming Gi-DREADDs (red rectangle) are expressed on the pyramidal neuron, upon CNO (yellow) binding to the mutated receptors, glutamatergic transmission onto the interneuron will be blocked which in turn will supress the perisomatic inhibition onto the pyramidal neuron and subsequently decrease gamma power.

Data presented in this chapter, contributes to the understanding of the underlying mechanism of Gi-DREADD induced pyramidal neuron silencing in the hippocampus. Specifically, the results suggest that excitatory activity in the hippocampus is essential for generation of brain oscillations in the beta and gamma range and this effect is dependent on the interplay within the pyramidal-interneuron network. One caveat of the current study is that one cannot exclude the possibility that the off-target expression of the DREADDs in interneurons may have contributed to this outcome. However, modulation of brain oscillations was not associated with locomotor or cognitive changes. Thus, it would be interesting to assess changes not only at the level of the LFP in the hippocampus but also for example in the mPFC while the animal subjects are performing a hippocampal-dependent task, as evidence from rodent studies showed increased hippocampal-prefrontal coherence and synchrony during a working memory task (Sigurdsson et al., 2010).

6.5 DREADD limitations

Despite their indisputable versatility, the use of DREADDs comes with limitations that users should consider when designing experiments that utilise these tools. Firstly, there are temporal limitations associated with the use of DREADDs. In contrast to optogenetics that have millisecond temporal resolution, DREADD activation is dependent on the time it takes the agonist to reach the brain and bind to the receptors which is in the range of tens of minutes after systemic injection for CNO. Indeed, the exposure study presented in Chapter 4 shows that CNO and clozapine peak in the brain 30 min post injection, with very little clozapine still being found in the brain and no CNO, 4h after higher dose of CNO injection. In addition, evidence from the LFP study in Chapter 5 shows that the effects on brain oscillations were still present 2h later. This is in line with findings showing increased gamma power in Gq-DREADD expressing mice 9h after two different doses of CNO (Alexander et al., 2009). This suggests that the prolonged physiological effects are not due to continuous activation of the DREADD by CNO but could be attributed to downstream changes in the signalling machinery (Alexander et al., 2009). Considering that effects of DREADD activation by different doses of CNO last beyond the window in which the agonist is present in the brain, suggests the inability to control the amount of 'stimulation' or 'inhibition' by simply altering the CNO dose. In addition, this also indicates that physiological changes caused by DREADD/CNO binding cannot be stopped once the activation was initiated. As a result, based on the local signalling machinery of each cell, DREADD effects are likely to be brain-area specific, and require pilot studies to assess the level of expression needed to elicit certain behaviours (Urban & Roth, 2015).

Moreover, there is the possibility that DREADD use is more versatile in mice compared to rats. This argument is twofold. Firstly, as mentioned above, the mouse brain is anatomically smaller than the rat brain. Thus, by using the same volume of viral construct, and same number of injection sites, a bigger region would be transfected in the mouse brain compared to rat and

subsequently a higher number of cells with express the constructs. Indeed, mouse studies reported hippocampal deficits in mice expressing Gi-DREADD in the hippocampus after injection of the same volume of viral construct as used in this thesis (Varela et al., 2016, Tuscher et al., 2018, Lopez, et al., 2016). Secondly, transgenic mouse lines are commonly used in neuroscience research. This enables more cell specific targeting of DREADDs by using Cre recombinase systems. For example, Urban et al., (2016) injected a cre-dependent DREADD in the dorsal raphe nucleus of transgenic mice expressing cre in serotonergic cells (Slc6a4-Cre mice, Gong et al., 2007). This enabled a specific manipulation of the raphe serotonergic neuronal population by CNO administration (Urban et al., 2016). Additionally, transgenic mice expressing DREADDs under the control of various promoters have been designed (Alexander et al., 2009; Zhu et al., 2016), which renders DREADDs even less invasive, eliminating the need for stereotaxic injection of the construct. While mouse models are commonly used in neuroscience because of their genetic manipulation potential, rats are thought to be better models for neuropharmacological research because of their different cognitive traits such as being faster learners in water (Whishaw & Tomie, 1996), being more social but also more impulsive than mice (Ellenbroek & Youn, 2016). Thus, in relation to DREADD use, mice could provide an excellent framework for investigating basic brain circuity while rats could prove to be better models for neuropharmacological, behavioural or drug screening studies.

Another important consideration is the type of cell the DREADDs are expressed in. Specifically, DREADDs can lead to different outcomes based on the number or types of receptors expressed by the targeted cells. CNO induced activation of the DREADD could lead to direct silencing/activation of these receptors or indirectly modulate downstream events as a consequence of DREADD activation (Smith et al., 2016). For example, Gi-DREADD-induced silencing is thought to be mediated by activation of GIRKs, the levels of GIRK expression is cell-type specific, which could lead to different effects based on the type of cell and brain area

in which the DREADDs are expressed (Rogan & Roth, 2011). Thus, different responses mediated by the same DREADD are dependent on the signalling machinery of each cell (Smith et al., 2016).

As seen in Chapter 2 and discussed above, there is an inter-animal variability of expression that is associated with the stereotaxic injection of DREADDs, but also the extent to which the constructs are expressed in a neuronal population will be sub-maximal. This can lead to changes in non-DREADD expressing neighbouring cells as shown by Vazey and Aston-Jones (2014). The investigators reported decreased discharge rate in non-DREADD cells as a consequence of Gq-DREADD activation of locus coeruleus norepinephrine cells in the presence of CNO (Vazey and Aston-Jones, 2014). Lastly, the use of inhibitory DREADDs should not be regarded as equivalent to lesions of the hippocampus. DREADDs will not abolish the hippocampal function, rather they will dampen down neuronal activity, as seen in the slice experiments presented in Chapter 2, where CNO/clozapine induced activation of the Gi-DREADD caused a 30-50% decrease in fEPSP slope from baseline.

Finally, the use of CNO as DREADD agonist is an important consideration before undertaking experiments. As shown in this thesis and reported by others (Gomez et al., 2017; MacLaren et al., 2016; Raper et al., 2017; Jendryka et al., 2019) CNO is reverse-metabolised to clozapine and is poorly brain penetrant. However, clozapine itself is not inert, and was shown to have different affinities at low doses as discussed in Chapter 3. Despite these recent reports, CNO cannot be deemed unsuitable in studies using DREADDs as evidence from the hundreds of scientific studies that have successfully used CNO as DREADD activator. More importantly, future studies should control for both DREADD agonist and DREADD expression itself by using vehicle controls and control viral vectors, in order to avoid misinterpretation of the data. Experiments in this thesis did not find non-DREADD effects of CNO at two doses widely used

in the literature (3 and 10 mg/kg). Still, to bypass this caveat, CNO intracerebral micro-infusions are an option. While delivery of DREADD agonists through micro-infusions would also provide greater specificity in terms of the desired target for DREADD manipulations, cannulations would make the approach more invasive, whereas the less invasive nature of DREADD activation is one of the main advantages of using DREADDs. Lastly, alternative agonists, such as perlapine and Compound 21 have been developed and present a promising pharmacokinetic (Chen et al., 2015; Thompson et al., 2018) and pharmacodynamic profile (Jendryka et al., 2019).

Nevertheless, DREADDs have been used successfully in many studies and their benefits in neuroscience research are beyond question. With thorough experimental design and appropriate controls, they can be useful tools in deconstructing a variety of behaviours.

6.6 Unanswered questions

Despite attempts to contribute to understanding of hippocampal function with the help of DREADDs, a number of questions remain unanswered. One of the main themes arising from this thesis concerns the mechanisms underlying the lack of behavioural effects observed throughout despite direct evidence of Gi-DREADD function *ex vivo* and *in vivo.* A few factors can contribute to this phenotype. Firstly, it is possible that compensatory mechanisms in extra-hippocampal areas (i.e. mPFC) are involved, although these are not recruited after hippocampal lesions for example (Morris et al., 1990). Secondly, considering that the dorsal hippocampus is anatomically large, complete targeting might be needed in order to observe changes at the behavioural level. Lastly, behavioural outcomes might be confounded if the CNO dose is sub-optimal. The answer is likely to be a combination of the above, by which silencing a limited population of pyramidal neurons in the dorsal hippocampus is not enough to cause cognitive deficits.

On the basis of immunohistological analysis presented in Chapter 2 and observations made during post-hoc confirmation of DREADD expression, the viral constructs spread 0.5 mm anterior and posterior from the injection site on the AP axis. Considering the dorsal hippocampus starts at AP: -1.8 mm posterior from bregma and the ventral hippocampus ends at AP: -7.3 mm from bregma in the Lister hooded rat (Moser et al., 1995), DREADD expression over 1 mm of the dorsal hippocampus would account for approximately 18% of the total volume of the hippocampus. Assuming that 18% of the hippocampal volume was inhibited by Gi-DREADD/CNO pairing (that assumes a high enough CNO dose as well), entails transfection was successful at both injection sites, CA1 and CA3 but also the DG that was not a direct site of injection. As discussed in Chapter 2, this pattern of expression was observed in the majority of animals. Moser and colleagues showed that as little as 26% of spared hippocampal tissue located at the dorsal pole is needed for intact spatial learning, and that dorsal hippocampus lesions of 40% of the total volume of the hippocampus are required to cause a spatial learning deficit (Moser et al., 1995). This suggests that in the current study, an inhibition of 18% of the total hippocampal volume restricted to mainly pyramidal cells in the dorsal hippocampus might not be enough to cause cognitive deficits.

Future studies could address this by increasing the number of viral delivery injection sites along the AP axis to ensure wider viral spread. In addition, to eliminate the possibility of CNO not reaching the brain to bind to DREADDs, CNO intracranial micro-infusions could be used as described by other studies (Shipman et al., 2019; Stachniak et al., 2014) and could draw comparisons between CNO systemic administration and CNO micro-infusion in the context of behavioural studies. Finally, to test whether the pyramidal neuron manipulation has a subtler role in hippocampal dependent tasks, the difficulty of these tasks could be addressed by increasing the ITI or memory load.

Next, it remains unclear whether the changes seen in brain oscillations are a direct effect of pyramidal neuronal silencing and reduced drive onto inhibitory interneurons or an indirect effect as a consequence of perturbations of other cells. In addition, it is unknown what the implications of changes in gamma power are, as no cognitive deficits were observed. The lack of spatial or short-term working memory impairments reported in this thesis is somewhat surprising considering the decreased gamma power reported by the LFP study. These results are in contrast to a previous report where investigators found increased hippocampal gamma power and CA3-CA1 coherence on a delayed spatial alternation modified circular version of a T-maze, at the T junction of the arms, where the rat had to make a decision to turn right or left. The report suggests gamma oscillations as a physiological mechanism by which CA3 and CA1 communicate to support memory retrieval (Montgomery & Buzsaki, 2007). On the basis of evidence from this study, suppression of excitatory transmission in the dorsal hippocampus resulting in decreased gamma power should in turn lead to spatial memory deficits. However, just because changes in electrical activity were correlated with changes in behaviour it does not mean that the electrophysiological profile is causally necessary for decreased performance on a behavioural task. Furthermore, it is important to note that while by using a Gi-DREADD and the behavioural tasks described in this thesis, there was no detectable memory impairment, it does not mean that a hippocampal deficit – that could be detected by using a different task – is not present. For example, as seen from post-hoc histological viral expression validation, in the current study the constructs were also transfected to the principal layer of the DG. Thus, future studies could test this model in a DG-dependent task, such as active place avoidance, that was reported to be sensitive to optogenetic manipulations of granule cells of dorsal DG (Kheirbek et al., 2013; van Dijk & Fenton, 2018).

In the current study, LFP recordings were not made while the animals were performing a task. Therefore, it would be interesting to record simultaneously from the dorsal hippocampus and mPFC - that is also known to be involved in working memory (Miller & Cohen, 2001) - of rats

expressing a hippocampal Gi-DREADD in the presence of CNO during testing on a hippocampal-dependent task, to assess whether the mPFC compensates for the decrease in gamma power and subsequently rectifies deficits. Additionally, future studies could investigate connections between mPFC and dorsal hippocampus by using a double DREADD approach. Specifically, two different inhibitory DREADDs (Gi-coupled kappa opioid receptor DREADD and hM4Di-DREADD) (Vardy et al., 2015), activated by two different ligands (SalB and CNO, respectively) could be expressed at the same time in the two distinct brain regions. Agonists of the DREADDs could inhibit each brain region individually or concomitantly and study the inter-play between the two areas during behaviour.

6.7 Conclusions

The current study employed a variety of techniques to enable the characterisation of chemogenetic tools in the hippocampus in relation to cognition. Some interesting paradoxes were reported. Specifically, expression of an inhibitory DREADD in pyramidal neurons of the dorsal hippocampus decreased excitatory transmission *ex vivo* in slices in the presence of CNO. *In vivo*, the agonist binding caused decreased power in the 10-150 Hz brain oscillation range as recorded by hippocampal LFP. However, these network changes did not translate into spatial, short-term working memory, object exploration or locomotor activity changes. Similarly, Gi-DREADD did not decrease novelty induced c-Fos activity. Expression of an excitatory DREADD in pyramidal neurons of the dorsal hippocampus also decreased excitatory transmission *ex vivo* in slices in the presence of CNO. *In vivo*, the agonist binding did not cause any statistically significant changes in the hippocampal LFP but there was an indication towards increased gamma power. Moreover, two rats showed epileptiform activity in the form of wet dog shakes which serves as a direct indicator of Gq-DREADD function. Additionally, CNO injection increased neuronal activity as measured by c-Fos in the hippocampus of Gq-DREADD expressing rats.

At the time some of the experiments were undertaken, they were the first ones to report on a couple of critical issues associated with DREADD use. Specifically, once the pharmacological inertness of CNO was brought into question (Gomez et al., 2017), the exposure study presented in Chapter 4 was the first one to assess the clozapine levels in the rat brain after CNO and clozapine injection. Aditionally, the decrease in excitatory transmission in the presence of CNO and clozapine in Gq-DREADD expressing slices in *ex vivo* electrophysiology experiments presented in Chapter 2 has not been reported until after experiments in this thesis were ended and is yet to be shown in rat slices. Finally, and perhaps most importantly, the experiments described in this thesis used the rat as a model instead of the mouse, which is more commonly used in DREADD literature. While this decision proved to be more challenging because of the fewer studies reported in the literature, using DREADDs in a rat model could serve as a better neuropharmacological research tool than the mouse.

To summarise, the data presented in this thesis demonstrate DREADD functionality in the rat hippocampus. However, the findings highlight the difficulties in using chemogenetics in such a complex and large brain region and emphasise the potential brain-area specific differences in outcomes when using chemogenetics.

Chapter 7

Appendix

7.1 Histology (LFP/ECoG Study I)

Exclusions were made based on histological validation of electrode placement and confirmation of viral expression. In this study, data from two dorsal hippocampal electrodes from Gi-DREADD rats were excluded due to one electrode not being found and no viral expression around the electrode that was placed too anterior for the second exclusion. One electrode from an EGFP rat was excluded as it was placed too anterior.

Figures **7.1 and 7.2** show the exact electrode positioning and viral spread around the area of the electrode in each rat from the study. The images indicate the depth electrode was positioned in or above the CA3 region in the dorsal hippocampus in most animals, with only a few electrodes being placed more anterior. In terms of viral expression, the EGFP construct was transfected around the injection sites in the CA1 and CA3 area but also the suprapyramidal blade of the DG. The Gi-DREADD showed good expression in the CA1, CA3 and suprapyramidal blade of the DG in 4 out of 7 rats, while the remainder 3 rats showed expression mostly restricted to the CA1 region.

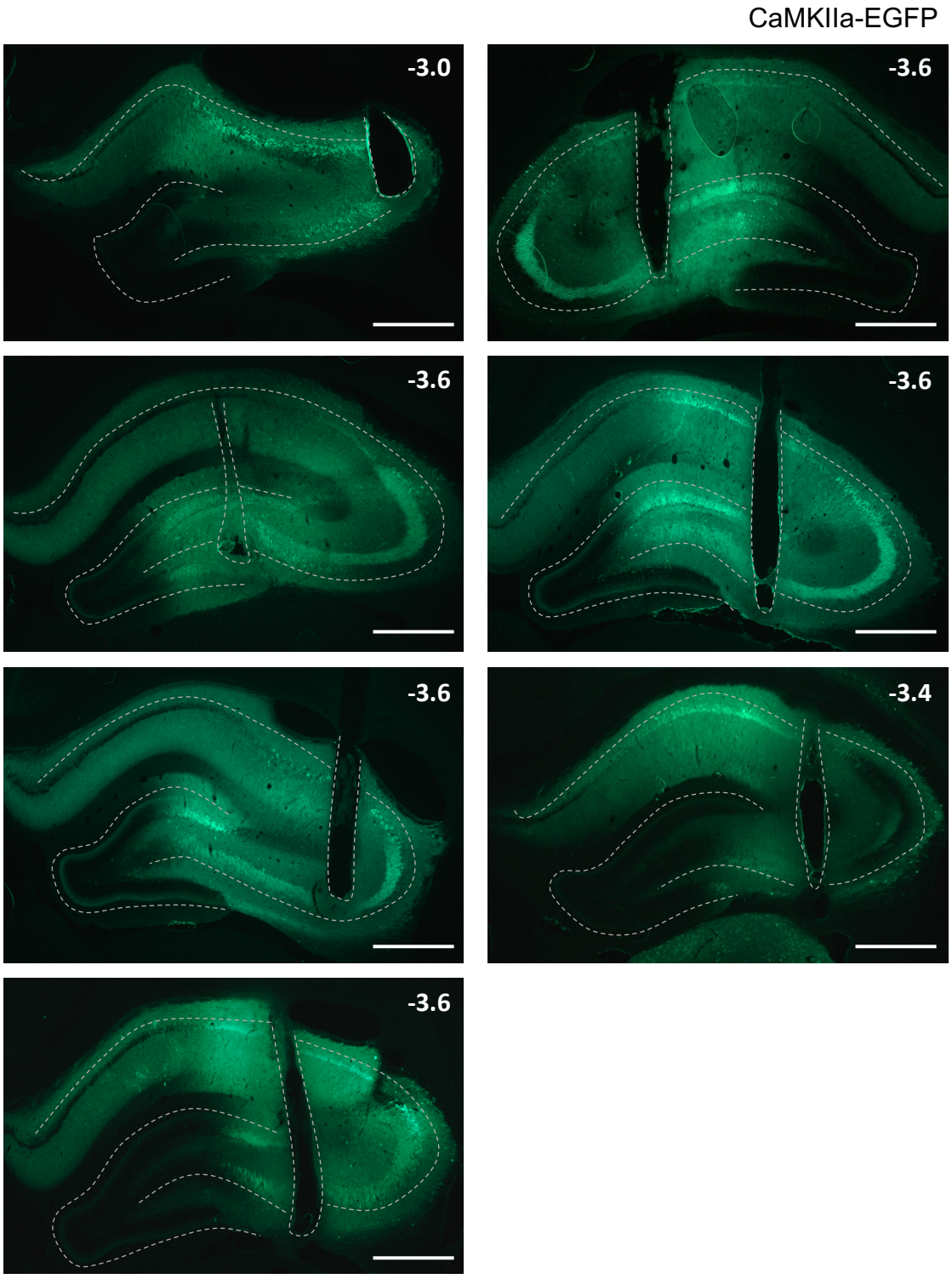


Figure 7.1: Electrode placement confirmation and EGFP-control expression validation

Epifluorescent images showing the expression of the EGFP tagged control construct (green) in the area surrounding the recording electrode from all the rats in the LFP/ECoG Study I. Outside of pyramidal layer is outlined by white dotted line. Electrode positioning is highlighted by the white dotted line. Each image represents a different rat. Numbers represent approximate AP coordinates. Scale bar = 500 µm.

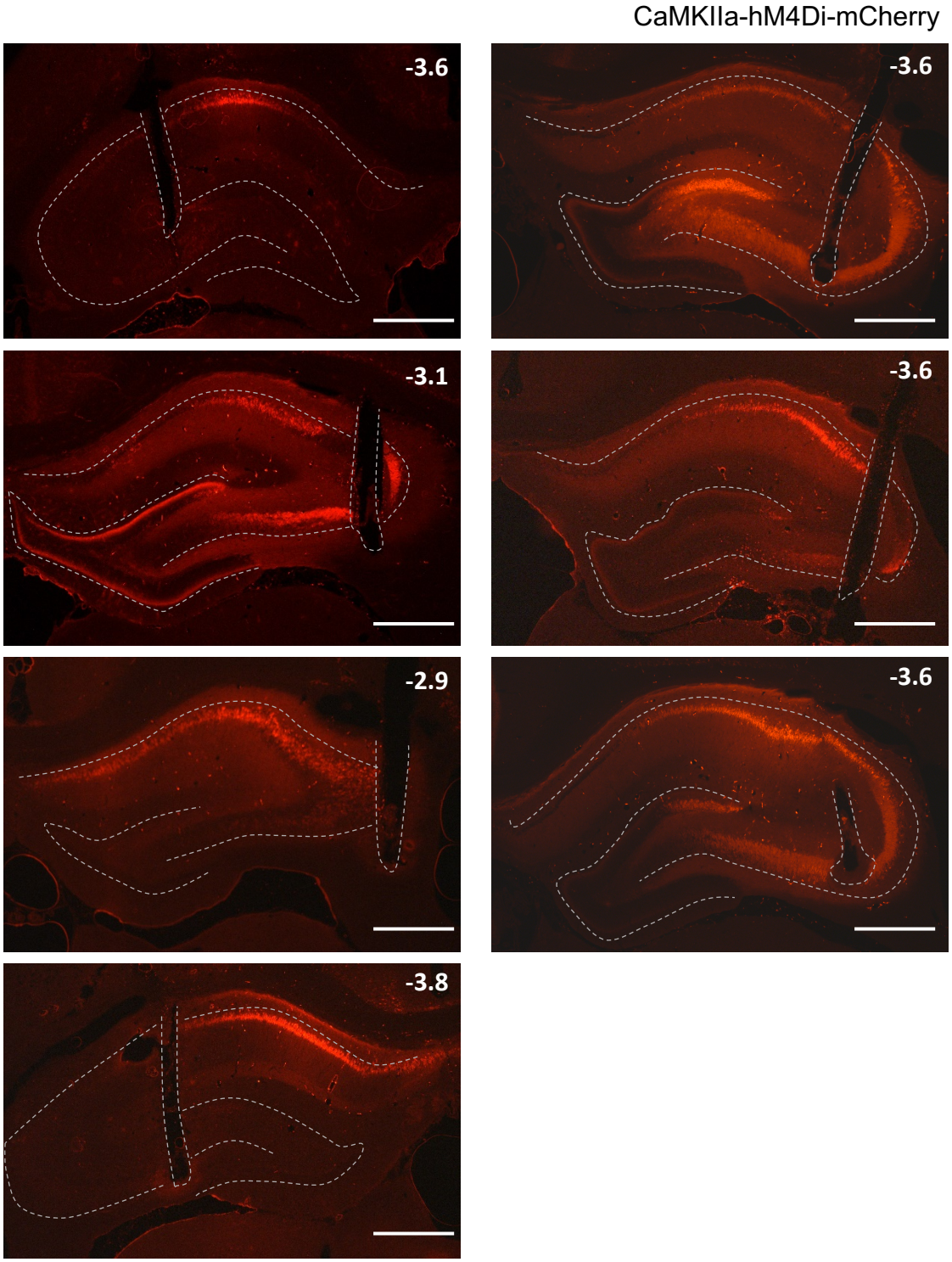


Figure 7.2: Electrode placement confirmation and Gi-DREADD expression validation

Epifluorescent images showing the expression of the mCherry tagged Gi-DREADD construct (red) in the area surrounding the recording electrode from all the rats in the LFP/ECoG Study I. Outside of pyramidal layer is outlined by white dotted line. Electrode positioning is highlighted by the white dotted line. Each image represents a different rat. Numbers represent approximate AP coordinates. Scale bar = 500 µm.

7.2 Resting state ECoG profile of rats expressing an inhibitory or excitatory DREADD in the dorsal hippocampus – study II

ECoG data recorded from a screw placed above the dorsal hippocampus during the second LFP/ECoG study are presented in Figures **7.3-7.5**. Statistical data can be found in Table **7.1**. Band power separation was done as described earlier: theta (4-10 Hz), beta (10-30 Hz), low gamma (30-50 Hz), high gamma (50-90 Hz) and high frequency oscillations (HFO, 90-150 Hz).

Overall there were no marked differences between saline or CNO (10 mg/kg) treatment amongst the three groups. There was a significant effect of time on the high gamma power in the Gi-DREADD group ($F(10, 198) = 1.95$, $P = 0.041$), which indicated that high gamma power was decreased over time. Additionally, as revealed by a Tukey's post hoc test and shown in **Figure 7.3**, there was a significant decrease in low gamma power in the Gi-DREADD group at specific time-points. There was also an indication of increased power in the 1-4 Hz range in EGFP-control group in the presence of CNO, as shown in **Figure 7.5B.**

Next, ECoG data recorded from a screw placed above the mPFC during the second LFP/ECoG study are presented in Figures **7.6-7.8**. Statistical data can be found in Table **7.2**.

Again, no statistically significant changes in ECoG signal were recorded from the mPFC screw in any of the three groups regardless of treatment, with the exception of a significant increase in the theta band in the presence of CNO in the Gi-DREADD group as revealed by an ANOVA analysis ($F(1, 198) = 4.05$, $P = 0.045$). Taken together these data suggest that the presence of an excitatory or inhibitory DREADD in the dorsal hippocampus does not impact on electrical activity – as recorded by an ECoG screw – in the mPFC.

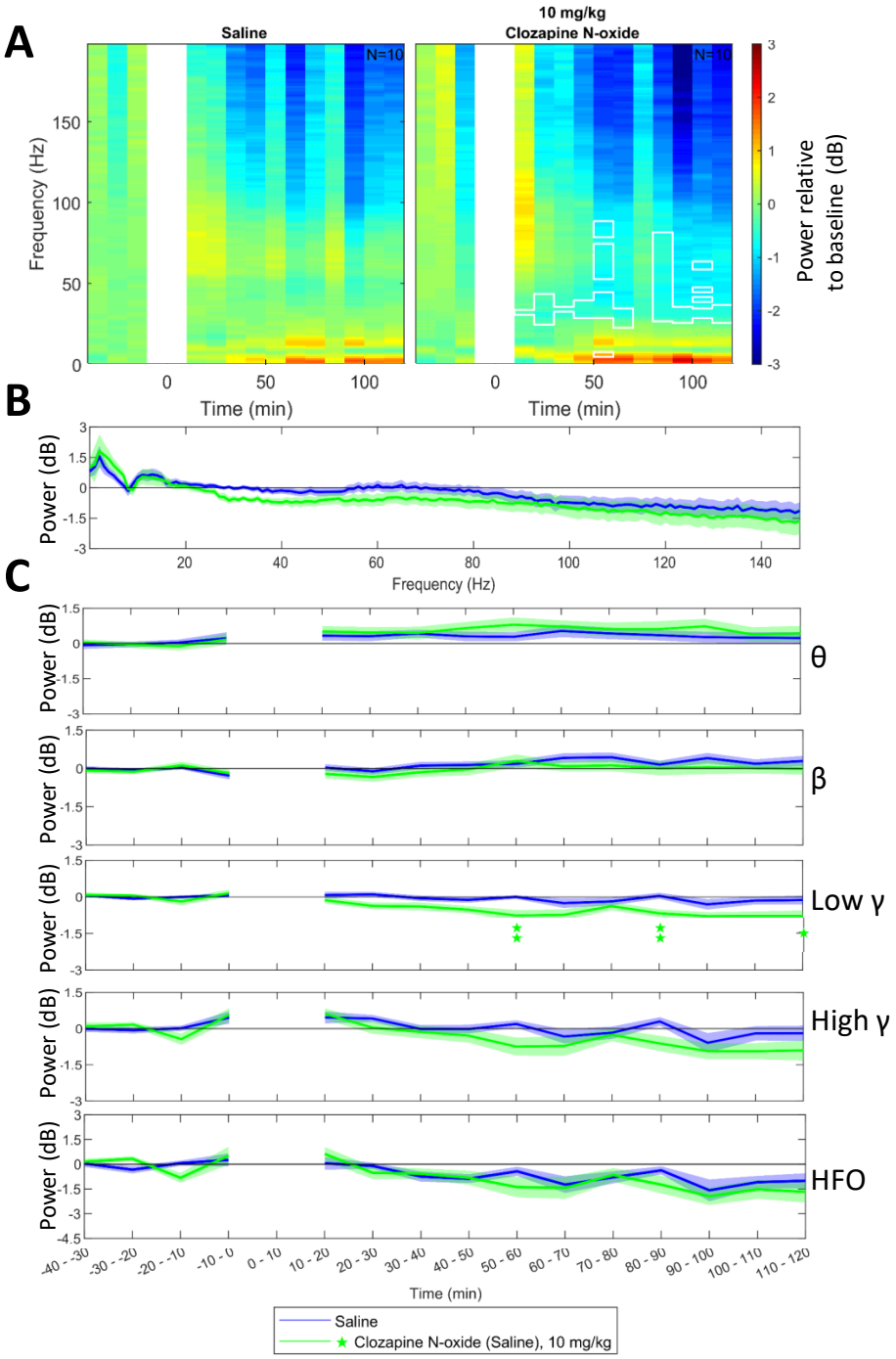


Figure 7.3: ECoG profile of dorsal hippocampus Gi-DREADD expressing rats.

(A) Baseline normalised spectrogram of ECoG signal recorded over 2h post injection from a screw placed above the dorsal hippocampus of rats expressing a Gi-DREADD after saline (left) or CNO (10 mg/kg) treatment (right). Area within the white line represents statistical significance compared to saline treatment at pixel level. Time point of 0 represents time of injection. (B) Power of brain oscillations (up to 150 Hz) over the 30-120 min post injection time interval. (C) Band power separation (from top to bottom) for theta, beta, low and high gamma and high frequency oscillations (HFO) over 2h recording illustrated in 10-min time bins. Missing data represents time of injection (T0). All data are shown as mean ± SEM values from n=10 rats and are baseline normalised. *P<0.05, **P<0.01, fit of a generalised linear mixed effect model and multiple comparison tests with Tukey's honest significance difference.

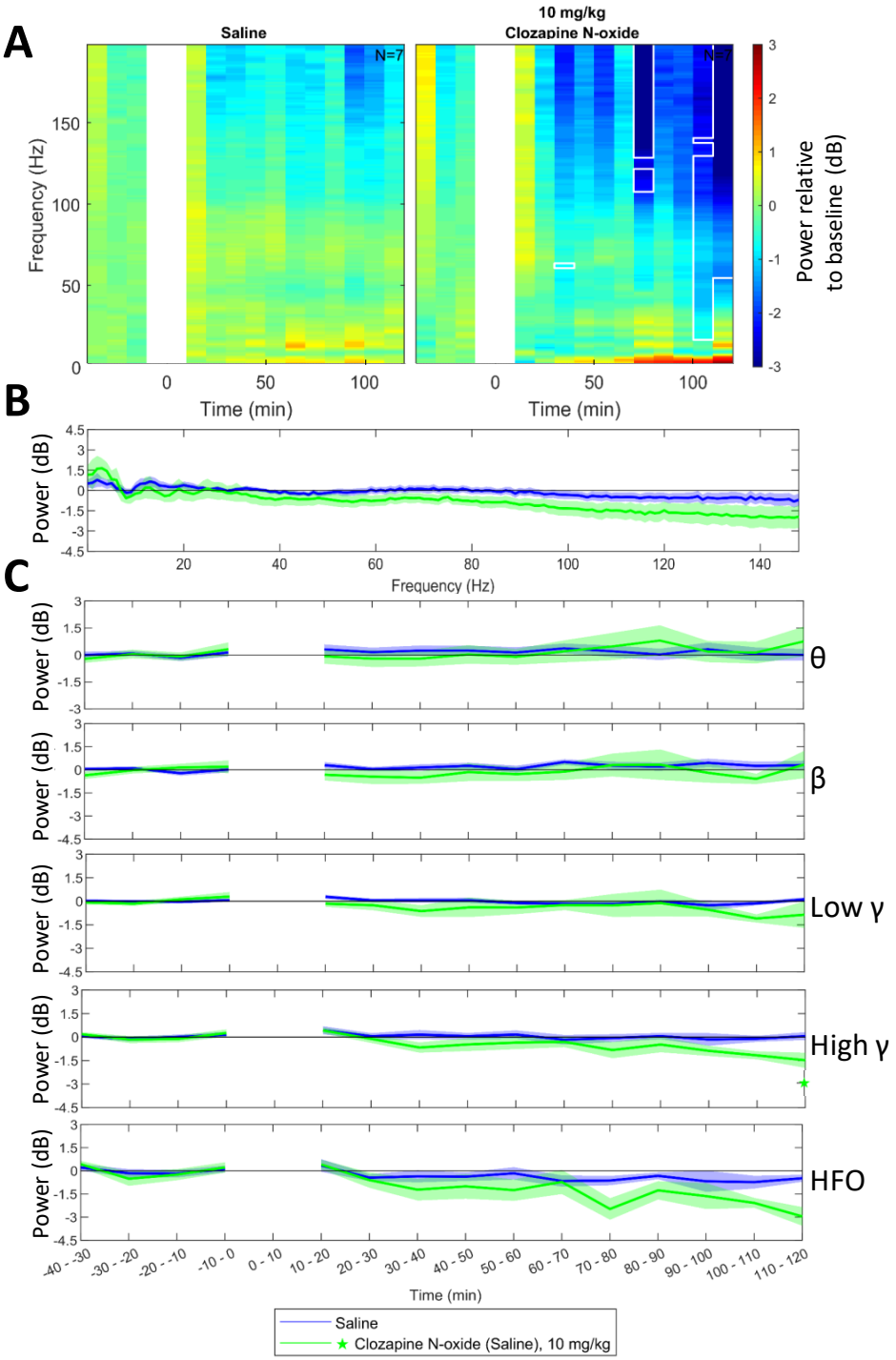


Figure 7.4: ECoG profile of dorsal hippocampus Gq-DREADD expressing rats.

(A) Baseline normalised spectrogram of ECoG signal recorded over 2h post injection from a screw placed above the dorsal hippocampus of rats expressing a Gq-DREADD after saline (left) or CNO (10 mg/kg) treatment (right). Area within the white line represents statistical significance compared to saline treatment at pixel level. Time point of 0 represents time of injection. (B) Power of brain oscillations (up to 150 Hz) over the 30-120 min post injection time interval. (C) Band power separation (from top to bottom) for theta, beta, low and high gamma and high frequency oscillations (HFO) over 2h recording illustrated in 10-min time bins. Missing data represents time of injection (T0). All data are shown as mean ± SEM values from n=7 rats and are baseline normalised. *P<0.05, fit of a generalised linear mixed effect model and multiple comparison tests with Tukey's honest significance difference.

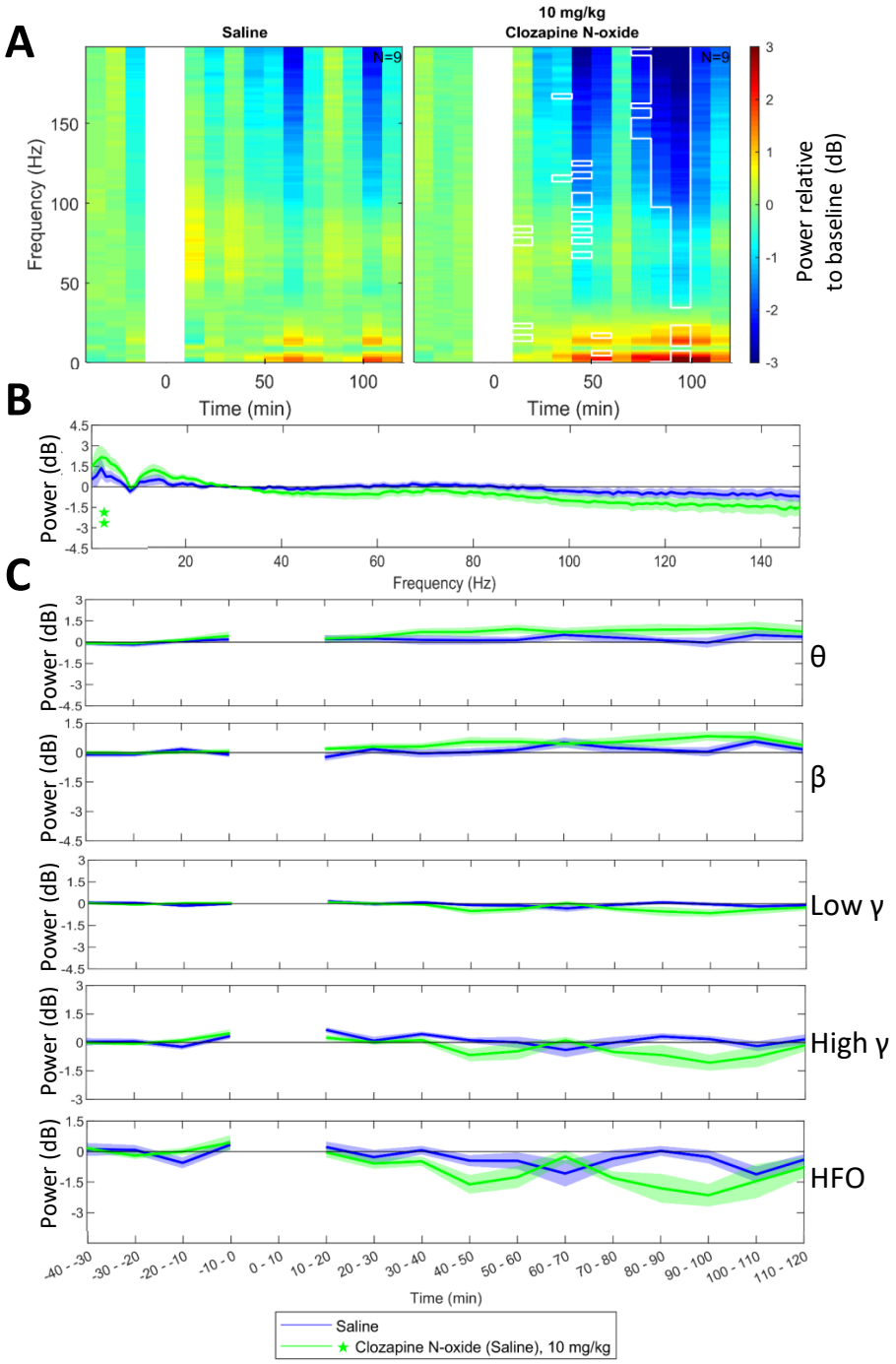


Figure 7.5: ECoG profile of dorsal hippocampus EGFP-control rats.

(A) Baseline normalised spectrogram of ECoG signal recorded over 2h post injection from a screw placed above the dorsal hippocampus of rats expressing a EGFP-control construct after saline (left) or CNO (10 mg/kg) treatment (right). Area within the white line represents statistical significance compared to saline treatment at pixel level. Time point of 0 represents time of injection. (B) Power of brain oscillations (up to 150 Hz) over the 30-120 min post injection time interval. (C) Band power separation (from top to bottom) for theta, beta, low and high gamma and high frequency oscillations (HFO) over 2h recording illustrated in 10-min time bins. Missing data represents time of injection (T0). All data are shown as mean ± SEM values from n=9 rats and are baseline normalised. **P<0.01, fit of a generalised linear mixed effect model and multiple comparison tests with Tukey's honest significance difference.

Band power	DREADD	Treatment		Time		Interaction		Post-hoc (p-values at different time bins)								
		F(dF1,dF2)	p	F(dF1,dF2)	p	F(dF1,dF2)	p	T30	T40	T50	T60	T70	T80	T90	T100	T110
θ	Gi	F(1, 198)= 0.54	0.47	F(10, 198) =0.25	0.99	F(10, 198) =0.32	0.97	1	0.99	0.95	1	1	1	0.99	1	1
	Gq	F(1, 132) =0.78	0.38	F(10, 132) =0.16	0.99	F(10, 132) =0.96703	0.48	1	1	1	1	1	0.99	1	1	0.99
	eGFP	F(1, 176) =0.008	0.93	F(10, 176) =0.64	0.78	F(10, 176) =0.53	0.53	0.98	0.97	0.6	1	0.99	0.76	0.245	0.99	0.99
β	Gi	F(1, 198)= 1.38	0.24	F(10, 198) =1.38	0.19	F(10, 198) =0.4	0.94	0.99	1	1	0.99	0.99	1	0.99	1	0.99
	Gq	F(1, 132) =1.81	0.18	F(10, 132) =0.2	0.89	F(10, 132) =0.51	0.88	0.99	1	1	0.99	1	1	0.99	0.98	1
	eGFP	F(1, 176) =2.99	0.085	F(10, 176) =1.79	0.065	F(10, 176) =0.89	0.54	0.99	0.89	0.99	1	0.99	0.91	0.19	1	1
Low γ	Gi	F(1, 198)= 1.45	0.23	F(10, 198) =1.23	0.27	F(10, 198) =1.28	0.25	0.96	0.8	**0.003**	0.46	0.99	**0.0096**	0.43	0.0545	**0.035**
	Gq	F(1, 132) =1.05	0.3	F(10, 132) =0.28	0.98	F(10, 132) =0.59	0.82	0.99	1	1	1	1	1	1	0.868	0.857
	eGFP	F(1, 176)= 0.06	0.81	F(10, 176) =0.77	0.65	F(10, 176) =1.62	0.1	1	0.99	0.99	0.99	0.99	0.48	0.54	1	1
High γ	Gi	F(1, 198)= 0.2	0.65	F(10, 198) =1.95	**0.041**	F(10, 198) =1.14	0.34	1	1	0.45	0.99	1	0.51	1	0.86	0.9
	Gq	F(1, 132) =0.0005	0.98	F(10, 132) =0.43	0.93	F(10, 132) =1.39	0.19	0.9	0.99	0.99	1	0.951	0.99	0.97	0.493	**0.019**
	eGFP	F(1, 176)= 1.25	0.26	F(10, 176) =1.24	0.27	F(10, 176) =1.57	0.12	1	0.92	0.99	0.99	0.99	0.6	0.14	0.99	1
HFO	Gi	F(1, 198)= 1.09	0.3	F(10, 198) =1.66	0.09	F(10, 198) =0.75	0.67	1	1	0.99	1	1	0.99	1	1	0.99
	Gq	F(1, 132) =0.008	0.93	F(10, 132) =0.42	0.94	F(10, 132) =1.31	0.23	0.99	1	0.99	1	0.575	0.99	0.99	0.959	0.078
	eGFP	F(1, 176)= 0.24	0.62	F(10, 176) =1.27	0.25	F(10, 176) =2.1	**0.027**	1	0.89	0.99	0.99	0.986	0.12	0.095	1	1

Table 7.1: Statistical table of ECoG signals recorded from the dorsal hippocampal screw in the presence of CNO

ANOVA results for the fit generalised linear model with treatment and time as fixed-effect predictor, separated by band power and viral construct for data presented in Figures 7.3-7.5. Comparison was made between vehicle and CNO treatments and statistically significant p values are underlined and written in bold.

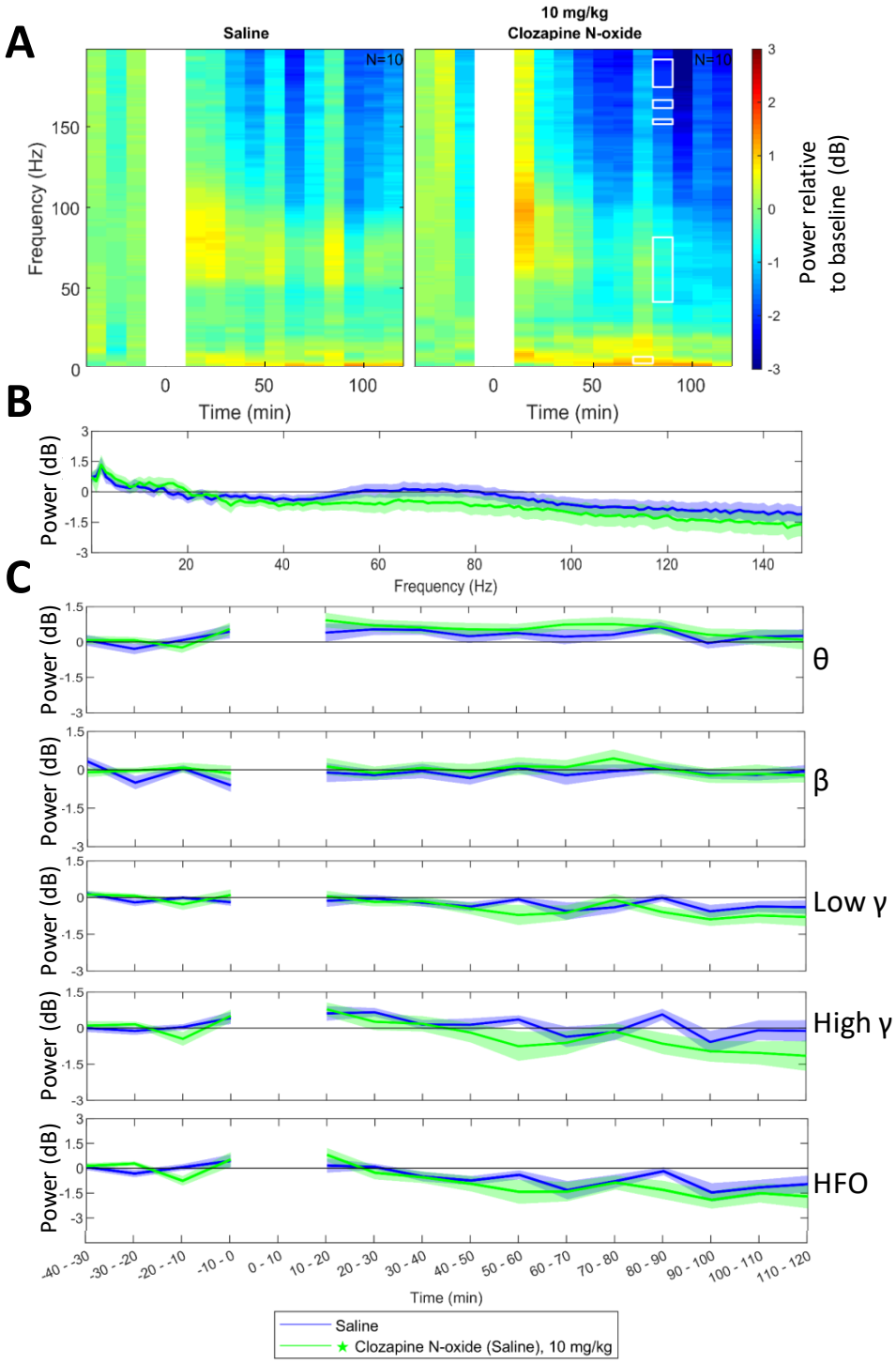


Figure 7.6: ECoG profile of mPFC Gi-DREADD expressing rats.

(A) Baseline normalised spectrogram of ECoG signal recorded over 2h post injection from a screw placed above the mPFC of rats expressing a Gi-DREADD after saline (left) or CNO (10 mg/kg) treatment (right). Area within the white line represents statistical significance compared to saline treatment at pixel level. Time point of 0 represents time of injection. (B) Power of brain oscillations (up to 150 Hz) over the 30-120 min post injection time interval. (C) Band power separation (from top to bottom) for theta, beta, low and high gamma and high frequency oscillations (HFO) over 2h recording illustrated in 10-min time bins. Missing data represents time of injection (T0). All data are shown as mean ± SEM values from n=10 rats and are baseline normalised.

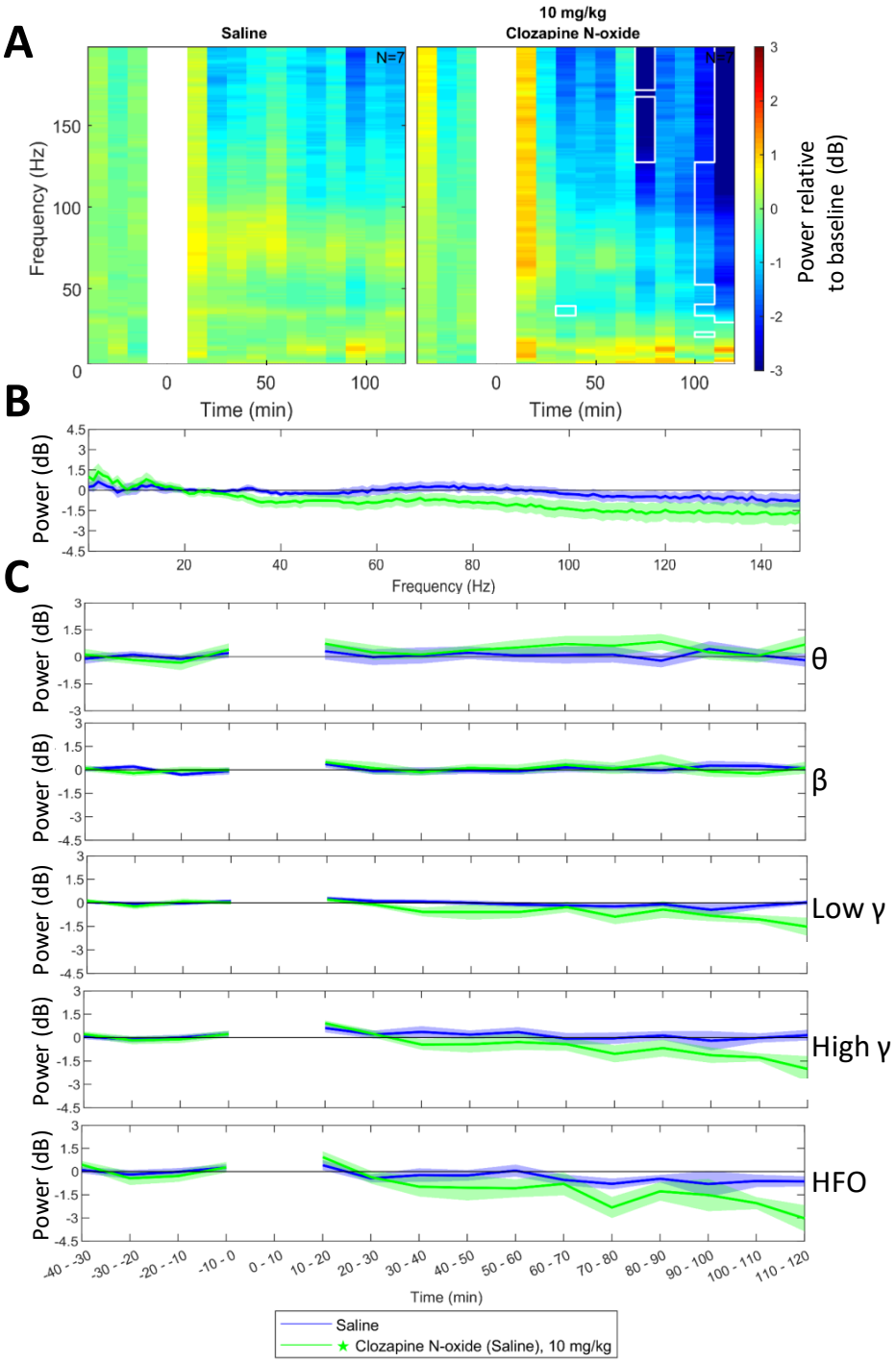


Figure 7.7: ECoG profile of mPFC Gq-DREADD expressing rats.

(A) Baseline normalised spectrogram of ECoG signal recorded over 2h post injection from a screw placed above the mPFC of rats expressing a Gq-DREADD after saline (left) or CNO (10 mg/kg) treatment (right). Area within the white line represents statistical significance compared to saline treatment at pixel level. Time point of 0 represents time of injection. (B) Power of brain oscillations (up to 150 Hz) over the 30-120 min post injection time interval. (C) Band power separation (from top to bottom) for theta, beta, low and high gamma and high frequency oscillations (HFO) over 2h recording illustrated in 10-min time bins. Missing data represents time of injection (T0). All data are shown as mean ± SEM values from n=7 rats and are baseline normalised. *P<0.05, fit of a generalised linear mixed effect model and multiple comparison tests with Tukey's honest significance difference.

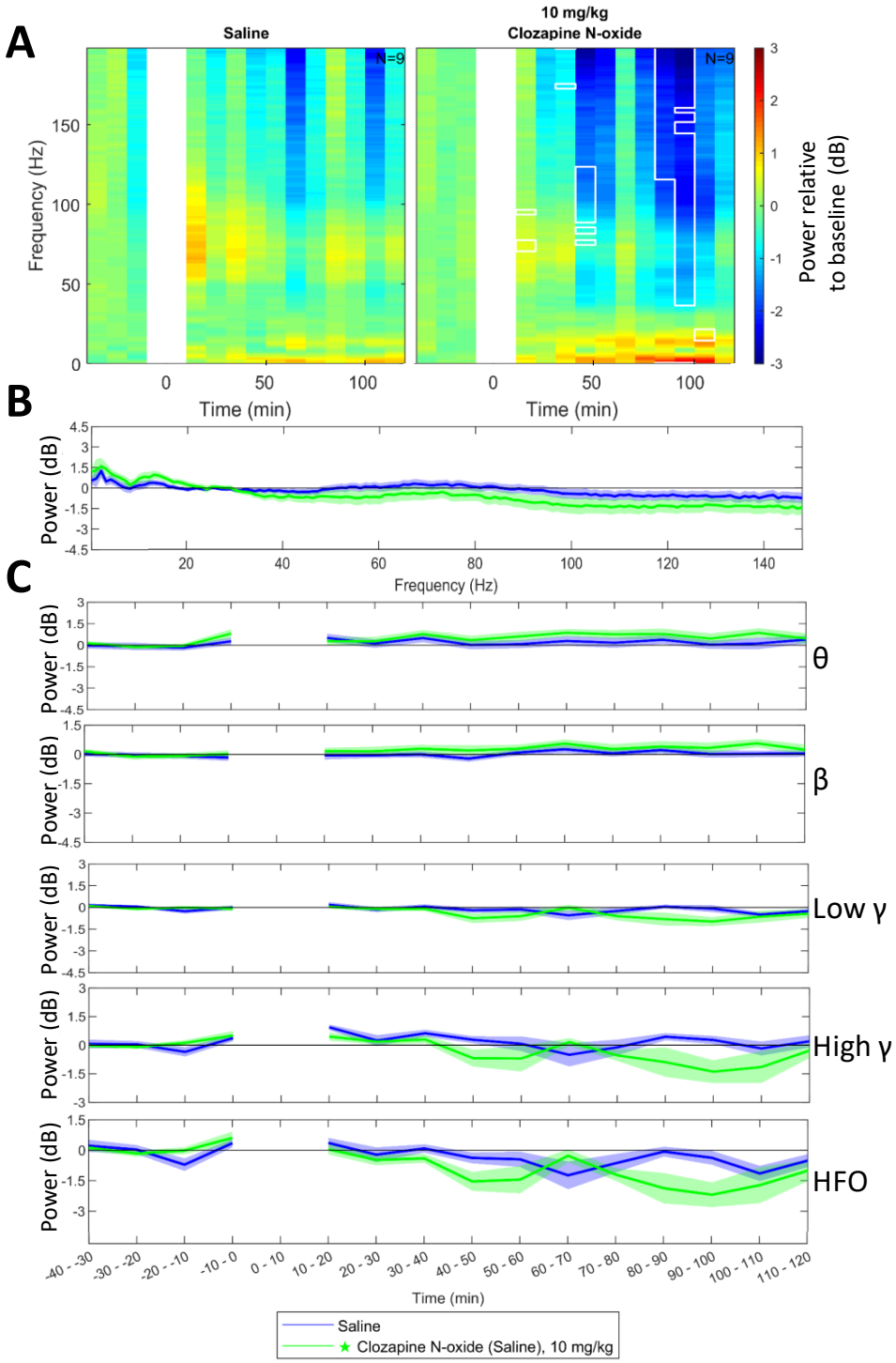


Figure 7.8: ECoG profile of mPFC EGFP-control expressing rats.

(A) Baseline normalised spectrogram of ECoG signal recorded over 2h post injection from a screw placed above the mPFC of rats expressing an EGFP-control after saline (left) or CNO (10 mg/kg) treatment (right). Area within the white line represents statistical significance compared to saline treatment at pixel level. Time point of 0 represents time of injection. (B) Power of brain oscillations (up to 150 Hz) over the 30-120 min post injection time interval. (C) Band power separation (from top to bottom) for theta, beta, low and high gamma and high frequency oscillations (HFO) over 2h recording illustrated in 10-min time bins. Missing data represents time of injection (T0). All data are shown as mean ± SEM values from n=9 rats and are baseline normalised.

Band power	DREADD	Treatment		Time		Interaction		Post-hoc (p-values at different time bins)								
		F(dF1,dF2)	p	F(dF1,dF2)	p	F(dF1,dF2)	p	T30	T40	T50	T60	T70	T80	T90	T100	T110
θ	Gi	F(1, 198)= 4.05	**0.045**	F(10, 198) =1.02	0.43	F(10, 198) =0.78	0.65	1	0.99	1	0.95	0.99	1	0.99	1	1
	Gq	F(1, 132) =1.02	0.32	F(10, 132) =0.43	0.93	F(10, 132) =0.84	0.593	1	1	1	0.99	0.99	0.71	1	1	0.94
	eGFP	F(1, 176) =0.63	0.43	F(10, 176) =0.86	0.57	F(10, 176) =0.95	0.49	1	0.99	0.97	0.94	0.93	0.99	0.99	0.6	1
β	Gi	F(1, 198)= 0.99	0.32	F(10, 198) =0.54	0.86	F(10, 198) =0.58676	0.82	1	0.99	1	0.99	0.93	1	1	1	1
	Gq	F(1, 132) =0.14	0.71	F(10, 132) =0.61	0.8	F(10, 132) =0.82	0.61	1	1	1	1	1	0.99	0.99	0.99	1
	eGFP	F(1, 176) =1.44	0.23	F(10, 176) =1.04	0.41	F(10, 176) =0.39	0.95	0.99	0.82	0.99	0.99	0.99	1	0.98	0.31	0.99
Low γ	Gi	F(1, 198)= 0.49	0.48	F(10, 198) =1.08	0.38	F(10, 198) =1.26	0.26	1	1	0.78	1	0.99	0.9	0.99	0.99	0.99
	Gq	F(1, 132) =0.025	0.87	F(10, 132) =0.54	0.86	F(10, 132) =1.29	0.25	0.99	0.99	0.99	1	0.99	1	1	0.83	**0.015**
	eGFP	F(1, 176) =0.17	0.68	F(10, 176) =0.94	0.5	F(10, 176) =1.55	0.12	1	0.99	0.99	0.99	0.99	0.63	0.55	1	1
High γ	Gi	F(1, 198)= 0.15	0.7	F(10, 198) =1.71	0.08	F(10, 198) =1.2592	0.26	1	1	0.69	1	1	0.52	1	0.91	0.81
	Gq	F(1, 132) =0.36	0.55	F(10, 132) =0.43	0.93	F(10, 132) =1.66	0.097	0.99	0.99	0.99	1	0.97	0.99	0.99	0.77	**0.011**
	eGFP	F(1, 176) =0.85	0.36	F(10, 176) =1.1	0.36	F(10, 176) =1.43	0.17	1	0.98	0.99	0.99	1	0.7	0.26	0.98	1
HFO	Gi	F(1, 198)= 1.39	0.24	F(10, 198) =2.01	**0.034**	F(10, 198) =0.83	0.6	1	1	0.97	1	1	0.93	1	1	0.99
	Gq	F(1, 132) =0.54	0.46	F(10, 132) =0.55	0.85	F(10, 132) =1.28	0.25	1	0.99	0.99	1	0.92	0.99	1	0.96	0.18
	eGFP	F(1, 176) =0.32	0.57	F(10, 176) =1.44	0.16	F(10, 176) =1.91	**0.0465**	1	0.94	0.99	0.99	1	0.22	0.21	1	1

Table 7.2: Statistical table of ECoG signals recorded from the mPFC screw in the presence of CNO

ANOVA results for the fit generalised linear model with treatment and time as fixed-effect predictor, separated by band power and viral construct for data presented in Figures 7.6-7.8. Comparison was made between vehicle and CNO treatments and statistically significant p values are underlined and written in bold.

7.3 Resting state LFP profile recorded from the mPFC from rats expressing an inhibitory or excitatory DREADD in the dorsal hippocampus – study II

Finally, LFP data recorded from a depth electrode placed in the mPFC during the second LFP/ECoG study are presented in Figures **7.9-7.11**. Statistical data can be found in Table **7.3**.

The statistical analysis revealed no effect of treatment in any of the groups at any of the band powers recorded. There were however some statistically significant effects of the treatment*time interaction in the EGFP-control group in a number of bands (theta: $F(10, 154) = 2.27$, $P = 0.017$; beta: $F(10, 154) = 2.08$, $P = 0.0296$; low gamma: $F(10, 154) = 2.08$, $P = 0.0295$). This can be explained by the data plotted in the spectrograms that illustrates that the power changes across the frequencies with every 10 min time-bin, not only during the recording but also during the baseline period, and that this constant fluctuation in band power is in opposite directions based on treatment, in the case of the Gi-DREADD group and the EGFP-control group.

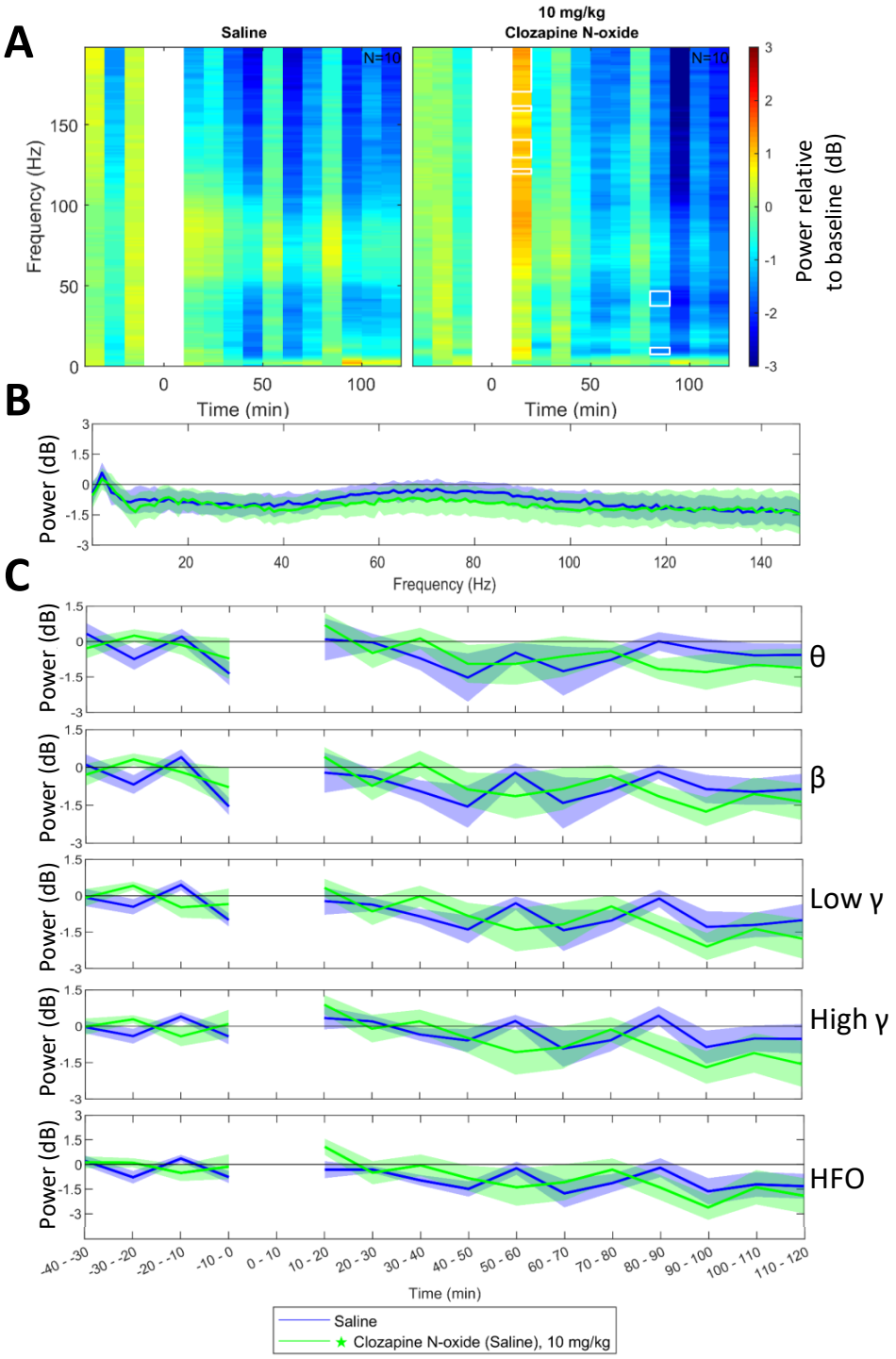


Figure 7.9: LFP profile of mPFC Gi-DREADD expressing rats.

(A) Baseline normalised spectrogram of LFP signal recorded over 2h post injection from a mPFC depth electrode in rats expressing hippocampal Gi-DREADD after saline (left) or CNO (10 mg/kg) treatment (right). Area within the white line represents statistical significance compared to saline treatment at pixel level. Time point of 0 represents time of injection. (B) Power of brain oscillations (up to 150 Hz) over the 30-120 min post injection time interval. (C) Band power separation (from top to bottom) for theta, beta, low and high gamma and high frequency oscillations (HFO) over 2h recording illustrated in 10-min time bins. Missing data represents time of injection (T0). All data are shown as mean ± SEM values from n=10 rats and are baseline normalised.

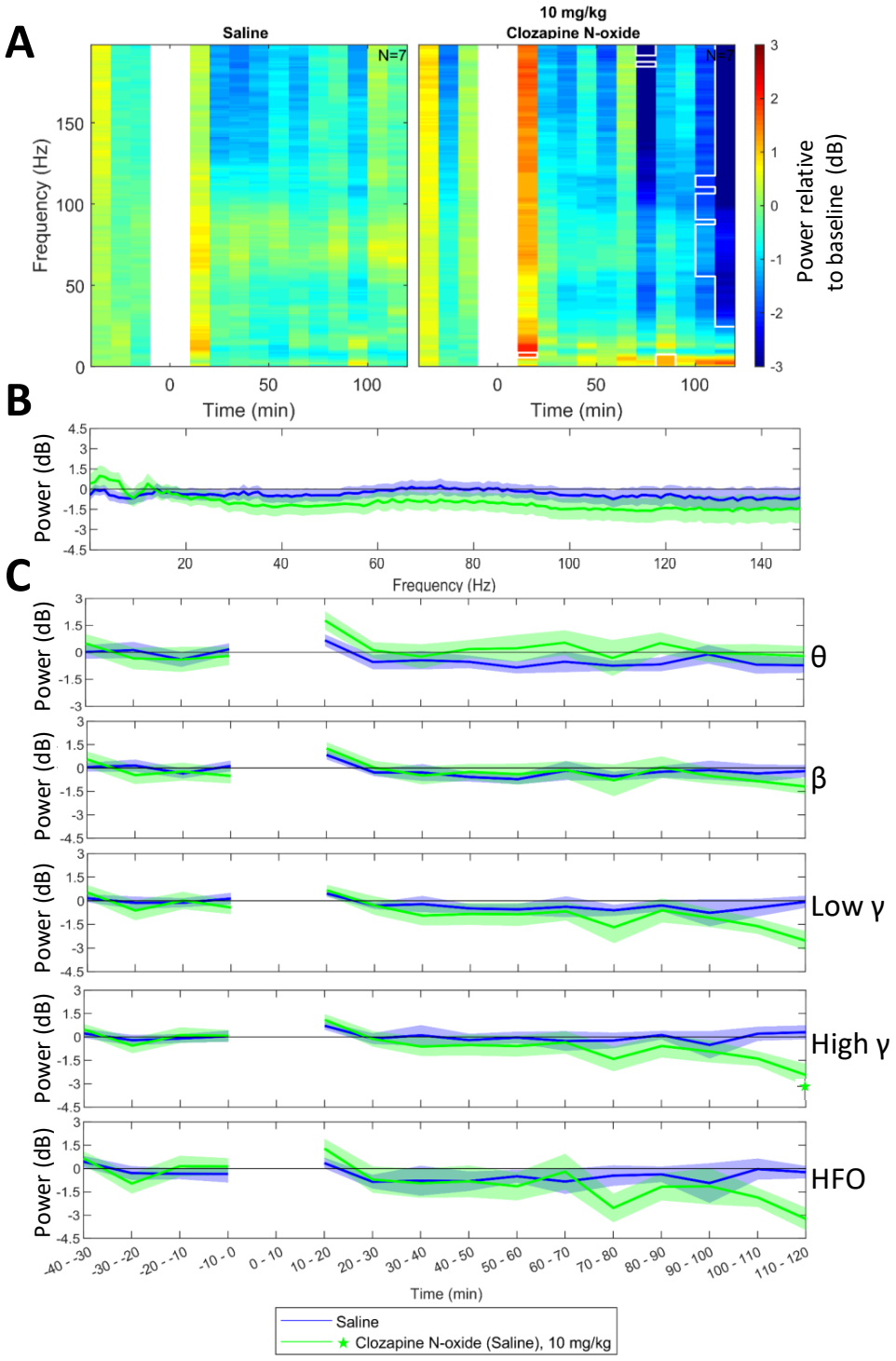


Figure 7.10: LFP profile of mPFC Gq-DREADD expressing rats.

(A) Baseline normalised spectrogram of LFP signal recorded over 2h post injection from a mPFC depth electrode in rats expressing hippocampal Gq-DREADD after saline (left) or CNO (10 mg/kg) treatment (right). Area within the white line represents statistical significance compared to saline treatment at pixel level. Time point of 0 represents time of injection. (B) Power of brain oscillations (up to 150 Hz) over the 30-120 min post injection time interval. (C) Band power separation (from top to bottom) for theta, beta, low and high gamma and high frequency oscillations (HFO) over 2h recording illustrated in 10-min time bins. Missing data represents time of injection (T0). All data are shown as mean ± SEM values from n=7 rats and are baseline normalised.

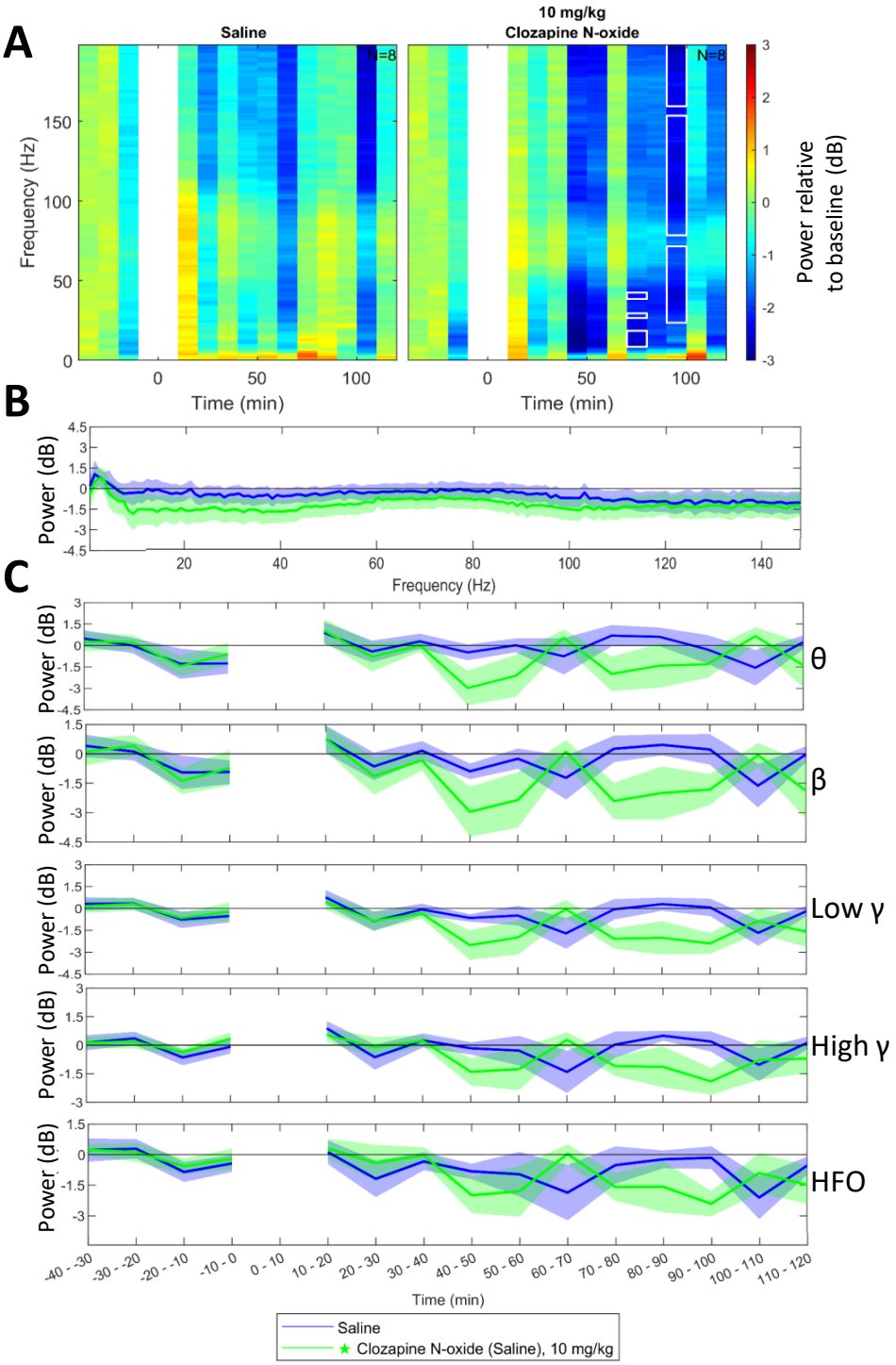


Figure 7.11: LFP profile of mPFC EGFP-control expressing rats.

(A) Baseline normalised spectrogram of LFP signal recorded over 2h post injection from a mPFC depth electrode in rats expressing hippocampal EGFP-control after saline (left) or CNO (10 mg/kg) treatment (right). Area within the white line represents statistical significance compared to saline treatment at pixel level. Time point of 0 represents time of injection. (B) Power of brain oscillations (up to 150 Hz) over the 30-120 min post injection time interval. (C) Band power separation (from top to bottom) for theta, beta, low and high gamma and high frequency oscillations (HFO) over 2h recording illustrated in 10-min time bins. Missing data represents time of injection (T0). All data are shown as mean ± SEM values from n=8 rats and are baseline normalised.

Band power	DREADD	Treatment		Time		Interaction		Post-hoc (p-values at different time bins)								
		F(dF1,dF2)	p	F(dF1,dF2)	p	F(dF1,dF2)	p	T30	T40	T50	T60	T70	T80	T90	T100	T110
θ	Gi	F(1, 198)= 0.9	0.34	F(10, 198) =1.28	0.24	F(10, 198) =1.25	0.26	0.99	1	1	1	1	0.98	0.99	1	1
	Gq	F(1, 132) =3.27	0.07	F(10, 132) =0.97	0.47	F(10, 132) =0.38	0.95	1	0.99	0.99	0.99	1	0.97	1	1	1
	eGFP	F(1, 154) =0.02	0.89	F(10, 154) =0.94	0.49	F(10, 154) =2.27	**0.017**	1	0.80	0.95	0.99	0.69	0.97	1	0.93	0.99
β	Gi	F(1, 198)= 0.94	0.34	F(10, 198) =1.06	0.39	F(10, 198) =1.34	0.21	0.99	0.99	0.99	1	1	0.99	0.99	1	1
	Gq	F(1, 132) =0.47	0.5	F(10, 132) =0.88	0.55	F(10, 132) =0.54	0.86	1	1	1	1	1	1	1	1	0.99
	eGFP	F(1, 154) =6.9e-05	0.99	F(10, 154) =1.03	0.42	F(10, 154) =2.08	**0.0296**	1	0.95	0.95	0.99	0.68	0.81	0.96	0.99	0.98
Low γ	Gi	F(1, 198)= 0.68	0.41	F(10, 198) =1.11	0.36	F(10, 198) =1.22	0.28	0.99	1	0.99	1	1	0.99	0.99	1	0.99
	Gq	F(1, 132) =0.09	0.76	F(10, 132) =0.44	0.93	F(10, 132) =1.13	0.35	1	1	1	1	0.99	1	1	0.99	0.11
	eGFP	F(1, 154) =0.11	0.74	F(10, 154) =1.35	0.21	F(10, 154) =2.08	**0.0295**	1	0.96	0.99	0.99	0.92	0.76	0.64	1	0.99
High γ	Gi	F(1, 198)= 0.66	0.42	F(10, 198) =1.05	0.4	F(10, 198) =1.15	0.33	1	1	0.97	1	1	0.95	0.99	1	0.99
	Gq	F(1, 132) =0.3	0.59	F(10, 132) =0.45	0.92	F(10, 132) =1.51	0.14	1	1	1	1	0.99	1	1	0.87	**0.0377**
	eGFP	F(1, 154) =0.17	0.68	F(10, 154) =1.22	0.28	F(10, 154) =1.6	0.11	1	0.99	0.99	0.96	0.99	0.97	0.77	1	1
HFO	Gi	F(1, 198) =2.45	0.12	F(10, 198) =0.89	0.54	F(10, 198) =1.07	0.39	1	1	0.99	1	1	0.99	0.99	1	1
	Gq	F(1, 132) =0.87	0.35	F(10, 132) =0.325	0.97	F(10, 132) =1.45	0.16	1	1	1	1	0.94	1	1	0.99	0.39
	eGFP	F(1, 154) =0.028	0.87	F(10, 154) =0.93	0.5	F(10, 154) =1.49	0.15	1	0.99	1	0.98	1	0.99	0.9	0.99	1

Table 7.3: Statistical table of LFP signals recorded from the mPFC depth electrode in the presence of CNO

ANOVA results for the fit generalised linear model with treatment and time as fixed-effect predictor, separated by band power and viral construct for data presented in Figures 7.9-7.11. Comparison was made between vehicle and CNO treatments and statistically significant p values are underlined and written in bold.

Bibliography

Ainge, J. A., Heron-Maxwell, C., Theofilas, P., Wright, P., de Hoz, L., & Wood, E. R. (2006). The role of the hippocampus in object recognition in rats: examination of the influence of task parameters and lesion size. *Behavioural Brain Research*, **167**(1), 183–195.

Aitta-Aho, T., Maksimovic, M., Dahl, K., Sprengel, R., & Korpi, E. R. (2019). Attenuation of novelty-induced hyperactivity of gria1-/- Mice by cannabidiol and hippocampal inhibitory chemogenetics. *Frontiers in Pharmacology*, **10**.

Alexander, G. M., Brown, L. Y., Farris, S., Lustberg, D., Pantazis, C., Gloss, B., Plummer, N. W., Jensen, P., & Dudek, S. M. (2018). CA2 neuronal activity controls hippocampal low gamma and ripple oscillations. *ELife*, **7**.

Alexander, G. M., Riddick, N. V., McCann, K. E., Lustberg, D., Moy, S. S., & Dudek, S. M. (2019). Modulation of CA2 neuronal activity increases behavioral responses to fear conditioning in female mice. *Neurobiology of Learning and Memory*, **163**.

Alexander, G. M., Rogan, S. C., Abbas, A. I., Armbruster, B. N., Pei, Y., Allen, J. A., Nonneman, R. J., Hartmann, J., Moy, S. S., Nicolelis, M. A., McNamara, J. O., & Roth, B. L. (2009). Remote Control of Neuronal Activity in Transgenic Mice Expressing Evolved G Protein-Coupled Receptors. *Neuron*, **63**(1), 27–39.

Alger, B. E., Nagode, D. A., & Tang, A. H. (2014). Muscarinic cholinergic receptors modulate inhibitory synaptic rhythms in hippocampus and neocortex. *Frontiers in Synaptic Neuroscience*, **6**.

Andersen, P., Morris, R., Amaral, D., Bliss, T., & O'Keefe, J. (2007). *The Hippocampus Book*. New York: Oxford University Press, Inc.

Anwyl, R. (1999). Metabotropic glutamate receptors: electrophysiological properties and role in plasticity. *Brain Research. Brain Research Reviews*, **29**(1), 83–120.

Armbruster, B. N., Li, X., Pausch, M. H., Herlitze, S., & Roth, B. L. (2007). Evolving the lock to fit the key to create a family of G protein-coupled receptors potently activated by an inert ligand. *PNAS*, **104**(12), 5163–5168.

Aschauer, D. F., Kreuz, S., & Rumpel, S. (2013). Analysis of Transduction Efficiency, Tropism and Axonal Transport of AAV Serotypes 1, 2, 5, 6, 8 and 9 in the Mouse Brain. *PLoS One*, **8**(9).

Ashby, C. R., & Wang, R. Y. (1996). Pharmacological actions of the atypical antipsychotic drug clozapine: A review. *Synapse*, **24**(4), 349–394.

Atasoy, D., Betley, J. N., Su, H. H., & Sternson, S. M. (2012). Deconstruction of a neural circuit for hunger. *Nature*, **488**(7410), 172–177.

Atasoy, D., & Sternson, S. M. (2018). Chemogenetic tools for causal cellular and neuronal biology. *Physiological Reviews*, **98**(1), 391–418.

Avaliani, N., Andersson, M., Runegaard, A. H., Woldbye, D., & Kokaia, M. (2016). DREADDs suppress seizure-like activity in a mouse model of pharmacoresistant epileptic brain tissue. *Gene Therapy*, **23**(10), 760–766.

Avoli, M., & Jefferys, J. G. R. (2016). Models of drug-induced epileptiform synchronization in vitro. *Journal of Neuroscience Methods*, **260**, 26–32.

Bannerman, D. M., Grubb, M., Deacon, R. M. J., Yee, B. K., Feldon, J., & Rawlins, J. N. P. (2003). Ventral hippocampal lesions affect anxiety but not spatial learning. *Behavioural Brain Research*, **139**(1–2), 197–213.

Bannerman, D. M., Deacon, R. M. J., Brady, S., Bruce, A., Sprengel, R., Seeburg, P. H., & Rawlins, J. N. P. (2004). A comparison of GluR-A-deficient and wild-type mice on a test battery assessing sensorimotor, affective, and cognitive behaviors. *Behavioral Neuroscience*, **118**(3), 643–647.

Bannerman, D. M., Deacon, R. M. J., Offen, S., Friswell, J., Grubb, M., & Rawlins, J. N. P. (2002). Double dissociation of function within the hippocampus: Spatial memory and hyponeophagia. *Behavioral Neuroscience*, **116**(5), 884–901.

Bannerman, D. M., Yee, B. K., Good, M. A., Heupel, M. J., Iversen, S. D., & Rawlins, J. N. P. (1999). Double dissociation of function within the hippocampus: A comparison of dorsal, ventral, and complete hippocampal cytotoxic lesions. *Behavioral Neuroscience*, **113**(6), 1170–1188.

Bannerman, D. M., Sprengel, R., Sanderson, D. J., McHugh, S. B., Rawlins, J. N. P., Monyer, H., & Seeburg, P. H. (2014). Hippocampal synaptic plasticity, spatial memory and anxiety. *Nature Reviews. Neuroscience*, **15**(3), 181–192.

Barker, G. R. I., & Warburton, E. C. (2011). When is the hippocampus involved in recognition memory? *The Journal of Neuroscience*, **31**(29), 10721–10731.

Barkus, C., Sanderson, D. J., Rawlins, J. N. P., Walton, M. E., Harrison, P. J., & Bannerman, D. M. (2014). What causes aberrant salience in schizophrenia? A role for impaired short-term habituation and the GRIA1 (GluA1) AMPA receptor subunit. *Molecular Psychiatry*, **19**(10), 1060–1070.

Bartos, M., Vida, I., & Jonas, P. (2007). Synaptic mechanisms of synchronized gamma oscillations in inhibitory interneuron networks. *Nature Reviews Neuroscience*, **8**(1), 45–56.

Beasley, C. L., & Reynolds, G. P. (1997). Parvalbumin-immunoreactive neurons are reduced in the prefrontal cortex of schizophrenics. *Schizophrenia Research*, **24**(3), 349–355.

Bender, D., Holschbach, M., & Stöcklin, G. (1994). Synthesis of n.c.a. carbon-11 labelled clozapine and its major metabolite clozapine-N-oxide and comparison of their biodistribution in mice. *Nuclear Medicine and Biology*, **21**(7), 921–925.

Bender, F., Gorbati, M., Cadavieco, M. C., Denisova, N., Gao, X., Holman, C., Korotkova, T., & Ponomarenko, A. (2015). Theta oscillations regulate the speed of locomotion via a hippocampus to lateral septum pathway. *Nature Communications*, **6**.

Bernstein, J. G., & Boyden, E. S. (2011). Optogenetic tools for analyzing the neural circuits of behavior. *Trends in Cognitive Sciences*, **15**(12), 592–600.

Bickel, U. (2005). How to measure drug transport across the blood-brain barrier. *NeuroRx*, **2**(1), 15–26.

Bird, C. M., & Burgess, N. (2008). The hippocampus and memory: Insights from spatial processing. *Nature Reviews Neuroscience*, **9**(3), 182–194.

Boehringer, R., Polygalov, D., Huang, A. J. Y., Middleton, S. J., Robert, V., Wintzer, M. E., Piskorowski, R. A., Chevaleyre, V., & McHugh, T. J. (2017). Chronic Loss of CA2 Transmission Leads to Hippocampal Hyperexcitability. *Neuron*, **94**(3), 642–655.

Boyden, E. S. (2011). A history of optogenetics: The development of tools for controlling brain circuits with light. *F1000 Biology Reports*, **3**(1).

Boyden, E. S., Zhang, F., Bamberg, E., Nagel, G., & Deisseroth, K. (2005). Millisecond-timescale, genetically targeted optical control of neural activity. *Nature Neuroscience*, **8**(9), 1263–1268.

Bragin, A., Engel, J., Wilson, C. L., Fried, I., & Mathern, G. W. (1999). Hippocampal and entorhinal cortex high-frequency oscillations (100-500 Hz) in human epileptic brain and in kainic acid-treated rats with chronic seizures. *Epilepsia*, **40**(2), 127–137.

Brancaccio, M., Maywood, E. S., Chesham, J. E., Loudon, A. S. I., & Hastings, M. H. (2013). A Gq-Ca2+ axis controls circuit-level encoding of circadian time in the suprachiasmatic nucleus. *Neuron*, **78**(4), 714–728.

Brandon, M. P., Bogaard, A. R., Libby, C. P., Connerney, M. A., Gupta, K., & Hasselmo, M. E. (2011). Reduction of theta rhythm dissociates grid cell spatial periodicity from directional tuning. *Science*, **332**(6029), 595–599.

Brandon, M. P., Koenig, J., Leutgeb, J. K., & Leutgeb, S. (2014). New and distinct hippocampal place codes are generated in a new environment during septal inactivation. *Neuron*, **82**(4), 789–796.

Broadbent, N. J., Gaskin, S., Squire, L. R., & Clark, R. E. (2009). Object recognition memory and the rodent hippocampus. *Learning and Memory*, **17**(1), 794–800.

Broadbent, N. J., Squire, L. R., & Clark, R. E. (2004). Spatial memory, recognition memory, and the hippocampus. *PNAS*, **101**(40), 14515–14520.

Broersen, L. M., & Uylings, H. B. M. (1999). Visual attention task performance in Wistar and Lister Hooded rats: Response inhibition deficits after medial prefrontal cortex lesions. *Neuroscience*, **94**(1), 47–57.

Bullitt, E. (1990). Expression of C-fos-like protein as a marker for neuronal activity following noxious stimulation in the rat. *Journal of Comparative Neurology*, **296**(4), 517–530.

Burger, C., Gorbatyuk, O. S., Velardo, M. J., Peden, C. S., Williams, P., Zolotukhin, S., Reier, P. J., Mandel, R. J., & Muzyczka, N. (2004). Recombinant AAV viral vectors pseudotyped with viral capsids from serotypes 1, 2, and 5 display differential efficiency and cell tropism

after delivery to different regions of the central nervous system. *Molecular Therapy*, **10**(2), 302–317.

Buzsáki, G. (2015). Hippocampal sharp wave-ripple: A cognitive biomarker for episodic memory and planning. *Hippocampus*, **25**(10), 1073–1188.

Buzsáki, G. (2002). Theta oscillations in the hippocampus. *Neuron*, **33**(3), 325–340.

Buzsáki, G., Anastassiou, C. A., & Koch, C. (2012). The origin of extracellular fields and currents-EEG, ECoG, LFP and spikes. *Nature Reviews Neuroscience*, **13**(6), 407–420.

Buzsáki, G., Lai-Wo S., L., & Vanderwolf, C. H. (1983). Cellular bases of hippocampal EEG in the behaving rat. *Brain Research Reviews*, **6**(2), 139–171.

Buzsáki, G., & Wang, X.-J. (2012). Mechanisms of Gamma Oscillations. *Annual Review of Neuroscience*, **35**(1), 203–225.

Bygrave, A. M., Jahans-Price, T., Wolff, A. R., Sprengel, R., Kullmann, D. M., Bannerman, D. M., & Kätzel, D. (2019). Hippocampal–prefrontal coherence mediates working memory and selective attention at distinct frequency bands and provides a causal link between schizophrenia and its risk gene GRIA1. *Translational Psychiatry*, **9**(1).

Bygrave, A. M., Masiulis, S., Kullmann, D. M., Bannerman, D. M., & Kätzel, D. (2019). Gene-environment interaction in a conditional NMDAR-knockout model of schizophrenia. *Frontiers in Behavioral Neuroscience*, **12**.

Calabrese, E. J., & Baldwin, L. A. (2002). Defining hormesis. *Human and Experimental Toxicology*, **21**(2), 91–97.

Cardin, J. A., Carlén, M., Meletis, K., Knoblich, U., Zhang, F., Deisseroth, K., Tsai, L. H., & Moore, C. I. (2009). Driving fast-spiking cells induces gamma rhythm and controls sensory responses. *Nature*, **459**(7247), 663–667.

Carter, M. E., Soden, M. E., Zweifel, L. S., & Palmiter, R. D. (2013). Genetic identification of a neural circuit that suppresses appetite. *Nature*, **503**(7474), 111–114.

Cassataro, D., Bergfeldt, D., Malekian, C., Van Snellenberg, J. X., Thanos, P. K., Fishell, G., & Sjulson, L. (2014). Reverse pharmacogenetic modulation of the nucleus accumbens reduces ethanol consumption in a limited access paradigm. *Neuropsychopharmacology*, **39**(2), 283–290.

Chang, W. H., Lin, S. K., Lane, H. Y., Wei, F. C., Hu, W. H., Lam, Y. W. F., & Jann, M. W. (1998). Reversible metabolism of clozapine and clozapine N-oxide in schizophrenic patients. *Progress in Neuro-Psychopharmacology and Biological Psychiatry*, **22**(5), 723–739.

Chen, X., Choo, H., Huang, X. P., Yang, X., Stone, O., Roth, B. L., & Jin, J. (2015). The first structure-activity relationship studies for designer receptors exclusively activated by designer drugs. *ACS Chemical Neuroscience*, **6**(3), 476–484.

Chow, B. Y., Han, X., Dobry, A. S., Qian, X., Chuong, A. S., Li, M., Henninger, M. A., Belfort, G. M., Lin, Y., Monahan, P. E., & Boyden, E. S. (2010). High-performance genetically

targetable optical neural silencing by light-driven proton pumps. *Nature*, **463**(7277), 98–102.

Chung, L. (2015). A Brief Introduction to the Transduction of Neural Activity into Fos Signal. *Development & Reproduction*, **19**(2), 61–67.

Clark, R. E., Zola, S. M., & Squire, L. R. (2000). Impaired recognition memory in rats after damage to the hippocampus. *The Journal of Neuroscience*, **20**(23), 8853–8860.

Clark, R. E., Broadbent, N. J., & Squire, L. R. (2005). Impaired remote spatial memory after hippocampal lesions despite extensive training beginning early in life. *Hippocampus*, **15**(3), 340–346.

Clemens, L. E., Jansson, E. K. H., Portal, E., Riess, O., & Nguyen, H. P. (2014). A behavioral comparison of the common laboratory rat strains Lister Hooded, Lewis, Fischer 344 and Wistar in an automated homecage system. *Genes, Brain and Behavior*, **13**(3), 305–321.

Cobb, S. R., Buhl, E. H., Halasy, K., Paulsen, O., & Somogyi, P. (1995). Synchronization of neuronal activity in hippocampus by individual GABAergic interneurons. *Nature*, **378**(6552), 75–78.

Cohen, S. J., Munchow, A. H., Rios, L. M., Zhang, G., Asgeirsdóttir, H. N., & Stackman, R. W. (2013). The rodent hippocampus is essential for nonspatial object memory. *Current Biology*, **23**(17), 1685–1690.

Colgin, L. L. (2013). Mechanisms and Functions of Theta Rhythms. *Annual Review of Neuroscience*, **36**(1), 295–312.

Colgin, L. L. (2011). Oscillations and hippocampal-prefrontal synchrony. *Current Opinion in Neurobiology*, **21**(3), 467–474.

Colgin, L. L. (2016). Rhythms of the hippocampal network. *Nature Reviews. Neuroscience*, **17**(4), 239–249.

Colgin, L. L., Denninger, T., Fyhn, M., Hafting, T., Bonnevie, T., Jensen, O., Moser, M. B., & Moser, E. I. (2009). Frequency of gamma oscillations routes flow of information in the hippocampus. *Nature*, **462**(7271), 353–357.

Conklin, B. R., Hsiao, E. C., Claeysen, S., Dumuis, A., Srinivasan, S., Forsayeth, J. R., Guettier, J. M., Chang, W. C., Pei, Y., McCarthy, K. D., Nissenson, R. A., Wess, J., Bockaert, J., & Roth, B. L. (2008). Engineering GPCR signaling pathways with RASSLs. *Nature Methods*, **5**(8), 673–678.

Cordella, A., Krashia, P., Nobili, A., Pignataro, A., La Barbera, L., Viscomi, M. T., Valzania, A., Keller, F., Ammassari-Teule, M., Mercuri, N. B., Berretta, N., & D'Amelio, M. (2018). Dopamine loss alters the hippocampus-nucleus accumbens synaptic transmission in the Tg2576 mouse model of Alzheimer's disease. *Neurobiology of Disease*, **116**, 142–154.

Coward, P., Wada, H. G., Falk, M. S., Chan, S. D., Meng, F., Akil, H., & Conklin, B. R. (1998). Controlling signaling with a specifically designed Gi-coupled receptor. *PNAS*, **95**(1), 352–357.

Craig, M. T., & McBain, C. J. (2015). Fast gamma oscillations are generated intrinsically in CA1 without the involvement of fast-spiking basket cells. *The Journal of Neuroscience*, **35**(8), 3616–3624.

Cullinan, W. E., Herman, J. P., Battaglia, D. F., Akil, H., & Watson, S. J. (1995). Pattern and time course of immediate early gene expression in rat brain following acute stress. *Neuroscience*, **64**(2), 477–505.

Danglot, L., Triller, A., & Marty, S. (2006). The development of hippocampal interneurons in rodents. *Hippocampus*, **16**(12), 1032–1060.

Davidson, B. L., Stein, C. S., Heth, J. A., Martins, I., Kotin, R. M., Derksen, T. A., Zabner, J., Ghodsi, A., & Chiorini, J. A. (2000). Recombinant adeno-associated virus type 2, 4, and 5 vectors: Transduction of variant cell types and regions in the mammalian central nervous system. *PNAS*, **97**(7), 3428–3432.

Daya, S., & Berns, K. I. (2008). Gene therapy using adeno-associated virus vectors. *Clinical Microbiology Reviews*, **21**(4), 583–593.

Deacon, R. M. J., & Rawlins, J. N. P. (2006). T-maze alternation in the rodent. *Nature Protocols*, **1**(1), 7–12.

Deacon, R. M. J., Bannerman, D. M., Kirby, B. P., Croucher, A., & Rawlins, J. N. P. (2002). Effects of cytotoxic hippocampal lesions in mice on a cognitive test battery. *Behavioural Brain Research*, **133**(1), 57–68.

Deng, W., Aimone, J. B., & Gage, F. H. (2010). New neurons and new memories: How does adult hippocampal neurogenesis affect learning and memory? *Nature Reviews Neuroscience*, **11**(5), 339–350.

Deng, W., Goldys, E. M., Farnham, M. M. J., & Pilowsky, P. M. (2014). Optogenetics, the intersection between physics and neuroscience: light stimulation of neurons in physiological conditions. *American Journal of Physiology. Regulatory, Integrative and Comparative Physiology*, **307**(11), R1292-302.

Dimidschstein, J., Chen, Q., Tremblay, R., Rogers, S. L., Saldi, G. A., Guo, L., Xu, Q., Liu, R., Lu, C., Chu, J., Grimley, J. S., Krostag, A. R., Kaykas, A., Avery, M. C., Rashid, M. S., Baek, M., Jacob, A. L., Smith, G. B., Wilson, D. E., Kosche, G., Kruglikov, I., Rusielewicz, T., Kotak, V. C., Mowery, T. M., Anderson, S. A., Callaway, E. M., Dasen, J. S., Fitzpatrick, D., Fossati, V., Long, M. A., Noggle, S., Reynolds, J. H., Sanes, D. H., Rudy, B., Feng, G., & Fishell, G. (2016). A viral strategy for targeting and manipulating interneurons across vertebrate species. *Nature Neuroscience*, **19**(12), 1743–1749.

Dittgen, T., Nimmerjahn, A., Komai, S., Licznerski, P., Waters, J., Margrie, T. W., Helmchen, F., Denk, W., Brecht, M., & Osten, P. (2004). Lentivirus-based genetic manipulations of cortical neurons and their optical and electrophysiological monitoring in vivo. *PNAS*, **101**(52), 18206–18211.

Dragunow, M., & Faull, R. (1989). The use of c-fos as a metabolic marker in neuronal pathway tracing. *Journal of Neuroscience Methods*, **29**(3), 261–265.

Dudek, S. M., Alexander, G. M., & Farris, S. (2016). Rediscovering area CA2: Unique properties and functions. *Nature Reviews Neuroscience*, **17**(2), 89–102.

Eldridge, M. A. G., Lerchner, W., Saunders, R. C., Kaneko, H., Krausz, K. W., Gonzalez, F. J., Ji, B., Higuchi, M., Minamimoto, T., & Richmond, B. J. (2016). Chemogenetic disconnection of monkey orbitofrontal and rhinal cortex reversibly disrupts reward value. *Nature Neuroscience*, **19**(1), 37–39.

Ellenbroek, B., & Youn, J. (2016). Rodent models in neuroscience research: Is it a rat race? *DMM Disease Models and Mechanisms*, **9**(10), 1079–1087.

Engel, A. K., & Fries, P. (2010). Beta-band oscillations-signalling the status quo? *Current Opinion in Neurobiology*, **20**(2), 156–165.

Ereshefsky, L., Watanabe, M. D., & Tran-Johnson, T. K. (1989). Clozapine: an atypical antipsychotic agent. *Clinical Pharmacy*, **8**(10), 691–709.

Fanselow, M. S., & Dong, H.-W. (2010). Are the dorsal and ventral hippocampus functionally distinct structures? *Neuron*, **65**(1), 7–19.

Fatemi, S. H., Reutiman, T. J., Folsom, T. D., & Thuras, P. D. (2009). GABA(A) receptor downregulation in brains of subjects with autism. *Journal of Autism and Developmental Disorders*, **39**(2), 223–230.

Ferguson, S. M., Eskenazi, D., Ishikawa, M., Wanat, M. J., Phillips, P. E. M., Dong, Y., Roth, B. L., & Neumaier, J. F. (2011). Transient neuronal inhibition reveals opposing roles of indirect and direct pathways in sensitization. *Nature Neuroscience*, **14**(1), 22–24.

Fitzgerald, P. J., Barkus, C., Feyder, M., Wiedholz, L. M., Chen, Y. C., Karlsson, R. M., Machado-Vieira, R., Graybeal, C., Sharp, T., Zarate, C., Harvey-White, J., Du, J., Sprengel, R., Gass, P., Bannerman, D., & Holmes, A. (2010). Does gene deletion of AMPA GluA1 phenocopy features of schizoaffective disorder? *Neurobiology of Disease*, **40**(3), 608–621.

Fozzard, H. A., Lee, P. J., & Lipkind, G. M. (2005). Mechanism of local anesthetic drug action on voltage-gated sodium channels. *Current Pharmaceutical Design*, **11**(21), 2671–2686.

Freund, T. F., & Buzsáki, G. (1998). Interneurons of the hippocampus. *Hippocampus*, **6**(4), 347–470.

Frush, D. P., & McNamara, J. O. (1986). Evidence implicating dentate granule cells in wet dog shakes produced by kindling stimulations of entorhinal cortex. *Experimental Neurology*, **92**(1), 102–113.

Fukata, Y., & Fukata, M. (2017). Epilepsy and synaptic proteins. *Current Opinion in Neurobiology*, **45**, 1–8.

Fung, S. J., Webster, M. J., Sivagnanasundaram, S., Duncan, C., Elashoff, M., & Weickert, C. S. (2010). Expression of interneuron markers in the dorsolateral prefrontal cortex of the developing human and in schizophrenia. *American Journal of Psychiatry*, **167**(12), 1479–1488.

Gandal, M. J., Edgar, J. C., Klook, K., & Siegel, S. J. (2012). Gamma synchrony: Towards a translational biomarker for the treatment-resistant symptoms of schizophrenia. *Neuropharmacology*, **62**(3), 1504–1518.

Garner, A. R., Rowland, D. C., Hwang, S. Y., Baumgaertel, K., Roth, B. L., Kentros, C., & Mayford, M. (2012). Generation of a synthetic memory trace. *Science*, **335**(6075), 1513–1516.

Ghosh, A., Ginty, D. D., Bading, H., & Greenberg, M. E. (1994). Calcium regulation of gene expression in neuronal cells. *Journal of Neurobiology*, **25**(3), 294–303.

Giannotti, G., Heinsbroek, J. A., Yue, A. J., Deisseroth, K., & Peters, J. (2019). Prefrontal cortex neuronal ensembles encoding fear drive fear expression during long-term memory retrieval. *Scientific Reports*, **9**(1), 10709.

Girardeau, G., Benchenane, K., Wiener, S. I., Buzsáki, G., & Zugaro, M. B. (2009). Selective suppression of hippocampal ripples impairs spatial memory. *Nature Neuroscience*, **12**(10), 1222–1223.

Givens, B. S., & Olton, D. S. (1990). Cholinergic and GABAergic modulation of medial septal area: effect on working memory. *Behavioral Neuroscience*, **104**(6), 849–855.

Godsil, B. P., Kiss, J. P., Spedding, M., & Jay, T. M. (2013). The hippocampal-prefrontal pathway: The weak link in psychiatric disorders? *European Neuropsychopharmacology*, **23**(10), 1165–1181.

Gomez, J. L., Bonaventura, J., Lesniak, W., Mathews, W. B., Sysa-Shah, P., Rodriguez, L. A., Ellis, R. J., Richie, C. T., Harvey, B. K., Dannals, R. F., Pomper, M. G., Bonci, A., & Michaelides, M. (2017). Chemogenetics revealed: DREADD occupancy and activation via converted clozapine. *Science*, **357**(6350), 503–507.

Gong, S., Doughty, M., Harbaugh, C. R., Cummins, A., Hatten, M. E., Heintz, N., & Gerfen, C. R. (2007). Targeting Cre recombinase to specific neuron populations with bacterial artificial chromosome constructs. *The Journal of Neuroscience*, **27**(37), 9817–9823.

Graves, A. R., Moore, S. J., Bloss, E. B., Mensh, B. D., Kath, W. L., & Spruston, N. (2012). Hippocampal Pyramidal Neurons Comprise Two Distinct Cell Types that Are Countermodulated by Metabotropic Receptors. *Neuron*, **76**(4), 776–789.

Gray, J. A. (1982). *The Neuropsychology of Anxiety: an Enquiry in to the Functions of the Septo-hippocampal System*. New York: Oxford University Press.

Gray, J. A., & McNaughton, N. (2000). *The Neuropsychology of Anxiety: an Enquiry in to the Functions of the Septo-hippocampal System* (2nd Editio). Oxford University Press.

Guettier, J.-M., Gautam, D., Scarselli, M., Ruiz de Azua, I., Li, J. H., Rosemond, E., Ma, X., Gonzalez, F. J., Armbruster, B. N., Lu, H., Roth, B. L., & Wess, J. (2009). A chemical-genetic approach to study G protein regulation of beta cell function in vivo. *PNAS*, **106**(45), 19197–19202.

Guru, A., Post, R. J., Ho, Y. Y., & Warden, M. R. (2015). Making sense of optogenetics. *International Journal of Neuropsychopharmacology*, **18**(11).

Hannapel, R., Ramesh, J., Ross, A., Lalumiere, R. T., Roseberry, A. G., & Parent, M. B. (2019). Postmeal optogenetic inhibition of dorsal or ventral hippocampal pyramidal neurons increases future intake. *ENeuro*, **6**(1).

Hansen, I. H., Agerskov, C., Arvastson, L., Bastlund, J. F., Sørensen, H. B. D., & Herrik, K. F. (2019). Pharmaco-electroencephalographic reponses in the rat differ between active and inactive locomotor states. *European Journal of Neuroscience*, **50**(2), 1948–1971.

Harris, K. D., Csicsvari, J., Hirase, H., Dragoi, G., & Buzsáki, G. (2003). Organization of cell assemblies in the hippocampus. *Nature*, **424**(6948), 552–556.

Hirst, W. D., Abrahamsen, B., Blaney, F. E., Calver, A. R., Aloj, L., Price, G. W., & Medhurst, A. D. (2003). Differences in the Central Nervous System Distribution and Pharmacology of the Mouse 5-Hydroxytryptamine-6 Receptor Compared with Rat and Human Receptors Investigated by Radioligand Binding, Site-Directed Mutagenesis, and Molecular Modeling. *Molecular Pharmacology*, **64**(6), 1295–1308.

Hoffman, G. E., Smith, M. S., & Verbalis, J. G. (1993). c-Fos and related immediate early gene products as markers of activity in neuroendocrine systems. *Frontiers in Neuroendocrinology*, **14**(3), 173–213.

Holt, W., & Maren, S. (1999). Muscimol inactivation of the dorsal hippocampus impairs contextual retrieval of fear memory. *The Journal of Neuroscience*, **19**(20), 9054–9062.

Hopkins, A. L., & Groom, C. R. (2002). The druggable genome. *Nature Reviews Drug Discovery*, **1**(9), 727–730.

Howard, M. W., Rizzuto, D. S., Caplan, J. B., Madsen, J. R., Lisman, J., Aschenbrenner-Scheibe, R., Schulze-Bonhage, A., & Kahana, M. J. (2003). Gamma Oscillations Correlate with Working Memory Load in Humans. *Cerebral Cortex*, **13**(12), 1369–1374.

Hu, K. hui, Li, Y. an, Jia, W., Wu, G. yan, Sun, L., Wang, S. rong, & Yu, L. hua. (2019). Chemogenetic activation of glutamatergic neurons in the motor cortex promotes functional recovery after ischemic stroke in rats. *Behavioural Brain Research*, **359**, 81–88.

Ilg, A. K., Enkel, T., Bartsch, D., & Bähner, F. (2018). Behavioral effects of acute systemic low-dose clozapine in wild-type rats: Implications for the use of DREADDs in behavioral neuroscience. *Frontiers in Behavioral Neuroscience*, **12**.

Jain, S., Ruiz de Azua, I., Lu, H., White, M. F., Guettier, J.-M., & Wess, J. (2013). Chronic activation of a designer G(q)-coupled receptor improves β cell function. *The Journal of Clinical Investigation*, **123**(4), 1750–1762.

Jann, M. W., Lam, Y. W., & Chang, W. H. (1994). Rapid formation of clozapine in guinea-pigs and man following clozapine-N-oxide administration. *Archives Internationales de Pharmacodynamie et de Therapie*, **328**(2), 243–250.

Jendryka, M., Palchaudhuri, M., Ursu, D., van der Veen, B., Liss, B., Kätzel, D., Nissen, W., & Pekcec, A. (2019). Pharmacokinetic and pharmacodynamic actions of clozapine-N-oxide, clozapine, and compound 21 in DREADD-based chemogenetics in mice. *Scientific Reports*, **9**(1).

Jobert, M., Wilson, F. J., Ruigt, G. S. F., Brunovsky, M., Prichep, L. S., & Drinkenburg, W. H. I. M. (2012). Guidelines for the recording and evaluation of pharmaco-eeg data in man: The international pharmaco-EEG society (IPEG): The IPEG pharmaco-EEG guideline committee. *Neuropsychobiology*, **66**(4), 201–220.

Jones, M. W., & Wilson, M. A. (2005). Theta rhythms coordinate hippocampal-prefrontal interactions in a spatial memory task. *PLoS Biology*, **3**(12), 1–13.

Kandratavicius, L., Alves Balista, P., Lopes-Aguiar, C., Ruggiero, R. N., Umeoka, E. H., Garcia-Cairasco, N., Bueno-Junior, L. S., & Leite, J. P. (2014). Animal models of epilepsy: Use and limitations. *Neuropsychiatric Disease and Treatment*, **10**, 1693–1705.

Keenan, W. T., Fernandez, D. C., Shumway, L. J., Zhao, H., & Hattar, S. (2017). Eye-drops for activation of DREADDs. *Frontiers in Neural Circuits*, **11**.

Kesner, R. P., Kirk, R. A., Yu, Z., Polansky, C., & Musso, N. D. (2016). Dentate gyrus supports slope recognition memory, shades of grey-context pattern separation and recognition memory, and CA3 supports pattern completion for object memory. *Neurobiology of Learning and Memory*, **129**, 29–37.

Kheirbek, M. A., Drew, L. J., Burghardt, N. S., Costantini, D. O., Tannenholz, L., Ahmari, S. E., Zeng, H., Fenton, A. A., & Henl, R. (2013). Differential control of learning and anxiety along the dorsoventral axis of the dentate gyrus. *Neuron*, **77**(5), 955–968.

Kim, J. J., & Fanselow, M. S. (1992). Modality-specific retrograde amnesia of fear. *Science*, **256**(5057), 675–677.

Koike, H., Demars, M. P., Short, J. A., Nabel, E. M., Akbarian, S., Baxter, M. G., & Morishita, H. (2016). Chemogenetic Inactivation of Dorsal Anterior Cingulate Cortex Neurons Disrupts Attentional Behavior in Mouse. *Neuropsychopharmacology*, **41**(4), 1014–1023.

Kong, D., Tong, Q., Ye, C., Koda, S., Fuller, P. M., Krashes, M. J., Vong, L., Ray, R. S., Olson, D. P., & Lowell, B. B. (2012). GABAergic RIP-Cre neurons in the arcuate nucleus selectively regulate energy expenditure. *Cell*, **151**(3), 645–657.

Kovács, K. A., O'Neill, J., Schoenenberger, P., Penttonen, M., Guerrero, D. K. R., & Csicsvari, J. (2016). Optogenetically blocking sharp wave ripple events in sleep does not interfere with the formation of stable spatial representation in the CA1 area of the hippocampus. *PLoS One*, **11**(10).

Kovács, K. J. (1998). c-Fos as a transcription factor: A stressful (re)view from a functional map. *Neurochemistry International*, **33**(4), 287–297.

Krashes, M. J., Koda, S., Ye, C. P., Rogan, S. C., Adams, A. C., Cusher, D. S., Maratos-Flier, E., Roth, B. L., & Lowell, B. B. (2011). Rapid, reversible activation of AgRP neurons drives feeding behavior in mice. *Journal of Clinical Investigation*, **121**(4), 1424–1428.

Lapray, D., Lasztoczi, B., Lagler, M., Viney, T. J., Katona, L., Valenti, O., Hartwich, K., Borhegyi, Z., Somogyi, P., & Klausberger, T. (2012). Behavior-dependent specialization of identified hippocampal interneurons. *Nature Neuroscience*, **15**(9), 1265–1271.

Lasztóczi, B., & Klausberger, T. (2016). Hippocampal Place Cells Couple to Three Different Gamma Oscillations during Place Field Traversal. *Neuron*, **91**(1), 34–40.

Leung, L. S., & Shen, B. (2006). Hippocampal partial kindling decreased hippocampal GABAB receptor efficacy and wet dog shakes in rats. *Behavioural Brain Research*, **173**(2), 274–281.

Li, H., Penzo, M. A., Taniguchi, H., Kopec, C. D., Huang, Z. J., & Li, B. (2013). Experience-dependent modification of a central amygdala fear circuit. *Nature Neuroscience*, **16**(3), 332–339.

Li, J. H., Jain, S., McMillin, S. M., Cui, Y., Gautam, D., Sakamoto, W., Lu, H., Jou, W., McGuinness, O. P., Gavrilova, O., & Wess, J. (2013). A novel experimental strategy to assess the metabolic effects of selective activation of a G(q)-coupled receptor in hepatocytes in vivo. *Endocrinology*, **154**(10), 3539–3551.

Lisman, J. E., Coyle, J. T., Green, R. W., Javitt, D. C., Benes, F. M., Heckers, S., & Grace, A. A. (2008). Circuit-based framework for understanding neurotransmitter and risk gene interactions in schizophrenia. *Trends in Neurosciences*, **31**(5), 234–242.

Lisman, J. E., & Jensen, O. (2013). The θ-γ neural code. *Neuron*, **77**(6), 1002–1016.

Little, S., & Brown, P. (2014). The functional role of beta oscillations in Parkinson's disease. *Parkinsonism & Related Disorders*, **20**.

Liu, Q., Balsters, J. H., Baechinger, M., Van Der Groen, O., Wenderoth, N., & Mantini, D. (2015). Estimating a neutral reference for electroencephalographic recordings: The importance of using a high-density montage and a realistic head model. *Journal of Neural Engineering*, **12**(5).

Liu, X., Ramirez, S., Pang, P. T., Puryear, C. B., Govindarajan, A., Deisseroth, K., & Tonegawa, S. (2012). Optogenetic stimulation of a hippocampal engram activates fear memory recall. *Nature*, **484**(7394), 381–385.

Liu, Y., McAfee, S. S., & Heck, D. H. (2017). Hippocampal sharp-wave ripples in awake mice are entrained by respiration. *Scientific Reports*, **7**(1).

López, A. J., Kramár, E., Matheos, D. P., White, A. O., Kwapis, J., Vogel-Ciernia, A., Sakata, K., Espinoza, M., & Wood, M. A. (2016). Promoter-specific effects of DREADD modulation on hippocampal synaptic plasticity and memory formation. *The Journal of Neuroscience*, **36**(12), 3588–3599.

Lyons, M. R., & West, A. E. (2011). Mechanisms of specificity in neuronal activity-regulated gene transcription. *Progress in Neurobiology*, **94**(3), 259–295.

Mably, A. J., & Colgin, L. L. (2018). Gamma oscillations in cognitive disorders. *Current Opinion in Neurobiology*, **52**, 182–187.

MacLaren, D. A. A., Browne, R. W., Shaw, J. K., Radhakrishnan, S. K., Khare, P., España, R. A., & Clark, S. D. (2016). Clozapine N-oxide administration produces behavioral effects in long-evans rats: Implications for designing DREADD experiments. *ENeuro*, **3**(5).

Mahler, S. V., Vazey, E. M., Beckley, J. T., Keistler, C. R., Mcglinchey, E. M., Kaufling, J., Wilson, S. P., Deisseroth, K., Woodward, J. J., & Aston-Jones, G. (2014). Designer receptors show role for ventral pallidum input to ventral tegmental area in cocaine seeking. *Nature Neuroscience*, **17**(4), 577–585.

Maksimovic, M., Aitta-aho, T., & Korpi, E. R. (2014). Reversal of novelty-induced hippocampal c-Fos expression in GluA1 subunit-deficient mice by chronic treatment targeting glutamatergic transmission. *European Journal of Pharmacology*, **745**, 36–45.

Manahan-Vaughan, D. (1997). Group 1 and 2 metabotropic glutamate receptors play differential roles in hippocampal long-term depression and long-term potentiation in freely moving rats. *The Journal of Neuroscience*, **17**(9), 3303–3311.

Mann, E. O., Suckling, J. M., Hajos, N., Greenfield, S. A., & Paulsen, O. (2005). Perisomatic feedback inhibition underlies cholinergically induced fast network oscillations in the rat hippocampus in vitro. *Neuron*, **45**(1), 105–117.

Manseau, F., Danik, M., & Williams, S. (2005). A functional glutamatergic neurone network in the medial septum and diagonal band area. *Journal of Physiology*, **566**(3), 865–884.

Manvich, D. F., Webster, K. A., Foster, S. L., Farrell, M. S., Ritchie, J. C., Porter, J. H., & Weinshenker, D. (2018). The DREADD agonist clozapine N-oxide (CNO) is reverse-metabolized to clozapine and produces clozapine-like interoceptive stimulus effects in rats and mice. *Scientific Reports*, **8**(1).

Mao, J. B., & Robinson, J. K. (1998). Microinjection of GABA-A agonist muscimol into the dorsal but not the ventral hippocampus impairs non-mnemonic measures of delayed non-matching-to-position performance in rats. *Brain Research*, **784**(1–2), 139–147.

Marchant, N. J., Whitaker, L. R., Bossert, J. M., Harvey, B. K., Hope, B. T., Kaganovsky, K., Adhikary, S., Prisinzano, T. E., Vardy, E., Roth, B. L., & Shaham, Y. (2016). Behavioral and Physiological Effects of a Novel Kappa-Opioid Receptor-Based DREADD in Rats. *Neuropsychopharmacology*, **41**(2), 402–409.

Martin, C., Beshel, J., & Kay, L. M. (2007). An olfacto-hippocampal network is dynamically involved in odor-discrimination learning. *Journal of Neurophysiology*, **98**(4), 2196–2205.

Mayford, M., Bach, M. E., Huang, Y. Y., Wang, L., Hawkins, R. D., & Kandel, E. R. (1996). Control of memory formation through regulated expression of a CaMKII transgene. *Science*, **274**(5293), 1678–1683.

Mazzone, C. M., Pati, D., Michaelides, M., DiBerto, J., Fox, J. H., Tipton, G., Anderson, C., Duffy, K., McKlveen, J. M., Hardaway, J. A., Magness, S. T., Falls, W. A., Hammack, S. E., McElligott, Z. A., Hurd, Y. L., & Kash, T. L. (2018). Acute engagement of Gq-mediated signaling in the bed nucleus of the stria terminalis induces anxiety-like behavior. *Molecular Psychiatry*, **23**(1), 143–153.

McCarthy, M. M., Moore-Kochlacs, C., Gu, X., Boyden, E. S., Han, X., & Kopell, N. (2011). Striatal origin of the pathologic beta oscillations in Parkinson's disease. *PNAS*, **108**(28), 11620–11625.

McEown, K., & Treit, D. (2010). Inactivation of the dorsal or ventral hippocampus with muscimol differentially affects fear and memory. *Brain Research*, **1353**, 145–151.

McHugh, S. B., Niewoehner, B., Rawlins, J. N. P., & Bannerman, D. M. (2008). Dorsal hippocampal N-methyl-d-aspartate receptors underlie spatial working memory performance during non-matching to place testing on the T-maze. *Behavioural Brain Research*, **186**(1), 41–47.

McNaughton, N., Ruan, M., & Woodnorth, M.-A. (2006). Restoring theta-like rhythmicity in rats restores initial learning in the Morris water maze. *Hippocampus*, **16**(12), 1102–1110.

McOmish, C. E., Lira, A., Hanks, J. B., & Gingrich, J. A. (2012). Clozapine-induced locomotor suppression is mediated by 5-HT2A receptors in the forebrain. *Neuropsychopharmacology*, **37**(13), 2747–2755.

Melia, K. R., Ryabinin, A. E., Schroeder, R., Bloom, F. E., Wilson, M. C., & Anokhin, P. K. (1994). Induction and Habituation of Immediate Early Gene Expression in Rat Brain by Acute and Repeated Restraint Stress. *The Journal of Neuroscience*, **14**(10), 5929–5938.

Miller, E. K., & Cohen, J. D. (2001). An Integrative Theory of Prefrontal Cortex Function. *Annual Review of Neuroscience*, **24**(1), 167–202.

Miller, E. K., & Cohen, J. D. (2001). An Integrative Theory of Prefrontal Cortex Function. *Annual Review of Neuroscience*, **24**(1), 167–202.

Miyake, N., Miyake, K., Yamamoto, M., Hirai, Y., & Shimada, T. (2011). Global gene transfer into the CNS across the BBB after neonatal systemic delivery of single-stranded AAV vectors. *Brain Research*, **1389**, 19–26.

Mizumori, S. J. Y., Perez, G. M., Alvarado, M. C., Barnes, C. A., & McNaughton, B. L. (1990). Reversible inactivation of the medial septum differentially affects two forms of learning in rats. *Brain Research*, **528**(1), 12–20.

Montgomery, S. M., & Buzsáki, G. (2007). Gamma oscillations dynamically couple hippocampal CA3 and CA1 regions during memory task performance. *PNAS*, **104**(36), 14495–14500.

Morgan, J. I., & Curran, T. (1991). Stimulus-transcription coupling in the nervous system: involvement of the inducible proto-oncogenes fos and jun. *Annual Review of Neuroscience*, **14**, 421–451.

Morgan, J. I., Cohen, D. R., Hempstead, J. L., & Curran, T. (1987). Mapping patterns of c-fos expression in the central nervous system after seizure. *Science*, **237**(4811), 192–197.

Morris, R. G. M., Schenk, F., Tweedie, F., & Jarrard, L. E. (1990). Ibotenate Lesions of Hippocampus and/or Subiculum: Dissociating Components of Allocentric Spatial Learning. *European Journal of Neuroscience*, **2**(12), 1016–1028.

Morris, R. (1984). Developments of a water-maze procedure for studying spatial learning in the rat. *Journal of Neuroscience Methods*, **11**(1), 47–60.

Moser, E. I., Kropff, E., & Moser, M.-B. (2008). Place cells, grid cells, and the brain's spatial representation system. *Annual Review of Neuroscience*, **31**, 69–89.

Moser, M. B., Moser, E. I., Forrest, E., Andersen, P., & Morris, R. G. M. (1995). Spatial learning with a minislab in the dorsal hippocampus. *PNAS*, **92**(21), 9697–9701.

Müller, C., & Remy, S. (2014). Dendritic inhibition mediated by O-LM and bistratified interneurons in the hippocampus. *Frontiers in Synaptic Neuroscience*, **6**(SEP).

Nanou, E., Lee, A., & Catterall, W. A. (2018). Control of excitation/inhibition balance in a hippocampal circuit by calcium sensor protein regulation of presynaptic calcium channels. *The Journal of Neuroscience*, **38**(18), 4430–4440.

Naso, M. F., Tomkowicz, B., Perry, W. L., & Strohl, W. R. (2017). Adeno-Associated Virus (AAV) as a Vector for Gene Therapy. *BioDrugs*, **31**(4), 317–334.

Nathanson, J. L., Yanagawa, Y., Obata, K., & Callaway, E. M. (2009). Preferential labeling of inhibitory and excitatory cortical neurons by endogenous tropism of adeno-associated virus and lentivirus vectors. *Neuroscience*, **161**(2), 441–450.

Neves, G., Cooke, S. F., & Bliss, T. V. P. (2008). Synaptic plasticity, memory and the hippocampus: A neural network approach to causality. *Nature Reviews Neuroscience*, **9**(1), 65–75.

Nguyen, R., Morrissey, M. D., Mahadevan, V., Cajanding, J. D., Woodin, M. A., Yeomans, J. S., Takehara-Nishiuchi, K., & Kim, J. C. (2014). Parvalbumin and GAD65 interneuron inhibition in the ventral hippocampus induces distinct behavioral deficits relevant to schizophrenia. *The Journal of Neuroscience*, **34**(45), 14948–14960.

Nicoletti, F., Bockaert, J., Collingridge, G. L., Conn, P. J., Ferraguti, F., Schoepp, D. D., Wroblewski, J. T., & Pin, J. P. (2011). Metabotropic glutamate receptors: from the workbench to the bedside. *Neuropharmacology*, **60**(7–8), 1017–1041.

Niswender, C. M., & Conn, P. J. (2010). Metabotropic glutamate receptors: physiology, pharmacology, and disease. *Annual Review of Pharmacology and Toxicology*, **50**, 295–322.

Ohira, K., Furuta, T., Hioki, H., Nakamura, K. C., Kuramoto, E., Tanaka, Y., Funatsu, N., Shimizu, K., Oishi, T., Hayashi, M., Miyakawa, T., Kaneko, T., & Nakamura, S. (2010). Ischemia-induced neurogenesis of neocortical layer 1 progenitor cells. *Nature Neuroscience*, **13**(2), 173–179.

O'Keefe, J., & Dostrovsky, J. (1971). The hippocampus as a spatial map. Preliminary evidence from unit activity in the freely-moving rat. *Brain Research*, **34**(1), 171–175.

O'Keefe, J., & Nadel, L. (1978). *The Hippocampus as a Cognitive Map*.

Olsen, R. K., Moses, S. N., Riggs, L., & Ryan, J. D. (2012). The hippocampus supports multiple cognitive processes through relational binding and comparison. *Frontiers in Human Neuroscience*, **6**, 146.

Olton, D. S., Becker, J. T., & Handelmann, G. E. (1979). Hippocampus, space, and memory. *Behavioral and Brain Sciences*, **2**(3), 313–322.

O'Neill, J., Senior, T., & Csicsvari, J. (2006). Place-selective firing of CA1 pyramidal cells during sharp wave/ripple network patterns in exploratory behavior. *Neuron*, **49**(1), 143–155.

Owen, S. F., Liu, M. H., & Kreitzer, A. C. (2019). Thermal constraints on in vivo optogenetic manipulations. *Nature Neuroscience*, **22**(7), 1061–1065.

Pang, K. C. H., Jiao, X., Sinha, S., Beck, K. D., & Servatius, R. J. (2011). Damage of GABAergic neurons in the medial septum impairs spatial working memory and extinction of active avoidance: Effects on proactive interference. *Hippocampus*, **21**(8), 835–846.

Papa, M., Pellicano, M. P., Welzl, H., & Sadile, A. G. (1993). Distributed changes in c-Fos and c-Jun immunoreactivity in the rat brain associated with arousal and habituation to novelty. *Brain Research Bulletin*, **32**(5), 509–515.

Pardridge, W. M. (2011). Drug transport in brain via the cerebrospinal fluid. *Fluids and Barriers of the CNS*, **8**(1).

Parnaudeau, S., O'Neill, P.-K., Bolkan, S. S., Ward, R. D., Abbas, A. I., Roth, B. L., Balsam, P. D., Gordon, J. A., & Kellendonk, C. (2013). Inhibition of mediodorsal thalamus disrupts thalamofrontal connectivity and cognition. *Neuron*, **77**(6), 1151–1162.

Pati, S., Salvi, S. S., Kallianpur, M., Banerjee, A., Maiti, S., Clement, J. P., & Vaidya, V. A. (2019). Chemogenetic activation of excitatory neurons alters hippocampal neurotransmission in a dose-dependent manner. *BioRxiv*, 595504.

Paxinos, G., & Watson, C. (2007). *The Rat Brain in Stereotaxic Coordinates* (6th ed.). San Diego: Acandemic Press.

Phillips, R. G., & LeDoux, J. E. (1992). Differential contribution of amygdala and hippocampus to cued and contextual fear conditioning. *Behavioral Neuroscience*, **106**(2), 274–285.

Piterkin, P., Cole, E., Cossette, M. P., Gaskin, S., & Mumby, D. G. (2008). A limited role for the hippocampus in the modulation of novel-object preference by contextual cues. *Learning and Memory*, **15**(10), 785–791.

Prusky, G. T., Harker, K. T., Douglas, R. M., & Whishaw, I. Q. (2002). Variation in visual acuity within pigmented, and between pigmented and albino rat strains. *Behavioural Brain Research*, **136**(2), 339–348.

Rajkumar, R., See, L. K. Y., & Dawe, G. S. (2013). Acute antipsychotic treatments induce distinct c-Fos expression patterns in appetite-related neuronal structures of the rat brain. *Brain Research*, **1508**, 34–43.

Rangel, L. M., Chiba, A. A., & Quinn, L. K. (2015). Theta and beta oscillatory dynamics in the dentate gyrus reveal a shift in network processing state during cue encounters. *Frontiers in Systems Neuroscience*, **9**(July).

Rankovic, Z., Brust, T. F., & Bohn, L. M. (2016). Biased agonism: An emerging paradigm in GPCR drug discovery. *Bioorganic and Medicinal Chemistry Letters*, **26**(2), 241–250.

Raper, J., Morrison, R. D., Daniels, J. S., Howell, L., Bachevalier, J., Wichmann, T., & Galvan, A. (2017). Metabolism and Distribution of Clozapine-N-oxide: Implications for Nonhuman Primate Chemogenetics. *ACS Chemical Neuroscience*, **8**(7), 1570–1576.

Rawlins, J. N. P., & Olton, D. S. (1982). The septo-hippocampal system and cognitive mapping. *Behavioural Brain Research*, **5**(4), 331–358.

Ray, R. S., Corcoran, A. E., Brust, R. D., Kim, J. C., Richerson, G. B., Nattie, E., & Dymecki, S. M. (2011). Impaired respiratory and body temperature control upon acute serotonergic neuron inhibition. *Science*, **333**(6042), 637–642.

Reisel, D., Bannerman, D. M., Schmitt, W. B., Deacon, R. M. J., Flint, J., Borchardt, T., Seeburg, P. H., & Rawlins, J. N. P. (2002). Spatial memory dissociations in mice lacking GluR1. *Nature Neuroscience*, **5**(9), 868–873.

Robinson, S., Todd, T. P., Pasternak, A. R., Luikart, B. W., Skelton, P. D., Urban, D. J., & Bucci, D. J. (2014). Chemogenetic silencing of neurons in retrosplenial cortex disrupts sensory preconditioning. *The Journal of Neuroscience*, **34**(33), 10982–10988.

Rogan, S. C., & Roth, B. L. (2011). Remote control of neuronal signaling. *Pharmacological Reviews*, **63**(2), 291–315.

Romberg, C., Raffel, J., Martin, L., Sprengel, R., Seeburg, P. H., Rawlins, J. N. P., Bannerman, D. M., & Paulsen, O. (2009). Induction and expression of GluA1 (GluR-A)-independent LTP in the hippocampus. *European Journal of Neuroscience*, **29**(6), 1141–1152.

Roth, B. L. (2016). DREADDs for Neuroscientists. *Neuron*, **89**(4), 683–694.

Roth, B. L., Sheffer, D. J., & Kroeze, W. K. (2004). Magic shotguns versus magic bullets: Selectively non-selective drugs for mood disorders and schizophrenia. *Nature Reviews Drug Discovery*, **3**(4), 353–359.

Ryabinin, A. E., Criado, J. R., Henriksen, S. J., Bloom, F. E., & Wilson, M. C. (1997). Differential sensitivity of c-Fos expression in hippocampus and other brain regions to moderate and low doses of alcohol. *Molecular Psychiatry*, **2**(1), 32–43.

Sakaguchi, M., Kim, K., Yu, L. M. Y., Hashikawa, Y., Sekine, Y., Okumura, Y., Kawano, M., Hayashi, M., Kumar, D., Boyden, E. S., McHugh, T. J., & Hayashi, Y. (2015). Inhibiting the activity of CA1 hippocampal neurons prevents the recall of contextual fear memory in inducible ArchT transgenic mice. *PLoS One*, **10**(6).

Sanderson, D. J., Good, M. A., Skelton, K., Sprengel, R., Seeburg, P. H., Rawlins, J. N. P., & Bannerman, D. M. (2009). Enhanced long-term and impaired short-term spatial memory in GluA1 AMPA receptor subunit knockout mice: Evidence for a dual-process memory model. *Learning and Memory*, **16**(6), 379–386.

Sanderson, D. J., & Bannerman, D. M. (2012). The role of habituation in hippocampus-dependent spatial working memory tasks: evidence from GluA1 AMPA receptor subunit knockout mice. *Hippocampus*, **22**(5), 981–994.

Sannino, S., Russo, F., Torromino, G., Pendolino, V., Calabresi, P., & De Leonibus, E. (2012). Role of the dorsal hippocampus in object memory load. *Learning and Memory*, **19**(5), 211–218.

Sasaki, K., Suzuki, M., Mieda, M., Tsujino, N., Roth, B., & Sakurai, T. (2011). Pharmacogenetic modulation of orexin neurons alters sleep/wakefulness states in mice. *PloS One*, **6**(5), e20360.

Scharfman, H. E. (2016). The enigmatic mossy cell of the dentate gyrus. *Nature Reviews Neuroscience*, **17**(9), 562–575.

Scheyltjens, I., Laramée, M. E., Van den Haute, C., Gijsbers, R., Debyser, Z., Baekelandt, V., Vreysen, S., & Arckens, L. (2015). Evaluation of the expression pattern of rAAV2/1, 2/5,

2/7, 2/8, and 2/9 serotypes with different promoters in the mouse visual cortex. *Journal of Comparative Neurology*, **523**(14), 2019–2042.

Schinkel, A. H., Wagenaar, E., Mol, C. A. A. M., & Van Deemter, L. (1996). P-glycoprotein in the blood-brain barrier of mice influences the brain penetration and pharmacological activity of many drugs. *Journal of Clinical Investigation*, **97**(11), 2517–2524.

Schomburg, E. W., Fernández-Ruiz, A., Mizuseki, K., Berényi, A., Anastassiou, C. A., Koch, C., & Buzsáki, G. (2014). Theta Phase Segregation of Input-Specific Gamma Patterns in Entorhinal-Hippocampal Networks. *Neuron*, **84**(2), 470–485.

Schotte, A., Janssen, P. F., Megens, A. A., & Leysen, J. E. (1993). Occupancy of central neurotransmitter receptors by risperidone, clozapine and haloperidol, measured ex vivo by quantitative autoradiography. *Brain Research*, **631**(2), 191–202.

Scofield, M. D., Boger, H. A., Smith, R. J., Li, H., Haydon, P. G., & Kalivas, P. W. (2015). Gq-DREADD selectively initiates glial glutamate release and inhibits cue-induced cocaine seeking. *Biological Psychiatry*, **78**(7), 441–451.

Seeman, P. (2014). Clozapine, a fast-off-D2 antipsychotic. *ACS Chemical Neuroscience*, **5**(1), 24–29.

Seidenbecher, T., Laxmi, T. R., Stork, O., & Pape, H. C. (2003). Amygdalar and hippocampal theta rhythm synchronization during fear memory retrieval. *Science*, **301**(5634), 846–850.

Sengupta, A., Winters, B., Bagley, E. E., & McNally, G. P. (2016). Disrupted prediction error links excessive amygdala activation to excessive fear. *The Journal of Neuroscience*, **36**(2), 385–395.

Shipman, M. L., Johnson, G. C., Bouton, M. E., & Green, J. T. (2019). Chemogenetic silencing of prelimbic cortex to anterior dorsomedial striatum projection attenuates operant responding. *ENeuro*, ENEURO.0125-19.2019.

Sigurdsson, T., Stark, K. L., Karayiorgou, M., Gogos, J. A., & Gordon, J. A. (2010). Impaired hippocampal-prefrontal synchrony in a genetic mouse model of schizophrenia. *Nature*, **464**(7289), 763–767.

Sik, A., Penttonen, M., Ylinen, A., & Buzsiki, G. (1995). Hippocampal CA1 Interneurons: An in vivo Intracellular Labeling Study. *The Journal of Neuroscience*, **75**(10), 6651–6665.

Silva, B. A., Mattucci, C., Krzywkowski, P., Murana, E., Illarionova, A., Grinevich, V., Canteras, N. S., Ragozzino, D., & Gross, C. T. (2013). Independent hypothalamic circuits for social and predator fear. *Nature Neuroscience*, **16**(12), 1731–1733.

Smith, K. S., Bucci, D. J., Luikart, B. W., & Mahler, S. V. (2016). DREADDs: Use and application in behavioral neuroscience. *Behavioral Neuroscience*, **130**(2), 137–155.

Sohal, V. S., Zhang, F., Yizhar, O., & Deisseroth, K. (2009). Parvalbumin neurons and gamma rhythms enhance cortical circuit performance. *Nature*, **459**(7247), 698–702.

Stachniak, T. J., Ghosh, A., & Sternson, S. M. (2014). Chemogenetic synaptic silencing of neural circuits localizes a hypothalamus→midbrain pathway for feeding behavior. *Neuron*, **82**(4), 797–808.

Sternson, S. M., & Roth, B. L. (2014). Chemogenetic tools to interrogate brain functions. *Annual Review of Neuroscience*, **37**, 387–407.

Stevenson, E. L., & Caldwell, H. K. (2014). Lesions to the CA2 region of the hippocampus impair social memory in mice. *European Journal of Neuroscience*, **40**(9), 3294–3301.

Strader, C. D., Gaffney, T., Sugg, E. E., Rios Candelore, M., Keys, R., Patchett, A. A., & Dixon, R. A. F. (1991). Allele-specific activation of genetically engineered receptors. *Journal of Biological Chemistry*, **266**(1), 5–8.

Sudarov, A., Zhang, X.-J., Braunstein, L., LoCastro, E., Singh, S., Taniguchi, Y., Raj, A., Shi, S.-H., Moore, H., & Ross, M. E. (2018). Mature Hippocampal Neurons Require LIS1 for Synaptic Integrity: Implications for Cognition. *Biological Psychiatry*, **83**(6), 518–529.

Sun, H. X., Wang, D. R., Ye, C. B., Hu, Z. Z., Wang, C. Y., Huang, Z. L., & Yang, S. R. (2017). Activation of the ventral tegmental area increased wakefulness in mice. *Sleep and Biological Rhythms*, **15**(2), 107–115.

Thompson, K. J., Khajehali, E., Bradley, S. J., Navarrete, J. S., Huang, X. P., Slocum, S., Jin, J., Liu, J., Xiong, Y., Olsen, R. H. J., Diberto, J. F., Boyt, K. M., Pina, M. M., Pati, D., Molloy, C., Bundgaard, C., Sexton, P. M., Kash, T. L., Krashes, M. J., Christopolous, A., Roth, B. L., & Tobin, A. B. (2018). DREADD Agonist 21 Is an Effective Agonist for Muscarinic-Based DREADDs in Vitro and in Vivo . *ACS Pharmacology & Translational Science*, **1**(1), 61–72.

Thompson, R. F., & Spencer, W. A. (1966). Habituation: A model phenomenon for the study of neuronal substrates of behavior. *Psychological Review*, **73**(1), 16–43.

Tipps, M., de Velasco, E. M. F., Schaeffer, A., & Wickman, K. (2018). Inhibition of pyramidal neurons in the basal amygdala promotes fear learning. *ENeuro*, **5**(5).

Trepanier, C., Lei, G., Xie, Y.-F., & MacDonald, J. F. (2013). Group II metabotropic glutamate receptors modify N-methyl-D-aspartate receptors via Src kinase. *Scientific Reports*, **3**, 926.

Tuscher, J. J., Taxier, L. R., Fortress, A. M., & Frick, K. M. (2018). Chemogenetic inactivation of the dorsal hippocampus and medial prefrontal cortex, individually and concurrently, impairs object recognition and spatial memory consolidation in female mice. *Neurobiology of Learning and Memory*, **156**, 103–116.

Tzakis, N., & Holahan, M. R. (2019). Social Memory and the Role of the Hippocampal CA2 Region. *Frontiers in Behavioral Neuroscience*, **13**.

Uhlhaas, P. J., & Singer, W. (2010). Abnormal neural oscillations and synchrony in schizophrenia. *Nature Reviews Neuroscience*, **11**(2), 100–113.

Upright, N. A., Brookshire, S. W., Schnebelen, W., Damatac, C. G., Hof, P. R., Browning, P. G. F., Croxson, P. L., Rudebeck, P. H., & Baxter, M. G. (2018). Behavioral effect of

chemogenetic inhibition is directly related to receptor transduction levels in Rhesus monkeys. *The Journal of Neuroscience*, **38**(37), 7969–7975.

Urban, D. J., & Roth, B. L. (2015). DREADDs (Designer Receptors Exclusively Activated by Designer Drugs): Chemogenetic Tools with Therapeutic Utility. *Annual Review of Pharmacology and Toxicology*, **55**(1), 399–417.

Urban, D. J., Zhu, H., Marcinkiewcz, C. A., Michaelides, M., Oshibuchi, H., Rhea, D., Aryal, D. K., Farrell, M. S., Lowery-Gionta, E., Olsen, R. H. J., Wetsel, W. C., Kash, T. L., Hurd, Y. L., Tecott, L. H., & Roth, B. L. (2016). Elucidation of the Behavioral Program and Neuronal Network Encoded by Dorsal Raphe Serotonergic Neurons. *Neuropsychopharmacology*, **41**(5), 1404–1415.

Urban, J. D., Clarke, W. P., Von Zastrow, M., Nichols, D. E., Kobilka, B., Weinstein, H., Javitch, J. A., Roth, B. L., Christopoulos, A., Sexton, P. M., Miller, K. J., Spedding, M., & Mailman, R. B. (2007). Functional selectivity and classical concepts of quantitative pharmacology. *Journal of Pharmacology and Experimental Therapeutics*, **320**(1), 1–13.

van Dijk, M. T., & Fenton, A. A. (2018). On How the Dentate Gyrus Contributes to Memory Discrimination. *Neuron*, **98**(4), 832-845.e5.

Vanderwolf, C. H. (1969). Hippocampal electrical activity and voluntary movement in the rat. *Electroencephalography and Clinical Neurophysiology*, **26**(4), 407–418.

VanElzakker, M., Fevurly, R. D., Breindel, T., & Spencer, R. L. (2008). Environmental novelty is associated with a selective increase in Fos expression in the output elements of the hippocampal formation and the perirhinal cortex. *Learning and Memory*, **15**(12), 899–908.

Vardy, E., Robinson, J. E., Li, C., Olsen, R. H. J., DiBerto, J. F., Giguere, P. M., Sassano, F. M., Huang, X. P., Zhu, H., Urban, D. J., White, K. L., Rittiner, J. E., Crowley, N. A., Pleil, K. E., Mazzone, C. M., Mosier, P. D., Song, J., Kash, T. L., Malanga, C. J., Krashes, M. J., & Roth, B. L. (2015). A New DREADD Facilitates the Multiplexed Chemogenetic Interrogation of Behavior. *Neuron*, **86**(4), 936–946.

Varela, C., Weiss, S., Meyer, R., Halassa, M., Biedenkapp, J., Wilson, M. A., Goosens, K. A., & Bendor, D. (2016). Tracking the Time-Dependent Role of the Hippocampus in Memory Recall Using DREADDs. *PloS One*, **11**(5), e0154374.

Vazey, E. M., & Aston-Jones, G. (2014). Designer receptor manipulations reveal a role of the locus coeruleus noradrenergic system in isoflurane general anesthesia. *PNAS*, **111**(10), 3859–3864.

Vekovischeva, O. Y., Zamanillo, D., Echenko, O., Seppälä, T., Uusi-Oukari, M., Honkanen, A., Seeburg, P. H., Sprengel, R., & Korpi, E. R. (2001). Morphine-induced dependence and sensitization are altered in mice deficient in AMPA-type glutamate receptor-A subunits. *The Journal of Neuroscience*, **21**(12), 4451–4459.

Vertes, R. P. (2005). Hippocampal theta rhythm: A tag for short-term memory. *Hippocampus*, **15**(7), 923–935.

Vetere, G., Kenney, J. W., Tran, L. M., Xia, F., Steadman, P. E., Parkinson, J., Josselyn, S. A., & Frankland, P. W. (2017). Chemogenetic Interrogation of a Brain-wide Fear Memory Network in Mice. *Neuron*, **94**(2), 363-374.e4.

Wang, H. S., Pan, Z., Shi, W., Brown, B. S., Wymore, R. S., Cohen, I. S., Dixon, J. E., & McKinnon, D. (1998). KCNQ2 and KCNQ3 potassium channel subunits: Molecular correlates of the M-channel. *Science*, **282**(5395), 1890–1893.

Wang, X., Zhang, C., Szábo, G., & Sun, Q. Q. (2013). Distribution of CaMKIIα expression in the brain in vivo, studied by CaMKIIα-GFP mice. *Brain Research*, **1518**, 9–25.

Watakabe, A., Ohtsuka, M., Kinoshita, M., Takaji, M., Isa, K., Mizukami, H., Ozawa, K., Isa, T., & Yamamori, T. (2015). Comparative analyses of adeno-associated viral vector serotypes 1, 2, 5, 8 and 9 in marmoset, mouse and macaque cerebral cortex. *Neuroscience Research*, **93**, 144–157.

Wettschureck, N., & Offermanns, S. (2005). Mammalian G proteins and their cell type specific functions. *Physiological Reviews*, **85**(4), 1159–1204.

Whishaw, I. Q., & Tomie, J. A. (1996). Of mice and mazes: similarities between mice and rats on dry land but not water mazes. *Physiology & Behavior*, **60**(5), 1191–1197.

Whissell, P. D., Tohyama, S., & Martin, L. J. (2016). The Use of DREADDs to Deconstruct Behavior. *Frontiers in Genetics*, **7**, 70.

White, M. D., Milne, R. V. J., & Nolan, M. F. (2011). A Molecular Toolbox for Rapid Generation of Viral Vectors to Up- or Down-Regulate Neuronal Gene Expression in vivo. *Frontiers in Molecular Neuroscience*, **4**.

Whittington, M. A., Traub, R. D., Kopell, N., Ermentrout, B., & Buhl, E. H. (2000). Inhibition-based rhythms: Experimental and mathematical observations on network dynamics. *International Journal of Psychophysiology*, **38**(3), 315–336.

Wiedholz, L. M., Owens, W. A., Horton, R. E., Feyder, M., Karlsson, R. M., Hefner, K., Sprengel, R., Celikel, T., Daws, L. C., & Holmes, A. (2008). Mice lacking the AMPA GluR1 receptor exhibit striatal hyperdopaminergia and “schizophrenia-related” behaviors. *Molecular Psychiatry*, **13**(6), 631–640.

Wiltgen, B. J., Sanders, M. J., Anagnostaras, S. G., Sage, J. R., & Fanselow, M. S. (2006). Context fear learning in the absence of the hippocampus. *The Journal of Neuroscience*, **26**(20), 5484–5491.

Wong, M. (2010). Too much inhibition leads to excitation in absence epilepsy. *Epilepsy Currents*, **10**(5), 131–132.

Woods, S., Clarke, N. N., Layfield, R., & Fone, K. C. F. (2012). 5-HT6 receptor agonists and antagonists enhance learning and memory in a conditioned emotion response paradigm by modulation of cholinergic and glutamatergic mechanisms. *British Journal of Pharmacology*, **167**(2), 436–449.

Wright, R. A., Johnson, B. G., Zhang, C., Salhoff, C., Kingston, A. E., Calligaro, D. O., Monn, J. A., Schoepp, D. D., & Marek, G. J. (2013). CNS distribution of metabotropic glutamate

2 and 3 receptors: transgenic mice and [^{3}H]LY459477 autoradiography. *Neuropharmacology*, **66**, 89–98.

Wu, G. Y., Liu, G. L., Zhang, H. M., Chen, C., Liu, S. L., Feng, H., & Sui, J. F. (2015). Optogenetic stimulation of mPFC pyramidal neurons as a conditioned stimulus supports associative learning in rats. *Scientific Reports*, **5**.

Yau, J. O. Y., & McNally, G. P. (2015). Pharmacogenetic excitation of dorsomedial prefrontal cortex restores fear prediction error. *The Journal of Neuroscience*, **35**(1), 74–83.

Yeh, C. Y., Asrican, B., Moss, J., Quintanilla, L. J., He, T., Mao, X., Cassé, F., Gebara, E., Bao, H., Lu, W., Toni, N., & Song, J. (2018). Mossy Cells Control Adult Neural Stem Cell Quiescence and Maintenance through a Dynamic Balance between Direct and Indirect Pathways. *Neuron*, **99**(3), 493-510.e4.

Yoshii, T., Hosokawa, H., & Matsuo, N. (2017). Pharmacogenetic reactivation of the original engram evokes an extinguished fear memory. *Neuropharmacology*, **113**, 1–9.

Yuan, P., & Grutzendler, J. (2016). Attenuation of β-amyloid deposition and neurotoxicity by chemogenetic modulation of neural activity. *The Journal of Neuroscience*, **36**(2), 632–641.

Zamanillo, D., Sprengel, R., Hvalby, Ø., Jensen, V., Burnashev, N., Rozov, A., Kaiser, K. M. M., Köster, H. J., Borchardt, T., Worley, P., Lübke, J., Frotscher, M., Kelly, P. H., Sommer, B., Andersen, P., Seeburg, P. H., & Sakmann, B. (1999). Importance of AMPA receptors for hippocampal synaptic plasticity but not for spatial learning. *Science*, **284**(5421), 1805–1811.

Zeelenberg, R., & Pecher, D. (2015). A method for simultaneously counterbalancing condition order and assignment of stimulus materials to conditions. *Behavior Research Methods*, **47**(1), 127–133.

Zemelman, B. V, Lee, G. A., Ng, M., & Miesenböck, G. (2002). Selective photostimulation of genetically chARGed neurons. *Neuron*, **33**(1), 15–22.

Zhan, C., Zhou, J., Feng, Q., Zhang, J. en, Lin, S., Bao, J., Wu, P., & Luo, M. (2013). Acute and long-term suppression of feeding behavior by POMC neurons in the brainstem and hypothalamus, respectively. *The Journal of Neuroscience*, **33**(8), 3624–3632.

Zhou, Q. G., Nemes, A. D., Lee, D., Ro, E. J., Zhang, J., Nowacki, A. S., Dymecki, S. M., Najm, I. M., & Suh, H. (2019). Chemogenetic silencing of hippocampal neurons suppresses epileptic neural circuits. *Journal of Clinical Investigation*, **129**(1).

Zhou, W., Cheung, K., Kyu, S., Wang, L., Guan, Z., Kurien, P. A., Bickler, P. E., Jan, L. Y., Cotten, J. F., Orser, B. A., Solt, K., & Zhang, J.-M. (2018). Activation of orexin system facilitates anesthesia emergence and pain control. *PNAS*, **115**(45), 10740–10747.

Zhu, H., Aryal, D. K., Olsen, R. H. J., Urban, D. J., Swearingen, A., Forbes, S., Roth, B. L., & Hochgeschwender, U. (2016). Cre-dependent DREADD (Designer Receptors Exclusively Activated by Designer Drugs) mice. *Genesis*, **54**(8), 439–446.

Zhu, H., Pleil, K. E., Urban, D. J., Moy, S. S., Kash, T. L., & Roth, B. L. (2014). Chemogenetic inactivation of ventral hippocampal glutamatergic neurons disrupts consolidation of contextual fear memory. *Neuropsychopharmacology*, **39**(8), 1880–1892.

Zhu, H., & Roth, B. L. (2014). DREADD: a chemogenetic GPCR signaling platform. *The International Journal of Neuropsychopharmacology*, **18**(1).

Zou, D., Chen, L., Deng, D., Jiang, D., Dong, F., McSweeney, C., Zhou, Y., Liu, L., Chen, G., Wu, Y., & Mao, Y. (2016). DREADD in parvalbumin interneurons of the dentate gyrus modulates anxiety, social interaction and memory extinction. *Current Molecular Medicine*, **16**(1), 91–102.